Adhesion Molecule Expression In Corneal Transplantation: A Target For Therapy?

By

Christelle C. Kerouedan

A Thesis Submitted To The Faculty Of Medicine
Of The University Of London
For The Degree Of
Doctor Of Philosophy

Department of Immunology
Imperial College London
Faculty of Medicine
Hammersmith Campus
Du Cane Road,
London, UK

May 2003

For Manon, Antoine, and Ronan

Sometimes

Sometimes things don't go after all,
from bad to worse. Some years, muscadel
faces down frost; green thrives; the crops don't fail,
Sometimes a man aims high, and all goes well.

A people sometimes will step back from war;
elect an honest man; decide they care
enough, that they can't leave some stranger poor.
Some men become what they were born for.

Sometimes our best efforts do not go
amiss; sometimes we do as we meant to.
The sun will sometimes melt a field of sorrow
that seemed hard frozen: may it happen for you.

SHEENAGH PUGH (b. 1950)

Acknowledgments

My gratitude goes to Pr Andrew George and Dr Frank Larkin my supervisors. I thank particularly Andrew, for his support and encouragements when times were tough, for his technical support and invaluable advice. I appreciated his understanding, his open-door policy, and overall, his human and friendly attitude. I am very grateful to Frank, for his time and his precious advice and assistance, especially in the ophthalmic field.

I also thank Fight for Sight for funding this project.

I thank the numerous people of our past and present team, for their technical and moral support, especially Dr Navid Ardjomand, Dr Richard Comer, Dr William King, Dr Tobias Hudde, and Pervinder Sagoo. I particularly express my gratitude to Dr Peter Reynolds, Dr PH Tan and Stefanos Theoharis, for always offering a helping hand and moral support.

I am also thankful to Mary Bowe and Cheryl Costello for their smile and good humour. I thank them particularly for helping me struggle with the paperwork, the administration or finance department, and for their support when fighting the odds.

I thank my family and my friends for their support and their words of encouragements, especially Sophie Tourdot and Fabien Sebille, (ex) colleagues and friends, who helped me to see the good side of things when I needed it the most.

Finally, but not the least, I thank my husband Ronan, who encouraged me right from the beginning and without whom this thesis would not be. I thank him for his love and his support, for lifting my moods and raising my ambitions all along. I also thank my children Antoine and Manon, who, in their very own way, gave me the will and the strength to continue, and who reminded me frequently (sometimes more than needed), that there is more to life than PCR, FACS and cell culture.

Abstract

Corneal diseases are a major cause of blindness worldwide. In many cases, transplantation is the only treatment. Corneal grafting is the most common and the most successful solid organ transplantation procedure in humans. This is due in part, to the immune privilege of the cornea. However, significant rejection is seen, in particular in inflamed or vascularised graft beds.

The specific immune mechanism of corneal allograft rejection is not fully understood, but it is associated with various degrees of neovascularisation, infiltration of the graft with inflammatory cells and elevated pro-inflammatory cytokines. These are responsible for the up-regulation of adhesion molecules, whose role in the pathogenesis of corneal allograft rejection was therefore investigated, as they could potentially provide a target for anti-adhesive therapy.

The expression of a large panel of adhesion molecules and the influence of pro-inflammatory cytokines were investigated using RT-PCR, FACS analysis, immunofluorescence and histology in mouse corneas or in a mouse corneal endothelium (MCE) cell line. The role of the relevant adhesion molecules was then further investigated using adhesion assays, and histology on a mouse model of corneal allograft rejection.

Among all the adhesion molecules tested, VCAM-1 was the only one constitutively expressed in the MCE cells. TNFα, and IL-1α to a lesser extent, increased its expression. IFNγ alone had no effect but acted synergistically on VCAM-1 up-regulation by TNFα. *Ex vivo*, VCAM-1 was also detected in the mouse corneal endothelium.

Adhesion assays and blocking experiments suggested a role for VCAM-1 and a yet unknown molecule, in the recruitment of inflammatory cells to the graft. Its expression at the donor-recipient interface of the allograft but not the isograft also supported its implication in the rejection process. Preliminary experiments using vitamin E or "intrabodies" to modulate the expression of VCAM-1 in the MCE cells were very encouraging. RT-PCR analysis of post-mortem human corneas, however, showed no expression of VCAM-1 or of the other adhesion molecules tested. These data highlight a fundamental difference between the two species.

Table of Contents

ACKNOWLEDGMENTS **5**

ABSTRACT **6**

TABLE OF CONTENTS **7**

LIST OF FIGURES **12**

LIST OF TABLES **17**

INTRODUCTION **19**

1.1- Transplantation in the eye **19**
1.1.1- Anatomy 19
1.1.1.1- Corneal epithelium 19
1.1.1.2- Bowman's layer 22
1.1.1.3- Stroma 22
1.1.1.4- Descemet's membrane 23
1.1.1.5- Corneal endothelium 23
1.1.2- Immune privilege 25
1.1.2.1- Passive mechanisms responsible for immune privilege in the eye 26
a) Blood-ocular barrier 26
b) Avascularity 26
c) Absence of APC 27
1.1.2.2- Active mechanisms responsible for immune privilege in the eye 28
a) Fas-ligand expression 28
b) Immunosuppressive agents 30
c) ACAID 31
1.1.3- Clinical aspects 32
1.1.3.1- Indications for transplantation 32
1.1.3.2- Success 33
1.1.3.3- Graft failure 34
1.1.3.4- Corneal allograft rejection 34

1.2- Adhesion molecules **42**
1.2.1- Cell adhesion molecules (CAMs) 42
1.2.1.1- The selectin family 44
a) L-Selectin 44
b) E-Selectin 46
c) P-Selectin 46
1.2.1.2- The immunoglobulin (Ig) superfamily 46
a) ICAMs 47

b) VCAM-1 49
c) PECAM-1 49
d) NCAM 49
1.2.1.3- The integrin family 50
a) LFA-1 52
b) VLA-4 52
1.2.1.4- Cell surface amino oxidases 53
1.2.2- The adhesion cascade 54
1.2.2.1- Tethering and rolling 54
1.2.2.2- Integrin activation 56
1.2.2.3- Firm adhesion 56
1.2.2.4- Transmigration 56
1.2.3- Cell adhesion molecules in the study 58

1.3- Adhesion molecules and the eye 60

MATERIALS AND METHODS 64

2.1- Specimens 64
2.1.1- Human Corneas 64
2.1.2- Murine Corneas 64

2.2- Mouse corneal transplantation 64

2.3- Cell culture 68
2.3.1- Cell lines 68
2.3.2- Culture media and conditions 69
2.3.3- Primary cultures of bovine corneal endothelial cells (BCE) 72
2.3.4- Preparation of BCE matrix 72
2.3.5- Primary cultures of human corneal endothelial cells (HCE) 73

2.4- RT-PCR 74
2.4.1- Preparation of samples 74
2.4.1.1- Corneal samples 74
2.4.1.2- Cells and other tissues 74
2.4.2- mRNA extraction 74
2.4.3- Reverse transcription 75
2.4.4- PCR 76
2.4.5- Primers sequences 77

2.5- Antibodies used in the study 79
2.5.1- Antibody purification 79
2.5.2- Summary of antibodies used in this study 79

2.6- Flow cytometry 82
2.6.1- Preparation of cells 82
2.6.2- Staining 82

2.7- Immunofluorescence **83**
2.7.1- Cytospins 83
2.7.2- Cell culture on slides 83
2.7.3- Preparation of corneal flat mounts 84
2.7.4- Fluorescent staining 84

2.8- Immunohistology **85**
2.8.1- Tissue preparation and cryostat sectioning 85
2.8.2- Staining 85

2.9- Adhesion assay **87**
2.9.1- Seeding of adherent cells 87
2.9.2- Purification of human Polymorphonuclear cells (PMN) 87
2.9.3- Purification of human Peripheral Blood Mononuclear Cells (PBMC) 88
2.9.4- Purification of human T cells 88
2.9.5- Purification of mouse splenocytes 89
2.9.6- Labelling of leukocytes 89
2.9.7- Adhesion assay 90

2.10- Modulation of VCAM-1 expression in MCE BALB/c cells **92**
2.10.1- Inhibition of VCAM-1 expression in MCE cells using Vitamin E 92
2.10.2- Inhibition of VCAM-1 expression in MCE cells by transfection of a single chain anti-VCAM-1 antibody 92

ADHESION MOLECULES IN THE MOUSE CORNEA **95**

3.1- Expression of adhesion molecules in the mouse cornea **95**
3.1.1-Expression of adhesion molecules mRNA in the mouse cornea 96
3.1.1.1- Expression of adhesion molecules mRNA in the MCE cell line 98
3.1.1.2- Expression of adhesion molecules mRNA in the excised cornea 104
3.1.2- Expression of adhesion molecules proteins in the mouse cornea 107
3.1.2.1- Expression of adhesion molecules proteins in the MCE cell line 107
a) Expression of adhesion molecules in the resting MCE cell line 109
b) Expression of adhesion molecules in MCE cells exposed to TNFα 112
c) Expression of adhesion molecules in MCE cells exposed to IFNγ 112
d) Expression of adhesion molecules in MCE cells exposed to IL1-α 114
e) Expression of adhesion molecules in MCE cells exposed to TNFα and IFNγ 114
f) Expression of adhesion molecules in MCE cells exposed to a cocktail of cytokines 116
g) Optimisation of cytokine effect on VCAM-1 expression in MCE cells .. 116
h) Synergistic effect of IFNγ and TNFα on the expression of VCAM-1 in MCE cells 118
i) Conclusion 121
3.1.2.2 Expression of adhesion molecules proteins in the excised cornea 121
3.1.3- Conclusion 128

3.2- Function of adhesion molecules in the mouse cornea 129
3.2.1- Adhesion of human and murine cell populations to MCE cells 133
3.2.1.1- Adhesion of human and murine cell populations to resting MCE cells 133
3.2.1.2- Adhesion of human and murine cells to stimulated MCE cells..... 135
3.2.2- Inhibition of human cells adhesion to MCE BALB/c cells 138
3.2.2.1- Jurkat T cells..... 138
3.2.2.2- Purified T cells..... 143
3.2.2.3- PBMC 146
3.2.2.4- PMN..... 146
3.2.3- Inhibition of murine cells adhesion to MCE BALB/c cells..... 151
3.2.3.1- Splenocytes 151
3.2.3.2- Macrophages..... 154
3.2.4- Conclusion 154

3.3- Consequences of adhesion molecules expression on corneal allograft fate 158
3.3.1- ICAM-1..... 158
3.3.2- VCAM-1 160
3.3.3- PECAM-1 160
3.3.4- Conclusion 160

3.4- Modulation of VCAM-1 expression in MCE cells 163
3.4.1- Inhibition of VCAM-1 expression using Vitamin E..... 163
3.4.2- Inhibition of VCAM-1 expression by anti-VCAM-1 single chain antibody 167
3.4.3- Conclusion 172

3.5- VCAM-1, a target for therapy in corneal transplantation?..... 172

ADHESION MOLECULES IN THE HUMAN CORNEA..... 176

4.1- Expression of adhesion molecules in the human cornea 176
4.1.1- Optimisation of RT-PCR for human adhesion molecules 177
4.1.2- Detection of mRNA for adhesion molecules in some human corneas 181
4.1.3- Expression of adhesion molecule proteins in human corneal endothelium 187
4.1.4- Conclusion 187

4.2- Generation of a human corneal endothelial (HCE) cell line..... 189
4.2.1- Generation of a BCE cell culture and matrix preparation 189
4.2.2- Generation of a HCE cell culture..... 189
4.2.3- Conclusion 190

4.3- Conclusion 192

DISCUSSION 194

5.1- Adhesion molecules and the mouse cornea..... 195

5.1.1- Expression of adhesion molecules in the mouse cornea 196
5.1.2- Function of adhesion molecules in the mouse cornea 201
5.1.3- Consequences of adhesion molecules expression on mouse corneal allograft fate 207
5.1.4- Modulation of VCAM-1 expression in MCE cells 209

5.2- Adhesion molecules and the human cornea 213
5.2.1- Expression of adhesion molecules in the human cornea 214
5.2.2- Generation of a human corneal endothelial (HCE) cell line 217

5.3- Conclusion 218

CREDITS 220

ABBREVIATIONS 221

REFERENCES 224

List of Figures

INTRODUCTION

Figure 1: Anatomy of the eye.....20

Figure 2: Cross-section of a normal mouse eye.....20

Figure 3: Histological structure of the cornea.....21

Figure 4: Mosaic of polygonal and hexagonal cells in the guinea pig corneal endothelium.....24

Figure 5: Direct/Indirect Presentation.....29

Figure 6: Biological activities of IFNγ.....37

Figure 7: Biological activities of TNFα.....38

Figure 8: Biological activities of IL-1α.....39

Figure 9: Homotypic and heterotypic molecular interactions.....43

Figure 10: The selectin family.....45

Figure 11: The immunoglobulin superfamily.....48

Figure 12: The integrin family.....51

Figure 13: The recruitment of leukocytes from the circulation.....55

MATERIALS AND METHODS

Figure 1: Mouse corneal transplantation.....66

Figure 2: Inverted-phase micrograph of a nearly confluent MCE cell culture.....70

Figure 3: Adhesion assay protocol diagram.....91

ADHESION MOLECULES IN THE MOUSE CORNEA

Figure 1: Collagen VIII mRNA expression in mouse corneal endothelial (MCE) cells and in one excised mouse cornea.....97

Figure 2: Adhesion molecules mRNA expression in resting mouse corneal endothelial (MCE) cells.....99

Figure 3: Adhesion molecules mRNA in mouse corneal endothelial (MCE) cells stimulated with cytokines.....100

Figure 4: Pixel Density analysis of adhesion molecules PCR products in mouse corneal endothelial (MCE) cells stimulated with TNFα.....101

Figure 5: Pixel Density analysis of adhesion molecules PCR products in mouse corneal endothelial (MCE) cells stimulated with IFNγ.....101

Figure 6: Pixel Density analysis of adhesion molecules PCR products in mouse corneal endothelial (MCE) cells stimulated with IL-1α.....103

Figure 7: Pixel Density analysis of adhesion molecules PCR products in mouse corneal endothelial (MCE) cells stimulated with TNFα, IL-1α and IFNγ.....103

Figure 8: Adhesion molecules mRNA expression in mouse corneal endothelial cells and excised mouse corneas with or without stimulation with cytokines.....105

Figure 9: Adhesion molecules mRNA expression in excised mouse corneas with or without stimulation with cytokines.....105

Figure 10: Effect of trypsin detachment on adhesion molecules detection in sEnd-1 cells, resting or stimulated with TNFα for 4 hours.....108

Figure 11: Expression of adhesion molecules in resting mouse corneal endothelial (MCE) cells.....110

Figure 12: Adhesion molecules expression in resting mouse corneal endothelial (MCE) cells.....111

Figure 13: VCAM-1 protein is constitutively expressed in two different strains of MCE cells.....111

Figure 14: Effect of TNFα on adhesion molecules expression in mouse corneal endothelial (MCE) cells.....113

Figure 15: Effect of IFNγ on adhesion molecules expression in mouse corneal endothelial (MCE) cells.....113

Figure 16: Effect of IL-1α on adhesion molecules expression in mouse corneal endothelial (MCE) cells.....115

Figure 17: Effect of the combined exposure to TNFα and IFNγ on adhesion molecules expression in MCE cells.....115

Figure 18: VCAM-1 expression only is up-regulated on MCE cells after exposure to a cocktail of TNFα, IFNγ and IL-1α.....117

Figure 19: Effect of cytokine doses on VCAM-1 expression in mouse corneal endothelial (MCE) cells.....117

Figure 20: Effect of the combined exposure to TNFα, IFNγ and IL-1α on VCAM-1 expression in mouse corneal endothelial (MCE) cells.....119

Figure 21: Effect of the combined exposure to TNFα, IFNγ and IL-1α on VCAM-1 expression in mouse corneal endothelial (MCE) cells.....120

Figure 22: Effect of the combined exposure to TNFα, IFNγ and IL-1α on VCAM-1 expression in mouse corneal endothelial (MCE) cells.....120

Figure 23: Adhesion molecule expression in MCE cells using fluorescent microscopy.....122

Figure 24: Adhesion molecule expression in flat mounts of mouse endothelium using fluorescent microscopy.....124

Figure 25: Optimisation of adhesion molecules staining on histological sections...125

Figure 26: Adhesion molecule expression in MCE cells cytospins.....126

Figure 27: Adhesion molecule expression in normal mouse corneas sections.....127

Figure 28: FACS profile of human Jurkat T cells prior to, and after staining with Calcein AM.....131

Figure 29: Standard curve of human Jurkat T cells after labelling with Calcein....131

Figure 30: Optimisation of the adhesion assay technique using DAP-3 / DVCAM and Jurkat T cells.....132

Figure 31: Adhesion of human cell populations on resting MCE BALB/c cells.....134

Figure 32: Adhesion of murine cell populations on resting MCE BALB/c cells....134

Figure 33: Adhesion of human cell populations on activated MCE BALB/c cells..136

Figure 34: Adhesion of murine cell populations on activated MCE BALB/c cells..136

Figure 35: Inhibition of human Jurkat T cells adhesion on resting MCE cells.....139

Figure 36: Inhibition of human Jurkat T cells adhesion on resting MCE cells.....140

Figure 37: Inhibition of human Jurkat T cells adhesion on stimulated MCE cells...141

Figure 38: Inhibition of human purified T cells adhesion on resting MCE cells....144

Figure 39: Inhibition of human purified T cells adhesion on stimulated MCE 145

Figure 40: Inhibition of human PBMC adhesion on resting MCE cells.....147

Figure 41: Inhibition of human PBMC adhesion on stimulated MCE cells.....148

Figure 42: Inhibition of human PMN adhesion on resting MCE cells.....149

Figure 43: Inhibition of human PMN adhesion on stimulated MCE cells.....150

Figure 44: Inhibition of murine splenocytes adhesion on resting MCE cells.....152

Figure 45: Inhibition of murine splenocytes adhesion on stimulated MCE cells....153

Figure 46: Inhibition of murine macrophages adhesion on resting MCE cells.....156

Figure 47: Inhibition of murine macrophages adhesion on stimulated MCE cells...157

Figure 48: ICAM-1 expression in transplanted mouse corneas sections.....159

Figure 49: VCAM-1 expression in transplanted mouse corneas sections.....161

Figure 50: PECAM-1 expression in transplanted mouse corneas sections.....162

Figure 51: Inhibition of VCAM-1 expression using Vitamin E.....165

Figure 52: Structure of intact antibody, antibody fragments and scFv construct....168

Figure 53: Inhibition of VCAM-1 expression using a single chain anti-VCAM-1 antibody transfection.....171

ADHESION MOLECULES IN THE HUMAN CORNEA

Figure 1: RT-PCR of GAPDH, ICAM-1, VCAM-1 and E-selectin mRNA in TNFα-treated EA-hy 926 cells.....178

Figure 2: Pixel density analysis of ICAM-1, VCAM-1 and E-Selectin PCR products visualised on an ethidium bromide stained gel.....180

Figure 3: RT-PCR of GAPDH, ICAM-1, VCAM-1 and E-Selectin mRNA in DAP-3, DVCAM, CHO and CHO-E cells.....182

Figure 4: RT-PCR of GAPDH, ICAM-1, VCAM-1 and E-Selectin mRNA in one human cornea.....183

Figure 5: Pixel density analysis of ICAM-1, VCAM-1 and E-selectin bands after TNFα stimulation of a human cornea for 1 to 32h.....185

Figure 6: Pixel density analysis of ICAM-1, VCAM-1 and E-selectin PCR products after stimulation of a human cornea for 4h with 0.1 to 10 ng/ml TNFα.....185

Figure 7: Adhesion molecule protein expression in human corneas.....188

Figure 8: Inverted-phase micrograph of a confluent 4th-passage BCE cell culture.191

Figure 9: Inverted-phase micrograph of HCE cells in culture (passage 0).....191

List of Tables

INTRODUCTION

Table 1A: Adhesion molecules studied in this project.....58

Table 1B: Adhesion molecules studied in this project.....59

MATERIALS AND METHODS

Table 1: Standardised grading scheme used in the characterisation of the different allograft rejection stages.....67

Table 2: Summary of human PCR details.....77

Table 3: Summary of mouse PCR details.....78

Table 4: Rabbit antibodies used in the study.....79

Table 5: Mouse antibodies used in the study.....80

Table 6: Rat antibodies used in the study.....81

ADHESION MOLECULES IN THE MOUSE CORNEA

Table 1: Adhesion of human and murine cell populations to MCE cells.....137

ADHESION MOLECULES IN THE HUMAN CORNEA

Table 1: RT-PCR analysis of adhesion molecule mRNA expression in human corneas.....186

CHAPTER 1

Introduction

Introduction

1.1- Transplantation in the eye

1.1.1- Anatomy

Cornea, the transparent structure in front of the eye, plays a vital role both in light transmission and refraction, and as a physical barrier to trauma and infection (figures 1 and 2). It forms one sixth of the ocular globe and constitutes, with the sclera, the outer layer of the eye. Cornea and sclera meet at a region called the limbus and provide a protective envelope and a structural support to intraocular contents.

The cornea is an avascular tissue and can be subdivided into three layers (figure 3), namely the epithelium, the substantia propria or stroma, and finally the endothelium. The stroma is separated from the epithelium by the Bowman's layer and from the endothelium by the Descemet's membrane. The anterior surface of the cornea is covered with the precorneal tear film that is re-established with each blink, about once every twenty seconds.

1.1.1.1- Corneal epithelium

The corneal epithelium, which is 50 to 90 μm in thickness, constitutes of five or six layers of squamous non-keratinised cells. The deepest of these, the basal epithelial cells form a palisade-like layer and are firmly anchored in a basal lamina and in the underlying Bowman's layer via a complex mesh of collagen fibrils and anchoring plaques.

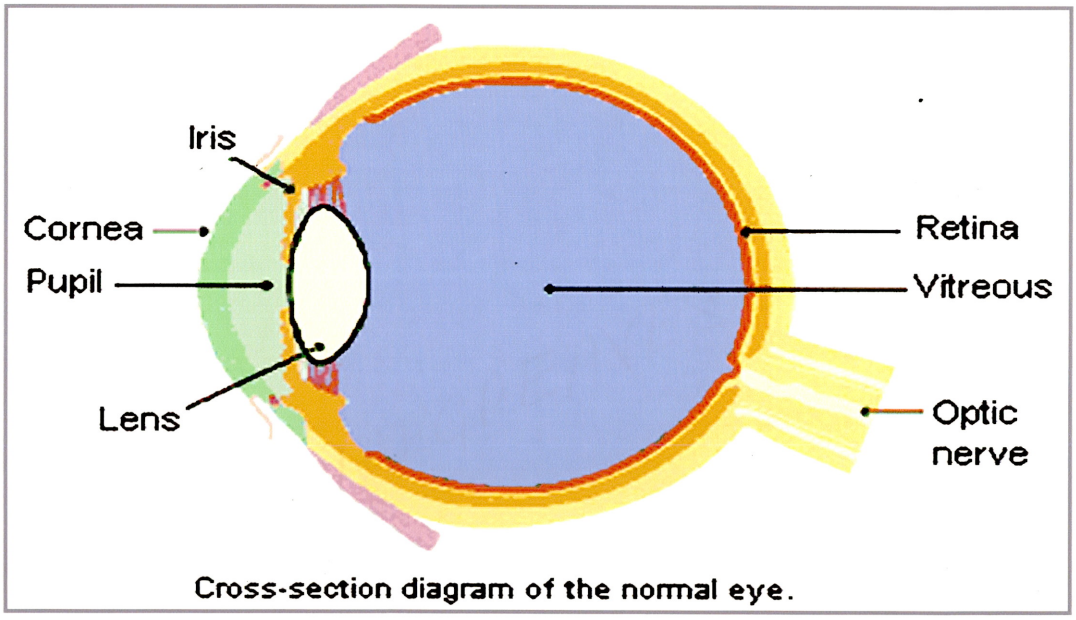


Figure 1: Anatomy of the human eye (courtesy of http://www.moorfields.org.uk).

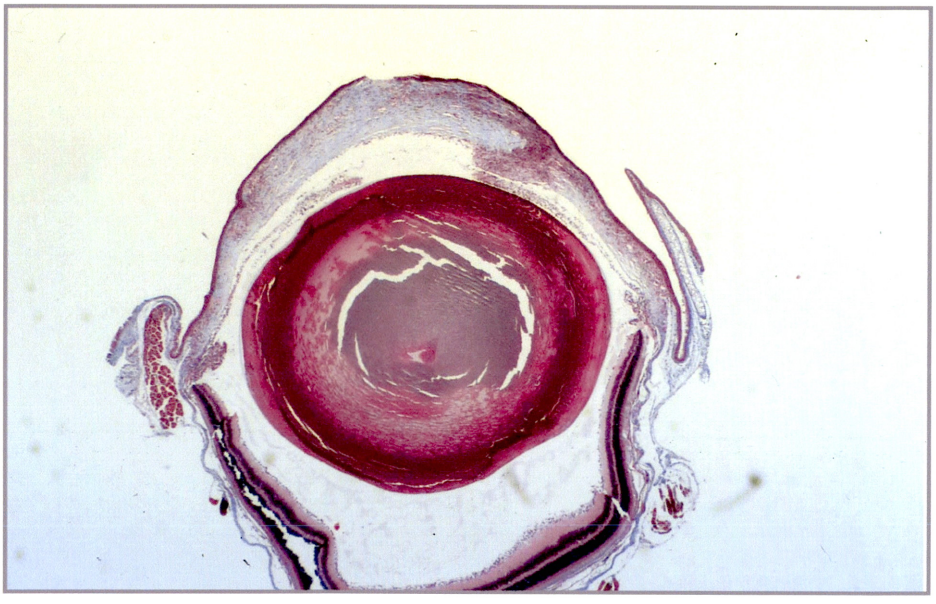


Figure 2: Cross-section of a normal mouse eye (Masson staining) (x50) (courtesy of Dr Navid Ardjomand).

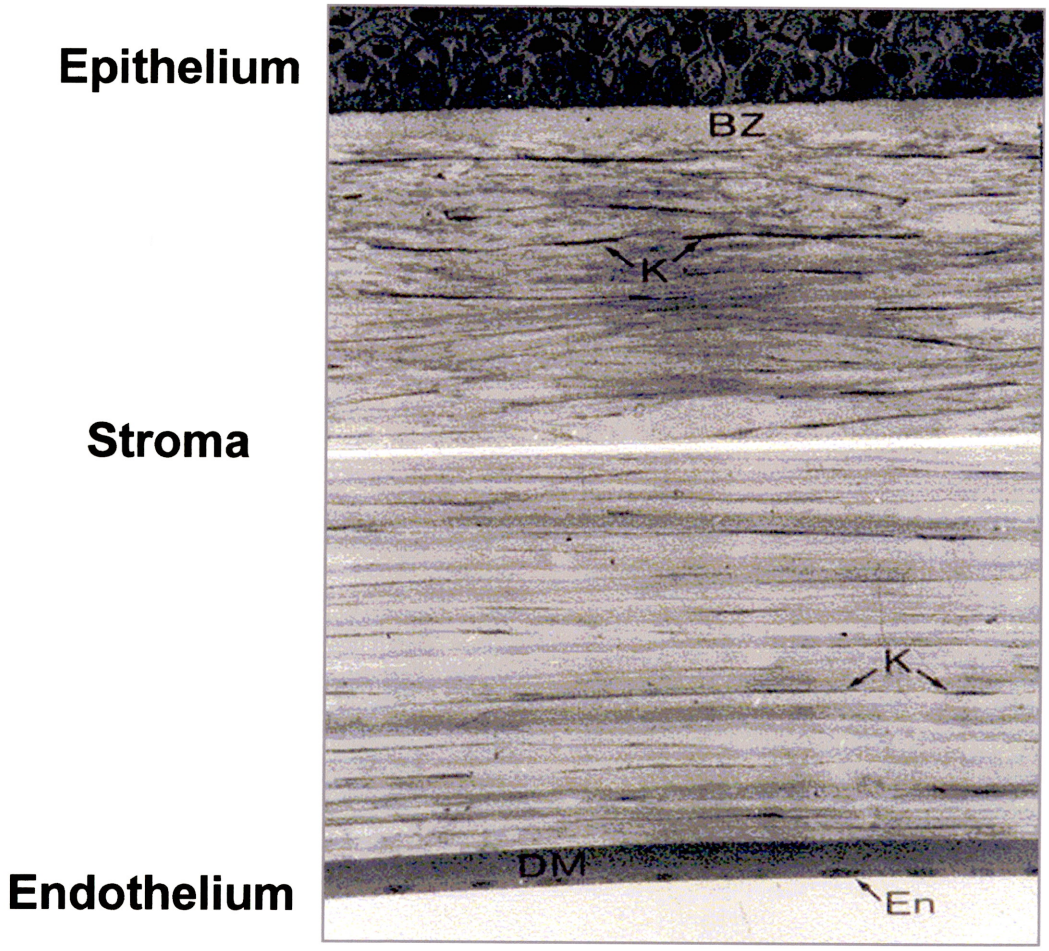


Figure 3: Histological structure of the cornea (adapted from Bron et al., 1997).
BZ= Bowman's Zone, K=Keratocytes, DM= Descemet's membrane and En=Endothelium

The second epithelial layer (also called "wing" or "umbrella" cells) and the next two or three layers are polyhedral cells, whereas the most superficial cells are mostly hexagonal (Bron *et al.*, 1997).

It was first thought that the division and then migration of basal epithelial cells ensured the renewal of epithelial cells. However, it is now recognised that the centripetal migration of cells derived from stem cells present in the nearby limbal basal layer ensures rapid repair of the damaged corneal epithelium in health (Forrester *et al.*, 1996). In cases of total epithelial and limbus loss (as in chemical injury of the ocular surface), the adjacent conjunctival epithelium is capable of resurfacing the whole cornea, though at a reduced rate; this epithelial phenotype is significantly less transparent than corneal epithelium and severe visual loss is the consequence (Bron *et al.*, 1997).

1.1.1.2- Bowman's layer

The Bowman's layer or anterior limiting lamina is an acellular structure (8-14 μm thick) immediately subjacent to the basal lamina of the epithelium. It constitutes of randomly arranged collagen fibrils that merge with the fibrils of the anterior stroma (Bron *et al.*, 1997).

1.1.1.3- Stroma

The stroma makes up about 90% of the corneal thickness (about 540 μm in the centre) and is mainly composed of regularly arranged type I collagen fibrils, parallel to each other and to the corneal surface. This precise organisation ensures the transparency of the cornea and is highly dependent on the state of hydration.

The normal stroma contains a relatively small number of cells, the keratocytes that lie between collagen fibers. Keratocytes have long flattened nuclei, stellate processes and are responsible for the synthesis during development, and then maintenance, of stromal collagen. When a small amount of stromal repair is needed, keratocytes become activated, migrate and transform into fibroblasts, finally leading to the formation of scar tissue (Bron *et al.*, 1997).

1.1.1.4- Descemet's membrane

As opposed to the Bowman's layer that is a modified zone of the anterior stroma, the Descemet's membrane or posterior limiting layer is well defined from the stroma. It separates the latter from the corneal endothelium. The Descemet's membrane is an 8-12 μm basement membrane composed of a fine latticework of collagen fibrils. It is rich in basement glycoproteins, laminin and collagen, especially types IV, V, VI and VIII and is capable of regeneration in case of injury (Bron *et al.*, 1997).

1.1.1.5- Corneal endothelium

The corneal endothelium (figure 4), directly in contact with the aqueous humour, is constituted of a single uninterrupted mosaic (4 to 6 μm) of polygonal and hexagonal cells, with a low regenerative rate. These cells are not of vascular but neuroectodermal origin. There are approximately 350 000 cells per cornea (3-4000 cells/mm^2) at birth, falling to 2500 cells/mm^2 in middle age and 2000 per mm^2 in old age (Waring *et al.*, 1982). A study by Bourne *et al.* estimated the endothelial cell loss rate at 0.6 +/- 0.5% per year in normal human cornea (Bourne *et al.*, 1997).

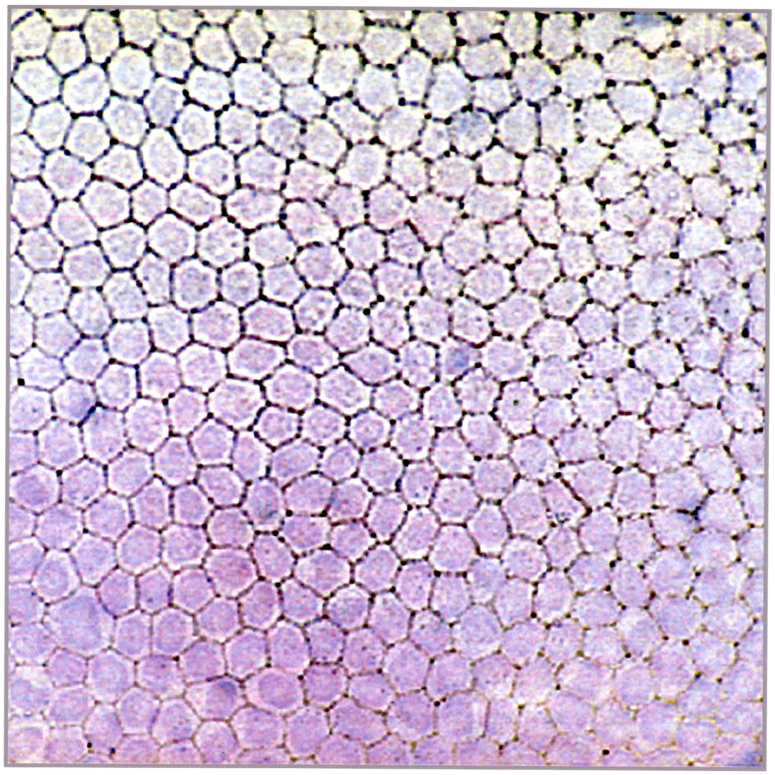


Figure 4: Mosaic of polygonal and hexagonal cells in the guinea pig corneal endothelium (x1000) (courtesy of Dr D.F.P. Larkin).

Lost cells are not replaced in human but the overall structure is maintained by spreading of adjacent cells, leading to a less homogeneous shape (polymegethism) of the endothelial cells.

The corneal endothelium has two functions. First, the endothelium acts as a barrier between the stroma and the aqueous humour. This barrier is leaky and allows penetration of small molecules, including oxygen and nutrients for the entire cornea (glucose, amino acids), from the anterior chamber of the eye to intercellular spaces. The second role of the endothelium is to pump water out of the stroma to maintain corneal deturgescence. Both the leak rate and the metabolic pump rate are in equilibrium so that the stromal content of water is always constant (78%). Damage to the endothelium, resulting in a cell density below 800 cells/mm^2, will affect the barrier function with water diffusing into the stroma leading to a thickening of the cornea (oedema) and loss of its transparency (Waring *et al.*, 1982).

1.1.2- Immune privilege

Corneal grafting is the most common and the most successful solid organ transplantation procedure in humans. In non-vascularised beds, the long-term (10 years) acceptance of allografts is about 60% (Williams *et al.*, 1997). Furthermore, this is achieved without HLA matching and with only a topical administration of immunosuppressive drugs. This high acceptance rate of corneal allografts is in part the result of immune privilege: this refers to the active phenomenon in which a graft of foreign tissue that would be rejected promptly if placed in a conventional site, enjoys prolonged (perhaps even permanent) survival when placed in a privileged site (Niederkorn *et al.*, 1990). Privileged sites include the eye (anterior chamber, corneal

stroma, and vitreous cavity), the brain, the maternal-foetal interface, testis and ovaries, the liver and the hamster cheek pouch. In addition, cornea is a privileged immune tissue (Hori *et al.*, 2000). In the case of corneal transplantation, privilege therefore arises from two aspects: it involves the transplantation of a privileged tissue, the cornea, into a privileged site, the anterior chamber of the eye.

The ocular immune privilege is the result of several protective factors that can be divided into the passive mechanisms that involve the ignorance of the antigen or its shedding from the immune system, and the active mechanisms that inhibit or deviate the normal immune response.

1.1.2.1- Passive mechanisms responsible for immune privilege in the eye

a) Blood-ocular barrier

The anterior chamber owes its privileged status to the blood-ocular barrier. In the eye, the blood supply is restricted to vessels of the ciliary bodies and of the retina. These vessels have many tight junctions that prevent penetration of cells and therefore constitute, respectively, the blood-aqueous barrier and the blood-retinal barrier.

Together, these two barriers form the blood-ocular barrier, which shields the anterior chamber from immune surveillance (Streilein *et al.*, 1993) by preventing access of immune response mediators (e.g. antibodies, T cells) to the eye.

b) Avascularity

The absence of both lymph and blood vessels of the cornea is thought to prevent the escape of alloantigens to the nearby lymphatic tissues, therefore blocking the

afferent arm of the immune response. As early as 1948, Medawar demonstrated that a skin graft transplanted to the anterior chamber of the eye of a specifically immunised rabbit, was destroyed only if it was vascularised (Medawar *et al.*, 1948). In addition, prevascularisation of the corneal bed has been shown to increase corneal graft failure (Pleyer *et al.*, 1992; Williams *et al.*, 1992).

c) Absence of APC

Many studies have examined the expression of Major Histocompatibility Complex (MHC) molecules on cornea (Fujikawa *et al.*, 1982; Whitsett and Stulting, 1984; Williams *et al.*, 1985). MHC class I antigens have been found on all corneal cell types (epithelium, stroma and endothelium); however, no class II antigen was detectable. Only a small number of HLA-DR^+ Langerhans cells (LC) were detected in corneal epithelium, near the limbus. This number was increased in inflammation and vascularisation (Williams *et al.*, 1985). This finding associated to the fact that professional APC (Antigen Presenting Cells) are characterised by a high level of MHC class II expression has led to the conclusion that the cornea was devoid of APC or "passenger cells". Indeed, the current dogma holds that the absence of LC in the central cornea (the only part used during transplantation) contributes to the protection of the allograft.

However, most recent information is that, contrary to what had previously been assumed, there are $CD11c^+$ MHC class II^- DCs in the epithelium and the anterior stroma of the normal mouse central cornea (Hamrah *et al.*, 2002; Hamrah *et al.*, 2003; Liu *et al.*, 2002) and MHC class II^- macrophages in the posterior stroma (Brissette-Storkus *et al.*, 2002). In addition, DCs were found capable of expressing

MHC class II antigens after transplantation and of migrating directly to the draining lymph nodes of the host (Liu *et al.*, 2002).

Alloantigens expressed on a graft can be recognised by recipient T cells via two distinct pathways: in the direct pathway, the natural antigen (not processed) is presented to recipient T cells by the donor MHC expressed on donor APC. The indirect pathway, however, involves the processing of the alloantigen by host APC and presentation via the recipient MHC to recipient T cells (figure 5). Before resident DCs and macrophages were identified, the general belief was that in corneal transplantation, recipient T cells were mainly sensitised by the indirect pathway. The recent findings suggest that both pathways of allorecognition might occur in corneal transplantation. It is also suggested that immune privilege might arise, not because of a lack of "passengers cells" in the central cornea but thanks to an active inhibition of corneal DC maturation (Hamrah *et al.*, 2002).

1.1.2.2- Active mechanisms responsible for immune privilege in the eye

a) Fas-ligand expression

Constitutive expression of CD95L (Fas-Ligand) on the corneal epithelium and endothelium is critical to its immune privileged status. CD95 or Fas is expressed on many cells but particularly on activated T cells. Interaction between CD95 on T cells and its ligand induces apoptosis of the $CD95^+$ cells. This mechanism has been shown to be involved in the protection of cornea from invading inflammatory cells (activated T cells, macrophages).

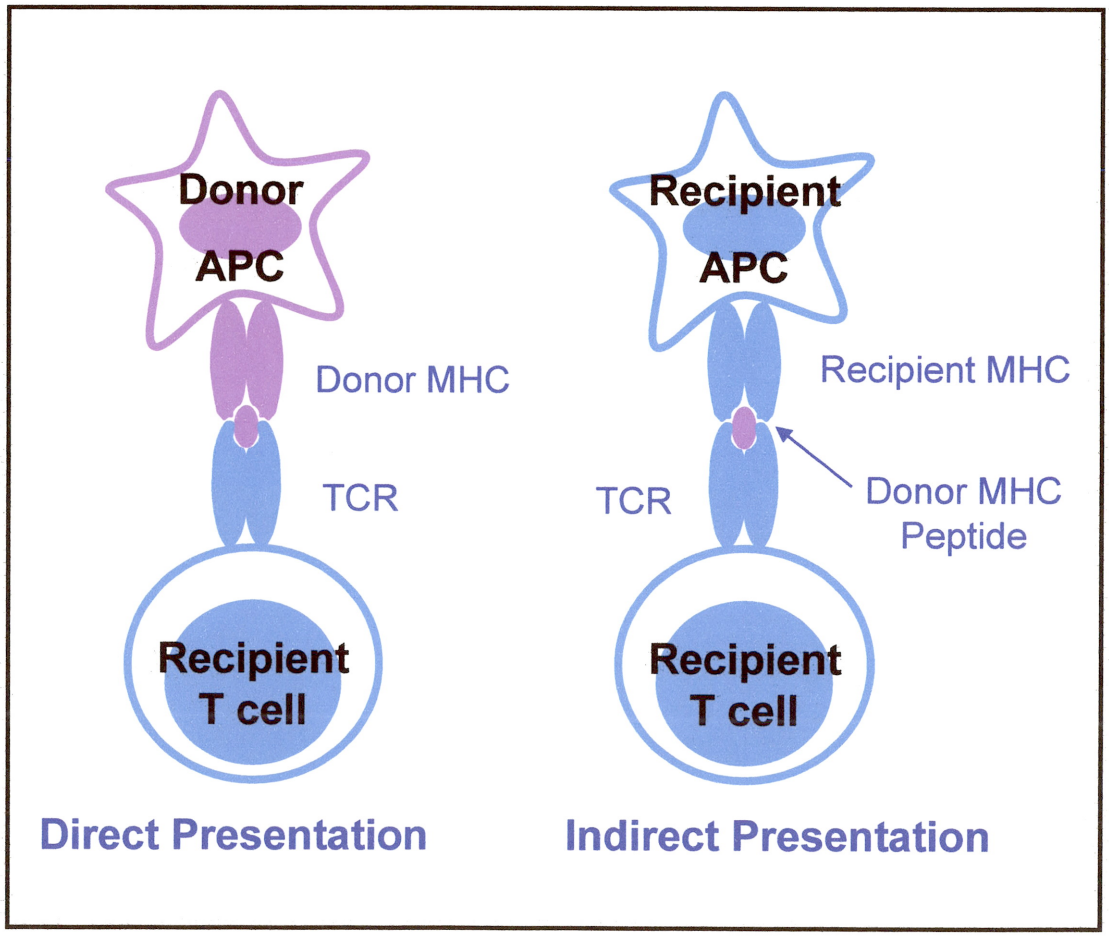


Figure 5: Direct/Indirect Presentation.
In the direct pathway of allorecognition, host or recipient T cells recognise determinant peptides of the intact donor MHC molecules displayed on the surface of donor cells. However, in the indirect pathway, donor MHC molecules are processed and presented to recipient T cells as peptides by recipient MHC molecules at the surface of recipient APC. This response is in the latter case restricted to the host rather than donor MHC.

Using a mouse corneal orthotopic allograft model, Stuart and al reported a survival rate of 45%. However, FasL$^-$ grafts (from B6-*gld* mice), or normal grafts transplanted to Fas$^-$ mice (B6-*gld*), were all rejected (Stuart *et al.*, 1997). Similarly, whereas both syngeneic and allogeneic corneal grafts survived almost indefinitely beneath the kidney capsule, transplants from Fas-deficient mice showed acute rejection (Hori *et al.*, 2000).

In some cases however, Fas-Ligand (FasL) expression was found to facilitate rejection by triggering a neutrophil mediated inflammatory response. While a soluble form of Fas-Ligand (entire extracellular domain) was associated with the recruitment of human neutrophils *in vitro* (Ottonello *et al.*, 1999), it was actually shown by Hohlbaum and co-workers that the natural form of soluble Fas-Ligand (sFasL) (matrix metalloproteinase-cleaved) suppressed the inflammatory response elicited by membrane-bound FasL *in vivo* (Hohlbaum *et al.*, 2000). This suggests a fine balance between the inflammatory properties of the membrane-bound FasL, which also possesses a cytotoxic activity (apoptosis), and the anti-inflammatory properties of the soluble form of FasL.

b) Immunosuppressive agents

Immune privilege is also the result of an immunosuppressive microenvironment. Cousins and co-workers reported high concentrations of transforming growth factor-beta (TGFβ) in normal aqueous humour. The β2 isoform is predominant and plays an important role in inhibiting lymphocyte activation and proliferation (Cousins *et al.*, 1991). Dekaris *et al.* also found that among patients undergoing keratoplasty, those with inflamed eyes had lower TGFβ2 levels than those with non-inflamed or normal

control eyes. In their study, levels of TGFβ2 lower than 1500 pg/ml were associated with poor prognosis of corneal allograft acceptance (Dekaris *et al.*, 2001).

IL-1 receptor antagonist (IL-1RA) is a naturally occurring IL-1 isoform secreted by cornea, also thought to have a suppressive effect: in rats, Torres and co-workers reported constitutive expression of the cytokine in non-grafted, contra lateral eyes, as well as in autografts and allografts (Torres *et al.*, 1996). Dana and co-workers, however, significantly improved the corneal allograft survival rate in mice treated topically with IL-1RA (Dana *et al.*, 1997) and the same team restored the capacity for inducing ACAID (see below) to soluble antigen (but not donor-derived alloantigen) in mouse corneal allografts, using a similar topical treatment with IL-1RA (Yamada *et al.*, 2000).

Other anti-inflammatory or immunosuppressive factors, including the α-melanocyte stimulating hormone (α-MSH), somatastatin, or thrombospondin-1 contribute to the inhibition or alteration of activated T cells and APC properties (Streilein *et al.*, 1993; Streilein *et al.*, 2002).

c) ACAID

Finally, but of crucial importance, is the anterior chamber-associated immune deviation or ACAID. This refers to a unique pattern of immune responses elicited by antigen injection in the anterior chamber of the eye, in which cellular immunity is down regulated to the advantage of humoral immunity: antigen-specific delayed-type hypersensibility (DTH) and complement-fixing antibodies are selectively suppressed whereas the production of alloantibodies is increased (Streilein *et al.*, 1993; Li *et al.*, 1996). Li *et al.* showed that ACAID was characterised by IL-10 but no IL-2, IFNγ or

IL-4 cytokine production. This is suggestive of a T-helper type 2 (Th2) dominated immune phenotype that cross regulates a Th1 cell population (Li *et al.*, 1996). Streilein and co-workers have proposed a hypothesis to try and explain the induction of ACAID. In the early ocular phase, the antigen is captured by ocular APC (from iris pigment epithelium, or ciliary bodies) under the influence of the immunosuppressive intraocular environment. These APC migrate to the blood stream via the trabecular meshwork and then specifically traffic to the marginal zone of the spleen. In the splenic phase, these APC secrete MIP-2 (macrophage inflammatory protein), a chemoattractant for CXCR2-bearing NK T cells and additional APC, which in turn create a novel immunomodulatory environment composed of TGFβ and IL-10. Finally, the third phase of ACAID induction sees the generation of regulatory T cells, T cells attracted to the site that see the ocular antigen in an immunomodulatory environment and differentiate into mediators of ACAID (Streilein *et al.*, 2002).

1.1.3- Clinical aspects

1.1.3.1- Indications for transplantation

Corneal transplantation, also known as corneal grafting or keratoplasty, refers to the surgical procedure in which abnormal host cornea is excised and replaced by a healthy donor cornea. The procedure may involve partial (lamellar keratoplasty) or full thickness grafting (penetrating keratoplasty).

Corneal diseases are a major cause of blindness worldwide. In many cases, transplantation is the only treatment. Therefore, most corneal allografts are performed to improve optical qualities of the cornea and thus improve vision. The

Corneal Transplant Follow up Study (CTFS) reported that 77% of the 4650 grafts registered between July 1987 and June 1991 were performed for optical reasons alone (Vail *et al.*, 1993). Some allografts are purely therapeutic (5.7% in the study above) with the aim of treating an infection disease unresponsive to conventional antimicrobial or antiviral therapy. Allografts are also performed to reconstruct or preserve corneal anatomy in eyes with severe structural changes (e.g. stromal thinning). Finally, a minority of corneal allografts is performed for cosmetic reasons.

The most frequent indication for corneal transplant by diagnosis include bullous keratopathy (endothelial failure), inflammation and keratoconus (Coster and Williams, 1992; Vail *et al.*, 1993; Inoue *et al.*, 2000; Maeno *et al.*, 2000) which, for example, accounted for 38%, 26% and 20% respectively in the Vail *et al.* study (Vail *et al.*, 1993).

1.1.3.2- Success

Corneal grafting is a common surgical procedure with more than 40,000 grafts performed in the United States and Canada in 1990 (Boisjoly *et al.*, 1993). Nonetheless and despite immune privilege, the long term outcome in corneal allotransplantation is paradoxical: while graft survival rate after 1, 5 and 10 years is as high as 90%, 74% and 62% respectively for low-risk groups (diagnosis of keratoconus, primary or secondary endothelial failure), figures for high-risk groups (acquired conditions that led to corneal inflammation or vascularisation) fall to 75%, 47% and less than 35% respectively (Williams *et al.*, 1997).

1.1.3.3- Graft failure

Risk factors associated with corneal allograft failure include: indications other than keratoconus or corneal dystrophy, a failed previous graft in the same eye, prior glaucoma or uveitis, inflammation at the time of grafting or oversized donor cornea (Australian Corneal Graft Registry (ACGR)) (Williams *et al.*, 1992). 'High risk' patients also include children. For instance, in one study analysing graft survival in infants (less than 13 months) with congenital corneal opacity, the overall survival rate for first grafts was only 61% at one year while the figures for subsequent grafts was even worse (Comer *et al.*, 2001).

Allograft rejection is the most common cause of graft failure. Combined data from both studies (CTFS and ACGR) show that rejection caused 32% of graft failures. Endothelial decompensation and infection caused respectively 20% and 14% of graft failures whereas technical reasons accounted for only 7% of failures (Waldock and Cook, 2000).

1.1.3.4- Corneal allograft rejection

Corneal allograft rejection is the most frequent cause for transplant failure. Alldrege and Krachmer (Alldredge and Krachmer, 1981) showed that rejection occurs at an average time of 8 months, however the same authors also reported an endothelial rejection as late as 9 years after graft.

Khodadoust and Silverstein firstly described the three types of corneal rejection, each affecting a different structure of the cornea, in a rabbit model (Khodadoust and Silverstein, 1969). Endothelial rejection is the most frequent in both low and high-risk groups (Pleyer *et al.*, 1992). It is also the most important clinically as it is

irreversible and leads to opacity of the cornea. Early signs of endothelial rejection include aqueous cells and small keratic precipitates. Rejection lines (aggregates of leukocytes destroying endothelial cells) are only seen in established rejection and are associated with stromal oedema. Epithelial rejection lines and subepithelial infiltrates indicate respectively an epithelial and a stromal rejection. Epithelial rejection occurs more often in high risk (10.5%) than in low-risk eyes (5.2%) (Pleyer *et al.*, 1992).

Most of the available information on the pathology of corneal allograft has been obtained from animal studies. Larkin *et al.*, in a study of rat corneal allograft rejection, observed an infiltration of T cells, macrophages, neutrophils and natural killer (NK) cells in both the aqueous humour and the rejected graft (epithelium, stroma or aggregated cells on endothelium). Most infiltrated cells expressed MHC class II antigens and a smaller number IL-2 receptor (IL2R). Interferon gamma (IFNγ) was also detected in the anterior stroma of the graft and in the recipient (peripheral) cornea (Larkin *et al.*, 1997b). These data are consistent with those of Sano *et al.*, who reported increased amounts of Interleukin-2 (IL-2) and IFNγ in rejected allografts in mice (Sano *et al.*, 1998). IFNγ is mainly produced by activated T cells and NK cells, and is responsible for macrophage activation and class II up-regulation, necessary for $CD4^+$ T cell mediated response (figure 6). Although at the time of grafting, no difference in IFNγ protein expression was detected in the aqueous humour of human diseased and control eyes (Dekaris *et al.*, 2001), a recent study, supported a role for IFNγ in corneal allograft rejection in human, as 10 out of 13 patients suffering from allograft rejection beneficiated from a treatment with anti

human IFNγ antibody-derived Fab. The same result was obtained in the 3 other patients after 3 courses of treatment (Skurkovich *et al.*, 2002).

Interleukin 1α (IL-1α) and Tumour Necrosis Factor alpha (TNFα) (proinflammatory cytokines) were detected in both syngeneic and allogeneic grafts in a rat (Larkin *et al.*, 1997b) and a mouse model (Sano *et al.*, 1998), whereas pulsatile increases in TNFα levels were also detected by bioassay in the aqueous humour of rabbit recipients of corneal allografts but not autografts (Rayner *et al.*, 2000).

In this model, Rayner *et al.* demonstrated that peaks of TNFα protein expression did not correlate with onset of rejection but that elevated mRNA for TNFα was detected before and during rejection of the allografts. TNFα is secreted by macrophages, monocytes, neutrophils, NK cells and $CD4^+$ T cells. It is a potent chemoattractant for neutrophils, that plays a role in macrophage activation, and in MHC class I and II up-regulation on leukocytes and lymphocytes progenitors (figure 7). IL-1 is mainly produced by monocytes but also by activated macrophages, peripheral neutrophils, B and T lymphocytes and endothelial cells. There are two forms of IL-1; IL-1β is the major form detected in humans, while IL-1α is predominant in mice. Both forms bind to the same receptor and share similar biological activities (figure 8): activation of lymphocytes (B and T helper), chemotactic action for leukocytes, promotion of monocyte and neutrophil adhesion, and stimulation of neovascularisation.

In a human study, the presence of TNFβ was associated with increased risk of rejection in inflamed eyes. In TNFβ negative patients, grafts were mainly accepted even among the "high risk" group of patients (Dekaris *et al.*, 2001).

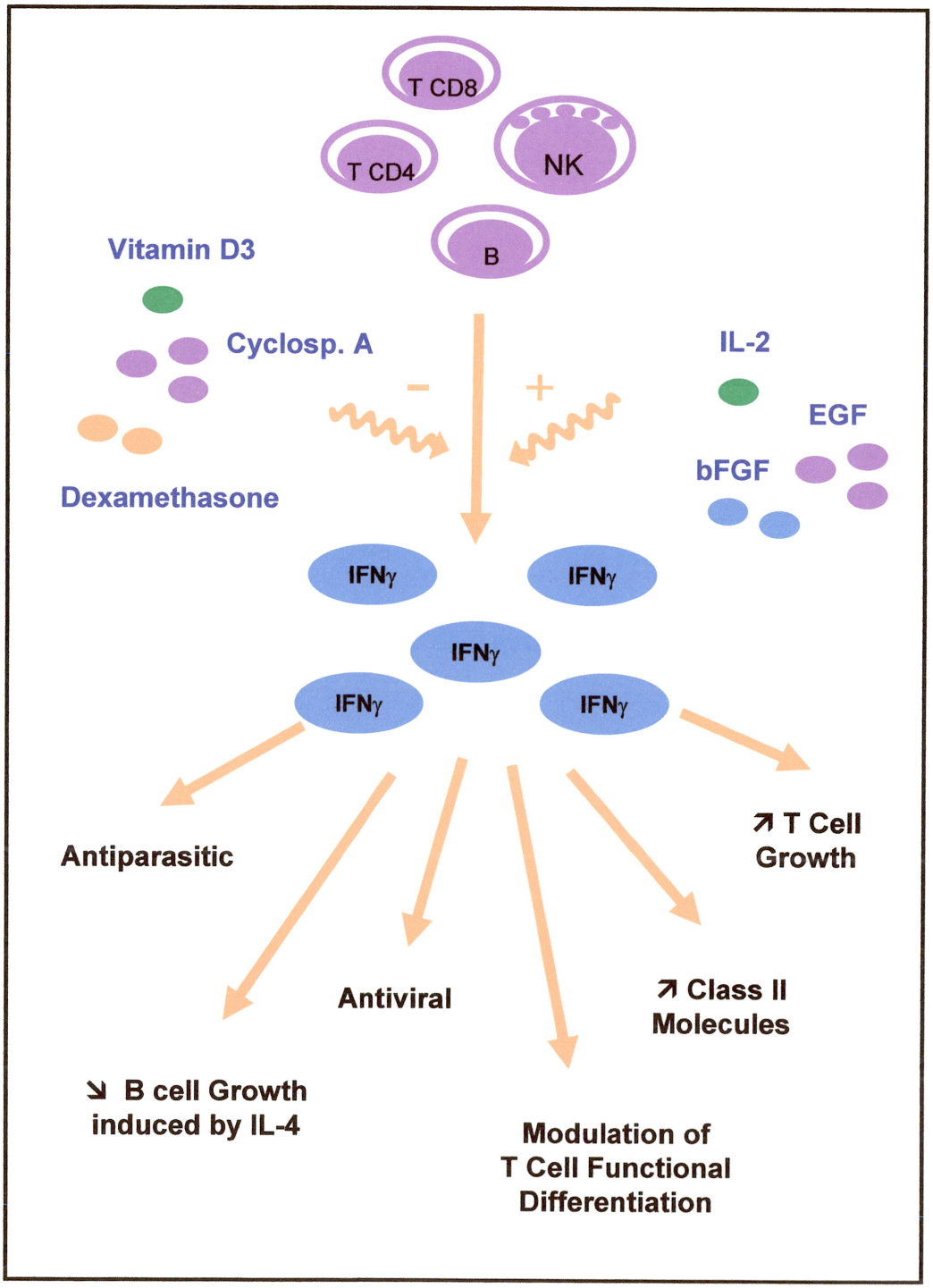


Figure 6: Representative biological activities of IFNγ.

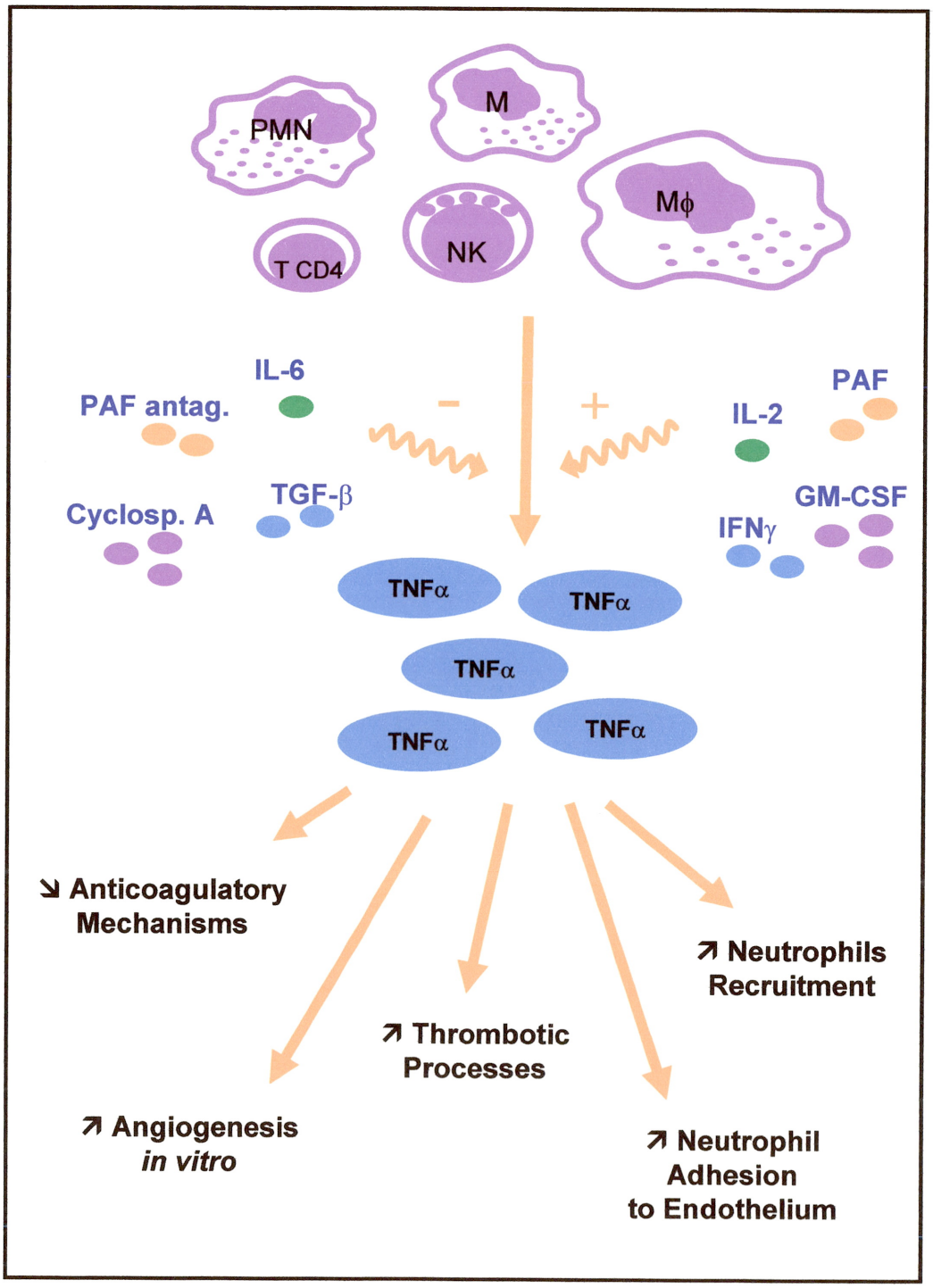


Figure 7: Representative biological activities of TNFα.

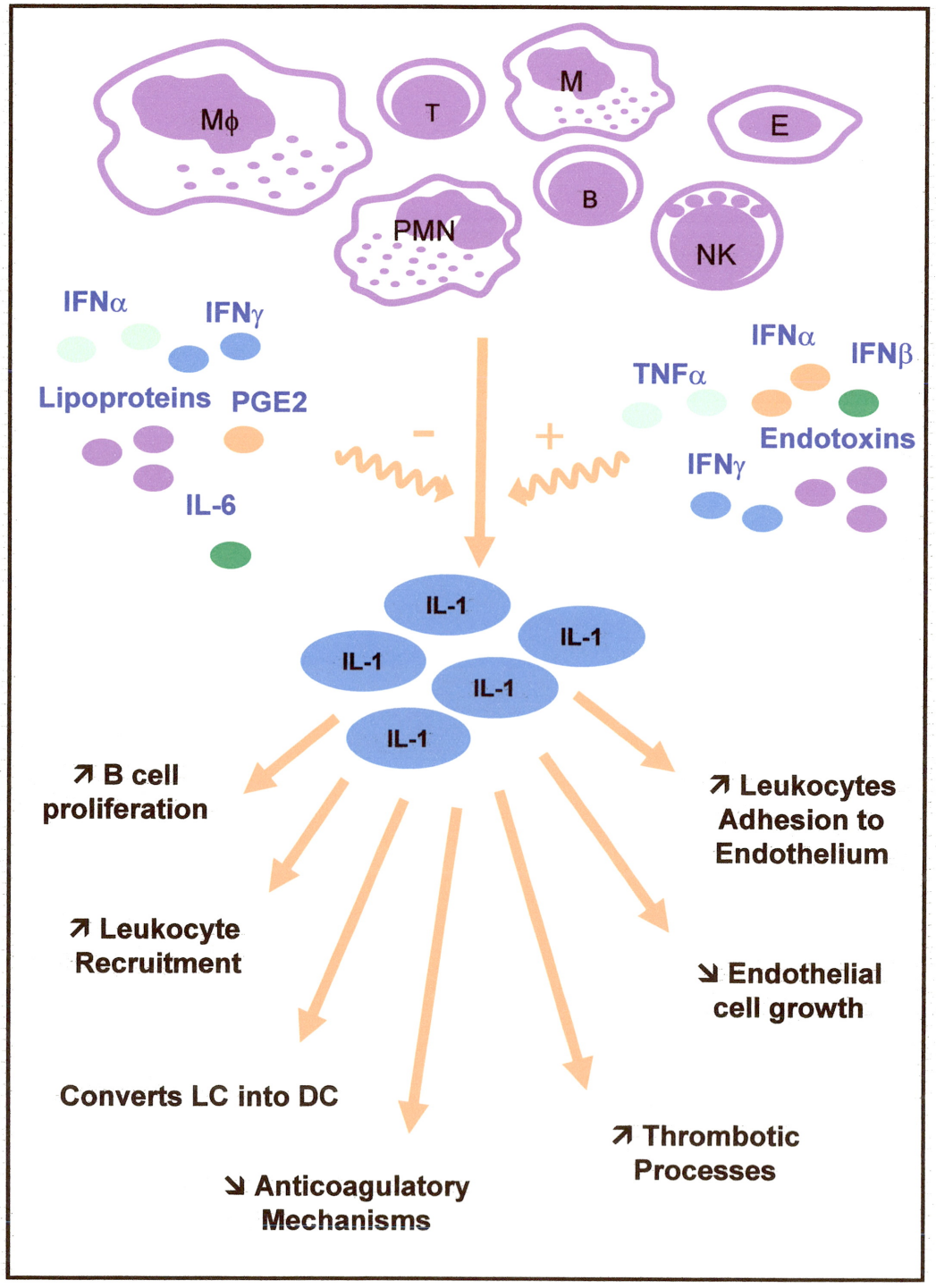


Figure 8: Representative biological activities of IL-1α.

In rats, Torres *et al.* also reported the presence of mRNA for IL-1α and TNFα in both syngeneic and allogeneic settings, as well as IL-6 and IL-10. However, they noted a decrease in the mRNA expression for these cytokines after 3 to 7 postoperative days (POD) in syngeneic grafts, whereas levels remained high or even increased until rejection in allografts (Torres *et al.*, 1996).

Similarly, in a mouse model, Zhu *et al.* reported an early phase where TNFα and IL-1α proteins were detected in allografts and to a lesser extent in isografts. At POD 7, these cytokines levels remained high or increased in allografts but decreased in syngeneic grafts (Zhu *et al.*, 1999).

King *et al.* also identified two phases in cytokines and chemokines expression in a Brown Norway to Lewis rat model, with an increase in IL-1β, IL-6, IL-10, IL12, RANTES (regulated upon activation of normal T cell expressed and secreted), monocyte chemoattractant protein MCP-1, and macrophage inducible proteins MIP-1α, MIP-1β, and MIP-2 until POD9, both in allo- and isografts, followed by a decrease in syngeneic graft or a further increase in allografts (King *et al.*, 2000). This early phase corresponds to the response to the transplantation process (surgical trauma) and leads to angiogenesis and migration/activation of inflammatory cells. Yamagami *et al.* also demonstrated a significant overexpression of RANTES, MIP-1α, MIP-1β, and MIP-2 and MCP mRNA in rejected allografts of C57Bl6, and to a lesser extent, of BALB/c mice corneas (Yamagami *et al.*, 1999). Noticeably, mRNA for IFNγ inducible protein IP-10, a Th1 associated chemokine, was found in high rejecting C57Bl6 corneas but not in low rejecting BALB/c corneas (Yamagami *et al.*, 1999).

Sano *et al.* and other studies demonstrated an important role of proinflammatory cytokines in the recognition of alloantigens and showed that Th1-helper cells rather than Th2 type are involved in the rejection process (Sano *et al.*, 1998). This was confirmed by Yamada *et al.* who observed an acceptance of corneal allografts in a model of Th2-biased mice (Yamada *et al.*, 1999).

This evidence and that of other studies (Joo *et al.*, 1995; Hegde and Niederkorn, 2000) show that the mechanism of graft destruction is more likely to involve a Delayed Type Hypersensitivity (DTH) rather than a cytotoxic T lymphocyte (CTL) response. However, contradictory results have been obtained and the role of $CD8^+$ CTLs in allograft rejection is not totally ruled out yet (Peeler *et al.*, 1985; Callanan *et al.*, 1988).

The nature of the Antigen Presenting Cells (APC) initiating corneal graft rejection is still unclear. A study in human from Filipec *et al.* suggests a role for dendritic cells (DC) in the presentation of alloantigens to T cells. In this immunohistochemical analysis of cellular infiltrates in rejecting grafts, DC (CD1a/MHC class II double positive cells) were detected in the deep epithelial layer and in the corneal stroma of rejected grafts (both non-inflamed and inflamed). There was however no evidence of DC in the control corneal tissue (Kuffova *et al.*, 1999).

It is now quite widely established that minor (non-MHC) rather than major histocompatibility (MHC) molecules play an important role in corneal allograft rejection. Nonetheless, the necessity and usefulness of MHC class I and class II matching is not completely defined yet (Sonoda and Streilein, 1992; Nicholls, 1996; Volker-Dieben *et al.*, 2000).

1.2- Adhesion molecules

1.2.1- Cell adhesion molecules (CAMs)

The last two decades has seen a vast increase in our understanding of cell adhesion molecules. Their critical role in many biological processes, including the immune and inflammation responses is now widely recognised. These cell surface proteins play a key role in antigen presentation, mediate the recruitment and extravasation of leukocytes to the site of inflammation, their migration through the extracellular matrix, and are finally involved in the interactions between effectors and target cells. Cell adhesion molecules mediate homotypic or heterotypic interactions between cells from the same or different origin. In addition, at the molecular level, interactions may occur in a homotypic (e.g. CD31 to CD31) or heterotypic manner (e.g. integrin to Ig-like molecule) (figure 9). Using their structural characteristics, cell adhesion molecules have been classified in four families, namely the cadherin family, the selectin family, the immunoglobulin-like superfamily (IgSF), and the integrin family. Some other molecules not classified among these families also emerge as potent adhesion molecules, as for instance the VAP-1 molecule, a cell surface amino oxidase. The following describes some families of adhesion molecules and some chosen members relevant for the study but is in no way an exhaustive list, nor can it be completely up to date as new adhesion molecules are discovered all the time. Table 1 (section 1.2.3-) gives more details about the adhesion molecules investigated in this study.

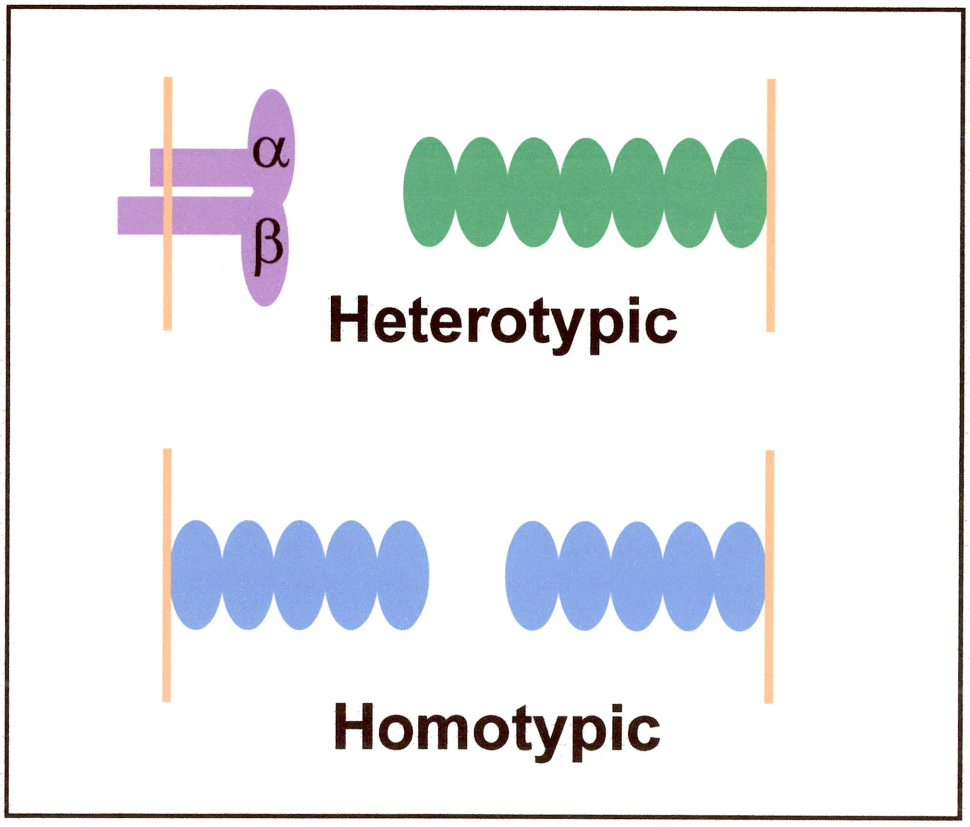


Figure 9: Homotypic and heterotypic molecular interactions.

1.2.1.1- The selectin family

To date, this family (figure 10) is composed of only three members, named after the cell-type on which they were first identified: L-Selectin (lymphocyte), E-Selectin (endothelium) and P-Selectin (platelet). Selectins are type I transmembrane glycoproteins containing an N-terminal lectin-like domain, an epidermal growth factor (EGF)-type domain followed by two (L-selectin), six (E-Selectin) or nine (P-Selectin) Short Consensus Repeat (SCR) motifs, a transmembrane domain and a short cytoplasmic tail. In P-Selectin, the cytoplasmic tail controls the storage of the adhesion molecule in granules. The N- terminus domain shares homology with the carbohydrate recognition domain found in calcium-dependent (C-type) lectins. This lectin domain is directly responsible for the interaction with cell surface lactosaminoglycans that possess a fucosylated, sialylated structure (Sialyl Lewis^x or Sle^x) (Bevilacqua, 1993; McEver, 1994; Varki, 1994). Selectins mediate the initial events of the cascade that leads to leukocyte recruitment to the site of inflammation.

a) L-Selectin

L-Selectin is found on most circulating lymphocytes, neutrophils and monocytes and, unlike the two others selectins, is expressed constitutively on the cell surface. L-Selectin activity is rapidly and transiently increased upon lymphocyte and neutrophil activation, then the molecule is shed from the cell surface (Bevilacqua, 1993).

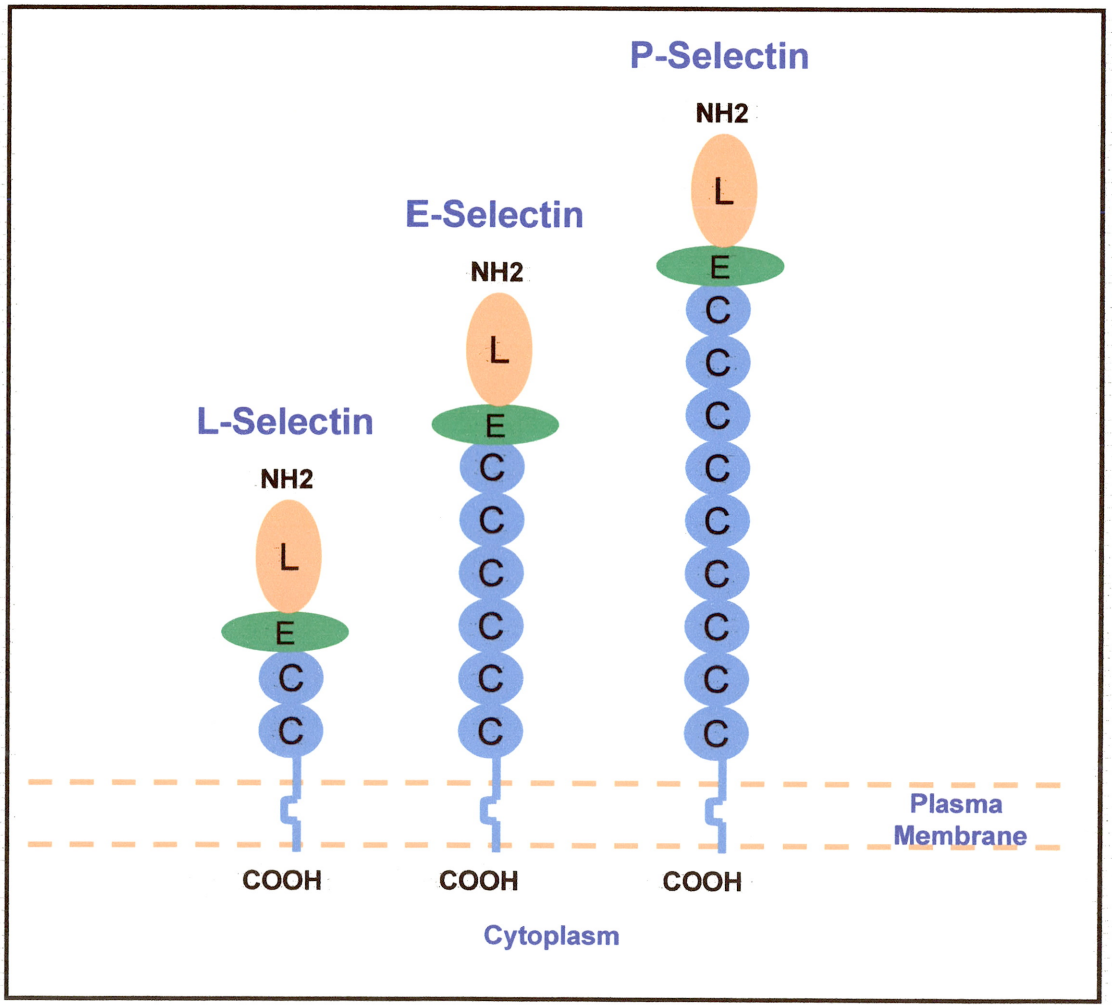


Figure 10: The selectin family.
Structurally, members of this family present an N-terminal lectin domain (L), an EGF (epidermal growth factor) -type domain (E), two to nine complement regulatory repeats (C) and a short cytoplasmic tail.

b) E-Selectin

E-Selectin is exclusively expressed on activated endothelium: it is rapidly synthesised and expressed on the surface of endothelial cells in response to LPS, IL-1, or TNFα stimulation. IFNγ does not induce E-Selectin expression but is however capable of prolonging the effect of TNFα (Bevilacqua, 1993). *In vitro*, E-Selectin reaches maximal expression after 4 to 6 hours and returns to its basal level after 24-48 hours (Bevilacqua, 1993).

c) P-Selectin

P-Selectin is constitutively expressed in megacaryocytes, platelets, and endothelial cells but is stored in α- and dense-granules (in platelets) and in Weibel-Palade bodies (in endothelial cells) in resting cells. Upon cellular activation by thrombin, histamine, or H_2O_2, P-Selectin is rapidly (within minutes) transported to the cell surface. Some studies report that de novo synthesis of P-Selectin can also occur following stimulation by TNFα or endotoxin (Hahne *et al.*, 1993).

1.2.1.2- The immunoglobulin (Ig) superfamily

Despite a wide variety in structure and function, all the members of the immunoglobulin superfamily IgSF (figure 11) have been grouped together because of the common immunoglobulin-like domain (two cysteines separated by 55 to 75 amino acids) they contain.

This family is very wide but the key members are the intercellular adhesion molecules (ICAM-1, ICAM-2 and ICAM-3), closely related in structure and function (ICAM-4 and -5 also recently identified), the vascular cell endothelial molecule

(VCAM-1 or CD106) and the platelet endothelial cell adhesion molecule (PECAM-1 or CD31). LFA-2 (CD2) binds to LFA-3 on leucocytes, endothelial and epithelial cells, and the neural cell adhesion molecule (NCAM) is particularly important during the development of the nervous system (Pigott and Power, 1993). The MHC class I and II molecules are also non-classical members of the family. Their role in antigen presentation is widely established and their implication in adhesion has been reported in several studies (Masuyama *et al.*, 1986; Pober and Cotran, 1991).

a) ICAMs

ICAMs (intercellular adhesion molecule) contain two to five extracellular Ig-like domains (figure 11). ICAM-1 is constitutively expressed at low level on resting endothelial cells and monocytes, and is inducible or up-regulated by LPS and various pro-inflammatory cytokines (IFNγ, IL-1, or TNFα) on a number of cells, both from the haematopoietic and non haematopoietic lineage (see table 1 for details). Unlike E-Selectin, ICAM-1 maximal expression is only reached after 6-12h. ICAM-2 is largely expressed on leukocytes and is constitutive at a high level on vascular endothelium. Its expression, unlike ICAM-1, cannot be up-regulated by cytokines. ICAM-3 is largely expressed on leukocytes but not on endothelial cells (Bevilacqua, 1993). Two new members of the ICAM family, ICAM-4/LW (Landsteiner-Wiener) on erythrocytes and ICAM-5 (telencephalin) have been recently identified. All ICAMs bind to the same ligand, LFA-1 (Yusuf-Makagiansar *et al.*, 2002).

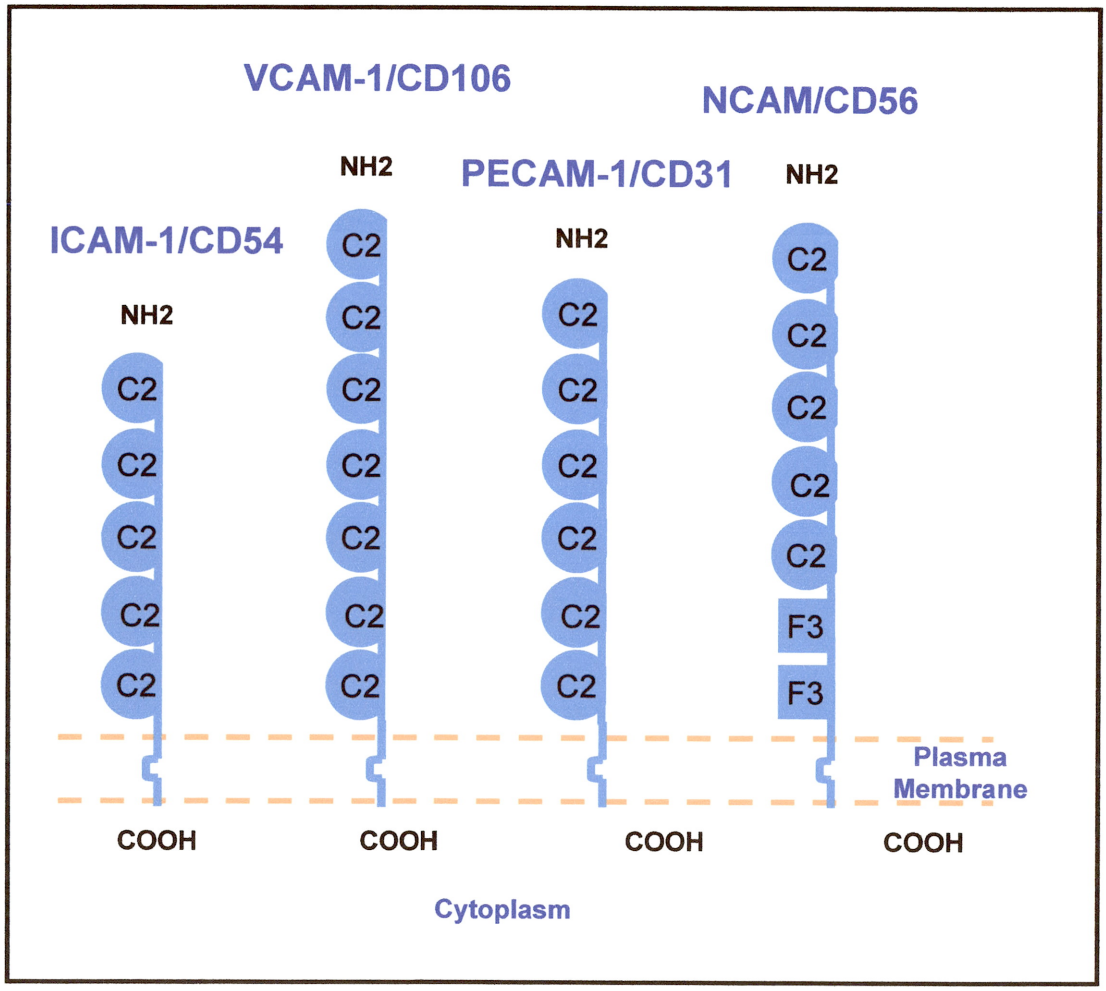


Figure 11: The immunoglobulin superfamily.
These members of the immunoglobulin superfamily contain five to seven Ig-like repeats (two cysteines separated by 55 to 75 amino acids) (C2) on their extracellular domain and present a short cytoplasmic tail. In addition, NCAM presents two fibronectin type III domains (F3).

b) VCAM-1

VCAM-1 (vascular cell adhesion molecule-1) presents seven Ig-like repeats on its extracellular domain (figure 11). It is predominantly expressed in vascular endothelium but has also been identified on tissue macrophages, DC, BM fibroblasts, myoblasts and myotubes and on non-vascular cells in joints, heart, muscle, kidney and brain (Koch *et al.*, 1991; Bevilacqua, 1993). Its expression is induced by pro-inflammatory cytokines and IL-4, in a kinetic similar to that of ICAM-1. VCAM-1 supports adhesion of lymphocytes and monocytes, but not neutrophils (except in rats (Davenpeck *et al.*, 1998)) through its interaction with the VLA-4 integrin (Bevilacqua, 1993).

c) PECAM-1

PECAM-1 (platelet endothelial cell adhesion molecule) is involved in both homophilic and heterophilic interactions. It is constitutively expressed on both leukocytes and endothelial cells and redistributes to the cell borders when cells come into contact as a monolayer. The homophilic interaction between endothelial and leukocyte CD31 mediates leukocyte transmigration through the endothelium (Bevilacqua, 1993).

d) NCAM

As ICAM-1, NCAM (neural cell adhesion molecule) presents five Ig-like repeats in its extracellular domain but also contains two fibronectin type III domains (figure 11). In human and mouse, NCAM is expressed in adult neural tissue and muscle as well as in many embryonic tissues. In human, but not in the mouse or the rat, NCAM is also expressed on haematopoietic cells, but is restricted to NK cells and a subset of

T cells (Barclay, 1997). Although its role on NK cells is still not clear, NCAM homotypic interaction with other NCAM molecules is involved in the control of neuronal development. The molecule has been included in the study because of the neuroectodermal origin of corneal endothelial cells.

1.2.1.3- The integrin family

Integrins are heterodimeric proteins composed of two non-covalently linked α– and β–chains, associated to the cytoskeleton via a short cytoplasmic tail. So far, 17 α–chains and 8 β–chains have been identified. The integrin family (figure 12) has been subdivided into subgroups according to their β-chain usage. The β1 integrin group is involved in interactions with the extracellular matrix and with basement membranes. These integrins also play a role in lymphocyte homing and leukocyte migration. One member of this subfamily, α4β1 (VLA-4) is particularly relevant as it is the ligand of VCAM-1, one of the molecules studied in this report. The β2 integrins, exclusively expressed on leukocytes, are particularly responsible for their recruitment to the site of inflammation. Among them is αLβ2 (LFA-1), the counter-receptor for ICAM-1. Most members of the integrin family bind more than one ligand and their specificities vary according to the cell type on which they are expressed. Integrins are constitutively expressed and require activation by specific signals (e.g. IL-8, thrombin, phorbol ester or T cell activation) to mediate adhesion. These signals induce a conformational change that enables the molecule to bind its ligand (Pigott and Power, 1993; Petruzzelli *et al.*, 1999).

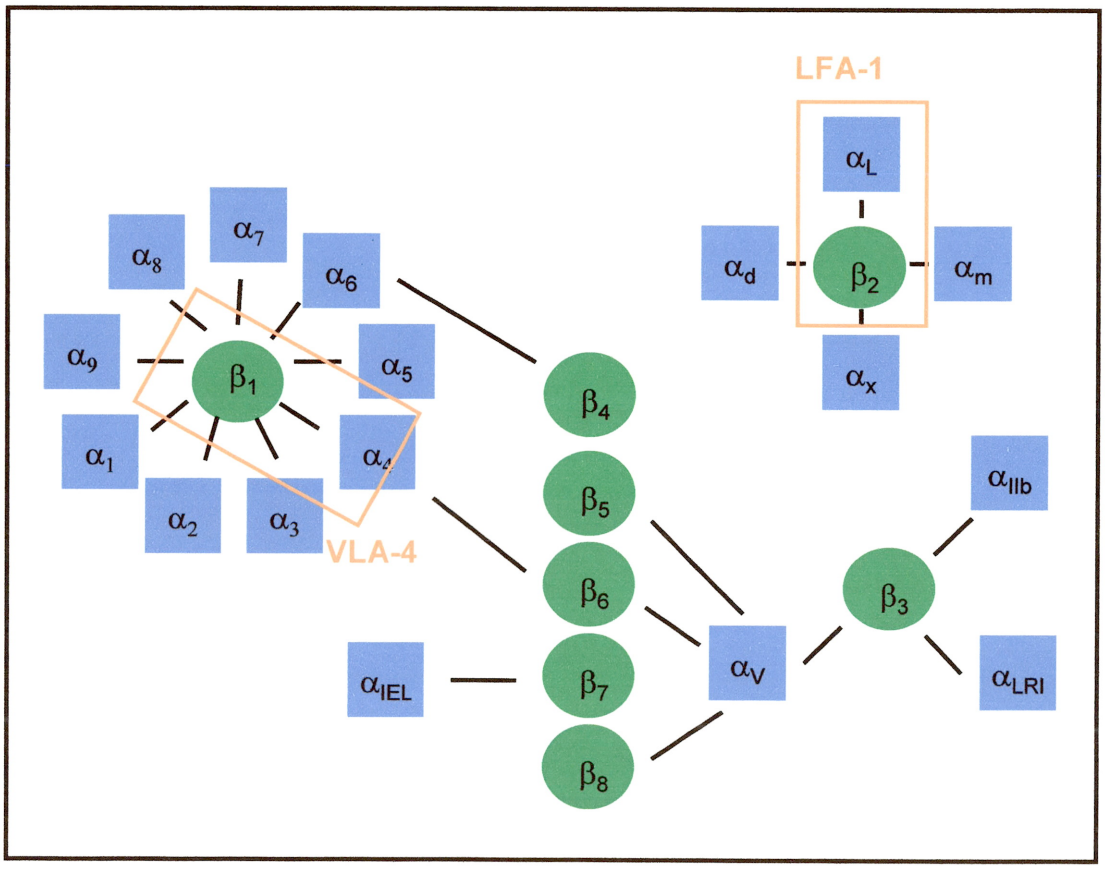


Figure 12: The integrin family (adapted from Petruzzelli et al).
Members of this family are composed of two non-covalently linked subunits, α and β, anchored in the cell membrane. The family is divided in sub-groups according to their β subunit usage.

a) LFA-1

LFA-1 (leukocyte function associated molecule) constitutes of a β2 (CD18) and of a αL (CD11a) integrin subunits. Both CD18 and CD11a are expressed on all leukocytes but CD11a is found with increased levels on memory T cells. Originally, LFA-1 was believed to bind to only three members of the IgSF, namely ICAM-1 (CD54), ICAM-2 (CD102) and ICAM-3 (CD50). However, two new members of the ICAM family, ICAM-4/LW (Landsteiner-Wiener) on red cells and ICAM-5 (telencephalin) have also been identified as LFA-1 ligands (Yusuf-Makagiansar *et al.*, 2002). Finally, the integrin also binds to JAM-1 (junctional adhesion molecule-1), another member of the IgSF. JAM-1 is involved in transendothelial migration of leukocytes (Ostermann *et al.*, 2002). LFA-1 mediates the adhesion of lymphocytes to many cells including endothelial cells.

b) VLA-4

VLA-4 belongs to the β1 integrins (VLA (very late) subfamily). It is constituted of a α4 (CD49d) and a β1 (CD29) subunit. VLA-4 is expressed on lymphocytes, monocytes, some granulocytes, and in some non-lymphoid tissues. α4 integrins are not expressed on neutrophils, except in rats where their low expression was found sufficient to mediate adhesion to rat VCAM-1 (Davenpeck *et al.*, 1998). VLA-4 binds VCAM-1 and fibronectin. It is involved in the migration of leukocytes from blood to tissue and does not require the tethering and rolling of leukocytes to mediate their firm adhesion to the endothelium (Barclay, 1997).

1.2.1.4- Cell surface amino oxidases

VAP-1 (vascular adhesion protein-1) is a glycosylated type II glycoprotein composed of two identical subunits forming a mushroom shape. Its structure differs from classical endothelial adhesion molecules, as it possesses an enzymatic activity within the globular head of its molecule. The enzyme is related to the SSAOs (semicarbazide-sensitive mono-amine oxidases), soluble enzymes responsible for the oxidative deamination of primary amines, leading to the formation of the relevant aldehyde and the release of hydrogen peroxide (H_2O_2) (Salmi and Jalkanen, 2001).

VAP-1 is detected in high endothelial cells of lymphatic organs, sinusoidal endothelial cells in the liver, synovial vessels, small caliber venules. It is also abundant in DC in the germinal centres, in smooth muscle cells and in fat cells. VAP-1 is however absent in endothelial cells from large vessels, epithelial or fibroblastic cells (Salmi and Jalkanen, 2001). Because the corneal endothelium does not behave as vascular endothelium, and because VAP-1 presents an untypical distribution, the molecule was included in this study.

VAP-1 is up-regulated on vasculature during inflammation such as allergy, synovitis or skin inflammation, in inflammatory bowel diseases. Studies in pigs and dogs showed that, in fact the molecule is stored in intracellular granules before its release in conditions of inflammation.

VAP-1 is involved in adhesion of lymphocytes to endothelium in synovial or PLN venules, and in hepatic sinusoidal endothelium, as part of the adhesion cascade. Under low-shear conditions, in the absence of selectins, VAP-1 support the adhesion and transmigration of lymphocytes probably by binding to them through an uncharacterized counter-receptor and through a covalent but transient bond between

the two cell types resulting from the deamination of a primary amine on the lymphocyte surface (Salmi and Jalkanen, 2001; Lalor *et al.*, 2002a).

1.2.2- The adhesion cascade

The recruitment of leukocytes from the blood vessels to a site of tissue injury or infection is crucial in the inflammation process. This involves a cascade of interactions between adhesion molecules on leukocytes and those on the endothelium (figure 13). Each step is mediated by a specific family of adhesion molecules: selectins are involved in the initiation of the cascade, whereas integrins and members of the immunoglobulin superfamily mediate the firm adhesion of leukocytes to the endothelium; finally the transmigration is achieved through homotypic and heterotypic interactions involving two other member of the Ig superfamily, PECAM-1 (CD31) and JAM-1 (Fuggle and Koo, 1998; Ostermann *et al.*, 2002), and the monoamine oxidase VAP-1 (Lalor *et al.*, 2002a).

1.2.2.1- Tethering and rolling

The initiation of this multistep process is mediated by selectins. Upon pro-inflammatory signals, P and E selectins are respectively transported to the endothelial cell surface or synthesised de-novo. Weak interactions between these molecules and their counterpart receptor on leukocytes (PSGL-1, Sialyl Lewis^x), associated with a rapid blood flow induce a characteristic movement of rolling of leukocytes on the endothelial cell surface. Rolling leukocytes also contribute to the recruitment of other leukocytes (secondary rolling) via L-selectin (Alon *et al.*, 1996).

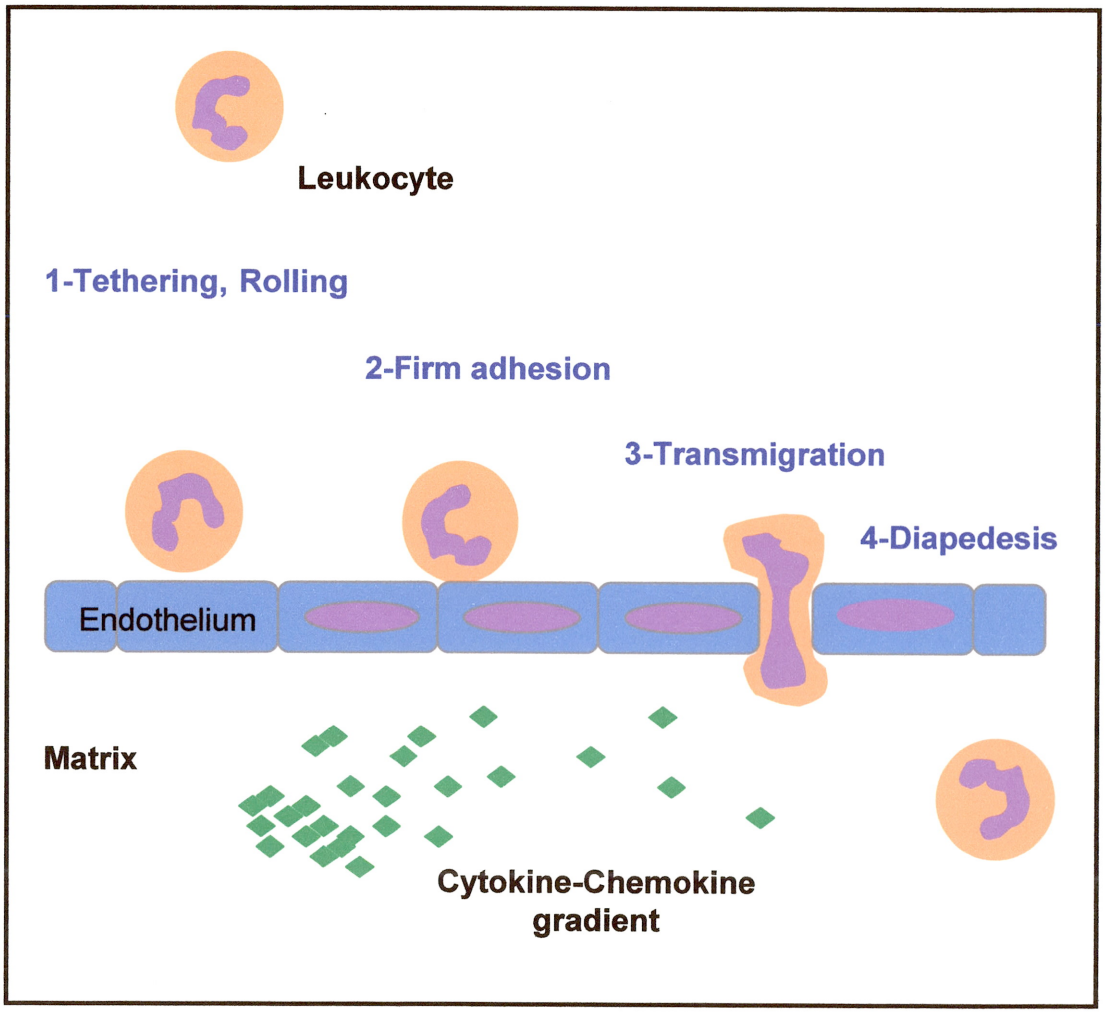


Figure 13: The recruitment of leukocytes from the circulation.
The recruitment of leukocytes is a complex event that can be divided in 4 steps: tethering and rolling, activation, adhesion, transmigration / extravasation. Selectins play a key role in the first stage of tethering and rolling, whereas integrins, activated by chemoattractants, mediate the leukocyte firm adhesion to the endothelium via their interactions with members of the Ig superfamily expressed on the endothelium.

1.2.2.2- Integrin activation

Rolling leukocytes are susceptible to signals in the environment such as chemokines (IL-8), cytokines (monocyte chemotactic protein (MCP1)), phospholipid platelet activating factor (PAF). These signals, produced both by leukocytes and by the endothelium, induce the activation of constitutively expressed integrins on the leukocyte surface, and a conformational change that allows them to interact with the members of the Ig family expressed on the activated endothelium.

Many chemokine receptors can respond to more than one chemokine, multiplying the numbers of combinations of interactions between the endothelium and leukocytes. Furthermore, the use of distinct chemokines at specific anatomical sites determines the specific subpopulation of recruited leukocytes (Ebnet and Vestweber, 1999).

1.2.2.3- Firm adhesion

The conformational change of integrins expressed on rolling leukocytes (LFA-1, VLA-4) mediates a high-avidity interaction with their counter-receptors on the activated endothelium (ICAM-1 and VCAM-1 respectively) and results in the firm adhesion and flattening of leukocytes to the endothelium. These leukocytes are then capable of supporting the rolling of further leukocytes through interactions between LFA-1 and ICAM-3.

1.2.2.4- Transmigration

CD31 (PECAM-1) and JAM-1 are critical in the process of leukocyte extravasation from blood vessels to lymphoid tissues or inflammation sites and are mainly concentrated on the cell borders. Both homotypic interactions between

endothelial CD31 and leukocyte CD31, and heterotypic interactions of CD31 with a putative ligand αVβ3 (Piali *et al.*, 1995), or of JAM-1 with LFA-1, mediate the transmigration of arrested leukocytes through the blood vessel wall (Ostermann *et al.*, 2002).

1.2.3- Cell adhesion molecules in the study

Adhesion Molecules	ICAM-1 (intercellular adhesion molecule-1)	VCAM-1 (vascular adhesion molecule-1)	PECAM-1 (platelet endothelial cell adhesion molecule-1)	NCAM (neural cell adhesion molecule)
CD Nomenclature	CD54	CD106	CD31	CD56
Alternate Name	–	INCAM-110	endoCAM, hec7	Leu-19 or NKH-1 antigen, Fasciclin II (drosophila)
Family	Ig superfamily	Ig superfamily	Ig superfamily	Ig superfamily
Distribution	•constitutive on monocytes, EC •inducible or up-regulated on B, T cells, thymocytes, DC, EC, fibroblasts, keratinocytes and epithelial cells	activated EC, tissue macrophages, DC, BM fibroblasts, myoblasts and myotubes	platelets, EC, monocytes, granulocytes, some T cells	•adult neural tissue and muscle, many embryonic tissues •NK cells and some T cells in human but not rat or mouse
Ligand	LFA-1, MAC-1 (CD11b/CD18), CD43	integrin $\alpha4\beta7$, $\alpha4\beta1$ (VLA-4)	CD31, CD38 ($\alpha V\beta3$ integrin)	CD56, chondroitin sulphate proteoglycans, NCAM-L1
Regulation	induced or up-regulated by LPS, IFNγ, IL-1β and TNFα	induced by IL-4, IFNγ, IL-1β and TNFα	•constitutive •down-regulated on T cells upon activation	transiently expressed during embryogenesis
Function	firm adhesion, signal transduction	firm adhesion, embryonic development	transmigration, signal transduction	control of neuronal development, not clear on NK cells

Table 1A: Adhesion molecules studied in this project.

Adhesion Molecules	E-Selectin	P-Selectin	VLA-4 (very late antigen-4)	LFA-1 (leukocyte function associated molecule-1)	VAP-1 (vascular adhesion protein-1)
CD Nomenclature	CD62E	CD62P	CD49d/CD29	CD11a/CD18	–
Alternate Name	ELAM-1 (endothelial leukocyte adhesion molecule-1), LECAM-2	LECAM-3, PADGEM, GMP-140	integrin α4β1, LPAM-2	integrin αLβ2	–
Family	selectin, C-type lectin	selectin, C-type lectin	β1 integrin	β2 integrin	cell surface amino oxidase
Distribution	activated endothelium	platelets, EC, megacaryocytes	•thymocytes, PBMC, NK cells, eosinophils, myelomonocytic cells •weak expression on adherent cells	•lymphocytes, granulocytes, monocytes and macrophages •increased levels on memory T cells	•synovial vessels, HSEC, smooth muscle cells, fat cells •DC in germinal centres
Ligand	Sialyl Lewis^x and related fucosylated N-actyl-lactosamines, L-Selectin	PSGL-1, sialylated, fucosylated lactosamino-glycans, L-Selectin	VCAM-1, fibronectin	ICAM-1, ICAM-2, ICAM-3, ICAM-4 and ICAM-5, JAM-1	Lectin-like molecule?
Regulation	rapid but transient up-regulation in inflammation, by LPS, TNFα and IL-1β	rapid (within mins) up-regulation with thrombin, histamine, PMA, peroxides or TNFα	slow up-regulation on T cells upon activation	•mainly constitutive •activation through TCR/CD3 complex or phorbol ester	•stored in intracellular granules •translocated onto luminal surface of EC at sites of inflammation (allergy, synovitis…)
Function	rolling, extravasation	rolling, extravasation	rolling, firm adhesion	firm adhesion	leukocyte rolling

Table 1B: Adhesion molecules studied in this project.
Keys: HSEC=hepatic sinusoidal endothelial cells, PSGL-1=P-Selectin glycoprotein ligand-1

1.3- Adhesion molecules and the eye

The specific immune mechanisms of corneal allograft rejection are not fully understood, but several studies reported various degrees of neovascularisation and infiltration of the graft with macrophages, T cells (Pepose *et al.*, 1985; Wackenheim-Urlacher *et al.*, 1995; Larkin *et al.*, 1997b; Kuffova *et al.*, 1999), the majority of which bear the helper T cell markers (Pepose *et al.*, 1985) and a small number of NK cells (in the early stage of rejection) (Larkin *et al.*, 1997b). Corneal allograft rejection is also associated with elevated pro-inflammatory cytokines (TNFα, IFNγ and IL-1β), as opposed to syngeneic grafts or accepted corneal allografts (Torres *et al.*, 1996; Sano *et al.*, 1998; King *et al.*, 2000).

Adhesion molecules are expressed on vascular endothelium upon stimulation with pro-inflammatory cytokines and play a key role in leukocyte recruitment and retention to the site of inflammation. Elner *et al.* (Elner *et al.*, 1991) reported an increase in ICAM-1 expression in the endothelium and stromal keratocytes of corneal tissue sections and in cultured human corneal endothelial (HCE) cells, after TNFα, IFNγ or IL-1β stimulation. The role of adhesion molecules in the pathogenesis of corneal allograft rejection deserves further investigation as they could potentially provide both a suitable marker for allograft rejection and a target for therapy, therefore preventing allograft rejection.

Many publications report studies of adhesion molecules in the cornea; most of them use an immunohistochemistry technique and a panel of monoclonal antibodies to determine the expression and distribution of adhesion molecules in normal, diseased or inflamed corneas.

Data are conflicting in some areas: ICAM-1 was found constitutively expressed on the endothelium of normal corneas in several reports (Foets *et al.*, 1992; Philipp and Gottinger, 1993; Philipp, 1994; Vorkauf *et al.*, 1995) but could not be detected by other authors (Whitcup *et al.*, 1993; Goldberg *et al.*, 1994). All reports however agree that ICAM-1 is expressed on stromal keratocytes and on basal epithelial cells. In inflamed or diseased corneas, authors reported a moderate to strong expression in corneal endothelium, in limbus vascular endothelium, stromal keratocytes and basal epithelium (Philipp and Gottinger, 1993; Whitcup *et al.*, 1993; Philipp, 1994). Similarly, stimulation of cultured human corneal endothelial (HCE) cells or whole corneas with pro-inflammatory cytokines induced ICAM-1 expression (Elner *et al.*, 1991; Pavilack *et al.*, 1992).

VCAM-1 was not found in normal corneas (Philipp and Gottinger, 1993; Goldberg *et al.*, 1994; Claesson *et al.*, 1997) except when organ cultured corneas were used (Foets *et al.*, 1992). VCAM-1 was expressed in inflamed and rejected corneas, and was localised to vascular endothelium in the stroma (Philipp and Gottinger, 1993; Goldberg *et al.*, 1994; Vorkauf *et al.*, 1995). In contrast to these findings, Pavilack *et al.* could not detect VCAM-1 expression on cytokine-stimulated corneas (Pavilack *et al.*, 1992).

Similarly, E-Selectin was not detected in normal corneas and was only weakly expressed in the stroma of vascularised corneas and the limbal vessels of inflamed or rejected corneas (Philipp and Gottinger, 1993; Goldberg *et al.*, 1994; Vorkauf *et al.*, 1995). E-Selectin was also reported on corneal endothelium in Vorkauf *et al.* (Vorkauf *et al.*, 1995).

P-Selectin was weakly expressed in normal corneal and vascular endothelium, but not in the stroma or the epithelium. Inflamed corneas showed increased expression both in vascular and in corneal endothelium (Vorkauf *et al.*, 1995).

Goldberg *et al.* found increased PECAM-1 in inflamed corneas on the epithelium and in the stroma. Interestingly, the only case of PECAM-1 expression in the endothelium was associated with VCAM-1 expression (Goldberg *et al.*, 1994).

All these findings are consistent with an increased expression of adhesion molecules in inflammation and rejection. Discrepancies between studies are however frequent. In addition, reports are difficult to analyse and compare as many authors refer to endothelium without distinguishing between vascular endothelium and corneal endothelium.

Aims of the study

Pro-inflammatory cytokines are associated with corneal allograft rejection. In the vascular endothelium, these cytokines induce the up-regulation of adhesion molecules, which are responsible for the recruitment of inflammatory cells. However less is known about the expression of adhesion molecules in the corneal endothelium. The aims of this thesis were therefore the following:

- Study the expression of adhesion molecules in normal and cytokine-stimulated corneas (using RT-PCR, FACS, histology).
- Study the role of adhesion molecules in the pathogenesis of corneal allograft rejection (using adhesion assays, histology in a mouse model of corneal allograft rejection).
- Identify a suitable target for gene therapy in order to prevent corneal allograft rejection.

CHAPTER 2

Materials and Methods

Materials and Methods

2.1- Specimens

2.1.1- Human Corneas

Dr D.F.P. Larkin (Institute of Ophthalmology, London) very generously provided corneas, from post-mortem human eyes unsuitable for transplantation, or from keratoconus recipients (Moorfields Eye Hospital's Eye Bank (London, UK)). Appropriate consent was obtained in all cases for harvesting and use of corneal tissues, which were stored for up to 4 weeks in Optisol GS (Chiron Ophthalmic, Irvine, CA) at 4°C. Donor age ranged from 40 to 88. Corneas were stimulated with various cytokines, washed in PBS (Oxoid, Basingstoke, UK), snap frozen and stored in -70°C until processing for RT-PCR.

2.1.2- Murine Corneas

Eyeballs from BALB/c mice used for others studies were removed within 20 mins of the animal death and stored in PBS at room temperature for up to 4h until the excision of the corneas. Corneas were then incubated with different cytokines, rinsed in PBS, snap frozen and stored at -70°C until use.

2.2- Mouse corneal transplantation

A mouse model of corneal allograft rejection was developed in the laboratory by Dr D.F.P. Larkin and Dr. Navid Ardjomand. In this model, female BALB/c mice (Harlan Olac, Bicester, UK) received orthotopic corneal allografts from female C3H/Hen mice (Harlan Olac). All transplants were performed by Dr. Navid

Ardjomand under appropriate Home Office licences. The center of the recipient cornea was marked with a 2.0 mm diameter trephine (Geuder, Germany) and excised using curved scissors. A 2.5 mm diameter full thickness corneal graft was marked with a trephine, cut out with a diamond knife from the center of the donor cornea and transplanted into the recipient corneal bed. The graft was secured with one continuous running 11/0 nylon suture (Ethicon, UK) that was removed 7 days after surgery (figure 1). At the completion of the procedure, the anterior chamber was reformed with sterile saline. All the grafts were observed 3 times a week until graft rejection occurred and the different stages of rejection were defined using a standardised grading scheme (table 1) adapted from Sonoda *et al.* (Sonoda and Streilein, 1993). A graft was technically successful if on day 7 (suture removal): 1) the cornea had become clear (grade 0-I) and 2) the animal had not developed a cataract.

Grafts were defined as rejected when the corneal clarity changed to grade III (opaque cornea, the iris cannot be clearly recognised). Eyeballs were collected on the day following suture removal (day 8) and at stage IV of rejection. They were then stored at -70°C until sectioning.

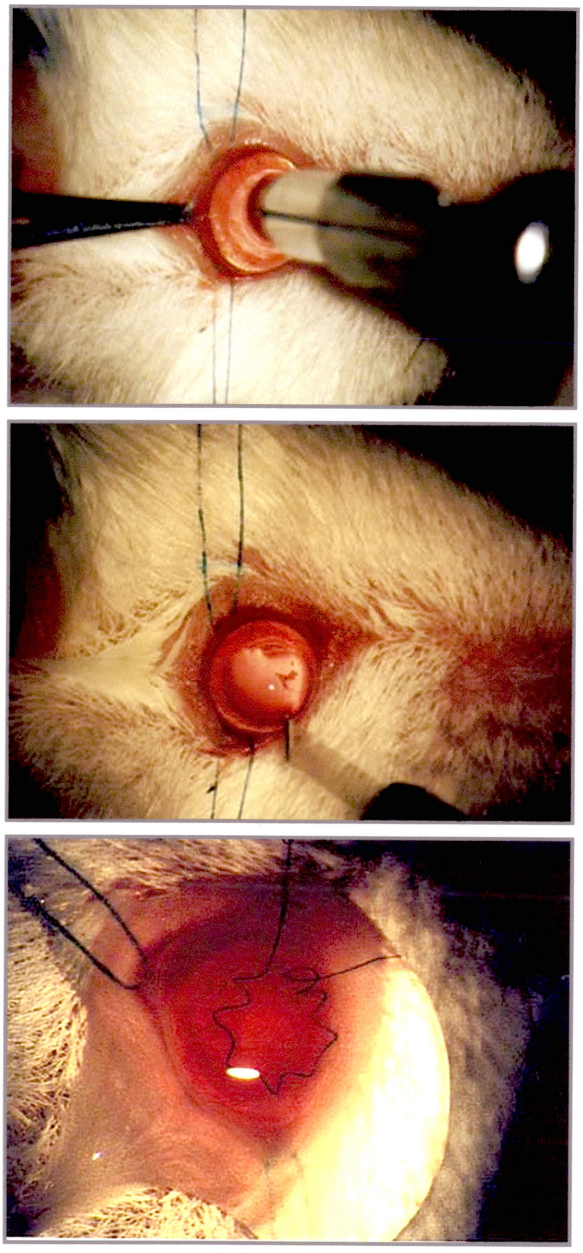


Figure 1: Mouse corneal transplantation (pictures courtesy of Dr Navid Ardjomand).
A 2.5 mm diameter full thickness corneal graft is marked with a trephine (A), cut out with a diamond knife from the centre of the donor cornea (B) and transplanted into a recipient corneal bed. The graft is then secured with a continuous running suture that is removed 7 days after surgery (C).

Grade	Description
0	clear cornea, no opacity
I	minimal epithelial opacities, anterior chamber and iris vessels easily visible
II	moderate corneal or anterior chamber opacity, iris vessels still visible
III	moderate corneal or anterior chamber opacity, only pupil margin visible
IV	complete corneal or anterior chamber opacity, no iris structure visible

Table 1: Standardised grading scheme used in the characterisation of the different allograft rejection stages.

2.3- Cell culture

2.3.1- Cell lines

EA-Hy 926

The EA-Hy 926 cell line, a hybridoma resulting from the fusion of human umbilical vein endothelial cells (HUVEC) and the A-549 lung epithelial carcinoma cell line, was originally a gift from Dr C.J.S. Edgell (Department of Pathology, School of Medicine, University of North Carolina) (Edgell *et al.*, 1983).

DAP-3/DVCAM

The mouse fibroblast cell line DAP-3 is MHC class II negative and thymidine kinase deficient, and is sensitive to neomycin. The DVCAM cells are DAP-3 cells transfected with a plasmid/gene construct encoding the human adhesion molecule VCAM-1. The construct also provides a resistance to geneticin disulphate (G418), a neomycin analogue (both cell lines were kindly provided by Prof. M. Ritter, Imperial College London).

CHO/CHO-E

CHO is a transformed cell line, of Chinese Hamster Ovarian origin, sensitive to zeocin. CHO-E cells consist of CHO cells transfected with a construct encoding the human adhesion molecule E-Selectin and resistance to zeocin (these cell lines were a gift from Prof. D.O. Haskard, Imperial College London) (Kao and Puck, 1968).

Jurkat

The transformed human T-cell line Jurkat was a gift from Dr G. Lombardi (Imperial College London) (Weiss *et al.*, 1984).

MCE BALB/c and MCE B6

Two mouse corneal endothelial cell (MCE) lines (figure 2) derived from BALB/c or C57BL6 mice were very generously provided by Prof. J. Niederkorn (University of Texas, Southwestern Medical Center, Dallas). The cells were immortalised with human papilloma virus genes E6 and E7 using pLXSN16E6/E7 disabled recombinant vector (Wilson *et al.*, 1995).

bEnd-1 and sEnd-1

The bEnd-1 and sEnd-1 cell lines are mouse endothelial cell lines derived from polyoma-induced hemangiomas in brain and in skin respectively. These cells were kindly provided by Dr Justin Mason (Imperial College London) (Hahne *et al.*, 1993).

J774A-1

J774 is an adherent transformed cell line derived from reticulum cell sarcoma that presents a macrophage morphology (Ralph *et al.*, 1976). These cells were kindly provided by Prof. D.O. Haskard.

2.3.2- Culture media and conditions

EA-Hy 926 and DAP cell lines were cultured in RPMI-1640 (Invitrogen, Groningen, Netherlands) supplemented with 10% heat-inactivated (30 mins at 56°C) Fetal Calf Serum (FCS) (Globepharm, Esher, UK), 2 mM L-glutamine (Invitrogen), 100 IU/ml penicillin and 100 μg/ml streptomycin (Invitrogen) and 1% sodium pyruvate (Sigma, Poole, UK). Cells reaching confluence were detached with trypsin (Sigma) and subcultured at a 1:3 ratio. DVCAM cells were cultured in the same medium supplemented with 200 μg/ml geneticin (G418 antibiotic) (Sigma).

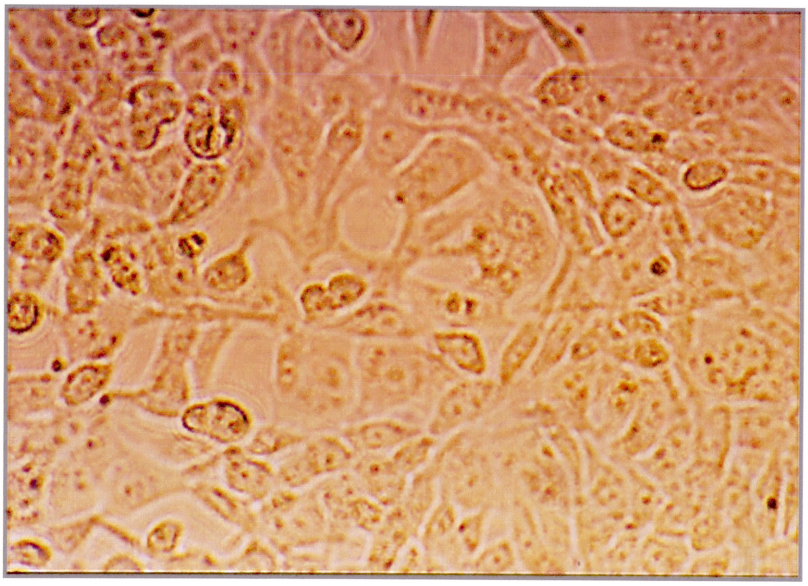


Figure 2: Inverted-phase micrograph of a nearly confluent MCE cell culture (x600).

Jurkat cells were grown in suspension in the above medium and routinely subcultured at a 1:10 ratio.

CHO cells were cultured in Nutrient Mixture Ham's F-12 (Invitrogen), supplemented with 10% heat-inactivated FCS, 2 mM L-glutamine, 50 U/ml penicillin and 50 μg/ml streptomycin (Invitrogen). CHOE cells were grown in the same medium, supplemented with 0.5% zeocin (Invitrogen).

MCE BALB/c and MCE B6 cells were cultured in Eagle's MEM medium with EBSS (Biowhittaker, Wokingham, UK) supplemented with 10% heat-inactivated FCS, 2 mM L-glutamine, 1% MEM vitamin solution (Biowhittaker), 1% sodium pyruvate and 1% penicillin/streptomycin fungizone mixture (Biowhittaker).

sEnd-1 and bEnd-1 were cultured on gelatin, in 175 cm^2 flasks (Costar, Cambridge, MA). 5 ml of 1% gelatin (Sigma) was used to cover the bottom of a flask and incubated at 37°C for 30 minutes. The gelatin was then aspirated and replaced by 15 ml of Dulbecco's MEM medium (Invitrogen) supplemented with 10% heat-inactivated FCS, 2 mM L-glutamine (Invitrogen), 50 U/ml penicillin and 50 μg/ml streptomycin (Invitrogen). In addition, 1% sodium pyruvate (Sigma) was also added to the sEnd-1 culture medium. The culture medium was then incubated for 30 to 60 minutes before the addition of the cells.

The J774 cells were cultured in Dulbecco's MEM (Invitrogen) supplemented with 10% heat-inactivated FCS, 100 U/ml penicillin and 100 μg/ml streptomycin.

All cells were cultured at 37°C in a 5% CO_2 humidified atmosphere, in a 750 ml /175 cm^2 flask (Helena Biosciences, Sunderland, UK) (except the sEnd-1 and bEnd-3 cells). At confluence, adherent cells were detached with trypsin (Sigma) and

subcultured at a 1:3 ratio (1:2 ratio for the sEnd-1 and bEnd-1 cells). All cells were regularly tested for mycoplasma and were not used unless clear of infection.

2.3.3- Primary cultures of bovine corneal endothelial cells (BCE)

Corneas were excised from bovine ocular globes obtained from a local slaughterhouse and washed for 5 mins in sterile PBS. The endothelial side of the cornea was then covered with approximately 500 μl of trypsin diluted 1:10 in PBS and incubated for 15 mins at 37°C. Endothelial cells were then gently scrapped off with an autoclaved metal spatula and rinsed from the endothelial surface using EMEM medium (Eagle's MEM with Earle's salts and Hepes buffer) (Sigma) containing 10% FCS. Dislodged cells were then washed in 10 ml medium at 300g for 5 mins. Pelleted cells from one bovine cornea were transferred to a 25-cm^2 flask (Becton Dickinson Labware, New Jersey, USA) in 10 ml of the above medium supplemented with 4 mM L-Glutamine, 50 μg/ml gentamicin (Invitrogen), 100 U/ml penicillin, 100 μg/ml streptomycin, 0.25 μg/ml amphotericin B solution (Invitrogen) and 150 μg/ml endothelial cell growth supplement (Sigma). Cultures were maintained at 37°C in a 5% CO_2 humidified atmosphere and medium was replaced twice a week.

2.3.4- Preparation of BCE matrix

BCE matrices were prepared as in Blake *et al.* (Blake *et al.*, 1997). Basically, BCE cells were trypsinised and cultured in a 35-mm petri dish until they were confluent. The cells were then washed once with PBS and incubated for 5 mins at room temperature (RT) with a detergent solution (0.5% sodium deoxycholate) (Sigma) to detach them from the underlying matrix. The remaining matrix was then

washed 5 times with EBSS (Ca^{2+} and Mg^{2+}-free Earle's Balanced Salt Solution) (Sigma) supplemented with 5 mM EDTA (Sigma) and buffered with 15 mM Hepes, 10 mM TES and 10 mM BES (all from Sigma). Matrices were then used immediately to grow HCE cells or were stored up to 4 weeks in buffered EBSS supplemented wit 1000 U/ml penicillin, 1 mg/ml streptomycin and 2.5 μg/ml amphotericin B solution (Sigma).

2.3.5- Primary cultures of human corneal endothelial cells (HCE)

Primary cultures of HCE cells were prepared according to the method of Blake *et al.* (Blake *et al.*, 1997). Excised human corneas were treated as bovine corneas in 150 μl of trypsin diluted 1:10 in PBS. After 30 mins of incubation at 37°C, endothelial cells were gently dislodged and washed in 10 ml EMEM containing 10% human serum derived from platelet-poor plasma (Sigma). The cell pellet from 2 corneas was then resuspended in 2 ml of culture medium (EMEM, 10% human serum, 4 mM L-Glutamine, 50 μg/ml gentamicin, 100 U/ml penicillin, 100 μg/ml streptomycin and 0.25 μg/ml amphotericin B solution, 150 μg/ml endothelial cell growth supplement, 5 μg/ml insulin, 5 μg/ml transferrin and 5 ng/ml sodium selenite solution (Sigma)) and plated in a 35-mm culture dish coated with BCE matrix (as detailed above) or collagen I (Biocoat®, Becton Dickinson Labware). Cultures were maintained at 37°C in a 5% CO_2 humidified atmosphere and medium was replaced every other day. Upon reaching confluence, cells were trypsinised for 1-2 mins and split at a 1:2 ratio.

2.4- RT-PCR

2.4.1- Preparation of samples

2.4.1.1- Corneal samples

Human corneas cut in quarters or whole mouse corneas (pool of 6 corneas per sample) were snap frozen for 5 mins in liquid nitrogen, then stored at –70°C until further use. When appropriate, samples were treated with cytokines (TNFα, IL-1α/β and/or IFNγ) (all from Peprotech EC Ltd, London, UK) before snap freezing. Before the mRNA extraction, the frozen human samples were incubated overnight in collagenase type I, S (150 U/ml) (Sigma) in order to ease the homogenisation of the tissues.

2.4.1.2- Cells and other tissues

Cells ($1x10^6$ cells per sample) were treated with cytokines (TNFα, IL-1α/β and/or IFNγ), then lysed using 1 ml RNazol ™ B (AMS Biotechnology, Oxon, UK), snap frozen in liquid nitrogen, and stored at -70°C. Other tissues used as positive controls for the PCR (mouse brain, spleen or liver) were snap frozen directly after the excision from the animal and stored at -70°C until further use.

2.4.2- mRNA extraction

Cell samples were thawed out and left on ice until the next stage of the mRNA extraction. Corneal samples incubated in collagenase were spun down for 5 mins at 13,000g (Eppendorf Centrifuge 5415 C) and the supernatant was removed. These samples and the other tissue samples (except mouse corneas) just removed from the -

70°C freezer were treated with 1 ml RNazol™ B containing phenol and guanidium salts. Mouse corneas were treated with 1ml of TRIzol® Reagent (Invitrogen).

All samples were then treated in the same way. Total cellular mRNA was extracted by phenol extraction: 100 μl of chloroform (Sigma) was added and samples were vortexed vigorously for 15 secs until the previously blue RNazol B or pink TRIzol turned white. They were left on ice for at least 10 mins and centrifuged at 13,000 g for 15 mins at 4°C. The upper aqueous phase (containing RNA) was then transferred to a fresh 1 ml microfuge tube containing an equal volume (500 μl) of ice-cold isopropanol (Sigma) and stored overnight at 4°C. The sample was centrifuged for 30 mins at 13,000g at 4°C, the supernatant was removed and the RNA was then washed once with 1 ml of ice-cold 75% ethanol (Sigma) and allowed to dry for 5-10 mins.

2.4.3- Reverse transcription

Each mRNA sample received 3.5 μl oligo (dT) (10 μg/ml) (Pharmacia Biotech, Milton Keynes, UK) and 10 μl autoclaved filtered deionised (afd) water. The sample was incubated at 60°C for 5 mins and then cooled on ice for 3 minutes. The mRNA was then reverse-transcribed using the following mix: 400 units of Moloney Murine Leukemia Virus Reverse Transcriptase (M-MLV RT) (Invitrogen), 10 μl of 5X First Strand Buffer (250 mM Tris-HCl (pH 8.3), 375 mM KCL, 15 mM $MgCl_2$) (Invitrogen), 5 μl of 100 mM dithiothreitol (DTT) (Invitrogen), 20 units of RNase Inhibitor (Roche, Lewes, UK) and 0.25 mM of each dNTP (Pharmacia Biotech). The mixture was then incubated for 40 mins at 37°C. Another 400 units of M-MLV RT

were added and incubated for a further 40 mins. Samples were finally heated at 70°C for 10 mins to stop the reaction.

2.4.4- PCR

All human PCR reactions were initially optimised (for annealing temperature and $MgCl_2$ concentration) using TNFα-stimulated (200 and 600 IU/ml) EA-Hy 926 cells. PCR for mouse GAPDH, ICAM-1, VCAM-1 and E-Selectin were optimised using the sEnd-1 cell line that constitutively expresses these molecules. The cell line was used as positive control in subsequent experiments. PCR for mouse NCAM-1 and VAP-1 were respectively optimised on mouse brain and liver tissues, whereas the Collagen VIII PCR was optimised using the MCE BALB/c cell line itself.

With the exception of GAPDH (30 cycles), all PCR reactions were carried out for 35 cycles using an Omnigene Thermal cycler (Hybaid, London, UK). Each cycle consisted of 94°C for 30 secs, x°C for 40 secs and 72°C for 1 min. The annealing temperature (x) was specific for each primer combination. Values for (x) are given in tables 2 and 3.

Each 20 μl PCR reaction consisted of: 0.5 U Taq polymerase (Qiagen, Hilden, Germany), 1X PCR reaction buffer (including 1.5mM $MgCl_2$) (Qiagen), 0.2mM of each dNTP, 1μM of each primer (MWG Biotech, Milton Keynes, UK) and 5μl of diluted cDNA (each cDNA sample was diluted 1:5). The PCR reaction was started at 94°C for 3 mins to denature all cDNA samples. Ten microlitres of PCR product and of 1 Kb Plus DNA Ladder (Invitrogen) were visualised by electrophoresis on a 1.5% agarose gel (Invitrogen) and ethidium bromide (Sigma) staining (10 mg/ml).

2.4.5- Primers sequences

All primers were obtained from MWG-Biotech. GAPDH (glyceraldehyde 3-phosphate dehydrogenase), or HPRT (Hypoxanthine Phospho-Ribosyl Transferase) housekeeping genes were used to standardise the experiments.

In our laboratory, F. Mirza designed the primers for human GAPDH, ICAM-1, VCAM-1 and E-Selectin while primers for mouse HPRT were designed by Dr R. Pillai. Primers for mouse ICAM-1, NCAM-1, VAP-1 and Collagen VIII were designed using the Gene Jockey software. Mouse GAPDH and VCAM-1 were designed according to Bowen *et al.* and mouse E-Selectin according to Khatib *et al.* (Bowen and Hunt, 1999; Khatib *et al.*, 1999).

Sequences of the primers, annealing temperatures and PCR products sizes for the human and the murine PCR are detailed in Tables 2 and 3 respectively.

mRNA	Sense Primer/Anti-Sense Primer	Ann. Temp. (°C)	PCR Product Size (bp)
GAPDH	5'-GCA GGG GGG AGC CAA AAG GG -3' 5'-TGC CAG CCC CAG CGT CAA AG -3'	58	567
ICAM-1	5'-TAT GGC AAC GAC TCC TTC T-3' 5'-CAT TCA GCG TCA CCT TGG -3'	58	219
VCAM-1	5'-ATG ACA TGC TTG AGC CAG G-3' 5'-GTG TCT CCT TCT TTG ACA CT-3'	58	241
E-Selectin	5'-CTC TGA CAG AAG AAG CCA AG-3' 5'-ACT TGA GTC CAC TGA AGC CA -3'	58	235

Table 2: Summary of human PCR details.

mRNA	Sense Primer/Anti-Sense Primer	Ann. Temp. (°C)	PCR Product Size (bp)
HPRT	5'-GTAATGATCAGTCAACGGGGGAC-3' 5'-CCAGCAAGCTTGCAACCTTAACCA	54	176
GAPDH	5'-TGA AGG TCG GTG TGA ACG GAT TTG GC-3' 5'-CAT GTA GGC CAT GAG GTC CAC CAC-3'	55	983
ICAM-1	5'-TTG TTC TCT AAT GTC TCC GAG G-3' 5'- TCA CAC TTC ACA GTT ACT TGG C-3'	59	404
VCAM-1	5'-CAA CGA TCT CTG TAC ATC CC-3' 5'-AGA GGC TGT ACA CTC TGC CT-3'	55	839
E-Selectin	5'-GTG CGG TGT ACG TCC TCT TGG-3' 5'-GAC TTG TAG GTG AAT TCT CCA GTA GT-3'	58	714
NCAM-1	5'-ATT CTT CCT GTG TCA AGT GG-3' 5'-ATC ACA GAC AAT CAC AGC ATC C-3'	57	309
VAP-1	5'-CTG GTG AAT GTG GTA TTG GTC C-3' 5'-GCC TGA GAT TCC AGA AGG-3'	56	409
COLLAGEN VIII	5'-CCT GGA CCC AAA GGA GAA GGT GG-3' 5'-CCT TTG GGG CCC GGA ATC CCA G-3'	66	329

Table 3: Summary of mouse PCR details.

2.5- Antibodies used in the study

2.5.1- Antibody purification

Supernatants (generous gift from Dr E. Eren) of hybridomas secreting clones of mouse anti-human VCAM-1 (1G11 and 60.9) were applied over 3-5 days to a protein G column (Sigma), using a peristaltic pump. Antibodies were then eluted with 2 ml of 0.1 M glycine pH 2.8 and collected in 50 µl neutralising Tris 1 M pH 8.8. They were finally buffer-exchanged into RPMI using PD10 columns (Sigma) and their concentration was determined by Optical Density (OD) at 280nm.

2.5.2- Summary of antibodies used in this study

All the antibodies mentioned in this thesis were titrated before use.

Specificity	Clone	Isotype	Form	Source	Dilution	Application
rabbit anti-mouse Ig FITC	-	IgG	purified	Dako	1:40	FACS, IF
rabbit anti-rat Ig FITC	-	IgG	purified	Dako	1:40	FACS, IF
rabbit anti-rat Ig biot.	-	IgG	purified	Vect Lab.	1 µg/ml	IH

Table 4: Rabbit antibodies used in the study.

Vect. Lab.=Vector Laboratories

IF=Immunofluorescence, IH=Immunohistology

Specificity	Clone	Isotype	Form	Source	Dilution	Application
mouse isotype control	11711.1	IgG1	Purified	R&D	10 µg/ml	FACS, IF
mouse isotype control	20102.1	IgG2a	Purified	R&D	10 µg/ml	FACS, IF
mouse anti-mouse class I (H-2Db)	28.14.8	IgG2a	Purified	Phar.	10 µg/ml	FACS
mouse anti-human ICAM-1	6.5B5	IgG1	Purified	(1)	10 µg/ml	IF
mouse anti-human VCAM-1	60.9	IgG1	Purified	(2)	10 µg/ml	AA
mouse anti-human VCAM-1	1G11	IgG1	Purified	(2)	2.5-10µg/ml	AA, IF
mouse anti-human E-Selectin	1.2B6	IgG1	Purified	(1)	2.5ug/ml	IF
mouse anti-human β2 integrin	TS1	IgG1	Sup.	(5)	neat	AA
mouse anti-human α4 integrin	MAX68P	IgG2b	Purified	(4)	10 µg/ml	AA
mouse anti-rat Thy1.1	OX7	IgG1	Purified	(3)	10 µg/ml	AA

Table 5: Mouse antibodies used in the study.

1=gift from I. Malik*, 2=purified from supernatant provided by Dr E.Eren, 3=gift from Prof M. Ritter*, 4=gift from Prof D.O. Haskard*, 5=gift from Dr F.M. Marelli-Berg*, Phar.=Pharmingen
AA=Adhesion Assay, IF=Immunofluorescence *=Imperial College London

Specificity	Clone	Isotype	Form	Source	Dilution	Application
rat isotype control	43414.11	IgG1	Purified	R&D	10 µg/ml	FACS, IF, IH, AA
rat isotype control	54447.11	IgG2a	Purified	R&D	5-10 µg/ml	FACS, IF, IH, AA
rat anti-mouse ICAM-1	YN1	IgG2a	purified	(1)	5-10 µg/ml	FACS, IF, IH, AA
rat anti-mouse VCAM-1	MK2.7	IgG1	purified	(1)	10 µg/ml	FACS, IF, IH, AA
rat anti-mouse E-Selectin	MES.1	IgG2a	purified	(1)	10 µg/ml	FACS, IF
rat anti-mouse P-Selectin	RB40	IgG1	purified	(1)	10 µg/ml	FACS, IF
rat anti-mouse PECAM-1	GC51	IgG2a	purified	(1)	10 µg/ml	FACS, IF, IH
rat anti-mouse β2 integrin	M18/2 (TIB-218)	IgG2a	purified	(1)	10 µg/ml	AA
rat anti-mouse α2 integrin	PS/2	IgG2b	purified	(1)	10 µg/ml	AA

Table 6: Rat antibodies used in the study.

1=gift from Prof D.O. Haskard, Imperial College London

AA=Adhesion Assay, IF=Immunofluorescence, IH=Immunohistology

2.6- Flow cytometry

2.6.1- Preparation of cells

Cells were detached from the flask using 5ml of Trypsin (Sigma) (or Cell Dissociation solution (Sigma) in the case of PECAM-1) and washed once for 10 mins in culture medium (4°C, 300 g (Jouan, CR412)). Cells were then washed once in FACS washing buffer: PBS containing 1% heat-inactivated FCS (Sigma), 0.1% sodium azide (NaN_3) (Sigma), and 5mM EDTA (Sigma), then counted and dispatched in a U-bottomed 96-well plate (Nunc, Roskilde, Danemark) at $0.5x10^6$ cells per well in a 200 μl suspension. Some cells were pre-treated with TNFα, IL-1α and/or IFNγ (all from Peprotech EC Ltd) before seeding in the 96-well plate.

2.6.2- Staining

All antibodies used for the staining were diluted in FACS buffer: PBS containing 1% heat-inactivated FCS, 0.1% sodium azide, and 5mM EDTA, supplemented with 10% of rabbit serum (Invitrogen) aggregated at 56°C for 30 mins. Antibodies were then centrifuged for 20 mins at 13,000g (Eppendorf Centrifuge 5415 C), at 4°C. Cells were spun down at 300 g, for 5 mins at 4°C and the plate flicked to remove the supernatant. Cells were then resuspended using a vortex and incubated with 50 μl of FACS buffer supplemented with aggregated rabbit serum. Cells were spun down at 300 g to remove the supernatant and incubated with 50 μl of the appropriate primary antibody (10 μg/ml) for 20 mins. Cells were kept on ice during the whole process. Cells were washed once in 200 μl of washing buffer at 300 g at 4°C and a rabbit anti-mouse FITC or a rabbit anti-rat FITC antibody (both from Dako, Ely, UK) was

added in 50 μl. After 20 mins at 4°C, cells were washed 3 times in 200 μl of washing buffer. Cells were then resuspended in 200 μl cold fixative solution: PBS-1% FCS-0.1% NaN_3-5mM EDTA containing 1% formaldehyde (Sigma), and transferred to FACS tubes (Becton Dickinson Labware) containing 200 μl fixative solution. Cells were then acquired on a FACS Coulter Epics XL-MCL (Coulter Corp., Miami, USA) or on a FACSCalibur (Becton Dickinson Immunocytometry Systems, California, US) and data were analysed using the CELLQuest software (Becton Dickinson Immunocytometry Systems).

2.7- Immunofluorescence

2.7.1- Cytospins

A cell suspension was prepared with 1-5x10^6 cells/ml in culture medium. Filter cards (Shandon SC, Pittsburg, PA) and then funnels were mounted on frosted microscope slides (Merck, Poole, UK). 100 μl of cell suspension was then added to each funnel and spun immediately for two mins at 550 rpm (Cytospin 2, Shandon SC). The filter mat was then reversed and 100 μl of cell suspension added again to each funnel. After another spin for two mins at 550 rpm, funnels and filter mats were carefully removed. Slides were left to dry overnight, wrapped in foil and stored at –20°C until further use. They were not fixed at this stage.

2.7.2- Cell culture on slides

Approximately 24h before staining, 2.5x10^5 cells were seeded in Flexiperm chambers (Sigma) attached onto Superfrost slides (Merck). The culture was then

gently washed with PBS before fluorescent staining. Flexiperm chambers were kept on the slides during the whole staining.

2.7.3- Preparation of corneal flat mounts

Mouse corneas freshly excised were washed in PBS, pressed between two frosted slides (Merck) and left to dry for 2 hours at 37°C. Once the corneas were dry, the two frosted slides were separated. The cornea was then gently removed using forceps, leaving the endothelium on one slide and the epithelium on the other one. Both slides were observed under light microscopy to distinguish between the two structures of the cornea and were marked as such. Slides were wrapped in foil and stored at –20°C until further use. They were not fixed at this stage.

2.7.4- Fluorescent staining

Fluorescent staining was carried out on MCE cells cytospins or cultured on glass slides, on whole human corneas or flat-mounts of mouse corneas. Cytospins, cultures and flat-mounts slides were fixed in a 50% methanol/ 50% acetone mixture for 10 mins, just prior to use. Slides and human corneas were washed twice in PBS and then incubated for 10 mins in PBS containing 10% aggregated rabbit serum. Slides were quickly dipped in PBS to remove serum excess and incubated with the appropriate primary antibody for 40 mins at 4°C in a humidified chamber. After 2 washes in PBS, slides were incubated with the appropriate secondary antibody (rabbit anti-mouse FITC or a rabbit anti-rat FITC antibody (both from Dako, Ely, UK)) for another 40 mins at 4°C in a humidified chamber. Slides were then washed twice in PBS and dried at RT. They were finally mounted in VECTASHIELD mounting medium for fluorescence containing DAPI (VECTOR Laboratories, Burlingame,

CA), a dye staining cell nuclei in blue. Human corneas were placed between two frosted slides glued together with paraffin just prior the analysis to prevent them from drying. Specimens were analysed on a fluorescent microscope, pictures were captured by a digital camera and analysed using the Metamorph Imaging software.

2.8- Immunohistology

2.8.1- Tissue preparation and cryostat sectioning

Mouse eyeballs collected at different stages of rejection, and spleens were snap frozen for 5 mins in liquid nitrogen, and then stored at –70°C until use. Samples were then mounted on a cryostat block using O.C.T. (Optimal Cutting Tissue) (Raymond A Lamb, London, UK) and left to warm up to –22°C in a cryostat (Bright Instruments, UK). Sections of 6 μm were then cut by Dr. Navid Ardjomand and deposed onto a multispot microscope slide (C.A. Hendley, Loughton, UK). Slides were left to dry overnight at RT before fixation in 100% acetone for 10 mins. Slides were then wrapped in foil and stored at –20°C until further use.

2.8.2- Staining

Antibody concentrations were optimised on MCE cells cytospins and on mouse spleens (ICAM-1, VCAM-1 and PECAM-1). Cryosections were thawed out in the foil for 10 mins at RT before staining whereas cytospins were fixed in a 50% methanol/ 50% acetone mixture for 10 mins, just prior to use. Slides were incubated for 30 mins with 5 μg/ml (ICAM-1, PECAM-1) or 10 μg/ml (VCAM-1) of primary antibody at RT in a humidified chamber. In the meantime, the appropriate secondary antibody (rabbit anti-mouse biotinylated or rabbit anti-rat biotinylated antibodies

(both from VECTOR Laboratories)) were diluted to a concentration of 1 μg/ml in PBS containing 2% mouse serum (Sigma) and incubated for 30 mins at RT before use. The cryosections were then washed twice in PBS and incubated for a further 20 mins with the appropriate secondary antibody at RT. The biotinylated secondary antibody was then detected using avidin covalently conjugated to an horseradish peroxidase enzyme provided in a VECTASTAIN® Elite ABC Kit prepared according to the manufacturer instructions (VECTOR Laboratories): 1drop of Reagent A and 1 drop of Reagent B were added to 2.5 ml of PBS, the solution was then mixed thoroughly and allowed to stand for 30 mins before use. Details on reagents A and B were not provided by the manufacturer (VECTOR Laboratories). Slides were incubated with 1 drop/well of this solution for 5 to 10 mins at RT and washed twice with PBS. The peroxidase substrate, DAB (diaminobenzidine) was prepared as recommended by the manufacturer (DAKO, Carpinteria, CA, USA): 1 drop of the DAB chromogen was added to 1ml of buffered substrate and the mixture was added to the slides for 1 min, or until a brown colour developed. Slides were then washed twice with tap water and counterstained in 0.1% Mayer's hematoxylin solution (Sigma) for 2 mins. After a wash under running tap water for 10 mins, slides were left to dry at RT and finally mounted in Kaiser's gelatin jelly (Merck).

2.9- Adhesion assay

2.9.1- Seeding of adherent cells

Cells were seeded in triplicates, onto a flat-bottomed 96-well plate (Nunc), 48 hours before the assay. Immediately before the assay, cells were gently washed twice with warm culture medium and left in 100 μl medium for the assay. When suitable, cells were treated with cytokines for 24h and/or were incubated for 30 mins with blocking antibodies, prior to the addition of labelled cells.

2.9.2- Purification of human Polymorphonuclear cells (PMN)

20 ml of whole blood were drawn on heparin (mucous) (5 IU/ml blood) (CP Pharmaceuticals Limited, Wrexham, UK) in a 50 ml conical tube. The tube was then filled up with 1X PBS kept at room temperature (RT) and inverted several times to homogenise the mixture. 25 ml of diluted blood were then gently laid on 15 ml Nycomed Lymphoprep (Nycomed Pharma AS, Oslo, Norway) and the tube was spun down at 300g, for 25 minutes, at RT without brake. After centrifugation, a whitish cloudy ring of cells (PBMC) was present in the upper part of the tube and was collected. The bottom of the tube contains a pellet of red blood cells (RBC) and PMN. The supernatant was collected (5 ml left) using a 25 ml pipette and discarded. The pellet was resuspended in cold sterile water and pipetted up and down on ice for exactly 30 seconds. PMN are less sensitive to lysis than RBC and are therefore preserved if this time is respected. The lysis was ended by the addition of 25ml cold 2X PBS. Cells were spun down at 300g for 5 minutes at 4°C. The supernatant was collected up to the 10 ml graduation: lysis of RBC produces a red opaque supernatant

that makes the localisation of the pellet very difficult. The lysis step using cold water was then repeated twice, the last centrifugation produces a white-greyish pellet of PMN. Cells were washed in medium and counted. When suitable, cells were incubated for 30 minutes with 50 ng/ml of Phorbol Myristate Acetate (PMA) (Sigma).

2.9.3- Purification of human Peripheral Blood Mononuclear Cells (PBMC)

The whitish cloudy ring of cells containing PBMC in the cell separation above was collected in a 50 ml tube. The tube was filled with 1X PBS at RT and the cells are spun down at 300g for 5 minutes at 20°C. The supernatant was discarded and the PBMC were resuspended in medium and counted. Half of the population was stimulated for 30 minutes with 50 ng/ml of PMA.

2.9.4- Purification of human T cells

Human T cells were purified by Dr W. Jordan from PBMC prepared as detailed above. PBMC were first incubated for 30 mins at 37°C in a tissue culture flask containing complete RPMI medium (RPMI supplemented with 100 IU/ml penicillin, 100 μg/ml streptomycin, 2mM L-glutamine, 1mM sodium pyruvate). Non adherent cells were then removed and resuspended in 1 ml of ice-cold complete RPMI medium containing a cocktail of the following antibodies, each at a final concentration of 10 μg/ml: anti-CD56, anti-CD14 (both from Dako), anti-CD11b and anti-CD19 (both purified from supernatants of in-house hybridomas cultures (OKM1 and BU12 respectively)). Cells were incubated with the antibody cocktail for 30 mins at 4°C. After one wash to remove excess antibody, cells were incubated with immunomagnetic beads coated with sheep anti-mouse IgG (Dynal, Oslo, Norway) at

a 4:1 bead to target cell ratio. The incubation was carried out on a roller, for 45 mins at 4°C, in a total volume of 1 ml. Bound cells were then removed using a magnet while non-bound cells were submitted to another round of purification, this time with a ratio of 2 beads/target cell. Cells were then counted and resuspended in complete medium supplemented with 10% heat-inactivated FCS before use in adhesion assay experiments.

2.9.5- Purification of mouse splenocytes

The spleens of two BALB/c mice were mashed in medium on a cell strainer (70μ) (Becton Dickinson Labware) using the plunger of a 5ml syringe. The suspension was then applied onto a second cell strainer on a 50 ml tube that was then filled with medium. The cells were spun down at 300g for 5 minutes and washed twice in 1X PBS. The pellet was then resuspended in 1X H-lyse buffer (Erythrocyte lysing kit, R&D Systems Europe Ltd) (2 ml / spleen) and incubated for 10 minutes at RT. The tube was then filled with 1X Wash Buffer (Erythrocyte lysing kit, R&D) and spun down at 300g for 5 minutes. Cells were resuspended in medium and counted. When suitable, the cells were incubated with 1 μg/ml PMA and 1 μg/ml ionomycin (Sigma) for 24h before being used in the adhesion assay.

2.9.6- Labelling of leukocytes

Calcein AM (acetoxymethyl) (Molecular Probes, Leiden, Netherlands) is a colourless dye that can permeate cells and becomes green fluorescent once hydrolysed.

Leukocytes were counted, washed once in warm sterile PBS and resuspended in culture medium containing 3 μM Calcein AM, with a maximum of $5x10^6$ cells per ml

of labelling medium. Cells were incubated for 1 hour at 37°C and washed once with warm medium for 10 mins at 300g.

2.9.7- Adhesion assay

Labelled cells were added to the adherent cells in 100 μl medium and incubated for 1 hour at 37°C. Medium was then gently removed, and cells were washed 3 times with warm medium to get rid of the unbound labelled cells. 100 μl of medium was left at the end of the assay and the plates were read on a fluorimeter (Cytofluor 2300). Wells containing medium or labelled cells only were not washed and constituted respectively the 0% and 100% controls required for the analysis (figure 3).

Adhesion assays were repeated at least three times but only representative data are presented in the results section of this thesis. To determine whether the difference in adhesion between resting and stimulated cells was significant, a Student's t-test was applied on triplicates from representative data (the data is assumed to be normally distributed when choosing this test).

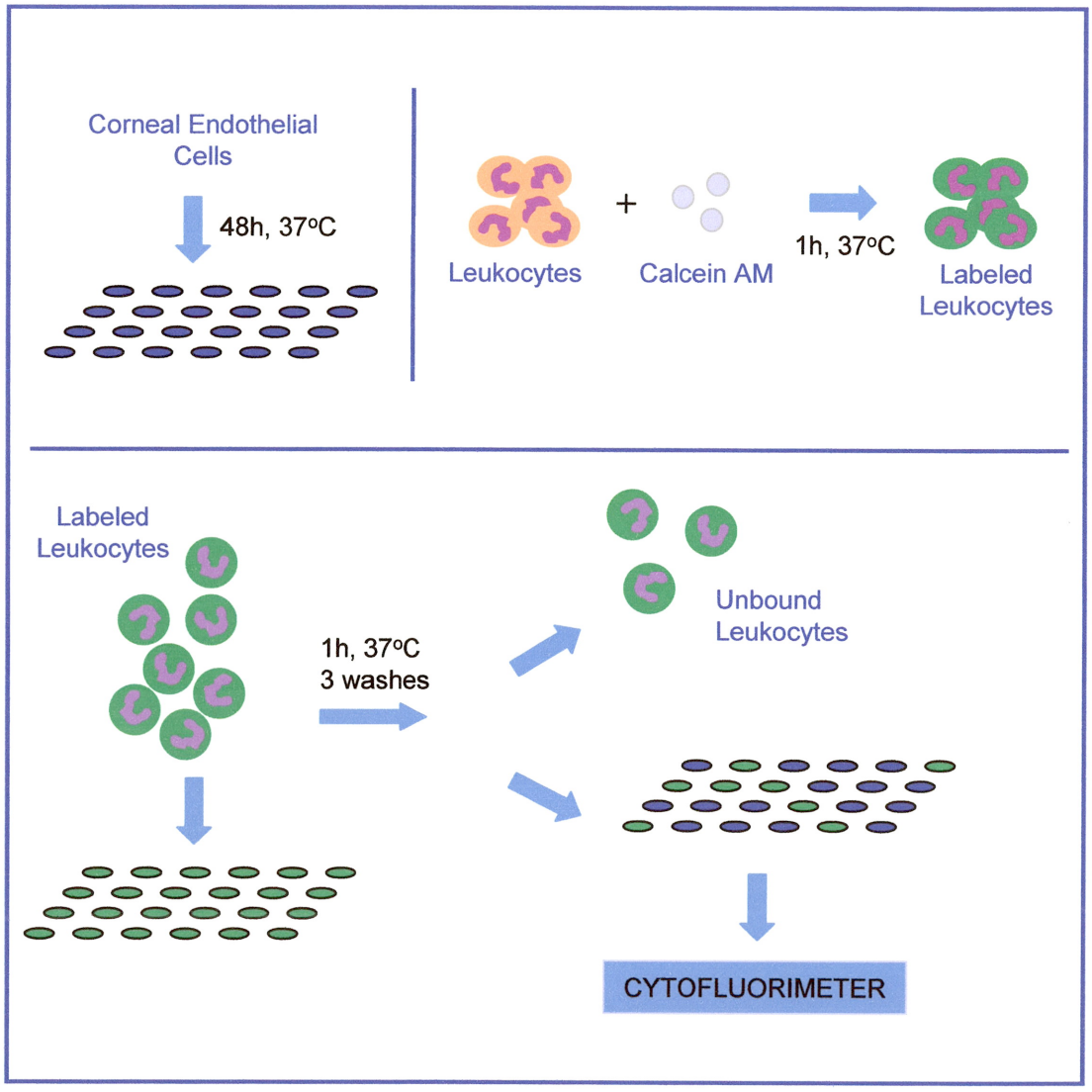


Figure 3: Adhesion assay protocol diagram.
Cell monolayers were seeded in triplicates, onto a flat-bottomed 96-well plate, 48 hours before the assay. Before the assay, leukocytes were incubated with Calcein AM, a dye taken in by cells, that becomes green fluorescent when hydrolysed. When suitable, monolayer cells were treated with cytokines for 24 hours and/or incubated for 30 mins with blocking antibodies, prior to the addition of labelled cells for 1 hour at 37°C. Plates were finally washed 3 times in warm medium and cells adherent to the monolayer were counted in a cytofluorimeter.

2.10- Modulation of VCAM-1 expression in MCE BALB/c cells

2.10.1- Inhibition of VCAM-1 expression in MCE cells using Vitamin E

MCE BALB/c cells were seeded at $0.5x10^6$ cells per well in a 24-well plate on day 0. On day 1, cells were washed with PBS and incubated with vitamin E (Sigma) for a further 24 hours at 37°C: the stock solution of vitamin E (0.02 M in ethanol) was diluted 1:20 in FCS and then appropriately in culture medium, in order to obtain a final concentration ranging from 20 to 500 μM. Cells were then washed in PBS and incubated with a combination of cytokines (20 ng/ml TNFα, 20 ng/ml IL-1α and 600 IU/ml IFNγ) for a further 8 hours at 37°C. Cells were finally detached with trypsin and the expression of VCAM-1 was analysed using Flow Cytometry as detailed above.

2.10.2- Inhibition of VCAM-1 expression in MCE cells by transfection of a single chain anti-VCAM-1 antibody

MCE BALB/c cells were seeded in a 24-well plate at a density of $0.5x10^6$ cells per well and were transfected the next day when about 70% confluent.

The cells were transfected by lipofection using LipofectAmine 2000 (Invitrogen) and the conditions optimised by Dr C. V. Arancibia-Carcamo. Basically, plasmid DNA was complexed with the LipofectAmine reagent by incubating the mixture in serum free medium for 30 minutes at RT, using a liposome:DNA ratio of 4 μl : 0.4 μg. The DNA:LipofectAmine complexes were then added to the cells and incubated for 3 hours at 37°C, 5% CO_2. After 3 hours, cells were washed once in PBS and grown in complete culture medium.

The following plasmids were used alone or in co-transfection:

-pCMV/EGFP (Clontech, Basingstoke, UK) encoding for a yellow variant of the Green Fluorescent Protein (GFP) under a CMV promoter.

-pE6/scFv (gift from Dr. P. Ramrakha, Imperial College London) encoding an scFv, a porcine VCAM-specific single chain antibody. When expressed in endothelial cells, the scFv "intrabody" binds to VCAM-1 as it is synthesised within the cell, and retains it within the endoplasmic reticulum. In porcine EC stably transfected, intracellular expression of the scFv "intrabodies" led to the inhibition of 90% of VCAM-1 expression and abolished VCAM-dependant adhesion of human leukocytes (Ramrakha *et al.*, submitted).

The day following transfection, cells were washed in PBS and incubated with a combination of cytokines (TNFα, IL-1α and IFNγ) for 24 hours at 37°C. The expression of VCAM-1 on the transfected cells was finally analysed by Flow Cytometry as detailed above.

CHAPTER 3

Adhesion Molecules in the Mouse Cornea

Adhesion molecules in the mouse cornea

3.1- Expression of adhesion molecules in the mouse cornea

As opposed to syngeneic grafts or accepted corneal allografts, the rejection of corneal grafts is accompanied by an elevation of pro-inflammatory cytokines (Torres *et al.*, 1996; Sano *et al.*, 1998; King *et al.*, 2000). In fact, King *et al.* identified an early phase where cytokines increased in both iso- and allografts. This early rise in cytokines corresponds to the response to surgical trauma. These levels of cytokines were however sustained (or further increased) only in the allografts (King *et al.*, 2000). As reviewed by Bevilacqua (Bevilacqua, 1993), pro-inflammatory cytokines are responsible for the induction or up-regulation of adhesion molecules in the vascular endothelium. We therefore investigated whether similar patterns of up-regulation occurred in the rejecting mouse corneal allograft.

The basal level of adhesion molecule expression and the influence of pro-inflammatory cytokines were investigated using RT-PCR, FACS analysis, immunofluorescence and histology. For this purpose, we used two different systems: a mouse corneal endothelial (MCE) cell line and whole excised corneas (or entire eyeballs for histology) both from BALB/c mice.

First, the endothelial origin of the cell line was confirmed. The neatly organized cobblestone-like morphology of the cells at confluence is typical of endothelial cells (chap. 2, fig. 2). Furthermore, an RT-PCR for collagen VIII, a marker specific for corneal endothelium confirmed the endothelial origin of the cell line. The collagen VIII molecule is found in the corneal endothelium, but not in the corneal stroma or epithelium (Kapoor *et al.*, 1988; Tamura *et al.*, 1991). Figure 1 shows a band at 329

bp, the expected size of the collagen VIII PCR product in both the MCE cell line and in the excised mouse cornea.

3.1.1-Expression of adhesion molecules mRNA in the mouse cornea

In order to investigate the presence of mRNA for adhesion molecules in these two models, we performed RT-PCR on samples incubated in control medium or in medium supplemented with various pro-inflammatory cytokines.

RT-PCR reactions for ICAM-1, VCAM-1 and E-Selectin were optimized using the bEnd-1 cell line (brain vascular endothelium), whereas RT-PCR reactions for NCAM-1 and VAP-1 were optimized on mouse brain and liver respectively.

The housekeeping genes, GAPDH or HPRT were used as internal controls to correct for the possible variations in mRNA quantities applied to the gel. The gel was then analysed using a densitometer, which converts the intensity of each band in Pixel Density (PD) units. This semi-quantitative technique gives indications of the variations in adhesion molecule mRNA levels, but cannot quantify mRNA as it is limited by a "plateau effect" in high quantities of mRNA. Pixel density is only proportional to the mRNA concentration during the amplification stage. In addition, for this reason and because of the variable efficiency between several sets of primers, comparison between different adhesion molecule patterns of expression must be interpreted with caution.

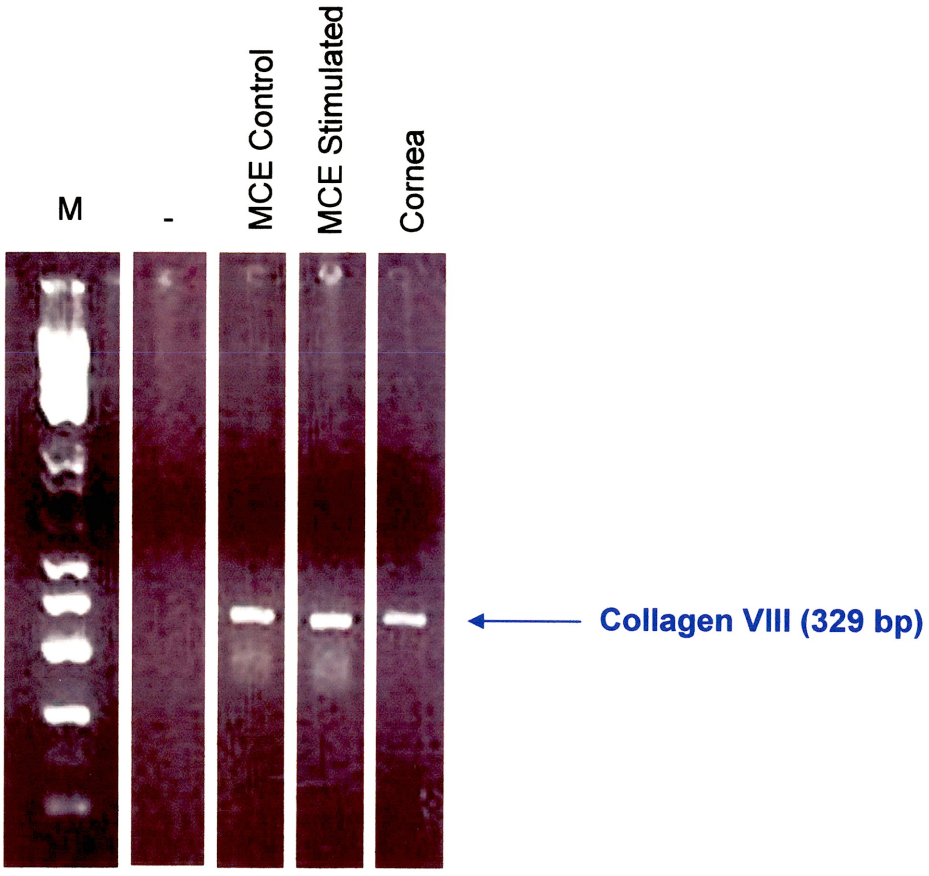


Figure 1: Collagen VIII mRNA expression in mouse corneal endothelial (MCE) cells and in one excised mouse cornea.
Total mRNA was extracted from mouse corneal endothelial cells (MCE BALB/c cells) and a pool of six mouse corneas, and was used in RT-PCR reactions specific for mouse collagen VIII, a specific marker for corneal endothelium.The gel shows the presence of Collagen VIII mRNA in both the MCE cell line (whether cells resting or stimulated with a triple combination of pro-inflammatory cytokines for 24 hours) and the excised tissue. This RT-PCR confirms the endothelial origin of the cell line and the presence of the endothelium on the excised corneal tissues used for RT-PCR. The PCR products were visualised by electrophoresis on a 1.5% agarose gel stained with ethidium bromide (10 mg/ml). Keys: M=Molecular weight marker; - = no cDNA.

3.1.1.1- Expression of adhesion molecules mRNA in the MCE cell line

Figure 2 presents a summary of the adhesion molecules tested by RT-PCR in the resting mouse corneal endothelial cell line. These molecules were tested in at least three batches of MCE cultures. Gel (A) demonstrates the presence of a faint band at 404 bp, the ICAM-1 PCR product. Stronger bands are detected at 839 and 714 bp, the respective sizes of the VCAM-1 and E-Selectin PCR products. Finally, PCR products for NCAM-1 (B) and VAP-1 (C) are also detected at the expected sizes of 309 and 409 bp respectively.

The MCE cells were then stimulated with various pro-inflammatory cytokines: TNFα (20 ng/ml), IFNγ (600 IU/ml), IL-1α (20 ng/ml) or a combination of the three cytokines. Figure 3 shows a summary of the PCR products obtained in the different conditions of stimulation. Figures 4, 5 6 and 7 present the Pixel Density (PD) analysis of representative PCR realized on cells stimulated respectively with TNFα, IFNγ, IL-α and the triple combination of cytokines.

As shown on figure 4, ICAM-1 mRNA was up-regulated upon stimulation with TNFα. The mRNA expression peaked after 4 hours of stimulation with a PD basal level increased nearly eight times. At 4h, the expression started to decrease, but the PD was still more than 5 times higher than in resting cells, after 24 hours of stimulation. VCAM-1 mRNA expression followed the same pattern but to a lesser extent, as the peak PD at 4h was only increased by 1.3 fold, and the level at 24h was less than 1.2 times the basal level. E-Selectin mRNA expression reached a maximum after 2 hours of TNFα stimulation, with nearly a two fold-increase in PD compared to the basal level.

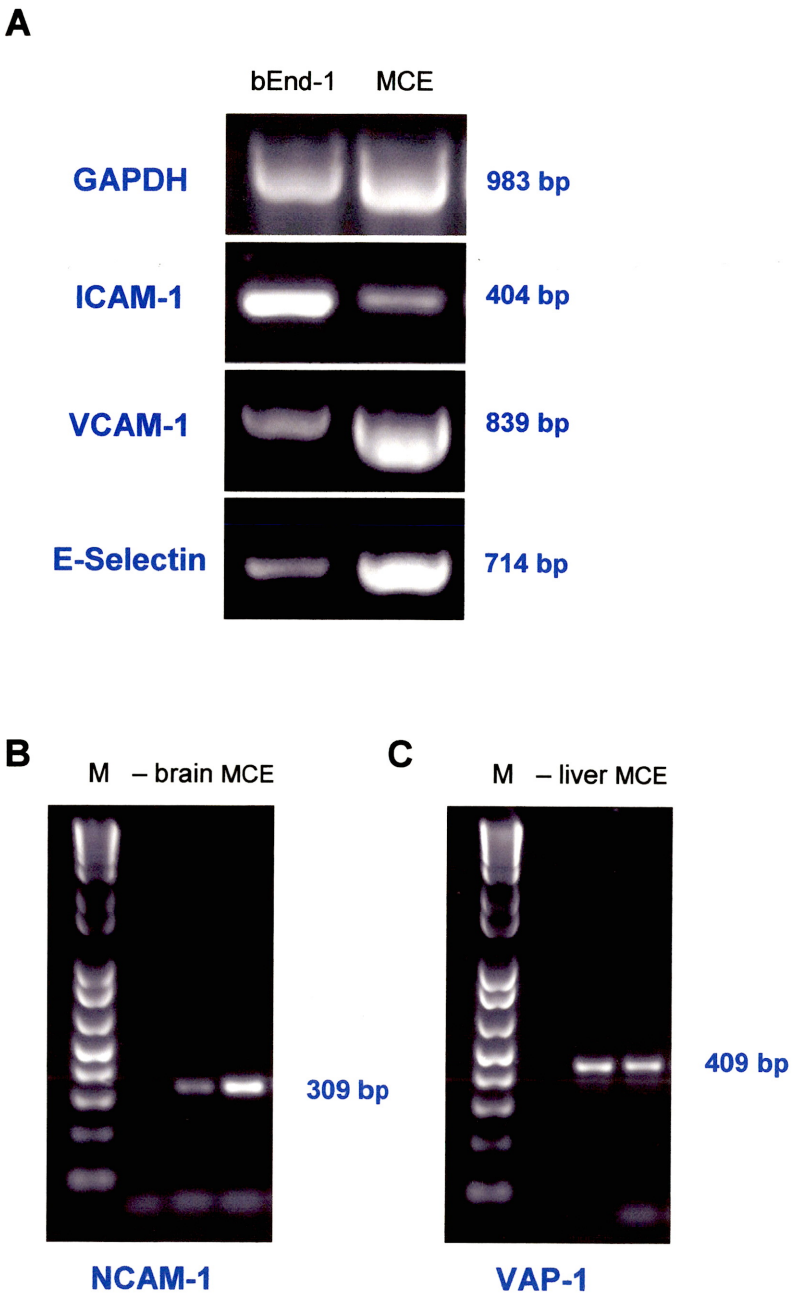


Figure 2: Adhesion molecules mRNA expression in resting mouse corneal endothelial (MCE) cells.
Total mRNA was extracted from mouse corneal endothelial cells (MCE BALB/c cells) and used in RT-PCR reactions specific for mouse adhesion molecules. Mouse brain endothelial cells (bEnd-1) were used as positive controls in the RT-PCR for ICAM-1, VCAM-1 and E-Selectin (A), whereas mouse brain and liver tissues were used as positive controls for the NCAM-1 (B) and VAP-1 (C) RT-PCR respectively. The figure presents the PCR products obtained after electrophoresis on a 1.5% agarose gel stained with ethidium bromide.
Keys: M=Molecular weight marker; - = no cDNA.

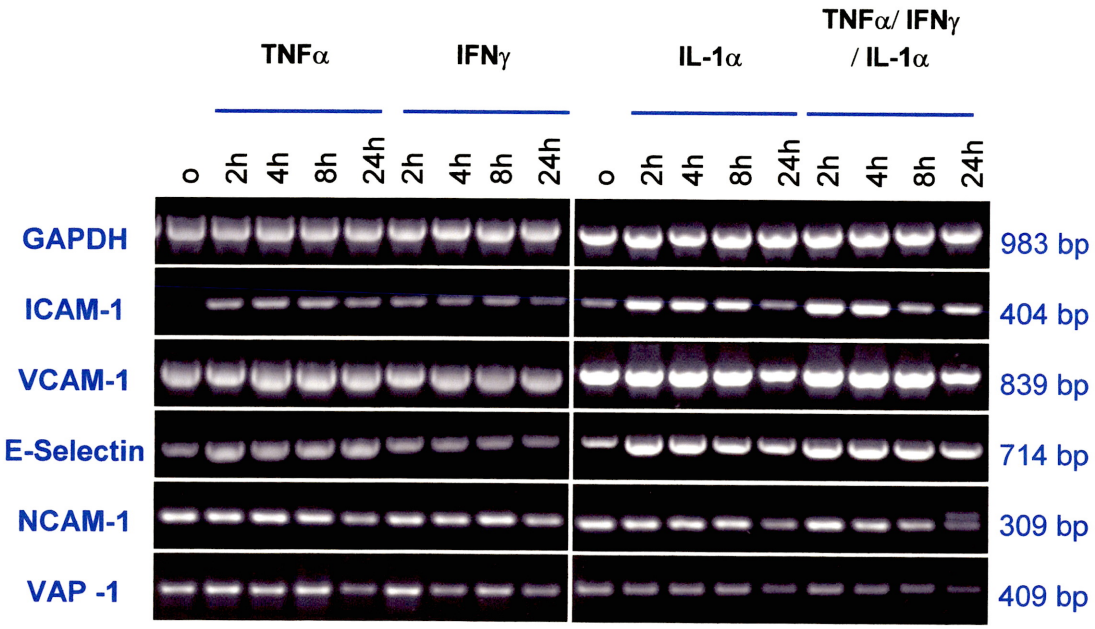


Figure 3: Adhesion molecules mRNA in mouse corneal endothelial (MCE) cells stimulated with cytokines.
Mouse corneal endothelial cells (MCE BALB/c) were stimulated with various cytokines (TNFα 20ng/ml, IFNγ 600 IU/ml, IL-1α 20 ng/ml) or a cocktail of the three cytokines for periods between 0 and 24h. Total mRNA was then extracted and used in RT-PCR reactions specific for mouse GAPDH, ICAM-1, VCAM-1, E-Selectin, NCAM-1 and VAP-1. The PCR products were then visualised by electrophoresis on an ethidium bromide-stained agarose gel.

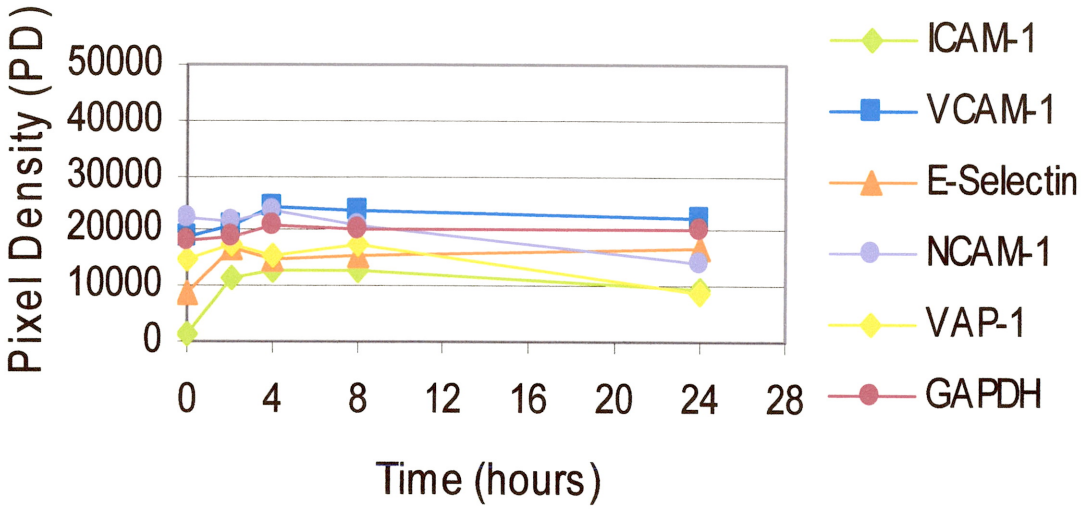


Figure 4: Pixel Density analysis of adhesion molecules PCR products in mouse corneal endothelial (MCE) cells stimulated with TNFα.
The gel shown in figure 3 was analysed using a densitometer. The graph shows the mean Pixel Density (PD) (not corrected for GAPDH) obtained for ICAM-1, VCAM-1, E-Selectin, NCAM-1 and VAP-1 PCR products in cells stimulated up to 24 hours with 20 ng/ml TNFα.

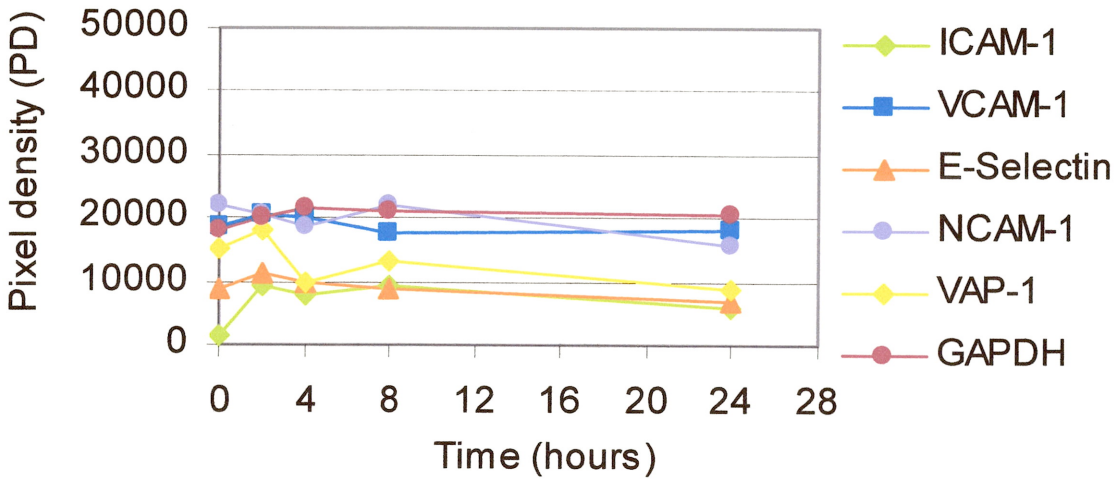


Figure 5: Pixel Density analysis of adhesion molecules PCR products in mouse corneal endothelial (MCE) cells stimulated with IFNγ.
The gel shown in figure 3 was analysed using a densitometer. The graph shows the mean Pixel Density (PD) (not corrected for GAPDH) obtained for ICAM-1, VCAM-1, E-Selectin, NCAM-1 and VAP-1 PCR products in cells stimulated up to 24 hours with 600 IU/ml IFNγ.

The level of expression remained approximately the same after 24 hours of stimulation. Upon stimulation with TNFα, levels of PD for NCAM-1 and VAP-1 were decreased 1.5 and 1.7 times respectively, as compared to their basal levels (figure 4).

IFNγ stimulation had a very moderate effect on the mRNA expression of VCAM-1 and E-Selectin in MCE cells, with only respectively a 1.1 and 1.3 fold-increase in PD after 2 hours of stimulation (figure 5). However, the PD for ICAM-1 was increased 5.7 times in 2 hours after stimulation with this same cytokine. After 24 hours, the PD remained 3.5 times higher than in resting cells. As with TNFα, NCAM-1 and VAP-1 mRNA expression decreased with time, to reach a PD respectively 1.4 and 1.7 times lower than in the resting cells (figure 5).

VCAM-1 mRNA expression was only moderately altered by the stimulation with IL-1α (only a 1.1 fold-increase in PD at 4 hours) (figure 6). ICAM-1 and E-Selectin PD were however increased 2.8 and 2.2 times respectively after 2 hours of stimulation. After 8 hours, the PD for ICAM-1 was still 2.3 times higher than in the non-stimulated cells, then it started to decrease to reach roughly the basal level after 24 hours (figure 6). At the same time, E-Selectin PD remained high with a 1.6 fold-increase, compared to the basal level (figure 6). Both NCAM-1 and VAP-1 PD levels were reduced by a factor of 2.1 after stimulation with IL-1α for 24 hours (figure 6).

Finally, stimulation with a combination of the three cytokines induced a 3.3 and 2.2 fold-increase in ICAM-1 and E-Selectin PD at 2 hours (figure 7). Levels remained high (1.9 and 1.7 times higher than basal levels respectively) after 24 hours of stimulation.

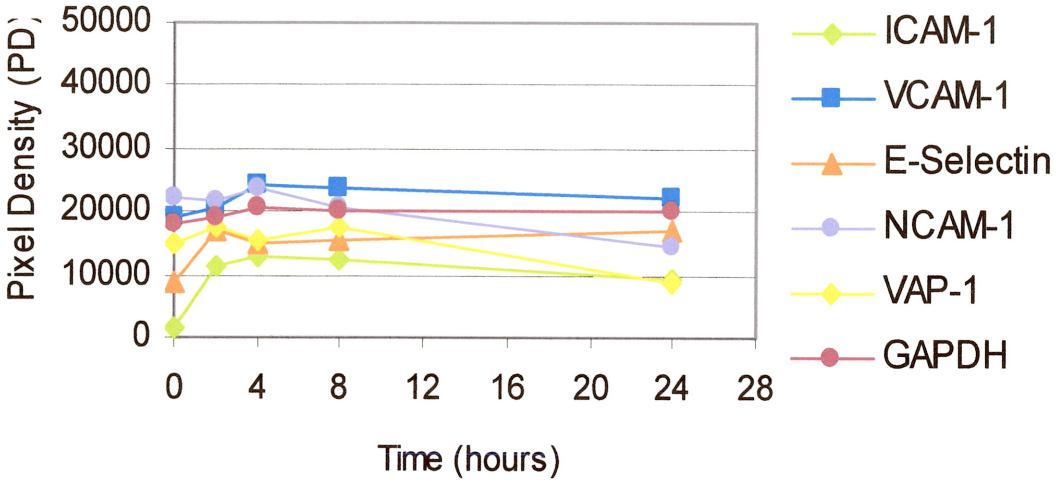


Figure 6: Pixel Density analysis of adhesion molecules PCR products in mouse corneal endothelial (MCE) cells stimulated with IL-1α.
The gel shown in figure 3 was analysed using a densitometer. The graph shows the mean Pixel Density (PD) (not corrected for GAPDH) obtained for ICAM-1, VCAM-1, E-Selectin, NCAM-1 and VAP-1 PCR products in cells stimulated up to 24 hours with 20 ng/ml IL-1α.

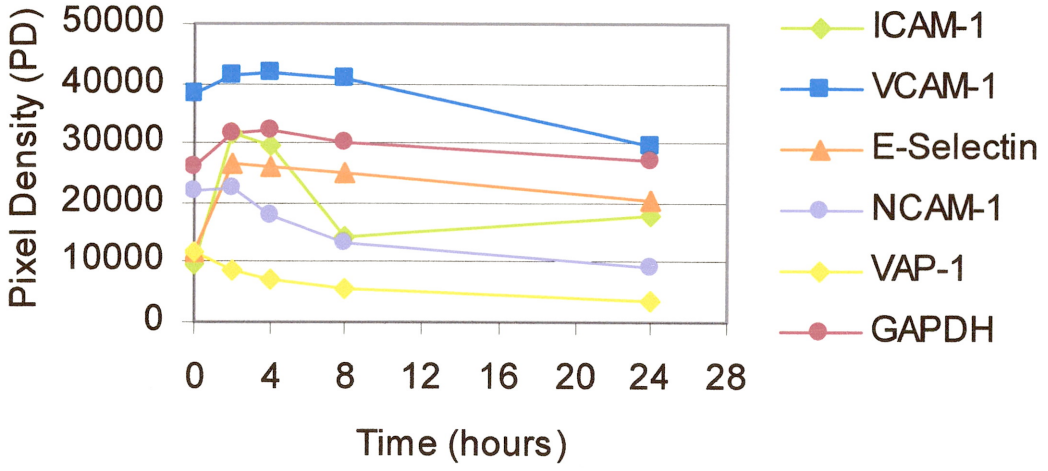


Figure 7: Pixel Density analysis of adhesion molecules PCR products in mouse corneal endothelial (MCE) cells stimulated with TNFα, IL-1α and IFNγ.
The gel shown in figure 3 was analysed using a densitometer. The graph shows the mean Pixel Density (PD) (not corrected for GAPDH) obtained for ICAM-1, VCAM-1, E-Selectin, NCAM-1 and VAP-1 PCR products in cells stimulated up to 24 hours with 20 ng/ml TNFα, 600 IU/ml IFNγ and 20 ng/ml IL-1α.

Again, levels of VCAM-1 mRNA were not very much affected by the triple stimulation with only a 1.1 increase in PD at 4 hours. As with the single cytokine stimulations, NCAM-1 and VAP-1 mRNA levels decreased with time (2.4 and 3.3 fold-decrease in PD respectively) (figure 7).

Altogether, these data show that, ICAM-1, E-Selectin and to a lesser extent VCAM-1 mRNA were up-regulated by TNFα, IL-1α and the triple combination. IFNγ, however, only slightly up-regulated the expression of ICAM-1 mRNA. NCAM-1 and VAP-1 mRNA expression decreased in time in all the conditions of stimulation.

3.1.1.2- Expression of adhesion molecules mRNA in the excised cornea

The expression of mRNA for these same adhesion molecules was then investigated *ex vivo* in excised mouse corneas. BALB/c mice corneas were excised from enucleated eyes and incubated for 4h with control medium or medium supplemented with the triple combination of cytokines (TNFα, IFNγ and IL-1α). After the incubation, specimens were snap frozen and stored at –70°C until the RT-PCR procedure. A pool of six mouse corneas was used in each condition. mRNA was extracted and the procedure followed as above with the MCE cell line.

Figure 8 shows the PCR products obtained from the excised mouse corneas and from MCE cells used here as controls for the experiment. Results of the gel analysis by densitometry are presented in figure 9 (VCAM-1 is presented separately as the amount of cDNA added in the PCR was 5 times lower than in the other PCR). As in the MCE cell line, ICAM-1 mRNA is present only in small amounts in the resting cornea whereas VCAM-1 mRNA is detected in much higher quantities (figure 8).

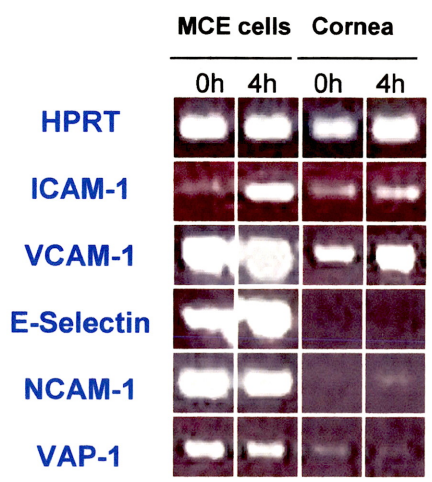


Figure 8: Adhesion molecules mRNA expression in mouse corneal endothelial (MCE) cells and excised mouse corneas with or without stimulation with cytokines.
Mouse corneal endothelial cells (MCE BALB/c) and a pool of six mouse corneas were incubated for 4 hours with control medium or medium containing a cocktail of three cytokines (TNFα 20 ng/ml, IFNγ 600 IU/ml, IL-1α 20ng/ml). Total mRNA was then extracted and used in RT-PCR reactions specific for mouse HPRT, ICAM-1, VCAM-1, E-Selectin, NCAM-1 and VAP-1. PCR products were visualised on a agarose gel stained with ethidium bromide.

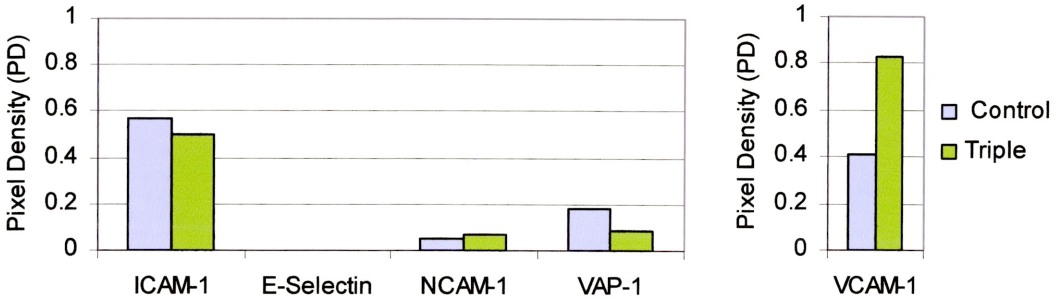


Figure 9: Adhesion molecules mRNA expression in excised mouse corneas with or without stimulation with cytokines.
A pool of six mouse corneas were incubated for 4 hours with control medium or medium containing a cocktail of three cytokines (TNFα 20 ng/ml, IFNγ 600 IU/ml, IL-1α 20ng/ml). Total mRNA was then extracted and converted in cDNA using reverse-transcriptase. 5μl of the cDNA preparation were then used in PCR reactions specific for mouse HPRT, ICAM-1, E-Selectin, NCAM-1 and VAP-1 (only 1μl for VCAM-1). The PCR products were finally visualised on a 1.5% agarose gel stained with 10 mg/ml ethidium bromide, analysed with a densitometer software. The graph shows the Pixel density analysis of this gel, after HPRT correction.

However, unlike the MCE cells, mouse corneas do not constitutively express E-Selectin or NCAM-1 mRNA. NCAM-1 mRNA, but not E-Selectin mRNA, is slightly induced by cytokines. VAP-1 mRNA is only found in very small quantities (figure 8).

Figure 9 presents the Pixel Density analysis of the gel presented in figure 8. Stimulation with cytokines increased the PD for NCAM-1 by 50%. The PD for ICAM-1 and VAP-1 were however decreased by 11% and 51% respectively. This variation of NCAM-1 mRNA expression needs to be interpreted with caution as the initial PD is 11 times lower than that of ICAM-1 and despite a 50% increase, the PD for NCAM-1 after stimulation remains nearly 8 times lower than the one for ICAM-1 (figure 9). However, and as detailed above, comparison between two sets of primers does not take into account differences in efficiency of amplification and the information provided is only of limited use unless PCR products are quantified.

VCAM-1 mRNA was detected in very high levels in the resting cornea; the stimulation with cytokines doubled this amount after 4 hours.

Taken together, these RT-PCR data show that the MCE cell line behaves very much like the mouse cornea tissue, when considering the mRNA expression of ICAM-1, VCAM-1, NCAM-1 and VAP-1. E-Selectin is the only adhesion molecule tested, that was detected in the cell line but not in the tissue. However, we need to bear in mind that the mRNA extracted from whole cornea tissues represents the mRNA not only from the endothelium (as in the MCE cell line), but also from the stroma and the epithelium of the cornea. Some discrepancies are therefore likely to arise. In addition, E-Selectin mRNA is detected in very low levels in the MCE cell line and might be below the threshold of detection in the whole cornea sample.

3.1.2- Expression of adhesion molecules proteins in the mouse cornea

The expression of adhesion molecule proteins in the mouse cornea was then investigated. First, we used FACS analysis on MCE cells incubated up to 48 hours, with control medium or medium containing pro-inflammatory cytokines. Protein expression was also analysed using 1) immunofluorescence on MCE cells cultured on glass slides or in flat-mounts of excised mouse corneas and 2) histology on eyeballs dissected from BALB/c mice.

3.1.2.1- Expression of adhesion molecules proteins in the MCE cell line

Trypsin is a rapid and effective reagent used routinely in our laboratory to detach cultured adherent cells from their support. The use of the reagent is however associated with enzymatic cleavage of some surface molecules. The effect of trypsin detachment on adhesion molecule detection was therefore determined using sEnd-1, a control cell line. Cells were detached using either a mild cell dissociation solution or trypsin. They were then stained for various adhesion molecules and the amount of adhesion molecules detected was determined by FACS analysis. Figure 10 compares the effect of cell detachment by the two reagents in resting (A) and activated cells (B). Figure 10A shows that the level of detection of ICAM-1 and E-Selectin are very similar with both cell detachment reagents. PECAM-1 detection, however, is reduced more than 4 times when trypsin is used. In stimulated cells (figure 10B), the level of detection is equivalent for all adhesion molecules tested, except again for PECAM-1 that is considerably decreased (4.6 fold) by trypsin detachment. Notably, murine PECAM-1 sensitivity to trypsin was also reported by Marelli-Berg and colleagues (Marelli-Berg *et al.*, 2000).

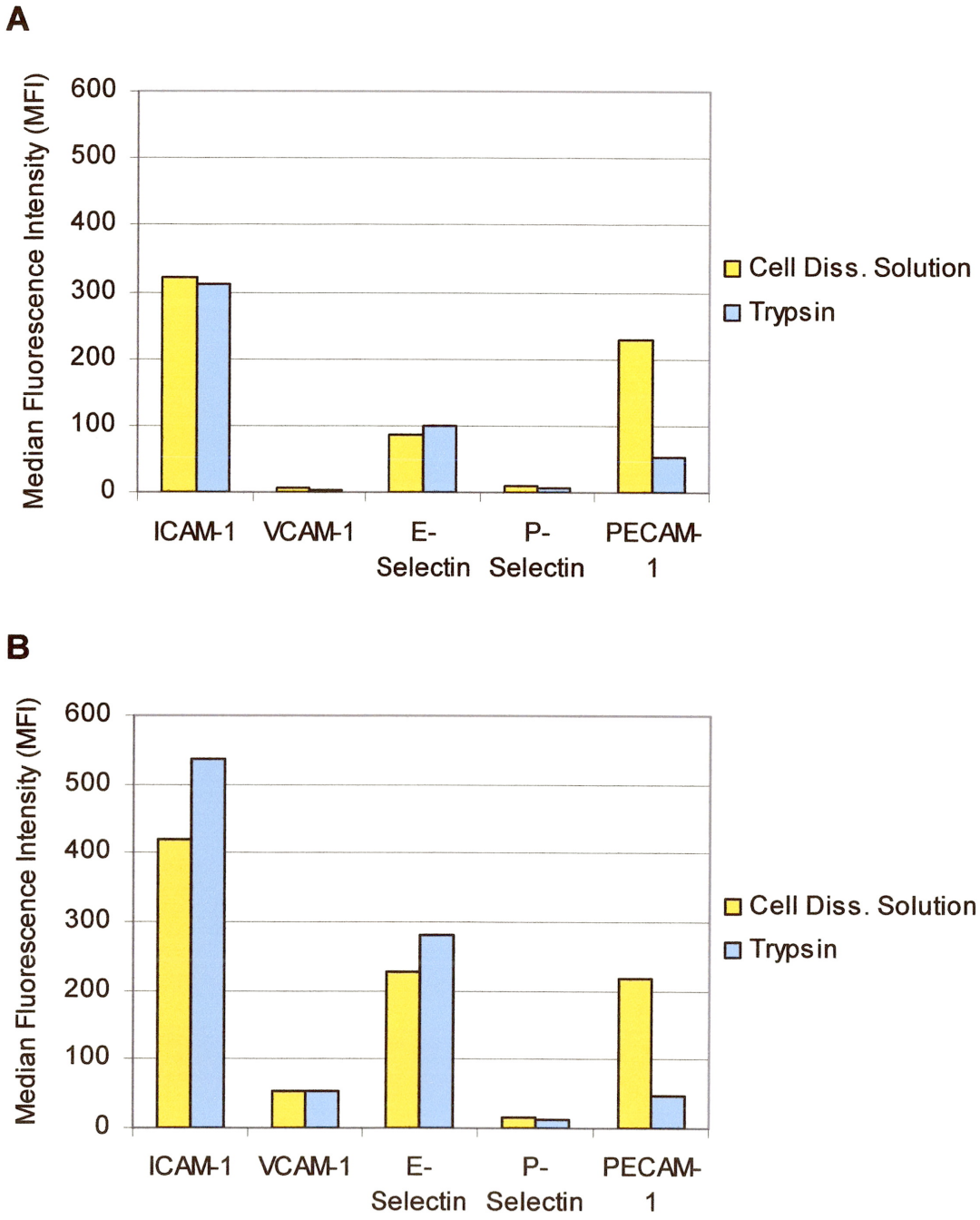


Figure 10: Effect of trypsin detachment on adhesion molecules detection in sEnd-1 cells, resting or stimulated with TNFα for 4 hours.
Resting sEnd-1 cells (A) or sEnd-1 cells stimulated with TNFα for 4 hours (B), were detached using trypsin or a cell dissociation solution, then stained with the relevant primary antibody and a secondary antibody conjugated to FITC, before cytofluorimetric analysis on a FACS Calibur. The level of adhesion molecules detected on cells detached with the two reagents is compared. The graphs show that among all the adhesion molecules tested, PECAM-1 is the only one whose level of detection is affected by trypsin detachment.

As the PECAM-1 molecule is removed by the trypsin treatment, we carried out all the PECAM-1 analysis on cells detached with the cell dissociation solution. However, all the other staining were performed on trypsinised cells, as it allowed shortening of the detachment step and therefore produced cells in better conditions for the subsequent staining.

a) Expression of adhesion molecules in the resting MCE cell line

Initially we stained resting MCE cells to determine the basal expression of the adhesion molecules on their surface. Figures 11 and 12 show respectively the FACS profiles and the Median Fluorescence Intensity (MFI) obtained for each staining. These are the representative data of one experiment repeated at least three times. The figures show the absence of PECAM-1 expression in the resting cells, a low expression of ICAM-1, E- and P-Selectin, and a very high constitutive expression of VCAM-1 (between 8 and 21 times the level of expression of ICAM-1, E- and P-Selectin) (figure 12). Positive controls are presented in figure 10. The constitutive expression of VCAM-1 was then confirmed on another mouse corneal endothelial cell line derived from MCE C57Bl6 mice, as shown on the FACS profiles presented on figure 13.

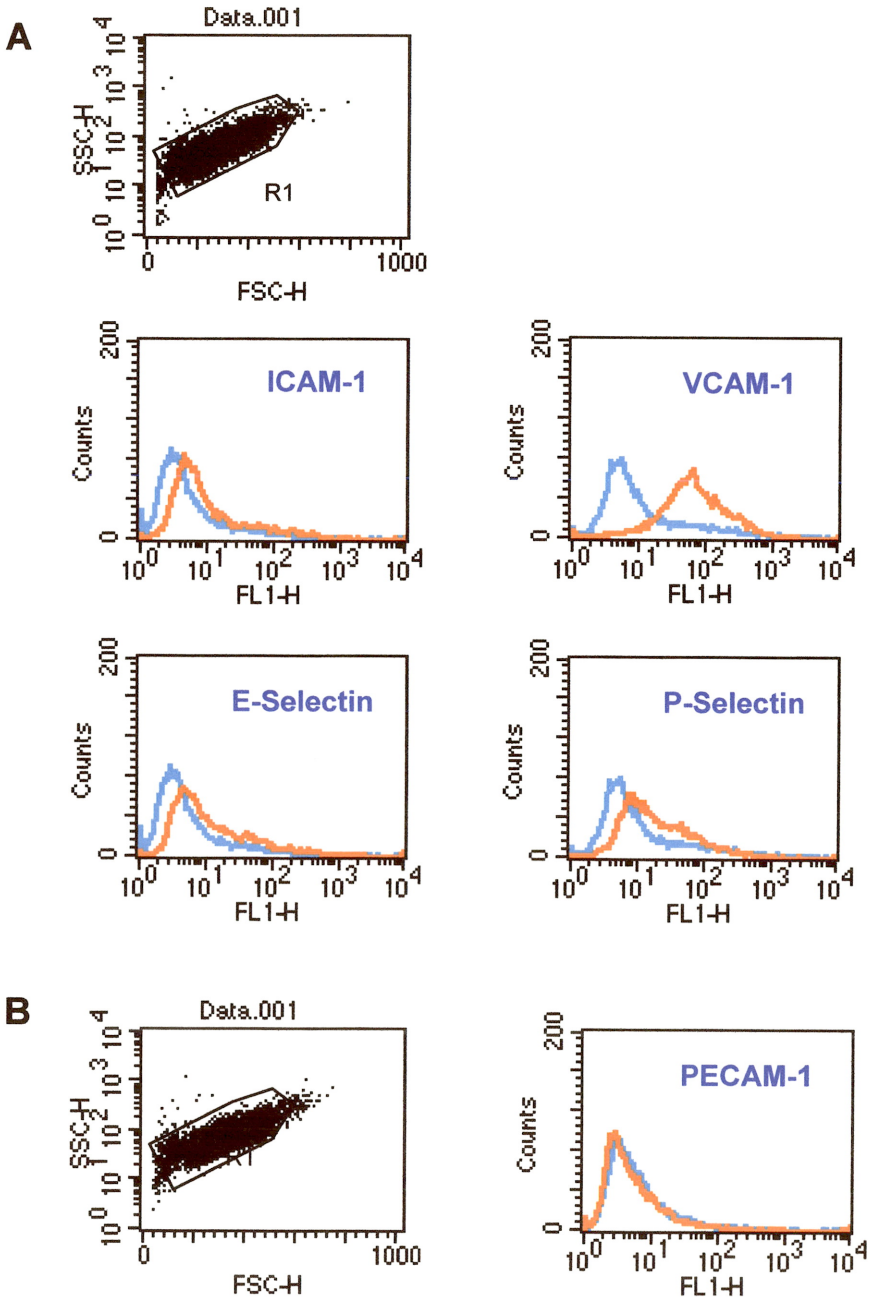


Figure 11: Expression of adhesion molecules in resting mouse corneal endothelial (MCE) cells.
Cultured cells were detached using trypsin (A) or cell dissociation solution (B), stained with the relevant primary antibody and a secondary antibody conjugated to FITC (FL1-H channel), before cytofluorimetric analysis on a FACS Calibur. The figure presents profiles of resting cells (orange) overlaid on isotype control profiles (blue). Dot blots present the gated population of MCE cells analysed in the experiment.

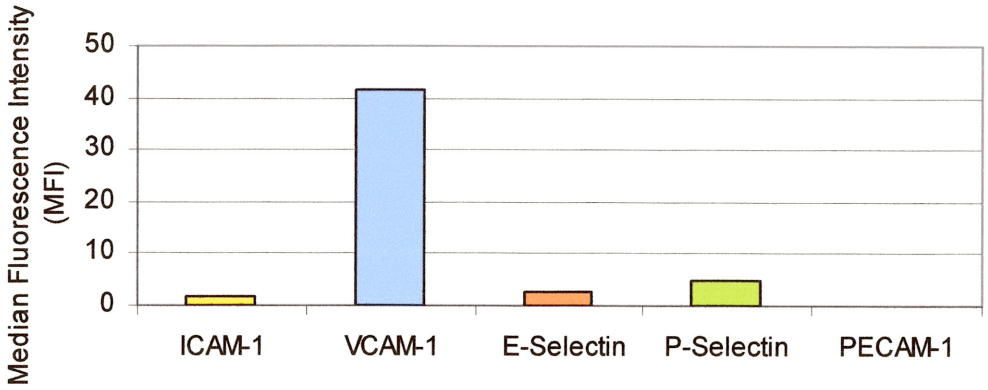


Figure 12: Adhesion molecules expression in resting mouse corneal endothelial (MCE) cells.
Cultured cells were detached using trypsin (or cell dissociation solution in the case of PECAM-1), stained with the relevant primary antibody and a secondary antibody conjugated to FITC, before cytofluorimetric analysis on a FACS Calibur. The graph presents the Median Fluorescence Intensity (MFI) obtained for each peak after deduction of the isotype control MFI. Positive controls are presented in figure 10.

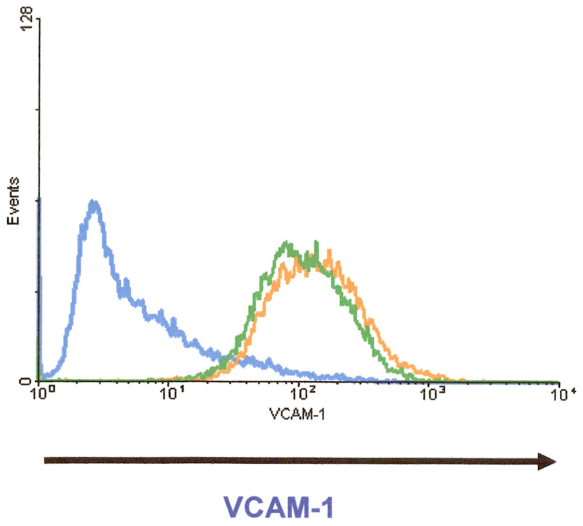


Figure 13: VCAM-1 protein is constitutively expressed in two different strains of MCE cells.
This figure presents the cytofluorimetric analysis of cultured mouse corneal endothelial (MCE) cells after staining with an isotype control antibody (blue) or an anti-mouse VCAM-1 antibody (10 μg/ml) (MCE BALB/c in orange and C57BL6 in green). Both cell lines show a constitutive expression of VCAM-1.

Cells were then stimulated up to 48 hours with TNFα, IFNγ, or IL-1α alone, a combination of TNFα and IFNγ or a combination of the three cytokines, before staining for adhesion molecules and FACS analysis. Results are presented in figures 14, 15, 16, 17 and 18 respectively. Experiments were repeated at least three times. One representative set of data is shown.

b) Expression of adhesion molecules in MCE cells exposed to TNFα

TNFα had virtually no effect on the expression of ICAM-1, PECAM-1, E- or P-Selectin proteins. However, the expression of VCAM-1 was increased nearly 2.5 times after 2 hours and was more than 3 times higher than in the resting cells after 24 hours of stimulation (figure 14). In endothelial cells, P-Selectin is stored in Weibel-Palade bodies, and is rapidly released upon cellular activation. The level of expression after 30 minutes of cytokine activation was therefore tested and was found similar to the level of expression in resting MCE cells (data not shown).

c) Expression of adhesion molecules in MCE cells exposed to IFNγ

IFNγ stimulation of the MCE cells increased the expression of P-Selectin only, but the 1.4 and 2 fold-increases at 4 and 24 hours respectively are not significant as the basal level was so low. Again, the level of P-Selectin expression at 30 mins was similar to the level in resting cells (data not shown). The stimulation with IFNγ had barely any effect on the other adhesion molecules tested, except on VCAM-1 expression that was decreased by nearly 18% after 24 hours (figure 15).

The 11.4 fold-increase in MHC class I expression demonstrates the activity of the IFNγ used in the experiment (figure 15).

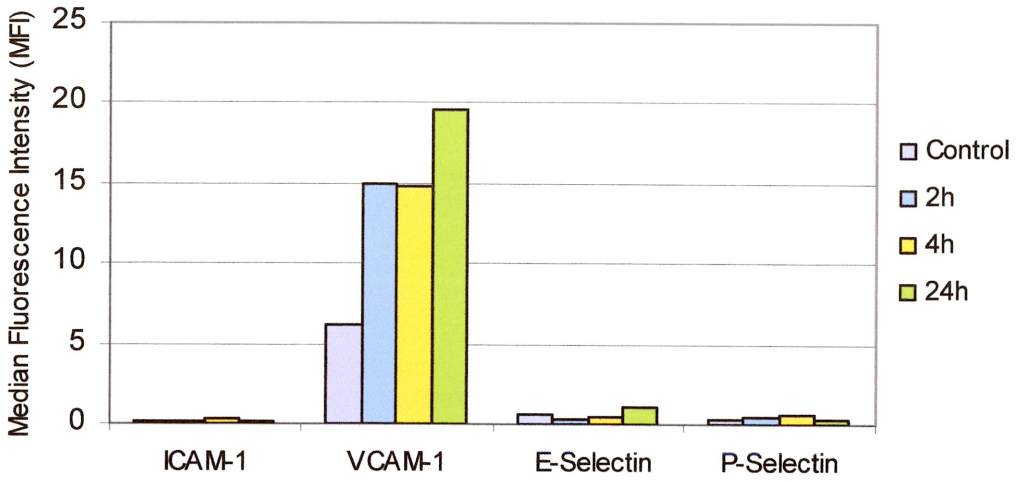


Figure 14: Effect of TNFα on adhesion molecules expression in mouse corneal endothelial (MCE) cells.
Cultured MCE cells were stimulated with 20 ng/ml TNFα for 0, 2 4 and 24 hours, detached using trypsin and stained as above before cytofluorimetric analysis. The graph presents the Median Fluorescence Intensity (MFI) obtained for each peak after deduction of the isotype control MFI.

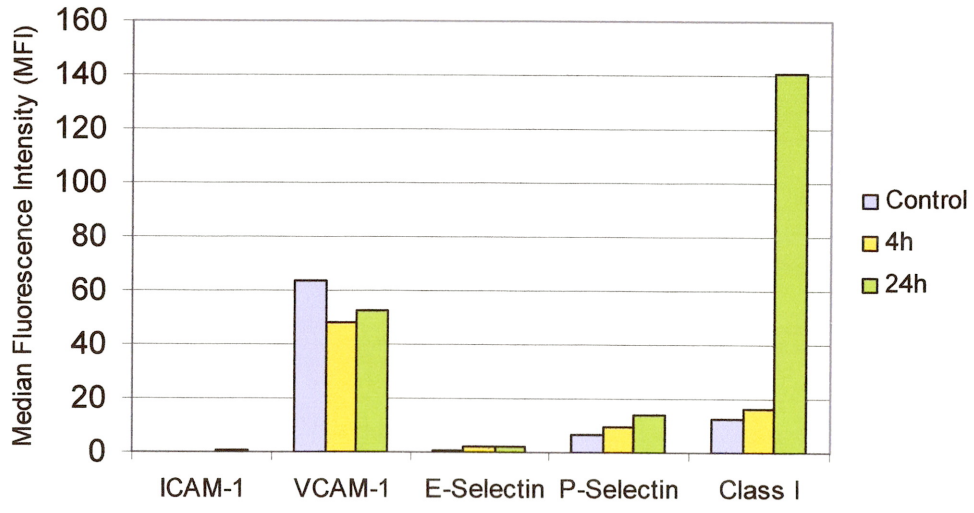


Figure 15: Effect of IFNγ on adhesion molecules expression in mouse corneal endothelial (MCE) cells.
As above, MCE cells were stimulated with 600 IU/ml IFNγ for 0, 4 and 24 hours, detached using trypsin and stained before cytofluorimetric analysis. The graph presents the Median Fluorescence Intensity (MFI) obtained for each peak after deduction of the isotype control MFI.

d) Expression of adhesion molecules in MCE cells exposed to IL1-α

Stimulation of MCE cells with IL-1α for 4 hours only induced a 21% increase in the expression of VCAM-1. This effect is minor compared to the 250% increase after stimulation with TNFα. IL1-α had no significant effect on the expression of other adhesion molecules tested in MCE cells (figure 16). The level of P-Selectin expression at 30 mins was similar to the basal level (data not shown).

e) Expression of adhesion molecules in MCE cells exposed to TNFα and IFNγ

The combined exposure to TNFα and IFNγ produced a more significant effect on the adhesion molecule expression in the MCE cells. After 24 hours, the expression of E- and P-Selectin were increased (60 and 10 times respectively) and the expression of ICAM-1 was induced (figure 17). However, considering the low levels of expression of these adhesion molecules in the resting cells, their level at 24 hours remained respectively 3, 5.3, and 12 times lower than the basal level of VCAM-1. This molecule was increased nearly twice after exposure to this combination of cytokines for 24 hours (figure 17).

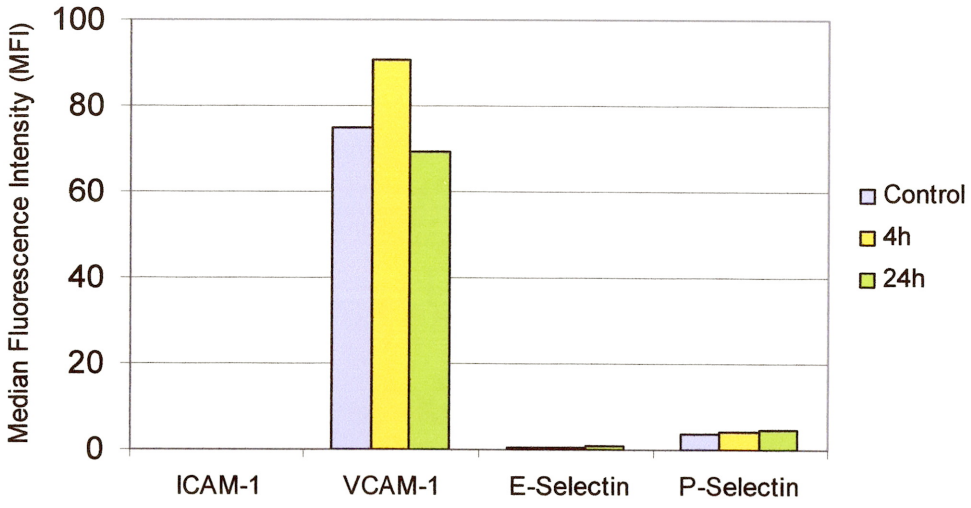


Figure 16: Effect of IL-1α on adhesion molecules expression in mouse corneal endothelial (MCE) cells.
Cultured MCE cells were stimulated with 20 ng/ml IL-1α for 0, 4 and 24 hours, detached using trypsin and stained as above before cytofluorimetric analysis. The graph presents the Median Fluorescence Intensity (MFI) obtained for each peak after deduction of the isotype control MFI.

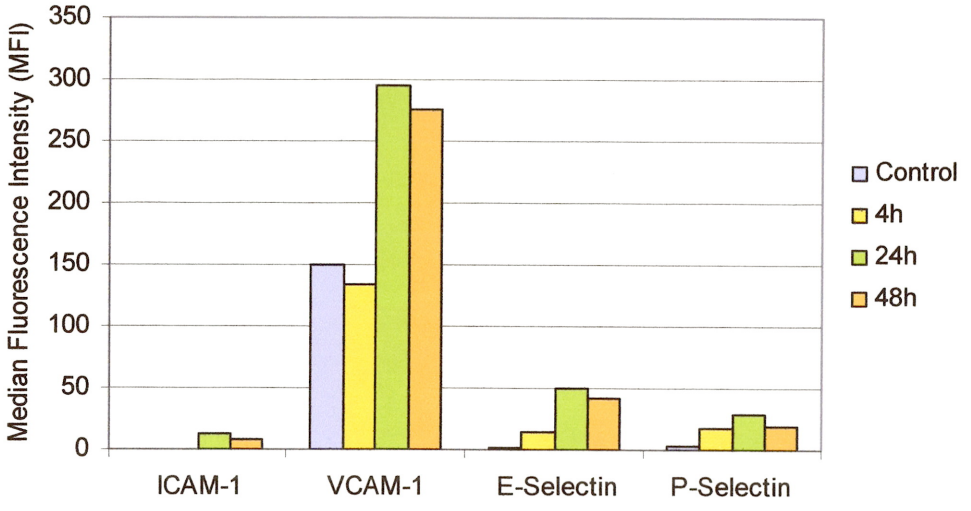


Figure 17: Effect of the combined exposure to TNFα and IFNγ on adhesion molecules expression in MCE cells.
Cultured MCE cells were stimulated with a combination of 20 ng/ml TNFα and 600 IU/ml IFNγ for 0, 4, 24 and 48 hours, detached using trypsin and stained as above before cytofluorimetric analysis. The graph presents the Median Fluorescence Intensity (MFI) obtained for each peak after deduction of the isotype control MFI.

f) Expression of adhesion molecules in MCE cells exposed to a cocktail of cytokines

The cocktail of cytokines had no effect on the expression of ICAM-1, nor PECAM-1 (figure 18). However, the expression of VCAM-1, E- and P-Selectin was increased 2.1, 4.4, and 1.6 times after 4 hours, and 2.7, 9, and 3.8 times after 24 hours of stimulation respectively. However, as in the previous experiment, the highest levels of E- and P-Selectin expression only reached 55% and 44% respectively of the basal expression of VCAM-1 in these cells (figure 18). We therefore concentrated our interest on VCAM-1 for the subsequent experiments.

g) Optimisation of cytokine effect on VCAM-1 expression in MCE cells

In order to obtain the optimal effect of pro-inflammatory cytokines on VCAM-1 expression, increased concentrations of TNFα and IFNγ were used to stimulate MCE cells.

Figure 19 shows the results of one representative experiment. At 4 hours, the expression of VCAM-1 showed a small 20% increase when the TNFα concentration was more than doubled (from 20 to 50 ng/ml). VCAM-1 expression was barely affected by the increase in IFNγ concentration from 600 to 1200 IU/ml. At 24 hours, the high dose of IFNγ only induced a 16% increase in VCAM-1 expression whereas increased doses in the TNFα/IL-1α combination did not further increase VCAM-1 expression after either 4 or 24 hours (figure 19).

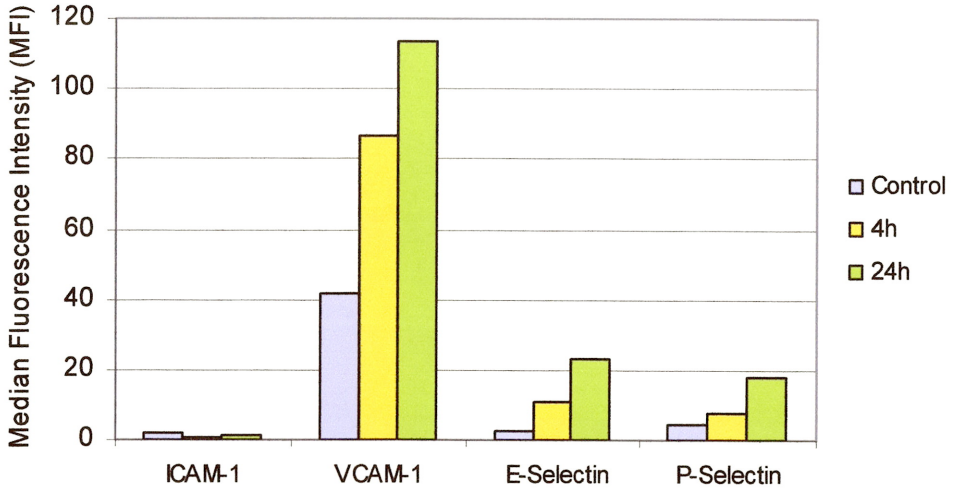


Figure 18: Effect of the exposure to a cocktail of TNFα, IFNγ and IL-1α on adhesion molecules expression in MCE cells.
Cultured MCE cells were stimulated with 20 ng/ml TNFα, 600 IU/ml IFNγ and 20 ng/ml IL-1α for 0, 4 and 24 hours, detached using trypsin and stained for adhesion molecules before cytofluorimetric analysis. The graph presents the Median Fluorescence Intensity (MFI) obtained for each peak after deduction of the isotype control MFI.

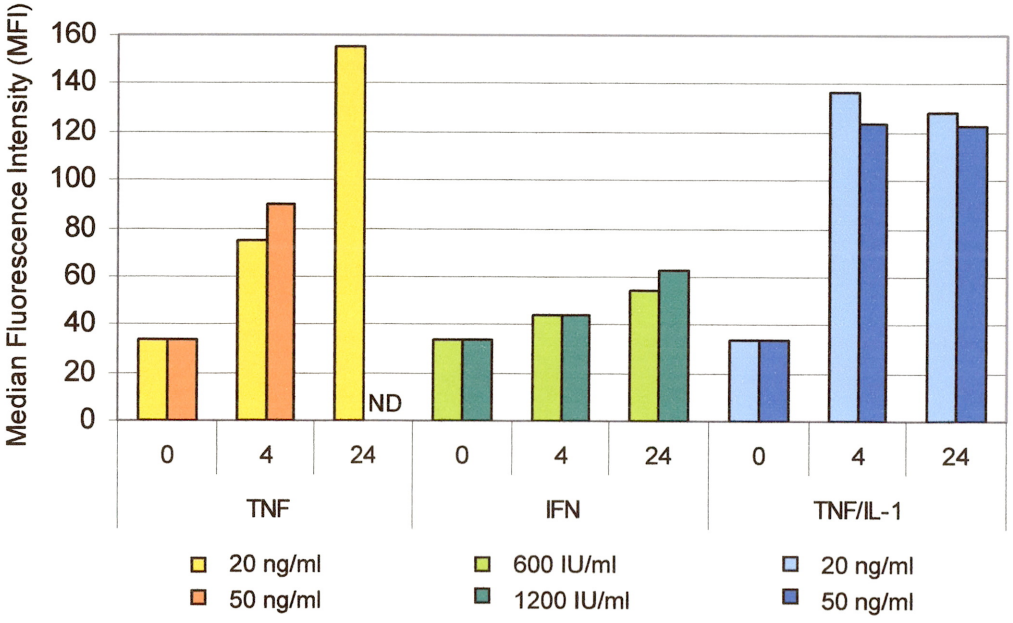


Figure 19: Effect of cytokine doses on VCAM-1 expression in mouse corneal endothelial (MCE) cells.
Cultured MCE cells were stimulated with various cytokines combinations for 0, 4 and 24 hours, detached using trypsin and stained for VCAM-1 before cytofluorimetric analysis. The graph presents the Median Fluorescence Intensity (MFI) of the VCAM-1 peak after deduction of the isotype control MFI.
Key: ND=not done

In HUVECs and in EA-hy-926, VCAM-1 is up-regulated after a 24h stimulation with a 10 ng/ml dose of TNFα (Thornhill *et al.*, 1993) (Iademarco *et al.*, 1995). Noticeably, this dose is also sufficient to increase the expression of ICAM-1 and E-Selectin in these cells (Thornhill *et al.*, 1993). In the same cells, Thornhill *et al.* found that IFNγ at 250 IU/ml had no effect on the expression of VCAM-1. At this dose, ICAM-1 was however up-regulated on HUVECs but not on EA-hy-926 (Thornhill *et al.*, 1993). Finally, in a study of mouse cardiac EC, Lidington and co-workers also demonstrated an up-regulation of VCAM-1 by a combination of 10 ng/ml TNFα and 10ng/ml IL-1β (Lidington *et al.*, 2002).

Doubling or more the concentration of cytokines only marginally increased the expression of VCAM-1 in MCE cells. We therefore carried out the subsequent experiments using the initial doses for the sake of comparison.

h) Synergistic effect of IFNγ and TNFα on the expression of VCAM-1 in MCE cells

The effects of the three cytokines (alone, in doublets or all together) on VCAM-1 expression were then compared. Figure 20 presents FACS profiles of MCE cells stained for VCAM-1. The FACS profiles of resting cells are compared with those of cells stimulated with single cytokines and their combinations. The Median Fluorescence Intensity (MFI) and the fold-increase are also presented in figures 21 and 22 respectively. These figures show that IFNγ and TNFα act in a synergistic way on VCAM-1 expression in MCE cells. The VCAM-1 expression on cells stimulated with both IFNγ and TNFα is 143% higher (5 times the amount in control cells) than the one for cells stimulated with TNFα alone (only twice the amount in the control cells).

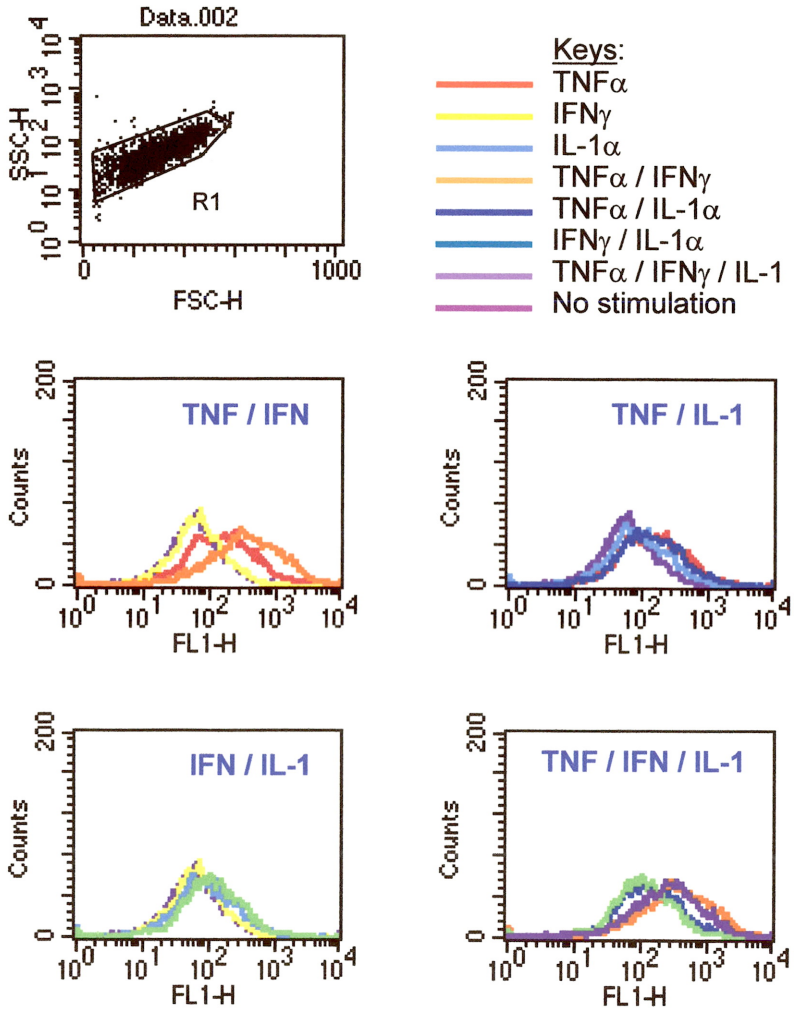


Figure 20: Effect of the combined exposure to TNFα, IFNγ and IL-1α on VCAM-1 expression in mouse corneal endothelial (MCE) cells.
Cultured cells were detached after 24 hours of incubation in the relevant cytokine combination, stained with an anti-mouse VCAM-1 antibody and a secondary antibody conjugated to FITC (FL1-H channel), before cytofluorimetric analysis on a FACS Calibur. In each panel (except lower right panel), the figure compares the profile of VCAM-1 detected in resting cells, in cells stimulated with a combination of two cytokines or with the relevant individual cytokines. In the lower right panel, the triple combination of cytokines is compared to the double combinations. Dot blots present the gated population of MCE cells analysed in the experiment.

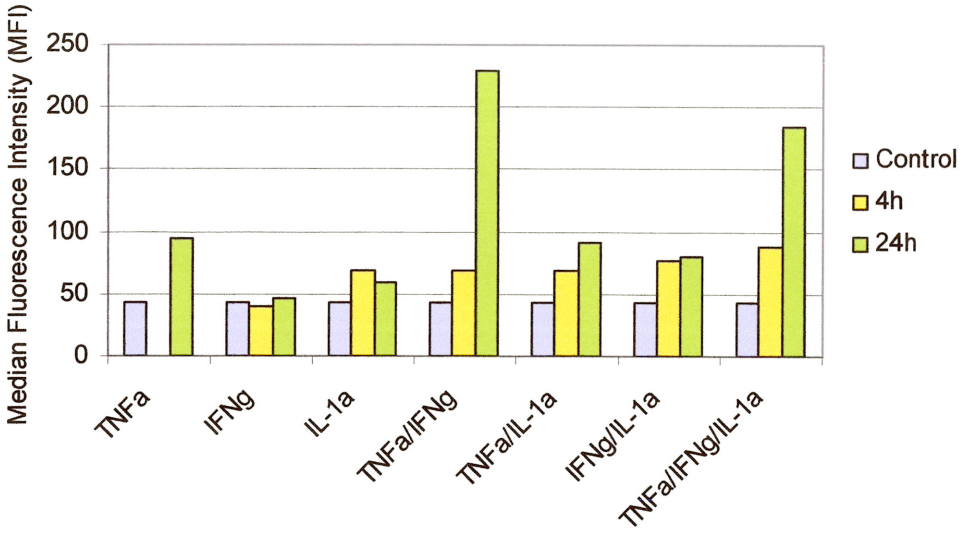


Figure 21: Effect of the combined exposure to TNFα, IFNγ and IL-1α on VCAM-1 expression in mouse corneal endothelial (MCE) cells.
Cultured cells were detached after 0, 4 or 24 hours of incubation in the relevant cytokine combination, stained for VCAM-1 and analysed on a FACS Calibur. The graph presents the Median Fluorescence Intensity (MFI) obtained for each peak after deduction of the isotype control MFI.

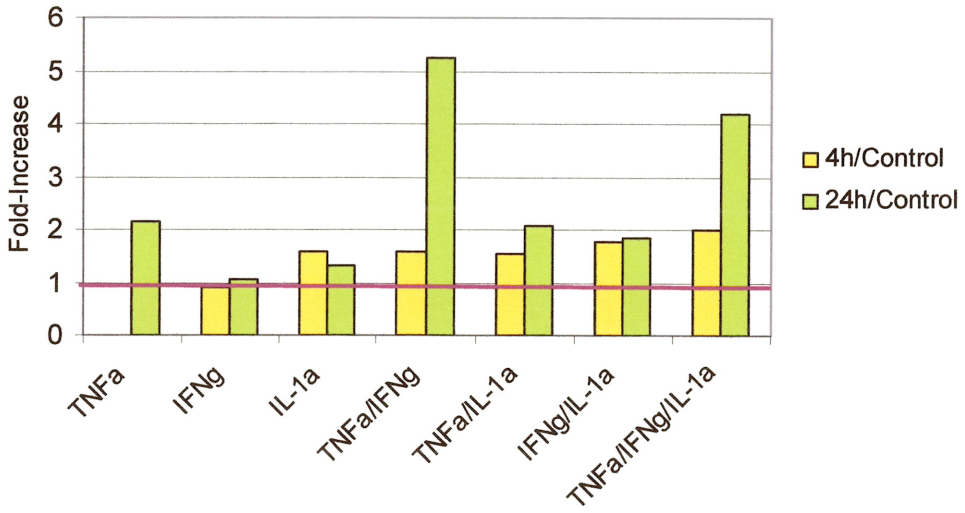


Figure 22: Effect of the combined exposure to TNFα, IFNγ and IL-1α on VCAM-1 expression in mouse corneal endothelial (MCE) cells.
As in figure 22, cells were detached after 0, 4 or 24 hours of incubation in the relevant cytokine combination and stained for VCAM-1 before FACS analysis. The graph presents the variation of VCAM-1 expression (expressed in fold-increase), in comparison to the expression in control cells.

The combination of the three cytokines does not further increase this effect (only 95% higher) (4.2 times the amount in control cells) (figures 21 and 22). The combinations TNFα/IL-1α and IFNγ/IL-1α do not increase VCAM-1 expression in comparison to the TNFα stimulation (figure 21). We therefore demonstrated a synergy between IFNγ and TNFα on the expression of VCAM-1 in MCE cells.

i) Conclusion

Among the adhesion molecules we tested by FACS on the MCE cell line, only VCAM-1 was significantly expressed on the resting cells. Its expression was up-regulated by TNFα alone but not (or very marginally) by IFNγ or IL-1α. A synergetic effect of IFNγ on the up-regulation of VCAM-1 expression by TNFα was however demonstrated in the MCE cells.

3.1.2.2- Expression of adhesion molecules proteins in the excised cornea

The presence of adhesion molecules in corneal endothelium was then analysed using immunofluorescent staining of mouse cornea flat-mounts and comparison with MCE cells grown on glass slides. MCE cell cultures were stained with primary antibodies specific for the following adhesion molecules: ICAM-1, VCAM-1, E- and P-Selectin, and PECAM-1. The antibody was then detected using a secondary antibody conjugated to FITC (green under fluorescent light). Slides were finally mounted in a mounting medium containing DAPI, a dye that stains cell nuclei in blue.

Among the one tested, VCAM-1 was the only adhesion molecule strongly detected in the cultures as shown on figure 23.

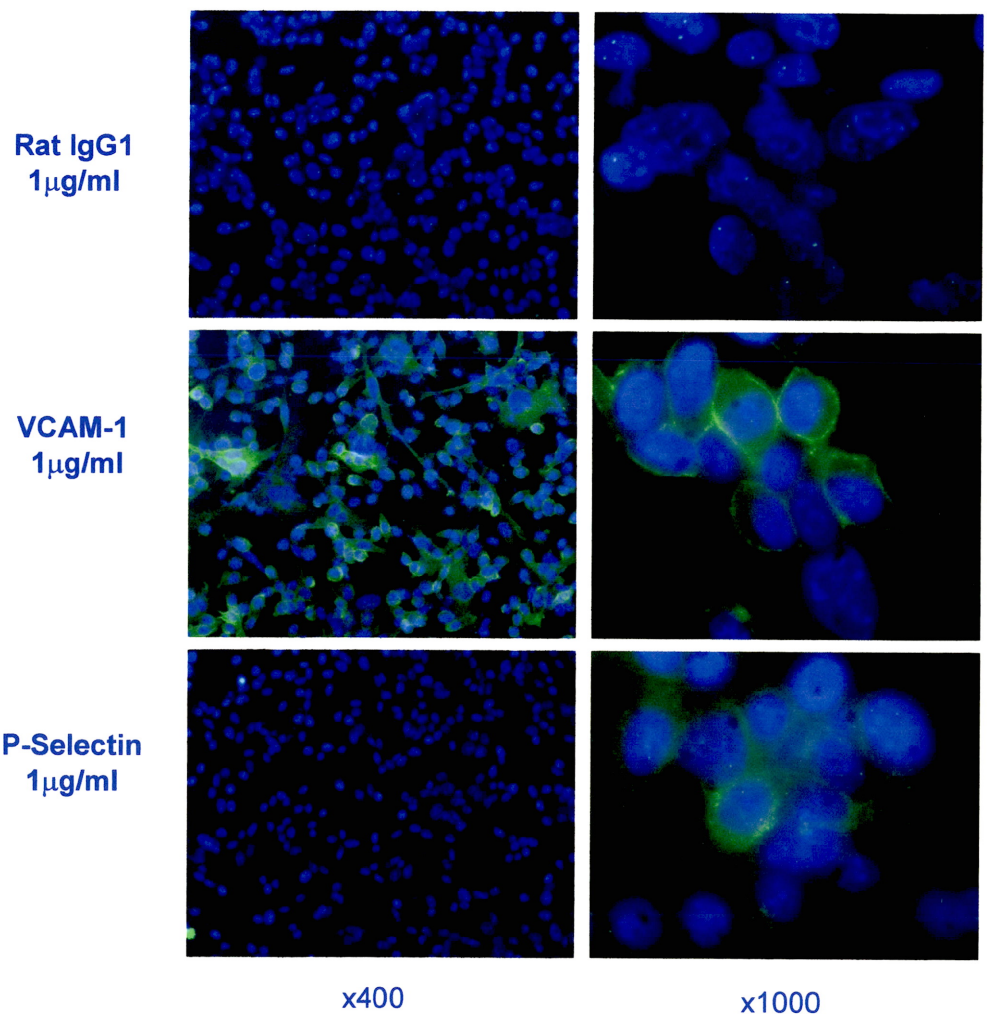


Figure 23: Adhesion molecule expression in MCE cells using fluorescent microscopy.
MCE cells were cultured on glass slides and stained with an anti-adhesion molecules primary antibody detected by a secondary antibody conjugated to FITC (green staining). Cells were finally dyed with DAPI, a fluorescent reagent that stains cells nuclei in blue. Analysis was performed under a fluorescent microscope (original magnification x400 or x1000) and the picture was captured with a digital camera. Staining for VCAM-1, and to a lesser extent for P-Selectin, only was detected in MCE cells. Staining for the other adhesion molecules produced pictures similar to the isotype control.

Positive cells presented a green staining mainly concentrated on the cellular surface. Some cells were slightly positive for P-Selectin but they were present in very small quantities. Slides stained for ICAM-1, E-Selectin and PECAM-1 (not shown) presented a staining similar to the rat IgG1 negative control presented on figure 23. These data confirm the data obtained by FACS analysis.

Flat mounts of mouse corneas were stained with the same range of antibodies, using the same technique. The results were similar to those obtained on the cell line. Among all the adhesion molecules tested, only VCAM-1 was detected in the cornea, both in the epithelium and the endothelium (figure 24).

To further confirm these data, cryosections of normal mouse eyeballs were stained with antibody against ICAM-1, VCAM-1 and PECAM-1 (the E- and P-Selectin staining could not be performed for technical reasons). Staining were optimized on mouse spleen sections (figure 25) and applied to MCE cells cytospins (figure 26). As expected, spleen sections were positive for the three adhesion molecules. In the spleen, ICAM-1 is expressed on DCs, T and B cells (white pulp) and on monocytes (red pulp). VCAM-1 is detected on macrophages of the red and white pulp (also on DCs) while PECAM-1 is expressed on some T cells, on monocytes and granulocytes.

Again, the FACS data obtained on the resting MCE cells were confirmed. MCE cells cytospins stained for VCAM-1 presented a discreet brown staining on their surface while those stained for both ICAM-1 and PECAM-1 were negative (figure 26).

The corneal endothelium was completely devoid of ICAM-1 staining as seen on figure 27. A discreet brown staining was however found mostly associated with keratocytes, in the corneal stroma and with epithelial cells.

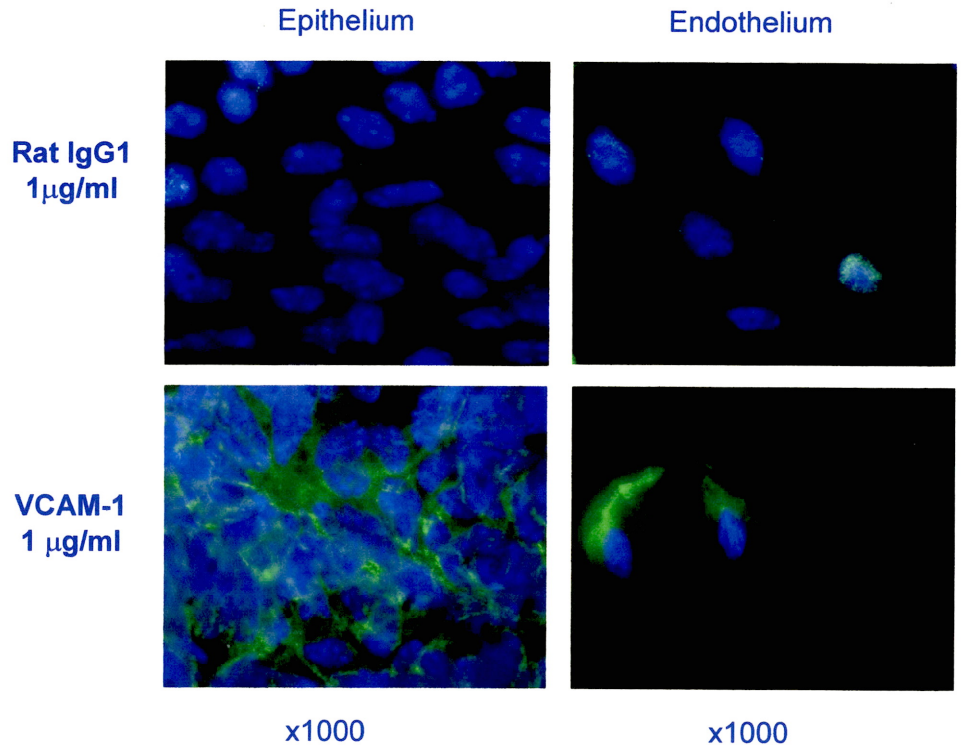
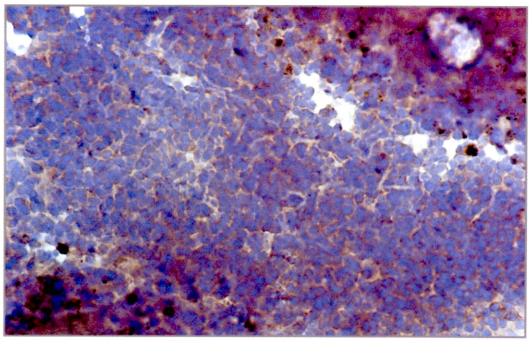
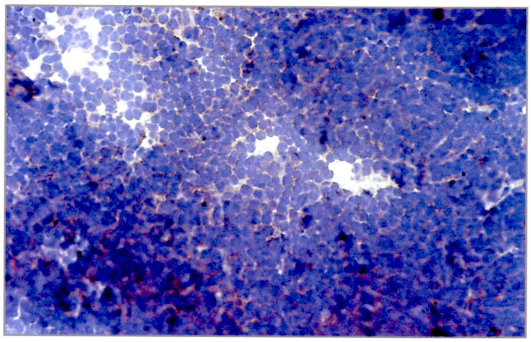


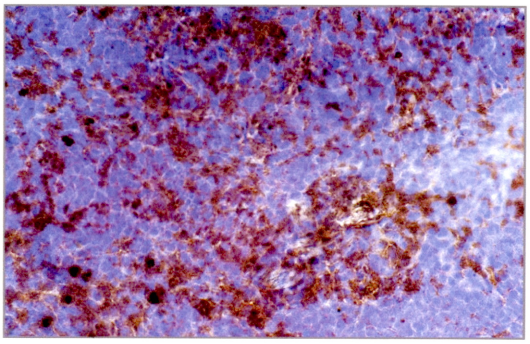
Figure 24: Adhesion molecule expression in flat mounts of mouse endothelium using fluorescent microscopy.
Mouse corneal endothelium and epithelium were dried on slides and stained with an anti-adhesion molecules primary antibody detected by a secondary antibody conjugated to FITC (green staining). Slides were finally dyed with DAPI, a fluorescent reagent that stains cells nuclei in blue. Analysis was performed under a fluorescent microscope (original magnification x1000) before capture of the picture with a digital camera. The staining for VCAM-1 was the only positive staining detected, both in the epithelium and the endothelium of the cornea.



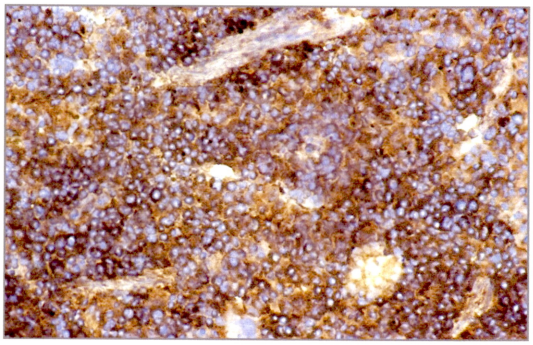
IgG2a



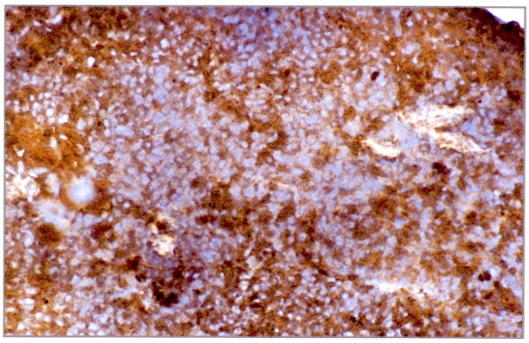
IgG1



ICAM-1



VCAM-1



PECAM-1

Figure 25: Optimisation of adhesion molecules staining on histological cryosections (x175).
Cryosections of normal mouse spleen were stained with the appropriate primary antibody (or the relevant isotype control: IgG1 for VCAM-1, IgG2a for ICAM-1 and PECAM-1) for 20 minutes, washed twice in PBS and incubated with a biotinylated secondary antibody for a further 20 minutes. The latter antibody was detected with an avidin-horse radish peroxidase-DAB system. Sections were finally counterstained with a 0.1% Mayer's hematoxillin solution, mounted and photographed.

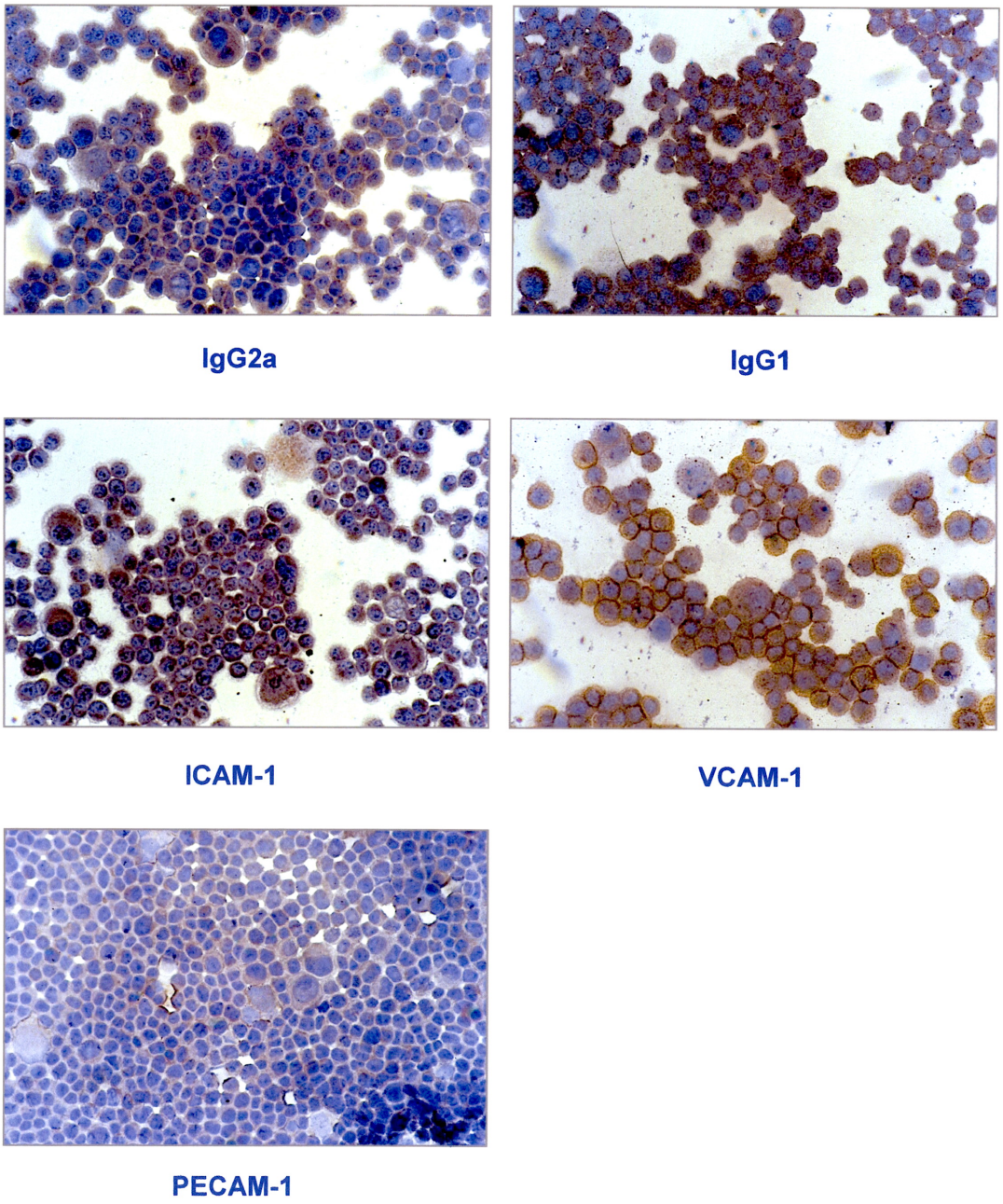
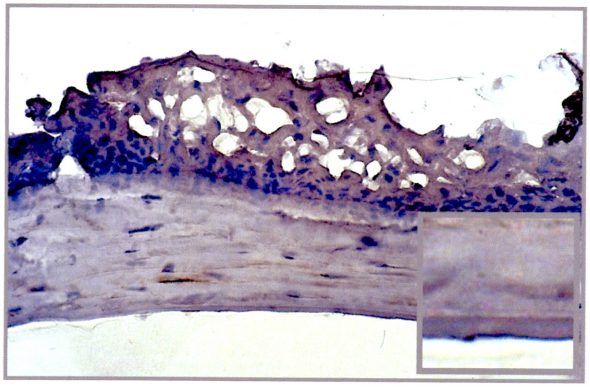
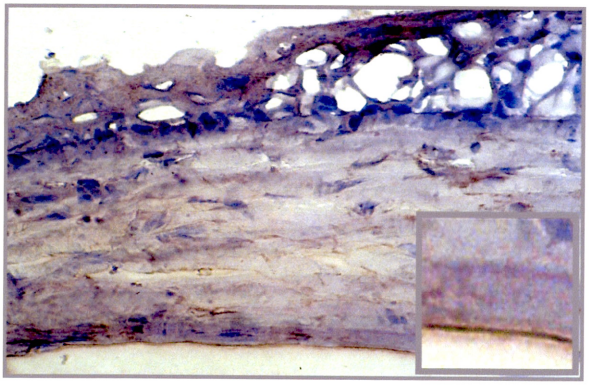


Figure 26: Adhesion molecules expression in MCE cells cytospins (x175). Cytospins of resting MCE cells were stained with the appropriate primary antibody for 20 minutes, washed twice in PBS and incubated with a biotinylated secondary antibody for a further 20 minutes. The latter antibody was detected with an avidin-horse radish peroxidase-DAB system. The sections were finally counterstained with a 0.1% Mayer's hematoxillin solution, mounted and photographed.

ICAM-1
(x200)
insert (x800)



VCAM-1
(x250)
insert (x800)



PECAM-1
(x100)
insert (x200)

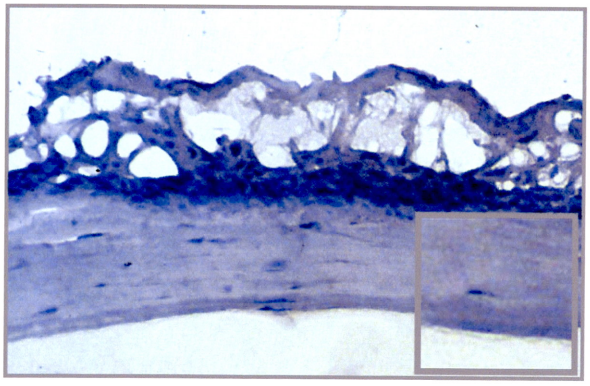


Figure 27: Adhesion molecules expression in normal mouse corneas sections.
Cryosections of normal mouse eyeballs were stained with the appropriate primary antibody for 20 minutes, washed twice in PBS and incubated with a biotinylated secondary antibody for a further 20 minutes. The latter antibody was detected with an avidin-horse radish peroxidase-DAB system. The sections were finally counterstained, mounted and photographed.

VCAM-1 on the other hand was expressed in corneal endothelial cells as attested by the presence of a brown staining associated with these cells. As for ICAM-1, some light staining could also be found associated with keratocytes and epithelial cells (figure 27).

Finally, no staining for PECAM-1 was detected in any of the corneal structures (figure 27).

3.1.3- Conclusion

Using RT-PCR, FACS analysis, immunofluorescence and histology, we looked at the expression of a panel of adhesion molecules in two models: 1) a mouse corneal endothelial (MCE) cell line and 2) whole excised corneas (or entire eyeballs for histology). Both were derived from BALB/c mice. We also investigated the effect of pro-inflammatory cytokines on this expression.

RT-PCR revealed small amounts of ICAM-1 mRNA, but higher quantities of E-Selectin, VCAM-1, NCAM-1 and VAP-1 mRNA in the MCE cell line. The quantity of ICAM-1 mRNA was strongly increased by all cytokines, either alone or in combination. TNFα, IL-1α and the combination of cytokines only mildly increased VCAM-1 and E-Selectin mRNA, whereas IFNγ showed no effect. NCAM-1 and VAP-1 mRNA decreased with times in all the conditions tested. Similar pattern were identified using whole excised mouse cornea, apart from the absence of E-Selectin mRNA in the tissue.

The FACS analysis, the immunofluorescence and the histology revealed a different pattern of protein expression and kinetics, suggesting post-transcriptional regulations. The VCAM-1 protein was the only adhesion molecule tested detected in

the cell line and in the whole tissue. Its expression was greatly increased by TNFα used alone. A synergetic effect of IFNγ on the up-regulation of VCAM-1 expression by TNFα was also demonstrated.

The study was then taken further by looking at the role of these adhesion molecules in the adhesion of cells to the corneal endothelium.

3.2- Function of adhesion molecules in the mouse cornea

An adhesion assay was set up in order to determine 1) the role of these adhesion molecules in the interaction between different cell populations and corneal endothelial cells and 2) the effect of pro-inflammatory cytokines, on these cell/cell interactions. Basically, fluorescently labelled cells from different human and murine populations were incubated with a monolayer of corneal endothelial cells, and after several washes to remove cells that did not adhere to the monolayer, labelled cells were counted. In subsequent experiments, the monolayer was incubated with pro-inflammatory cytokines (TNFα, IFNγ and IL-1) prior to the assay, in order to determine their influence on cell adhesion. Finally, some blocking antibodies were applied to the monolayer before the assay, in order to define the relative role of adhesion molecules and their ligands in the adhesion process of the different cell populations tested.

The first step consisted in labelling the cells added to the monolayer. Figure 28 presents a FACS profile of Jurkat T cells before and after labelling with calcein AM. As shown on this figure, all the cells are labelled after incubation for 1 hour with the dye. Labelled cells were then plated at different concentrations and the amount of

fluorescence in each well was determined using a fluorimeter. A direct relationship was established between the number of cells added to the well and the amount of fluorescence detected by the fluorimeter (figure 29).

The adhesion assay technique was then optimised using Jurkat T cells and the DAP-3 and DVCAM cell lines. Adherent cells (DAP-3 and DVCAM) were grown as a monolayer and incubated with calcein AM-labelled T cells. Unbound T cells were washed away and the remaining attached cells were counted using a fluorimeter. Results are presented in figure 30. DVCAM cells, mouse cells transfected with the gene for human VCAM-1, supported the binding of about 60-70% of the T cells added, versus only 30% for their non transfected counterparts (DAP-3 cells). The adhesion of T cells was partially blocked (down to 35% / 40%) with an anti-VCAM-1 blocking antibody (1G11), whereas an irrelevant antibody (OX7) or a non-blocking anti-VCAM-1 antibody (60.9) had no effect on the adhesion (figure 30).

This experiment showed that the assay was working and that the technique could be used to study first, the amount of labelled cells adhesion onto monolayers and secondly, using various blocking antibodies, the effect of specific adhesion molecules interactions with their ligands.

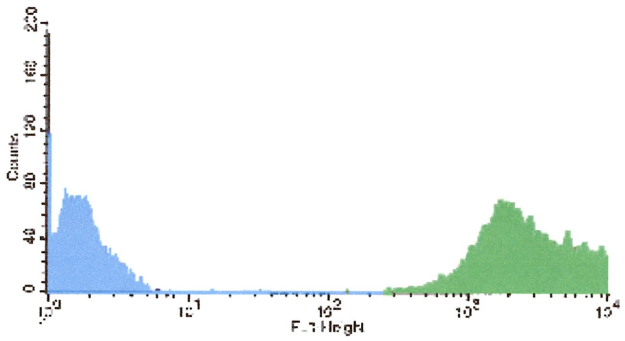


Figure 28: FACS profile of human Jurkat T cells prior to, and after staining with Calcein AM.
Human Jurkat T cells were resupended in culture medium containing 3 μM Calcein AM, for 1h at 37°C. The dye permeates the cells and becomes green fluorescent once hydrolysed. The figure presents an overlay of Jurkat T cells before (blue) and after (green) labelling and shows that all the cells are labelled with Calcein AM.

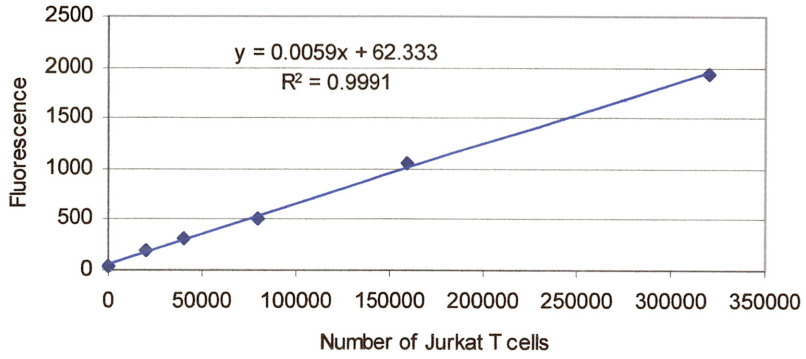


Figure 29: Standard curve of human Jurkat T cells after labelling with Calcein AM.
Human Jurkat T cells were labelled with 3 μM Calcein AM, for 1h at 37°C. Cells were then plated in a flat-bottom 96-well plate at different concentrations, in triplicates. The resulting fluorescence for each well was then analysed using a fluorescence plate reader. The graph shows a direct relationship between the number of labelled cells and the amount of fluorescence detected.

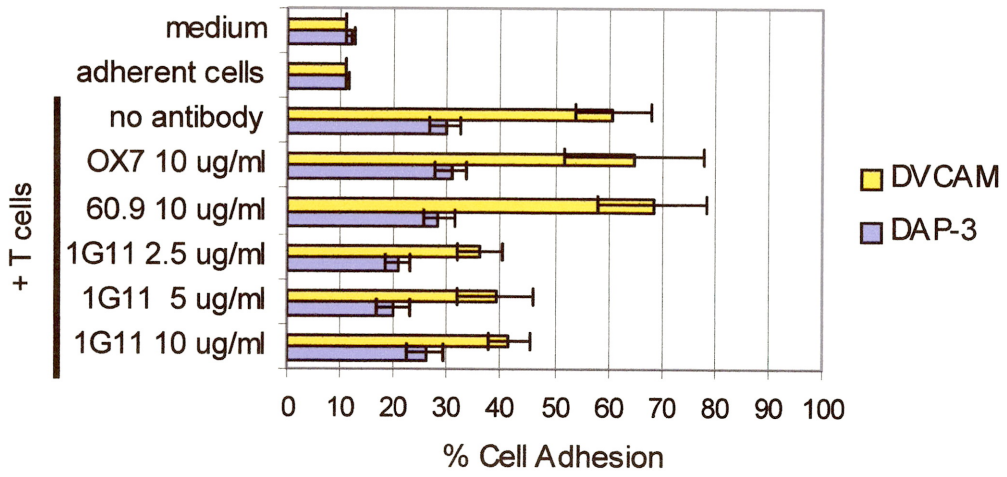


Figure 30: Optimisation of the adhesion assay technique using DAP-3 / DVCAM and Jurkat T cells.

Calcein AM-labelled Jurkat T cells were incubated for 1h at 37°C with a monolayer of DAP-3 or DVCAM cells. Non-adherent cells were washed and remaining cells were counted using a fluorimeter. For blocking conditions, monolayer cells were incubated for 30 min. with antibodies, prior to the addition of labelled T cells. Some wells containing labelled cells only were not washed and constituted the 100%. The graph shows a specific adhesion of human T cells on DVCAM but not DAP-3 cells. The adhesion is partially blocked by a blocking anti-VCAM-1 antibody (1G11), but not by a non blocking (60.9) or irrelevant antibody (OX7).

3.2.1- Adhesion of human and murine cell populations to MCE cells

3.2.1.1- Adhesion of human and murine cell populations to resting MCE cells

Several populations, both human (T cells, PBMC and PMN) (figure 31) and murine (splenocytes and macrophages) (figure 32) were tested for adhesion properties on resting MCE cells. The figures present representative data from experiments carried out at least three times.

Figure 31 shows that, when added to the monolayer of resting mouse corneal cells, about 65% of Jurkat T cells adhere to the monolayer. When purified T cells are added to the monolayer (as opposed to the cell line), only around 9% of the cells remain after the washes. The percentage increases however to more than 38% (more than 320% increase) when T cells are stimulated with PMA and ionomycin before the adhesion test.

In the same way, Polymorphonuclear cells (PMN), and to a lesser extent Peripheral Blood Mononuclear cells (PBMC), see their percentage of adherence increased from 21 to 44% (+109%) and from 20 to 25% (+25%) respectively, after stimulation with PMA for 30 minutes. Overall, stimulated human populations adhere more to the MCE cells monolayer than their resting counterparts (figure 31).

Among the murine populations tested (figure 32), the macrophages proved to adhere the most, with more than 63% of the cells remaining after the washes. Stimulated macrophages were not tested. As for PBMC and PMN, about 20% of splenocytes adhered to the corneal cell monolayer, but their stimulation with PMA and ionomycin for 24h did not increase their capacity of adherence.

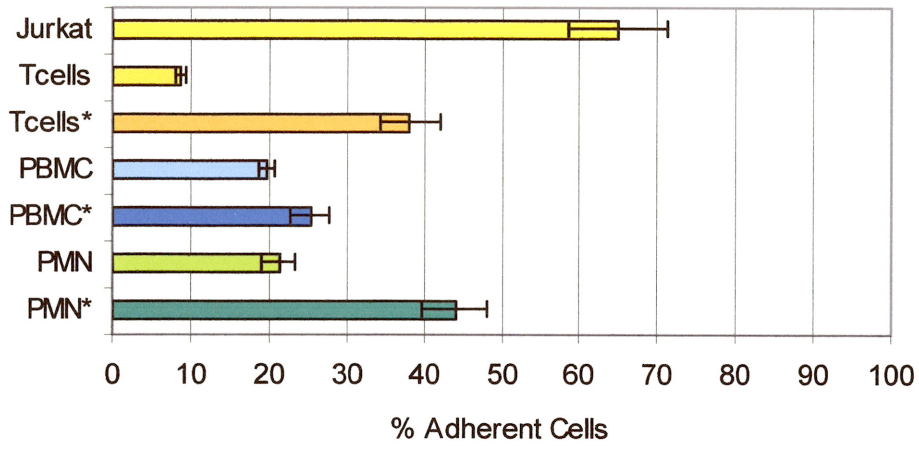


Figure 31: Adhesion of human cell populations on resting MCE BALB/c cells.
Calcein AM-labelled human cells were incubated for 1h at 37°C with a monolayer of MCE BALB/c cells. Non-adherent cells were washed and remaining cells were counted using a fluorimeter. Some wells containing labelled cells only were not washed and constituted the 100%. The graph presents the percentage of adherent cells for each cell population. Cells stimulated prior to the adhesion assay are labelled with a star (*). Keys: PBMC=Peripheral Blood Mononuclear Cells and PMN=Polymorphonuclear Cells.

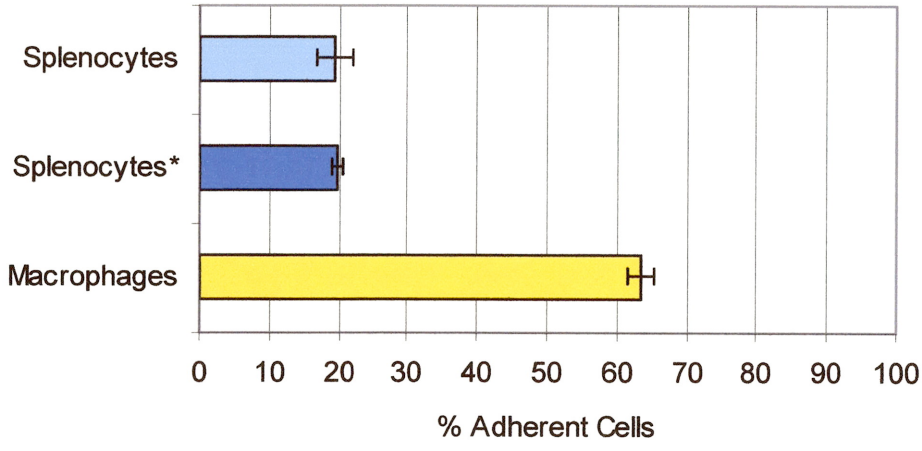


Figure 32: Adhesion of murine cell populations on resting MCE BALB/c cells.
As above, murine cells were labelled with Calcein AM before an incubation for 1h at 37°C with a monolayer of MCE BALB/c cells. Non-adherent cells were washed and the remaining cells were counted. The graph shows the percentage of adherent cells, using, for each cell population, the total number of cells added to the monolayer (wells not washed) as 100%. Populations labelled with a star (*) were stimulated prior to the assay.

3.2.1.2- Adhesion of human and murine cells to stimulated MCE cells

The same populations were then tested for their capacity to adhere to MCE cells stimulated for 24 hours with pro-inflammatory cytokines. Figure 33 presents the percentage of adherence of human cells to the monolayer whereas figure 34 presents the percentage of adherence of murine populations.

As in the case of resting MCE cells, the stimulation of purified T cells and PMN increased their capacity to adhere to the stimulated monolayer (from 16 to 44% (+175%) for purified T cells and from 27 to around 51% (+89%) for PMN). Stimulation of PBMC, however, did not increase their adherence (24% when stimulated versus 29%) (figure 33). Finally, the number of splenocytes adherent to the stimulated MCE monolayer did not increase after their activation (from 27 to 22% (-18%)) (figure 34).

The stimulation of the MCE cells did not affect much the capacity of Jurkat cells and macrophages to adhere with around 68% and 65% adherent cells respectively in the case of activated MCE cells, versus 65% and 63% in the case of resting MCE cells. Activated PBMC adhered roughly in the same way to the stimulated monolayer (24%) than to the resting cells (25%) whereas resting PBMC adhered more when MCE cells were activated (29% versus 20% on resting MCE cells). This is equivalent to a 45% increase.

Purified T cells adherence was increased by 78% (from around 9% to 16%) and by 16% (from 38% to 44%), in the case of resting and stimulated T cells respectively. In the same way, both unstimulated and stimulated PMN adhered more to the activated monolayer (27 and 51%) than to the resting MCE cells (21 and 44%).

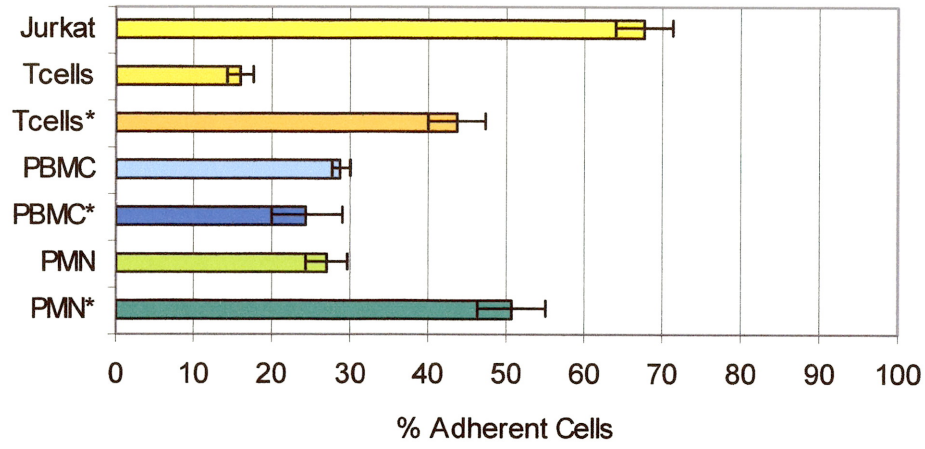


Figure 33: Adhesion of human cell populations on activated MCE BALB/c cells.
As above, calcein AM-labelled human cells were incubated for 1h at 37°C with a monolayer of MCE BALB/c cells, stimulated with a combination of pro-inflammatory cytokines for 24 hours. After several washes, adherent cells were counted using a fluorimeter. The graph presents for each cell population the percentage of adherent cells. Cells stimulated prior to the adhesion assay are labelled with a star (*). Keys: PBMC=Peripheral Blood Mononuclear Cells and PMN=Polymorphonuclear Cells.

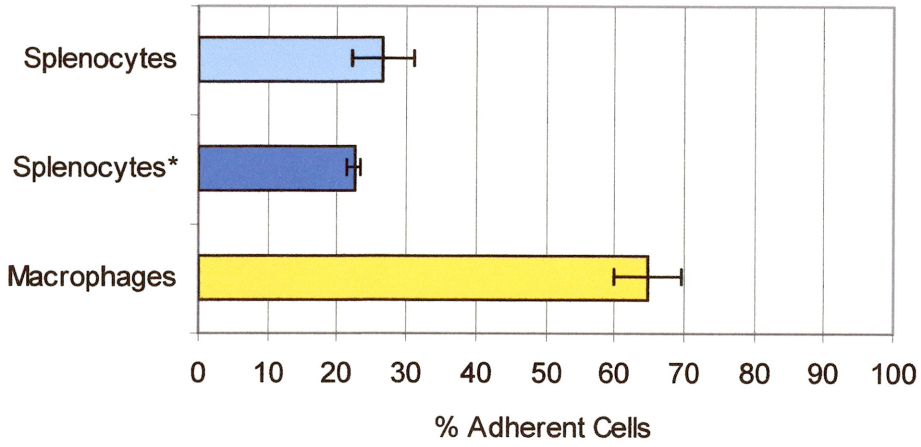


Figure 34: Adhesion of murine cell populations on activated MCE BALB/c cells.
As previously described, murine cells were labelled with calcein AM before an incubation for 1h at 37°C with a monolayer of MCE BALB/c cells, activated with cytokines for 24 hours. Non-adherent cells were washed and the remaining cells counted. The graph shows the percentage of adherent cells, for each cell population.

This is equivalent to a 29% and a 16% increase in adherence of resting and stimulated PMN respectively.

Overall, the stimulation of the human populations added to the monolayer produced a greater effect on the increase of adhesion, than the stimulation of the monolayer itself. Table 1 summarises all these results.

	Resting MCE cells		Stimulated MCE cells		
Population	Adhesion to MCE (%)	Variation no*/*(%)	Adhesion to MCE* (%)	Variation no*/*(%)	Variation MCE/MCE*(%)
Jurkat	65	NA	68	NA	+5
T cells	9	+322**	16	+175**	+78**
T cells*	38		44		+16
PBMC	20	+25**	29	-17	+45**
PBMC*	25		24		-4
PMN	21	+109**	27	+89**	+29*
PMN*	44		51		+16
Spleno	19	+5	27	-18	+42*
Spleno*	20		22		+10**
Macrophages	63	NA	65	NA	+3

Table 1: **Adhesion of human and murine cell populations to MCE cells**.
This table presents for all cell populations tested, the percentage of cells adhering to resting (MCE) and stimulated (MCE*) cells after adhesion assays carried out in different conditions of stimulation (columns 2 and 4). The total number of cells added to the MCE monolayer is used as 100% adhesion.
The table also presents the variation between the adhesion of resting and stimulated (*) cells to resting (column 3) and stimulated MCE (column 5).
Finally, the table shows the variation in cell adhesion between resting and stimulated MCE cells (column 6).
Keys: NA= not applicable, * $P < 0.1$; ** $P < 0.05$, significant difference between resting and stimulated cells (Student's t-test performed on triplicates from representative data presented in figures 31 to 34).

3.2.2- Inhibition of human cells adhesion to MCE BALB/c cells

In the following experiments (figures 35 to 43), we attempted to block the adhesion of the human populations previously tested, using several antibodies directed against adhesion molecules or their ligands and the relevant isotype controls. Anti-mouse antibodies were used to investigate the adhesion via adhesion molecules expressed on the MCE side of the interaction (YN1; anti-ICAM-1, MK2.7; anti-VCAM-1) while anti-human antibodies were used to investigate the role of those expressed on the tested human populations (TS1; anti- β2 integrin subunit of human LFA-1; MAX68P; anti- α4 integrin subunit of human VLA-4).

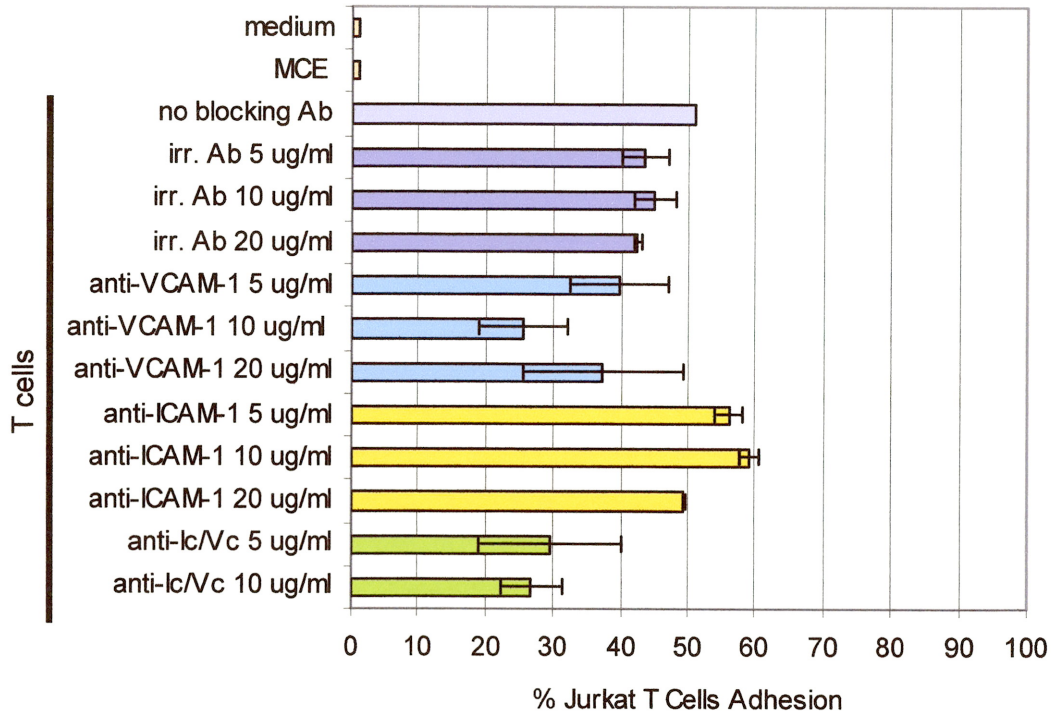
Tables presented in these figures show the percentage inhibition for each antibody using the condition with no blocking antibody as 100%. Experiments were repeated at least twice. Representative data are shown.

3.2.2.1- Jurkat T cells

The first experiments tested the ability to block the adhesion of Jurkat T cells to resting (figures 35 and 36) or activated (figure 37) MCE cells.

The adhesion of Jurkat T cells to resting corneal cells was not blocked by YN1, an anti-mouse ICAM-1 antibody tested at 5 to 20 μg/ml. MK2.7, however, an antibody directed against mouse VCAM-1, was able to inhibit their adhesion with a maximum of 49.8% when used at 10 μg/ml. The combination of the two antibodies did not further decrease the number of Jurkat cells adherent to the monolayer (figure 35). The anti-mouse ICAM-1 antibody YN1 was not used in subsequent experiments, whereas MK2.7, the anti-mouseVCAM-1 antibody was used at its optimal blocking concentration of 10 μg/ml, as determined with this experiment.

A

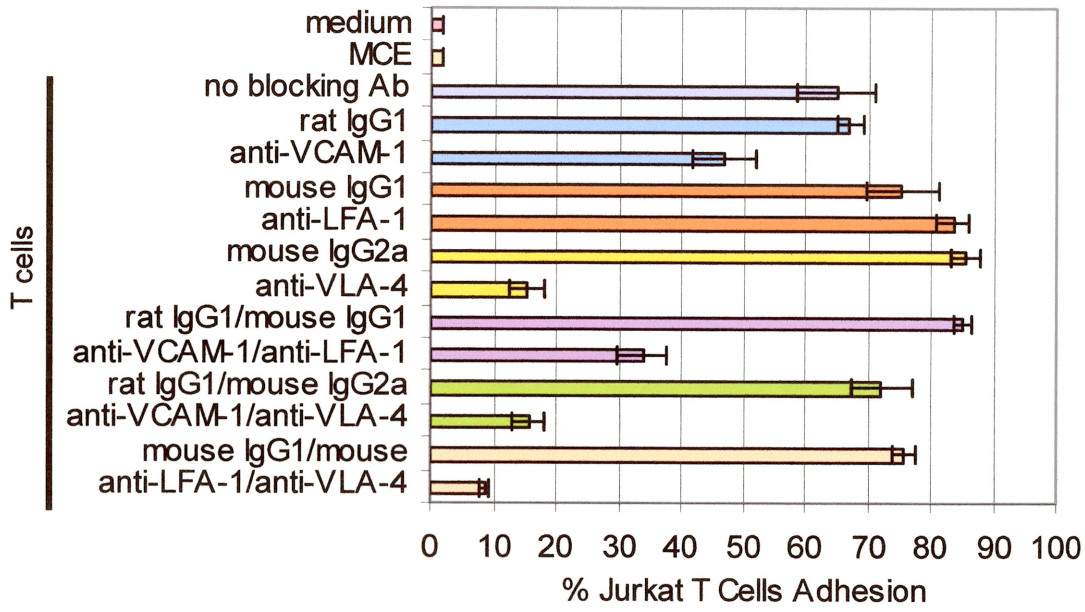


B

Condition	Inhibition (%)
irr. Ab 5 μg/ml	14.6
irr. Ab 10 μg/ml	11.7
irr. Ab 20 μg/ml	16.6
anti-VCAM-1 5 μg/ml	21.8
anti-VCAM-1 10 μg/ml	49.8
anti-VCAM-1 20 μg/ml	26.8
anti-ICAM-1 5 μg/ml	-9.9
anti-ICAM-1 10 μg/ml	-15.9
anti-ICAM-1 20 μg/ml	3.0
anti-ICAM/VCAM 5 μg/ml	42.0
anti-ICAM/VCAM 10 μg/ml	47.4

Figure 35: Inhibition of human Jurkat T cells adhesion on resting MCE cells.
Jurkat T cells labelled with calcein AM were incubated for 1h at 37°C with a monolayer of MCE cells. In blocking conditions, monolayer cells were incubated for 30 min. with antibodies, prior to the addition of labelled T cells. After several washes, the remaining adherent cells were counted using a fluorimeter. Graph (A) presents for each condition the percentage of adherent cells, using the unwashed wells as 100%. Table (B) summarises the % of inhibition using the condition with no blocking antibody as 0% of inhibition. Keys: irr.=irrelevant, Ab=antibody, Ic=ICAM-1, Vc=VCAM-1

A

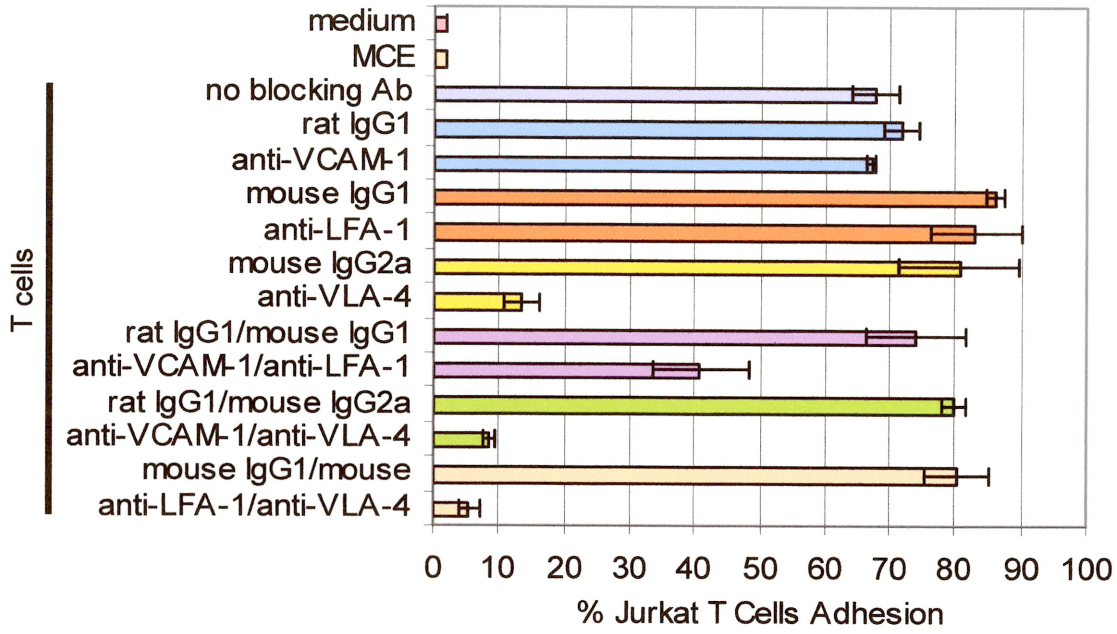


B

Condition	Inhibition (%)
rat IgG1	-3.5
anti-VCAM-1	27.9
mouse IgG1	-16.1
anti-LFA-1	-28.6
mouse IgG2a	-31.9
anti-VLA-4	76.6
rat IgG1/mouse IgG1	-31.2
anti-VCAM-1/anti-LFA-1	47.8
rat IgG1/mouse IgG2a	-11.2
anti-VCAM-1/anti-VLA-4	75.9
mouse IgG1/mouse IgG2a	-16.8
anti-LFA-1/anti-VLA-4	86.7

Figure 36: Inhibition of human Jurkat T cells adhesion on resting MCE cells.
The assay was performed as described in figure 36, using a different range of blocking antibodies. Calcein AM-labelled Jurkat T cells were incubated for 1h at 37°C with a monolayer of MCE cells. In blocking conditions, monolayer cells were incubated for 30 min. with antibodies, prior to the addition of labelled T cells. After several washes, the remaining adherent cells were counted. Graph (A) presents for each condition the percentage of adherent cells, using the unwashed wells as 100%. Table (B) summarises the % of inhibition using the condition with no blocking antibody as 0% of inhibition.

A



B

Condition	Inhibition (%)
rat IgG1	-5.8
anti-VCAM-1	0.9
mouse IgG1	-27.1
anti-LFA-1	-22.8
mouse IgG2a	-19.1
anti-VLA-4	80.1
rat IgG1/mouse IgG1	-9.3
anti-VCAM-1/anti-LFA-1	39.4
rat IgG1/mouse IgG2a	-18.0
anti-VCAM-1/anti-VLA-4	87.4
mouse IgG1/mouse IgG2a	-18.5
anti-LFA-1/anti-VLA-4	91.8

Figure 37: Inhibition of human Jurkat T cells adhesion on stimulated MCE cells.
The assay was performed as described in figure 37, using a stimulated monolayer of MCE cells. In blocking conditions, monolayer cells were incubated for 30 min. with antibodies, prior to the addition of labelled T cells. After several washes, the remaining adherent cells were counted. Graph (A) presents for each condition the percentage of adherent cells, using the unwashed wells as 100%. Table (B) summarises the % of inhibition using the condition with no blocking antibody as 0% of inhibition.

The role of LFA-1 and VLA-4 in the adhesion of Jurkat T cells to MCE cells was then investigated. Figure 36A and 37A show that the antibody directed against the β2 subunit of the human integrin LFA-1 had no effect on the adhesion of Jurkat T cells to MCE cells, whether resting or activated. Blocking with an anti-mouse VCAM-1 antibody proved to be less effective than in the previous experiment (49.2%) (figure 35B), but nonetheless knocked down nearly 28% of the adhesion (figure 36B) in the case of resting MCE cells. No effect was observed when activated MCE cells were blocked with this antibody alone (figure 37B). However, the effect was restored in both conditions of MCE cells (47.8 and 39.4%) when using a combination of anti-VCAM-1 and of anti-β2 integrin subunit (LFA-1 subunit), previously shown to be totally ineffective to reduce the adhesion of Jurkat to MCE cells. This strongly suggests an artifact in the anti-VCAM-1 alone condition, rather than a synergetic effect of the two antibodies directed against mouse VCAM-1 and against the human β2 integrin subunit of LFA-1.

Figure 36A and 37A demonstrate that the antibody directed against the α4 integrin subunit of human VLA-4 is able to decrease the adhesion of these cells by 76.6% in the case of resting MCE cells, and by more than 80% in the case of activated monolayer cells. This strongly suggests a role for an interaction via VLA-4 in this adhesion process. The combination of anti-VCAM-1 and anti-VLA-4 further decreased the adhesion of Jurkat cells only in the case of activated MCE cells (87.4% inhibition), suggesting these molecules have a greater role in the adhesion of Jurkat cells to activated than resting corneal cells.

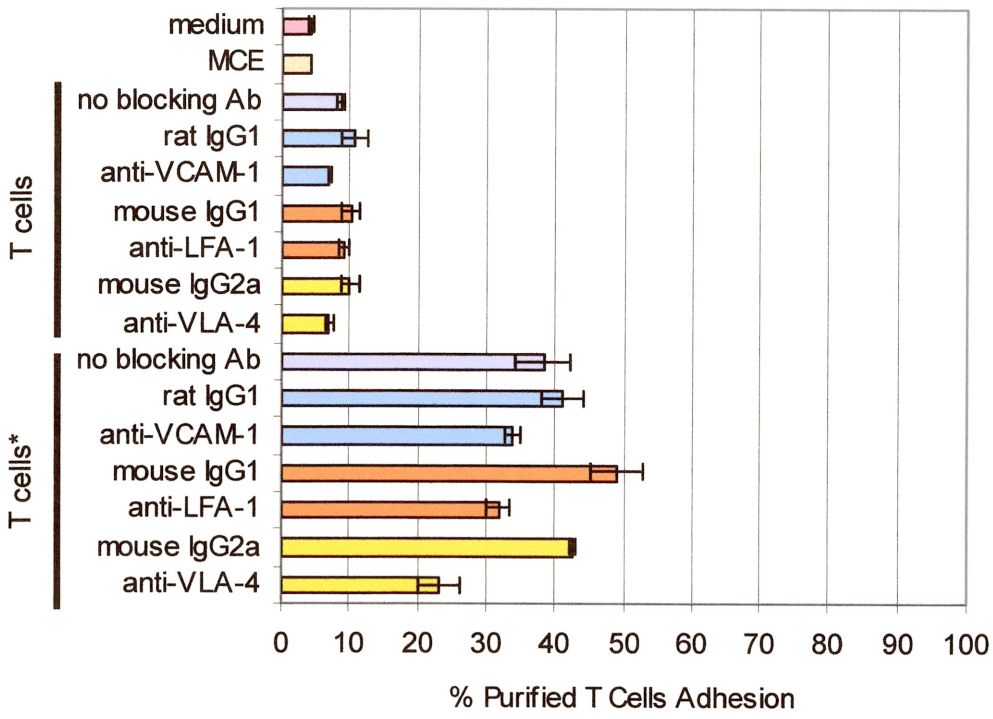
3.2.2.2- Purified T cells

The subsequent experiments then tested the ability of these antibodies to inhibit the adhesion of purified T cells to MCE cells, whether resting as presented in figure 38 or activated by pro-inflammatory cytokines as shown on figure 39. On the resting monolayer, the anti-mouse VCAM-1 antibody (MK2.7) decreased the adhesion of resting T cells by nearly 20% and of stimulated T cells by nearly 12% (figure 38). On the activated monolayer, the effect was more striking with 45% inhibition for resting T cells and nearly 33% for activated T cells. The isotype control for the latter condition presented however a 16% inhibition (figure 39).

The anti-human β2 integrin subunit (LFA-1 subunit) antibody had no effect on the adhesion of resting T cells to resting MCE cells. However, nearly 17% of adhesion was inhibited when T cells only were stimulated. The adhesion was even further reduced when MCE cells were stimulated (24% inhibition) (figures 38 and 39).

The antibody against human VLA-4 was able to decrease the T cell / MCE cell interaction in all cases with a decrease by 20% and 39%, when resting and activated T cells respectively were incubated with resting MCE cells (figure 38), and with a decrease by 57% and 55% when the same populations were added to an activated monolayer. Although the isotype also presented an inhibitory effect (22%) in the latter case, the inhibition by the anti-VLA-4 antibody was still very high (figure 39).

A



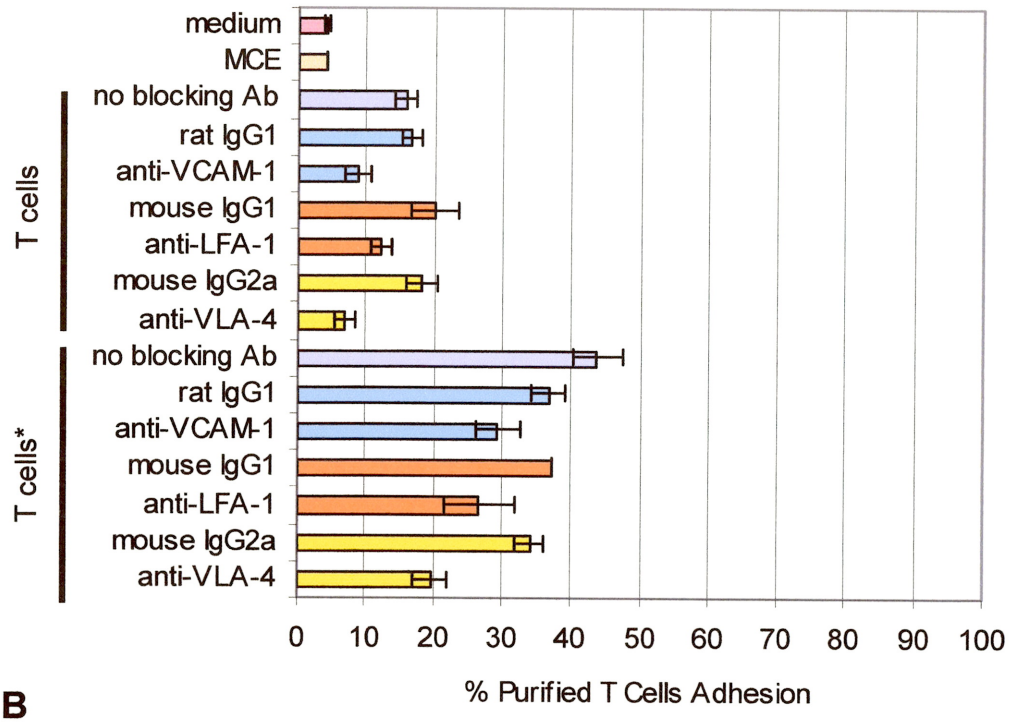
B

	Condition	Inhibition (%)
T cells	rat IgG1	-21.6
	anti-VCAM-1	19.6
	mouse IgG1	-16.1
	anti-LFA-1	-4.3
	mouse IgG2a	-15.3
	anti-VLA-4	19.6
T cells*	rat IgG1	-7.5
	anti-VCAM-1	11.8
	mouse IgG1	-28.0
	anti-LFA-1	16.8
	mouse IgG2a	-11.2
	anti-VLA-4	39.1

Figure 38: Inhibition of human purified T cells adhesion on resting MCE cells.

Human purified T cells were incubated for 24 hours with control medium or medium containing 5 μg/ml PMA and 100 υg/ml ionomycin (*). After labelling with Calcein AM, and incubation with a monolayer of resting MCE cells, non-adherent cells were washed and the remaining adherent cells were counted . In blocking conditions, monolayer cells were incubated for 30 min. with antibodies, prior to the addition of labelled T cells. Graph (A) presents for each condition the percentage of adherent cells, using the unwashed wells as 100%. Table (B) summarises the % of inhibition using the condition with no blocking antibody as 0% of inhibition.

A



B

	Condition	Inhibition (%)
T cells	rat IgG1	-5.4
	anti-VCAM-1	45.4
	mouse IgG1	-26.5
	anti-LFA-1	24.1
	mouse IgG2a	-13.7
	anti-VLA-4	57.0
T cells*	rat IgG1	16.1
	anti-VCAM-1	32.8
	mouse IgG1	14.9
	anti-LFA-1	38.8
	mouse IgG2a	22.1
	anti-VLA-4	55.2

Figure 39: Inhibition of human purified T cells adhesion on stimulated MCE cells.
Unlike the previous experiment, the assay was performed using a monolayer of stimulated MCE cells, incubated with resting or stimulated (*) human purified T cells. Graph (A) presents for each condition the percentage of adherent cells, using the unwashed wells as 100%. Table (B) summarises the % of inhibition using the condition with no blocking antibody as 0% of inhibition.

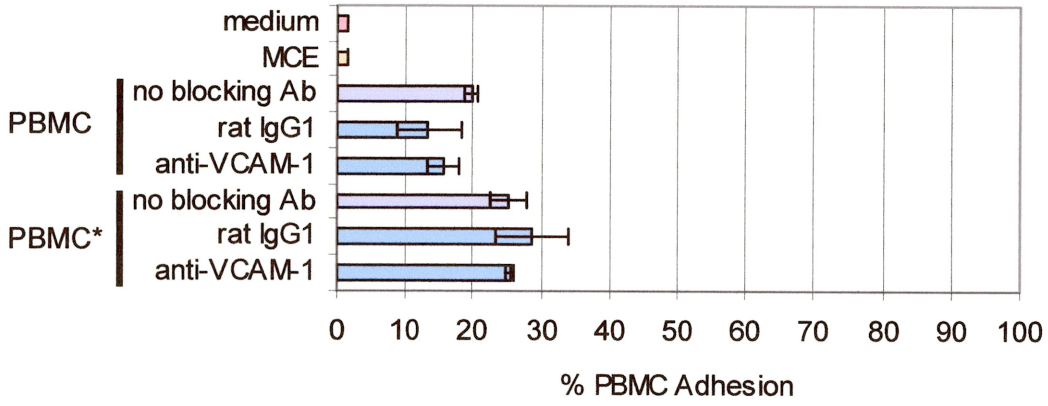
3.2.2.3- PBMC

The anti-VCAM-1 antibody was used to block the adhesion of Peripheral Blood Mononuclear cells (PBMC) to resting (figure 40) or activated (figure 41) MCE cells. Only when both populations were stimulated, did the antibody have an effect (nearly 19% inhibition) on the adhesion (figure 41 A and B). In the other cases, there was no detectable effect or the effect was equivalent to the one of the isotype control (figures 40A and 41A). No other antibodies were tested on these combinations of adhesion assays.

3.2.2.4- PMN

As for PBMC, the anti-VCAM-1 antibody was the only one tested. It showed almost no effect, whether in the case of resting cells or activated one (except a slight inhibition (8.4%) of activated PMN adhesion to resting MCE cells) (figures 42 and 43). The experiments on these cell populations were not pursued.

A

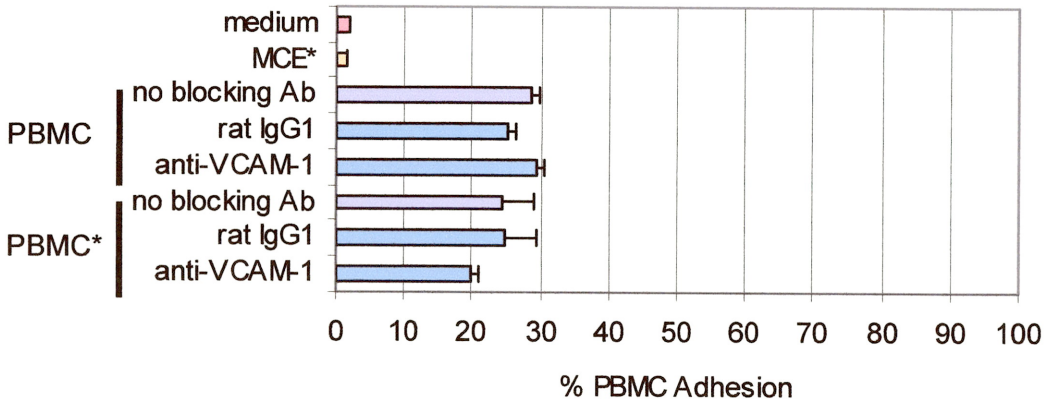


B

	Condition	Inhibition (%)
PBMC	rat IgG1	31.7
	anti-VCAM-1	20.1
PBMC*	rat IgG1	-13.5
	anti-VCAM-1	-0.9

Figure 40: Inhibition of human PBMC adhesion on resting MCE cells.
Human Peripheral Blood Mononuclear Cells (PBMC) were incubated for ½ an hour with control medium or medium containing 50 ng/ml PMA (*). An adhesion assay was then performed using a monolayer of resting MCE cells. In blocking conditions, monolayer cells were incubated for 30 min. with antibodies, prior to the addition of labelled PBMC. After several washes, remaining cells were counted. Graph (A) presents for each condition the percentage of adherent cells, using the unwashed wells as 100%. Table (B) summarises the % of inhibition using the condition with no blocking antibody as 0% of inhibition.

A

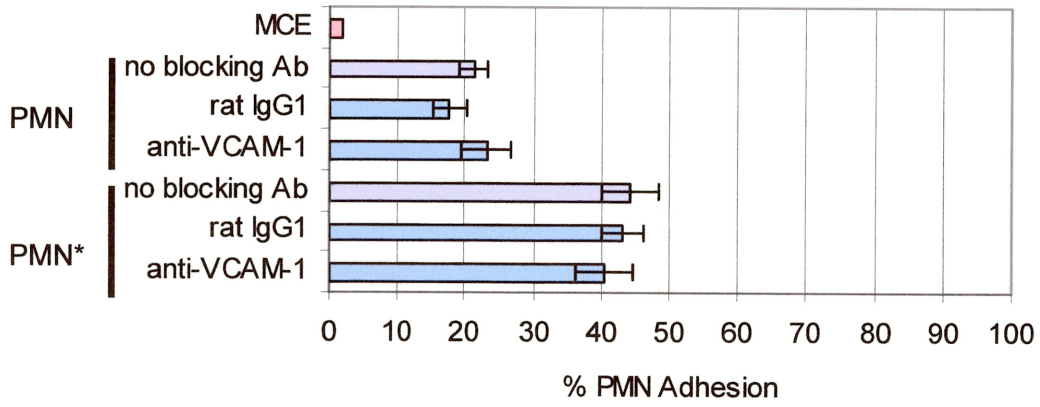


B

	Condition	Inhibition (%)
PBMC	rat IgG1	11.9
	anti-VCAM-1	-2.1
PBMC*	rat IgG1	-1.2
	anti-VCAM-1	18.6

Figure 41: Inhibition of human PBMC adhesion on stimulated MCE cells.
Human PBMC were prepared, stimulated and labelled as in figure 41. The assay was however performed on MCE cells stimulated for 24 hours with pro-inflammatory cytokines. Graph (A) presents for each condition the percentage of adherent cells, using the unwashed wells as 100%. Table (B) summarises the % of inhibition using the condition with no blocking antibody as 0% of inhibition.

A

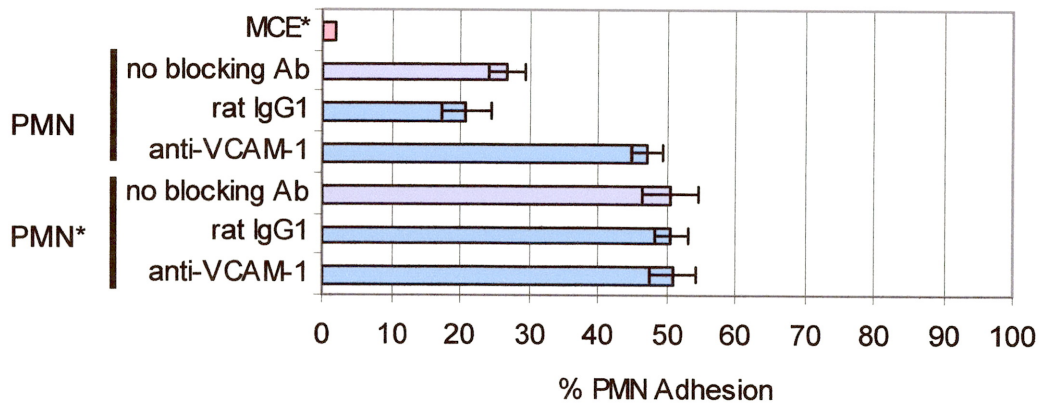


B

	Condition	Inhibition (%)
PMN	rat IgG1	17.1
	anti-VCAM-1	-8.8
PMN*	rat IgG1	1.9
	anti-VCAM-1	8.4

Figure 42: Inhibition of human PMN adhesion on resting MCE cells.
Human Polymorphonuclear cells (PMN) were incubated for ½ an hour with control medium or medium containing 50 ng/ml PMA (*). An adhesion assay was then performed using a monolayer of resting MCE cells. In blocking conditions, monolayer cells were incubated for 30 min. with antibodies, prior to the addition of labelled PMN. After several washes, remaining cells were counted. Graph (A) presents for each condition the percentage of adherent cells, using the unwashed wells as 100%. Table (B) summarises the % of inhibition using the condition with no blocking antibody as 0% of inhibition.

A



B

	Condition	Inhibition (%)
PMN	rat IgG1	22.7
	anti-VCAM-1	-74.9
PMN*	rat IgG1	-0.2
	anti-VCAM-1	-0.8

Figure 43: Inhibition of human PMN adhesion on stimulated MCE cells.
Human Polymorphonuclear cells (PMN) were prepared, stimulated and labelled as in figure 43. The adhesion assay was however performed using a monolayer of MCE cells, stimulated for 24 hours with pro-inflammatory cytokines. Graph (A) presents for each condition the percentage of adherent cells, using the unwashed wells as 100%. Table (B) summarises the % of inhibition using the condition with no blocking antibody as 0% of inhibition.

3.2.3- Inhibition of murine cells adhesion to MCE BALB/c cells

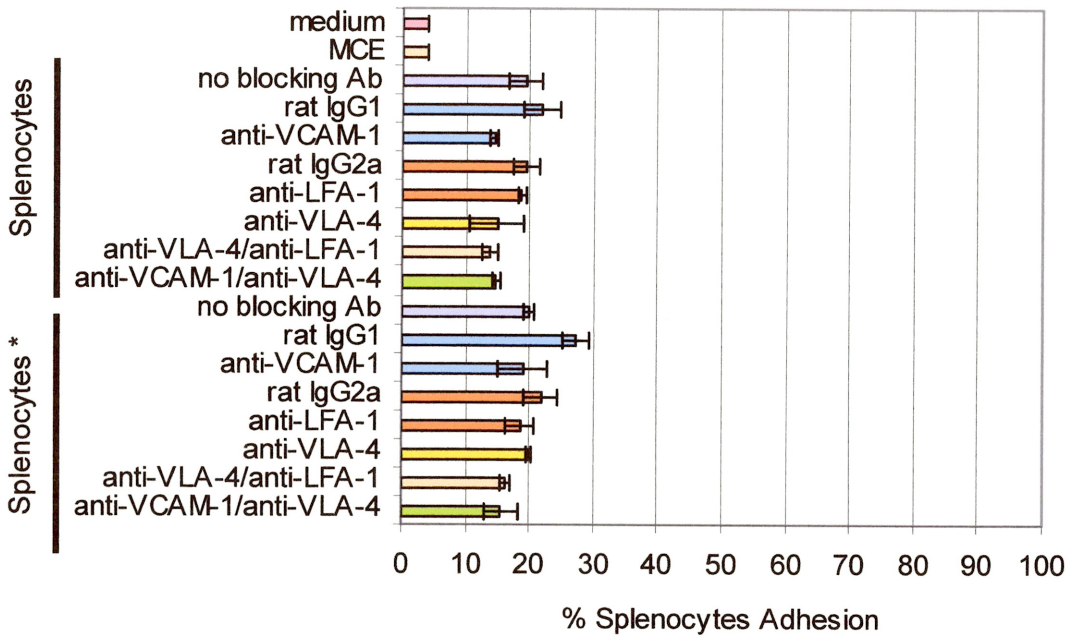
In the following experiments, we used antibodies against adhesion molecules or their ligands to inhibit the adhesion of murine populations (splenocytes and macrophages) to mouse corneal endothelial cells. All the antibodies used to investigate both sides of the interactions were directed against the mouse species (MK2.7; anti-mouse VCAM-1, M18/2; anti-mouse β2 integrin subunit of LFA-1, PS/2; anti-mouse α4 integrin subunit of VLA-4).

3.2.3.1- Splenocytes

Figure 44 presents the inhibition of adhesion of resting and activated splenocytes to resting corneal cells whereas figure 45 presents the same experiment carried out after the stimulation of corneal cells with pro-inflammatory cytokines.

The anti-mouse VCAM-1 antibody (MK2.7) was only able to block the adhesion of normal resting splenocytes. Their adhesion to both resting and stimulated corneal cells was decreased by more than 25% (figures 44 and 45) in the presence of this antibody. However, the antibody showed almost no ability to block the adhesion of activated splenocytes (figures 44 and 45). The antibody directed against the murine β2 integrin LFA-1 showed almost no effect either, whether on resting or activated cells. The antibody inhibited the adhesion of resting splenocytes to activated MCE by nearly 19%, but the isotype control for this condition also decreased the adhesion by 11%. The anti-mouse VLA-4, on the other hand was able to decrease the adhesion of resting splenocytes to unstimulated and stimulated MCE cells by 22.8% and 21.4% respectively, but as in the case of the anti-VCAM-1 antibody, the anti-VLA-4 was not able to inhibit the adhesion of activated splenocytes.

A



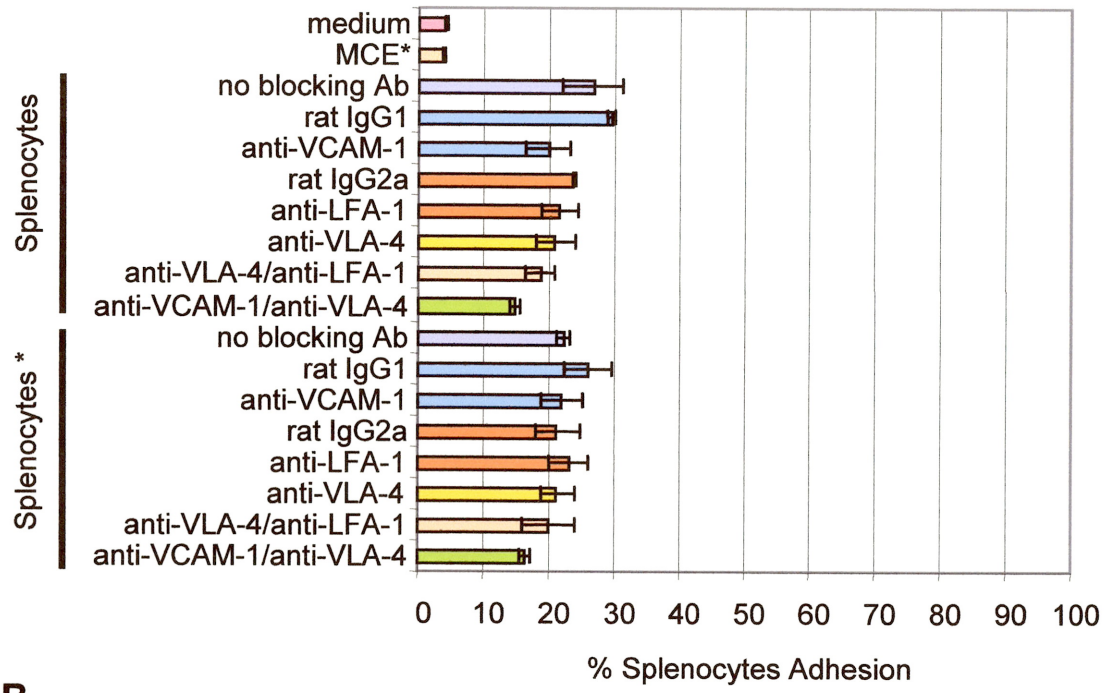
B

	Condition	Inhibition (%)
Spleno	rat IgG1	-13.4
	anti-VCAM-1	25.4
	rat IgG2a	-0.3
	anti-LFA-1	2.8
	anti-VLA-4	22.8
	anti-VLA-4/ rat IgG2a	34.3
	anti-VLA-4/anti-LFA-1	29.5
	anti-VCAM-1/anti-VLA-4	23.9
Spleno*	rat IgG1	-37.2
	anti-VCAM-1	4.4
	rat IgG2a	-10.1
	anti-LFA-1	6.0
	anti-VLA-4	-0.6
	anti-VLA-4/ rat IgG2a	16.6
	anti-VLA-4/anti-LFA-1	18.2
	anti-VCAM-1/anti-VLA-4	21.4

Figure 44: Inhibition of murine splenocytes adhesion on resting MCE cells.

Murine splenocytes were incubated for 24h with control medium or medium containing 1 μg/ml PMA and 1 υg/ml ionomycin (*). An adhesion assay was then performed using a monolayer of resting MCE cells. Graph (A) presents for each condition the percentage of adherent cells, using the unwashed wells as 100%. Table (B) summarises the % of inhibition using the condition with no blocking antibody as 0% of inhibition.

A



B

	Condition	Inhibition (%)
Spleno	rat IgG1	-10.5
	anti-VCAM-1	25.6
	rat IgG2a	11.0
	anti-LFA-1	18.8
	anti-VLA-4	21.4
	anti-VLA-4/ rat IgG2a	26.5
	anti-VLA-4/anti-LFA-1	29.6
	anti-VCAM-1/anti-VLA-4	44.4
Spleno*	rat IgG1	-16.0
	anti-VCAM-1	2.0
	rat IgG2a	4.4
	anti-LFA-1	-3.2
	anti-VLA-4	4.4
	anti-VLA-4/ rat IgG2a	16.2
	anti-VLA-4/anti-LFA-1	10.4
	anti-VCAM-1/anti-VLA-4	27.0

Figure 45: Inhibition of murine splenocytes adhesion on stimulated MCE cells.
Murine splenocytes were prepared, stimulated and labelled as in figure 45. The adhesion assay was however performed using a monolayer of MCE cells, stimulated for 24 hours with pro-inflammatory cytokines. Graph (A) presents for each condition the percentage of adherent cells, using the unwashed wells as 100%. Table (B) summarises the % of inhibition using the condition with no blocking antibody as 0% of inhibition.

An inhibition of activated splenocytes adhesion was detected only when the anti-VLA-4 was associated with an anti-VCAM-1 (21.4% and 27% inhibition for resting and activated MCE cells respectively) or to a lesser extent with an anti-LFA-1 (18.2% and 10.4% inhibition) antibody. On resting splenocytes, the same combinations slightly increased the effect produced by the antibodies alone (figure 44 and 45).

3.2.3.2- Macrophages

The adhesion of macrophages to mouse corneal cells was very high (63% and 65% of cells adhered to the resting and activated monolayer respectively). This adhesion could not be inhibited by any of the antibodies used previously, at least not more than with the isotype controls (figures 46A and 47A). Only when both macrophages and MCE cells were activated, the VLA-4 antibody was able to decrease the adhesion by nearly 30%. Finally, the combination anti-VCAM-1/anti-VLA-4 had barely any effect on the adhesion of macrophages (figures 46 and 47).

3.2.4- Conclusion

An adhesion assay was set up in order to investigate 1) the role of adhesion molecules in the adhesion of different human and murine populations to mouse corneal cells and 2) the influence of pro-inflammatory cytokines on this process.

The study revealed that overall the stimulation of the cells increased the capacity of the different populations tested to adhere to corneal endothelial cells (except in the case of mouse splenocytes). However, the study also showed, that this effect on the adhesion was greater when the cells added to the monolayer, as opposed to the monolayer itself, were activated.

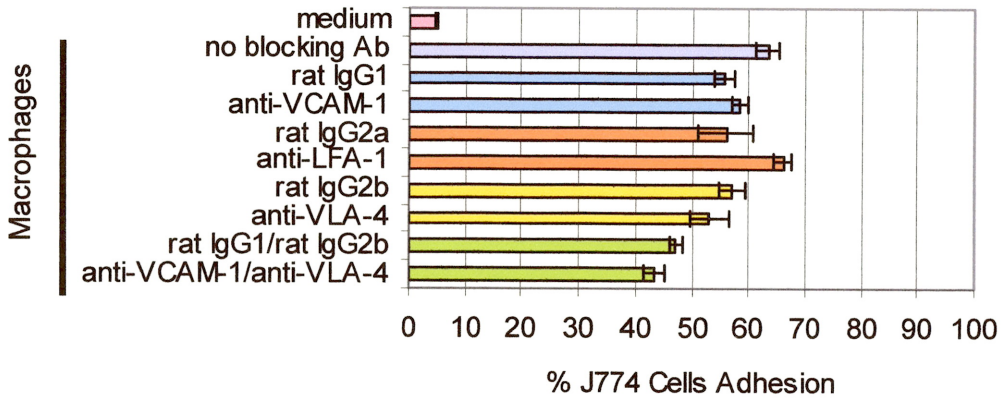
Our series of adhesion assays also showed that the ICAM-1 / LFA-1 interaction had probably a very small role to play, if any, in the adhesion of the cell populations tested to mouse corneal endothelial cells. The anti-mouse ICAM-1 Ab was only tested on Jurkat T cells and produced no effect at the range of concentration tested. This result is in agreement with the absence of ICAM-1 on MCE cells. The adhesion *via* the integrin LFA-1 was also investigated. On resting MCE cells, the antibody decreased the adhesion of activated purified T cells but had no effect on Jurkat, resting purified T cells, splenocytes or macrophages. We reached the same conclusions when the assays were performed on stimulated MCE cells, except that the antibody was also able to greatly decrease the adhesion of resting purified T cells. This antibody was not tested on PBMC and PMN.

The VCAM-1 / VLA-4 interaction, on the other hand, plays certainly a bigger part in the adhesion of leukocytes to MCE cells. Both antibodies, used either alone or in conjunction, were able to greatly reduce the adhesion of T cells or splenocytes to the MCE cell line. These data are in agreement with our previous results showing the constitutive expression of VCAM-1 only on MCE cells and its up-regulation by pro-inflammatory cytokines.

Interestingly, the association of the antibody directed against the α4 subunit of VLA-4 with an antibody against the β2 subunit of LFA-1 or against the mouse VCAM-1 molecule was able to reduce the adhesion of activated splenocytes to both resting and activated MCE cells, whereas these antibodies used alone had no effect.

Preliminary experiments on PBMC, PMN and mouse macrophages showed that VCAM-1 was probably not involved in their interaction with MCE cells, but further work is needed to provide a more definite answer on this matter.

A

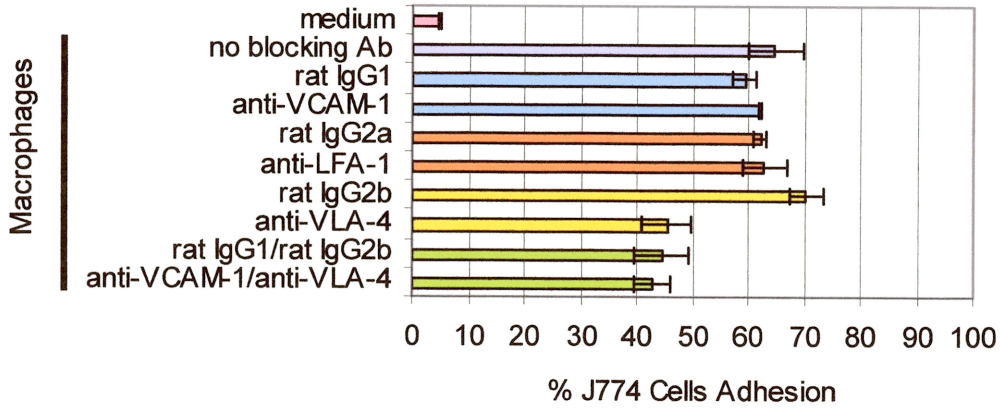


B

Condition	Inhibition (%)
rat IgG1	12.2
anti-VCAM-1	7.8
rat IgG2a	11.6
anti-LFA-1	-4.3
rat IgG2b	10.0
anti-VLA-4	16.2
rat IgG1/rat IgG2b	25.6
anti-VCAM-1/anti-VLA-4	31.6

Figure 46: Inhibition of murine macrophages adhesion on resting MCE cells.
Murine macrophages and resting MCE cells were used in an adhesion assay performed as previously described. Graph (A) presents for each condition the percentage of adherent cells, using the unwashed wells as 100%. Table (B) summarises the % of inhibition using the condition with no blocking antibody as 0% of inhibition.

A



B

Condition	Inhibition (%)
rat IgG1	8.2
anti-VCAM-1	4.2
rat IgG2a	4.2
anti-LFA-1	2.8
rat IgG2b	-8.7
anti-VLA-4	29.8
rat IgG1/rat IgG2b	31.3
anti-VCAM-1/anti-VLA-4	34.1

Figure 47: Inhibition of murine macrophages adhesion on stimulated MCE cells.
The experiment described in figure 47 was repeated using a monolayer of MCE cells, stimulated for 24 hours with pro-inflammatory cytokines. Graph (A) presents for each condition the percentage of adherent cells, using the unwashed wells as 100%. Table (B) summarises the % of inhibition using the condition with no blocking antibody as 0% of inhibition.

3.3- Consequences of adhesion molecules expression on corneal allograft fate

VCAM-1 was found expressed constitutively in both a cell line derived from mouse corneal endothelium (MCE cells), and in excised corneal tissues. Experiments showed that its expression was increased by pro-inflammatory cytokines (TNFα, IFNγ and IL-1α) and that the molecule, and its ligand VLA-4 were involved in the interaction of these MCE cells with T cells or splenocytes. We then looked at the impact of the VCAM-1 molecule on corneal allograft rejection using histology.

Female BALB/c mice received orthotopic corneal grafts from female C3H/Hen (allografts) or BALB/c mice (syngeneic grafts). Once the rejection of allografts was established (grade III: opaque cornea, iris could not be recognised), eye balls from both syngeneic and allografts were removed and stored at -70°C until sectioning. Cryosections were then stained with anti-mouse adhesion molecule (ICAM-1, VCAM-1 and PECAM-1) antibodies detected with an avidin-horse radish peroxidase-DAB system. The sections were finally counterstained, mounted and photographed. Results are presented in figures 48 to 50. Due to technical problems, only one eye per condition was stained.

3.3.1- ICAM-1

As in the ungrafted cornea, the expression of ICAM-1 in the isograft was mainly associated with fibroblastic cells of the stroma and the endothelium did not show any staining. The allograft was characterized by a huge infiltration of cells in the stroma, with which ICAM-1 staining was associated (figure 48).

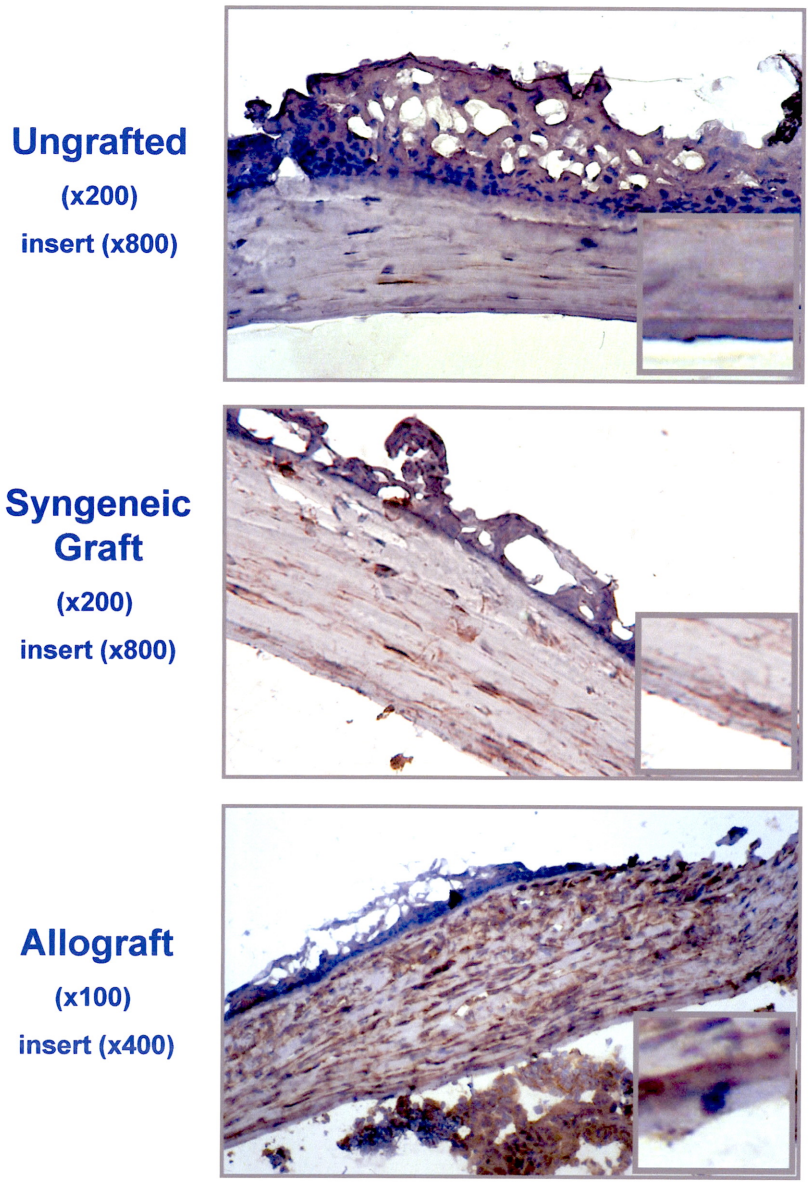


Figure 48: ICAM-1 expression in transplanted mouse corneas sections.
Female BALB/c mice received orthotopic corneal grafts from female C3H/Hen (allografts) or BALB/c mice (syngeneic grafts). Once the rejection of allografts was established (opaque cornea, iris could not be recognised), eyeballs from both syngeneic and allografts were removed and stored at -70°C until sectioning. Cryosections were then stained with an anti-mouse ICAM-1 (YN1) antibody for 20 minutes, washed twice in PBS and incubated with a biotinylated secondary antibody for a further 20 minutes. The latter antibody was detected with an avidin-horse radish peroxidase-DAB system. The sections were finally counterstained, mounted and photographed.

3.3.2- VCAM-1

Again, the staining of VCAM-1 in the syngeneic graft looks very much the same as in the ungrafted cornea, with staining associated with stromal fibroblastic cells and endothelial cells. The allograft is largely infiltrated by inflammatory cells and a very strong staining is visible at the donor / host interface. Some staining is also associated with invading blood vessels. Staining of the endothelium is not detected, mainly because of the damage sustained by this structure of the rejected cornea (figure 49).

3.3.3- PECAM-1

Unlike the ungrafted cornea that was completely devoid of staining for PECAM-1, the syngeneic graft presents some staining in the outer part of the stroma. The rest of the stroma and the others structures of the cornea do not present any staining for PECAM-1. The allograft, on the other hand, presents a strong staining for PECAM-1, first associated to keratocytes of the stroma and secondly a patchy staining presumably associated to blood vessels invading the rejected tissue. Cells adherent to the endothelium were also found positive for PECAM-1 (figure 50).

3.3.4- Conclusion

In respect to ICAM-1, VCAM-1 and PECAM-1 expression in the cornea, syngeneic grafts behave very much like the ungrafted cornea. These adhesion molecules are however far more expressed in the rejected cornea with staining associated to infiltrated cells and with blood vessels for VCAM-1 and PECAM-1. A very strong staining for VCAM-1 was also detected at the donor / host interface.

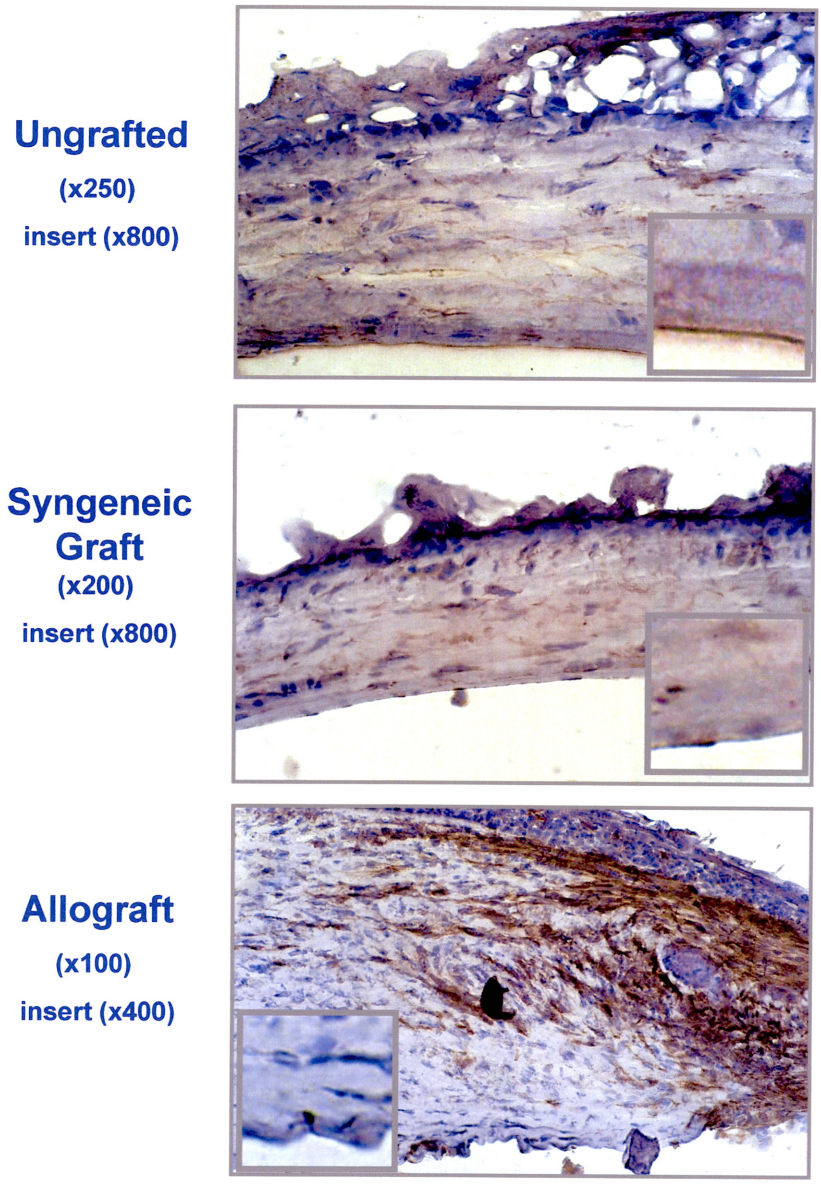


Figure 49: VCAM-1 expression in transplanted mouse corneas sections.
Female BALB/c mice received orthotopic corneal grafts from female C3H/Hen (allografts) or BALB/c mice (syngeneic grafts). Once the rejection of allografts was established (opaque cornea, iris could not be recognised), eyeballs from both syngeneic and allografts were removed and stored at -70°C until sectioning. Cryosections were then stained with an anti-mouse VCAM-1 (MK2.7) antibody for 20 minutes, washed twice in PBS and incubated with a biotinylated secondary antibody for a further 20 minutes. The latter antibody was detected with an avidin-horse radish peroxidase-DAB system. The sections were finally counterstained, mounted and photographed.

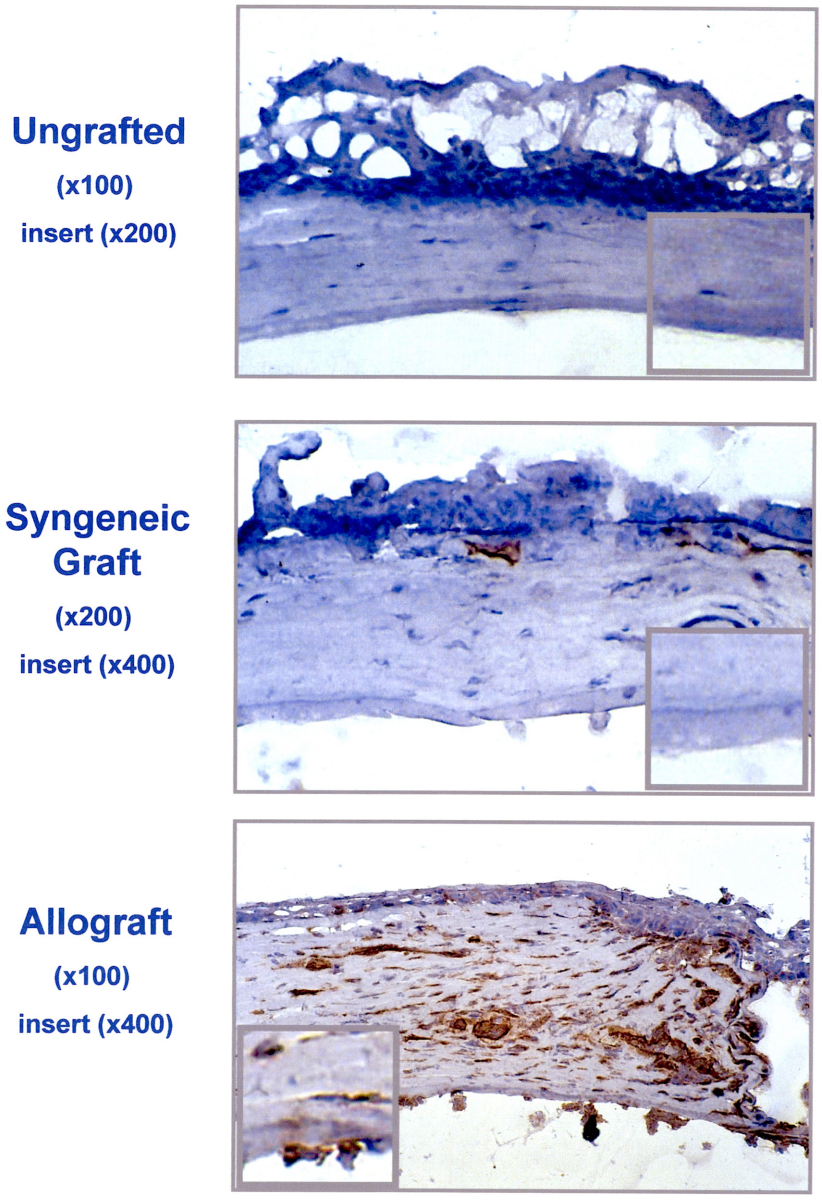


Figure 50: PECAM-1 expression in transplanted mouse corneas sections.
Female BALB/c mice received orthotopic corneal grafts from female C3H/Hen (allografts) or BALB/c mice (syngeneic grafts). Once the rejection of allografts was established (opaque cornea, iris could not be recognised), eyeballs from both syngeneic and allografts were removed and stored at -70°C until sectioning. Cryosections were then stained with an anti-mouse PECAM-1 (GC51) antibody for 20 minutes, washed twice in PBS and incubated with a biotinylated secondary antibody for a further 20 minutes. The latter antibody was detected with an avidin-horse radish peroxidase-DAB system. The sections were finally counterstained, mounted and photographed.

In the allograft, no conclusion can be drawn on the expression of these adhesion molecules in the endothelium, this structure being too damaged at this late stage of rejection.

3.4- Modulation of VCAM-1 expression in MCE cells

As demonstrated previously, VCAM-1 has been found in mouse corneal endothelial (MCE) cells and has been associated 1) with an increase in cell adhesion to these same cells and 2) with rejection in a mouse corneal allograft. Reducing its expression or its up-regulation by pro-inflammatory cytokines may therefore help preventing corneal allograft rejection. Two different techniques have been tested in order to diminish VCAM-1 expression: the first one involves the use of Vitamin E whereas the second uses a single chain antibody directed against VCAM-1.

3.4.1- Inhibition of VCAM-1 expression using Vitamin E

Vitamin E is the strongest physiological antioxidant present in cellular membranes and plasma lipoproteins. There are eight naturally occurring forms of vitamin E with antioxidant activity, four tocopherols (α, β, γ and δ) and four tocotrienols (α, β, γ and δ). Alpha-tocopherol is the biologically most active one (Blatt *et al.*, 2001). Although it was claimed for more than 50 years that vitamin E therapy was an effective treatment of heart diseases, theses findings were only recently confirmed by epidemiologic and clinical studies (as reviewed by Chan *et al.* (Chan, 1998)). Aside from its antioxidative properties, vitamin E is thought to modulate inflammatory response, possibly by inhibiting the activation of NF-κB by oxidants, PMA or TNFα in a number of cells. NF-κB is a reduction-oxidation (redox)-sensitive transcriptional

factor, regulator of many genes, including ICAM-1 and VCAM-1 (Janeway CA, 2001). *In vitro* studies have shown that supplementation of endothelial cells with vitamin E decreases monocyte-endothelial adhesion in HUVECs (Faruqi *et al.*, 1994), and suppresses IL-1β-induced expression of ICAM-1, VCAM-1 and E-Selectin in human aortic endothelial cells (HAECs) (Wu *et al.*, 1999). Zapolska-Downar and co-workers reported a decrease in TNFα or IL-1β-induced up-regulation of VCAM-1 but not ICAM-1 in HUVECs after treatment with alpha-tocopherol (Zapolska-Downar *et al.*, 2000).

A primary cell model for adult large vessel endothelium has been recently developed in our laboratory: primary endothelial cells are derived from human saphenous veins routinely removed in varicose vein surgery or vascular and coronary bypass operations. In this model (HSVECs), VCAM-1 (among other adhesion molecules) is up-regulated by pro-inflammatory cytokines (TNFα, IFNγ and IL-1β) (Tan *et al.*, submitted) and vitamin E has been shown to reduce significantly this up-regulation. The reagent was therefore tested on our MCE cells model.

Basically, MCE cells were incubated for 24 hours with concentrations of vitamin E ranging from 0 to 500 μM, washed once in PBS and further incubated for 8 hours with control medium (MCE) or medium containing a cocktail of pro-inflammatory cytokines (TNFα 20 ng/ml, IFNγ 600 IU/ml and IL-1α 20 ng/ml) (MCE*). Cells were then detached with trypsin and the expression of mouse VCAM-1 was analysed by Flow Cytometry. Results are presented in figure 51. As expected, the figure shows that the stimulation of MCE cells by pro-inflammatory cytokines has led to an up-regulation of VCAM-1 expression (more than 3 times as seen on the bottom panel of figure 51).

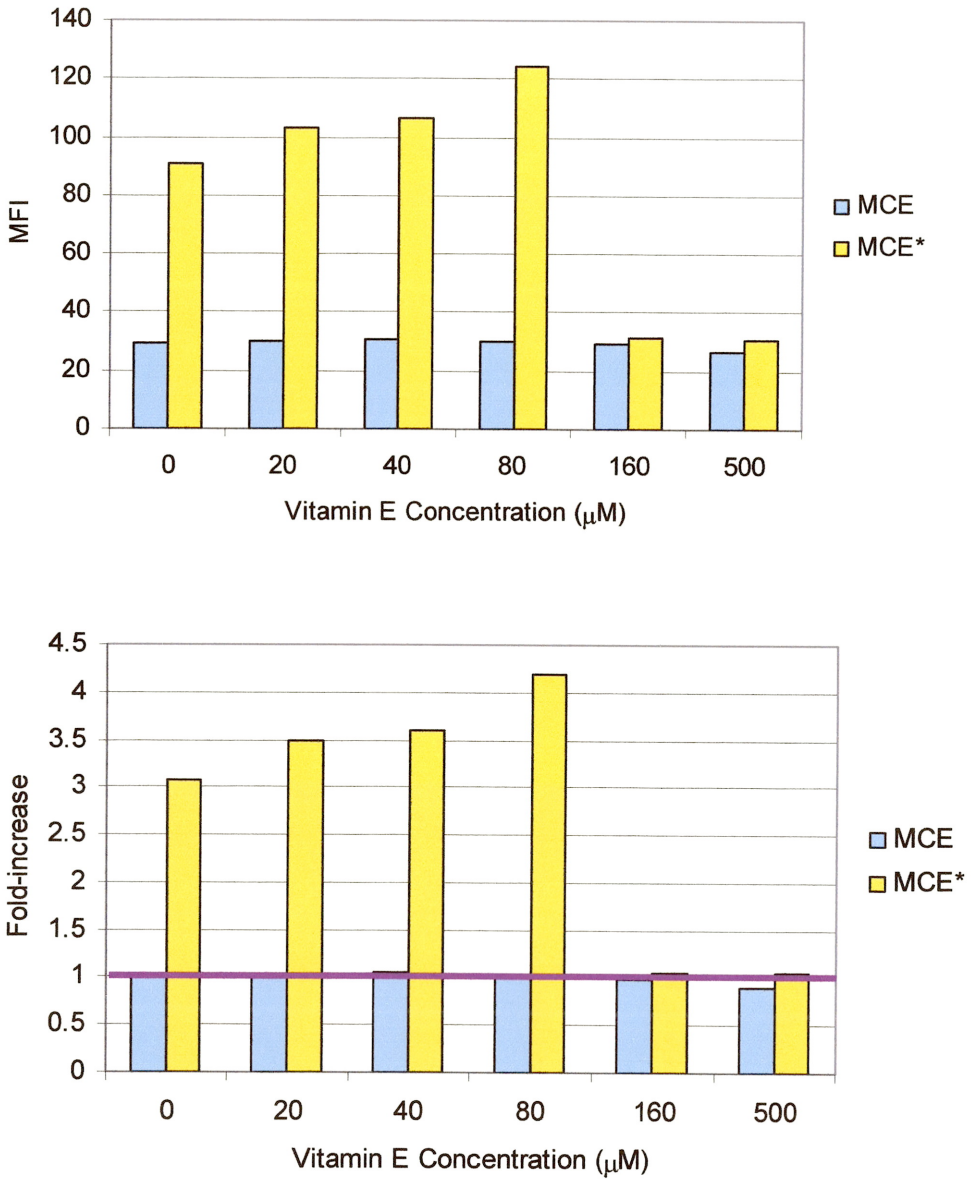


Figure 51: Inhibition of VCAM-1 expression using Vitamin E.
MCE cells were seeded in a 24-well plate and incubated for 24 hours with various concentrations of vitamin E (0 to 500 μM). Cells were then washed once in PBS and further incubated for 8 hours with control medium (MCE) or a medium containing a cocktail of pro-inflammatory cytokines (TNFα, IFNγ and IL-1) (MCE*). Cells were finally detached with trypsin and the expression of VCAM-1 was analysed using flow cytometry. The top panel presents the Median Fluorescence Intensity, whereas the bottom panel shows the fold-increase in VCAM-1 expression with 1 being the value of VCAM-1 expression in resting MCE not exposed to Vitamin E.

The figure also shows that in resting MCE cells, the expression of VCAM-1 is not affected by the pre-incubation with vitamin E, even at the very high dose of 500 μM. Stimulated MCE cells, on the other hand, see their VCAM-1 expression increased by low concentrations (20 to 80 μM), but decreased by high doses (160 and 500 μM) of vitamin E. The up-regulation of VCAM-1 reached a maximum at the 80 μM dose, with VCAM-1 expression more than 4 times higher than the level in resting MCE cells. At 160 and 500 μM, vitamin E completely inhibited the up-regulation of VCAM-1 expression, whose level remained the same as in resting cells. This experiment showed the powerful capacity of vitamin E to prevent the up-regulation of VCAM-1 in this cell model. However, when repeated a second time, the inhibitory effect of vitamin E was not detected: at the lowest doses (20 to 80 μM), the expression of VCAM-1 was increased in a pattern similar to the previous experiment. The highest doses (160 and 500 μM) however had no inhibitory effect on VCAM-1 up-regulation by the cocktail of cytokines (data not shown). These experiment have produced conflicting data, however the lack of inhibitory effect in the second set of data is probably due to a human error in the distribution of the vitamin E reagent. The experiment needs obviously repeating but the results of the first set of data are very encouraging. This first set of data is also consistent with those obtained on HSVECs in our laboratory (unpublished data). In these cells, vitamin E had a pro-inflammatory effect at lower doses (60 and 120 μM) while a reduction in mRNA expression was observed after treatment with a higher dose (240 μM).

3.4.2- Inhibition of VCAM-1 expression by anti-VCAM-1 single chain antibody

The intracellular antibody or intrabody technology uses the specific and high-affinity-binding properties of immunoglobulin molecules. Briefly, in this strategy, cells are transfected with the gene of an antibody directed against the target molecule, antibodies are then synthesised by the cell and are directed to a particular cellular compartment to down-regulate or inactivate specifically the target molecule. A key factor in the development of this technique is the use of single-chain antibodies (scFv). Single-chain antibodies are composed of the heavy- and light-chain variable domains (V_H and V_L) of the immunoglobulin molecule, separated by a flexible polypeptide linker that ensures stability to the molecule (figure 52) (Bird *et al.*, 1988; Huston *et al.*, 1988). Because the constant portion of the Ig has no role in antigen binding, it is not included in the construct. The result is a small molecule with high-affinity and selective binding properties, simple enough to require minimum assembly (Richardson and Marasco, 1995). Intrabodies may be used to block or stabilise molecular interactions, modulate enzyme function, (by occluding an active site, sequestering a substrate or fixing the enzyme in an active or inactive state), or even sequester targets in particular cellular compartments (Rondon and Marasco, 1997). The latter approach was used in this study. In our unit, a single chain antibody directed against pig VCAM-1 surface receptor was developed. One approach consists in constructing the scFv from a pre-existing hybridoma secreting a monoclonal antibody specific for the target molecule. Alternatively, the scFv used in this study was constructed from a phage-display antibody library: antibody genes (V_H and V_L domains, cloned in a phage (bacterial virus) vector, are fused to a coat protein of the phage to allow display of the antibody on the phage surface.

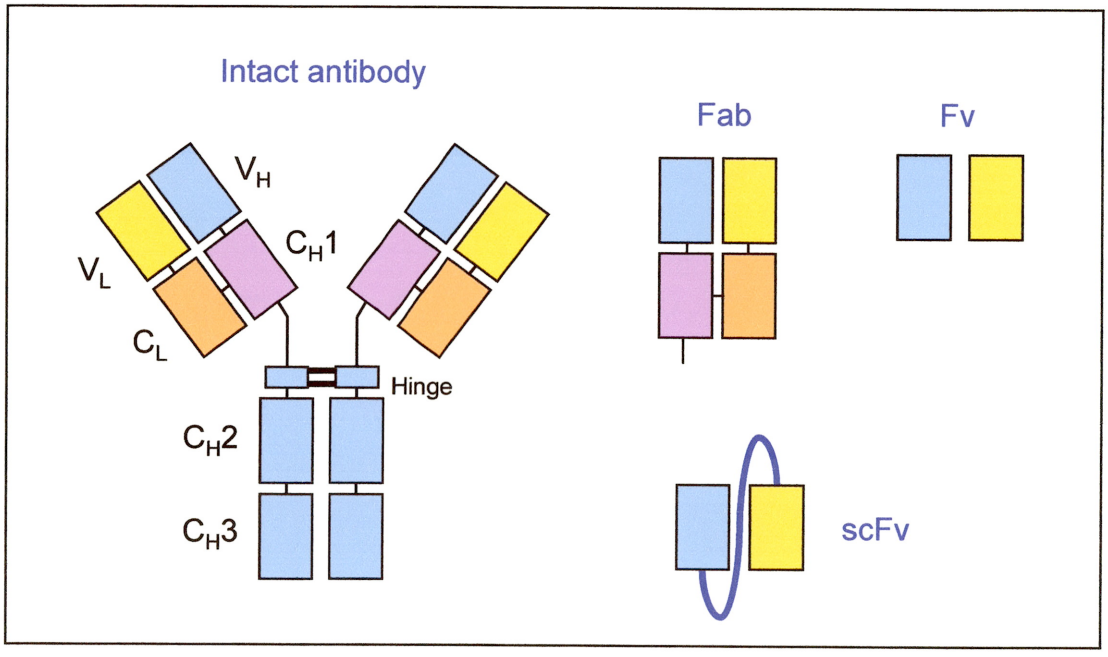


Figure 52: Structure of intact antibody, antibody fragments and scFv construct (adapted from Richardson et al, 1995).
Keys: C_H, heavy-chain constant domain; V_H heavy-chain variable domain; C_L, light-chain constant domain; V_L, light-chain variable domain; Fv, variable-region fragment; scFv, single-chain variable region fragment. The V_H and V_L domains of the scFv construct are separated by a flexible linker peptide.

Antibody-expressing phages are then separated from non-expressing phages by incubation with the antigen (in our case DAP-3 cells transfected with the gene encoding for porcine VCAM) (Ramrakha *et al.*, submitted). Selected phages are then used to infect and multiply in *E. coli*, therefore enriching for this population. After several rounds of selection, two phages clones specific for porcine VCAM were identified and, after PCR amplification, were cloned into a mammalian expression vector to produce scFv constructs suitable for transfection. A C-terminal retention signal (KDEL amino acid motif –Lys-Asp-Glu-Leu) was also added to the construct to sequester the intrabodies in the endoplasmic reticulum (ER). Intracellular expression of these scFv intrabodies led a 90 % reduction in VCAM-1 expression and abolished VCAM-dependant adhesion of human leukocytes (Ramrakha *et al.*, submitted). The intrabodies were tested in our MCE cell line model.

Briefly, MCE cells were co-transfected with different ratios of GFP and scFv/E6 plasmids. Plasmid scFv/E6 contains the gene for the scFv directed against pig VCAM-1, constructed as detailed above. When run through a flow cytometre, GFP-transfected cells are positive on the FL-1 channel (green) and allow selective analysis of transfected versus non-transfected cells. Finally, the different GFP/E6 ratios allow the analysis of the dose-response effect of plasmid scFv/E6. After transfection, cells were left to recover, and then stimulated with pro-inflammatory cytokines for 24 hours. Cells were then detached with trypsin and the expression of VCAM-1 was analysed by FACS analysis.

Figure 53 presents the results of one experiment. The top panel presents the median fluorescence intensity (MFI) detected in all cells regardless if they were transfected or not. The bottom panel expresses the fold-increase in VCAM-1

expression with 1 being the value of VCAM-1 expression in resting untransfected MCE cells.

The figure shows that on untransfected cells, the stimulation with pro-inflammatory cytokines increased the expression of VCAM-1 more than five times (figure 53, bottom). In both resting and activated MCE cells, the addition of the transfecting reagent lipofectamine alone, or the transfection with GFP alone (GFP:scFv 1:0) did not modify the level of VCAM-1 expression. In resting MCE cells, the transfection with both GFP and the single chain antibody (scFv) had no effect on the basal expression of VCAM-1 cells, even when a high ratio of scFv (GFP:scFv 1:3) was used. In activated cells, however, transfection with GFP:scFv decreased the expression of VCAM-1 by 5.4% (GFP:scFv 1:1) to nearly 13% when a GFP:scFv ratio of 1:3 was used (figure 53, top). In this latter case, the expression of VCAM-1 remained nearly 4.7 times higher than in resting cells, but a 13% reduction in expression is nonetheless a good achievement considering that only about 20% of the cells were transfected in this experiment, as attested by the number of "green" cells (cells transfected with GFP alone and positive on FACS on the FL-1 channel). The experiment needs therefore repeating and higher transfection rates should further reduce the expression of VCAM-1 in the MCE cells. These encouraging data are besides supported by recent results in our laboratory: MCE cells stably transfected with the scFv/E6 plasmid present a great reduction in VCAM-1 constitutive expression (Dr S. Alam, unpublished data).

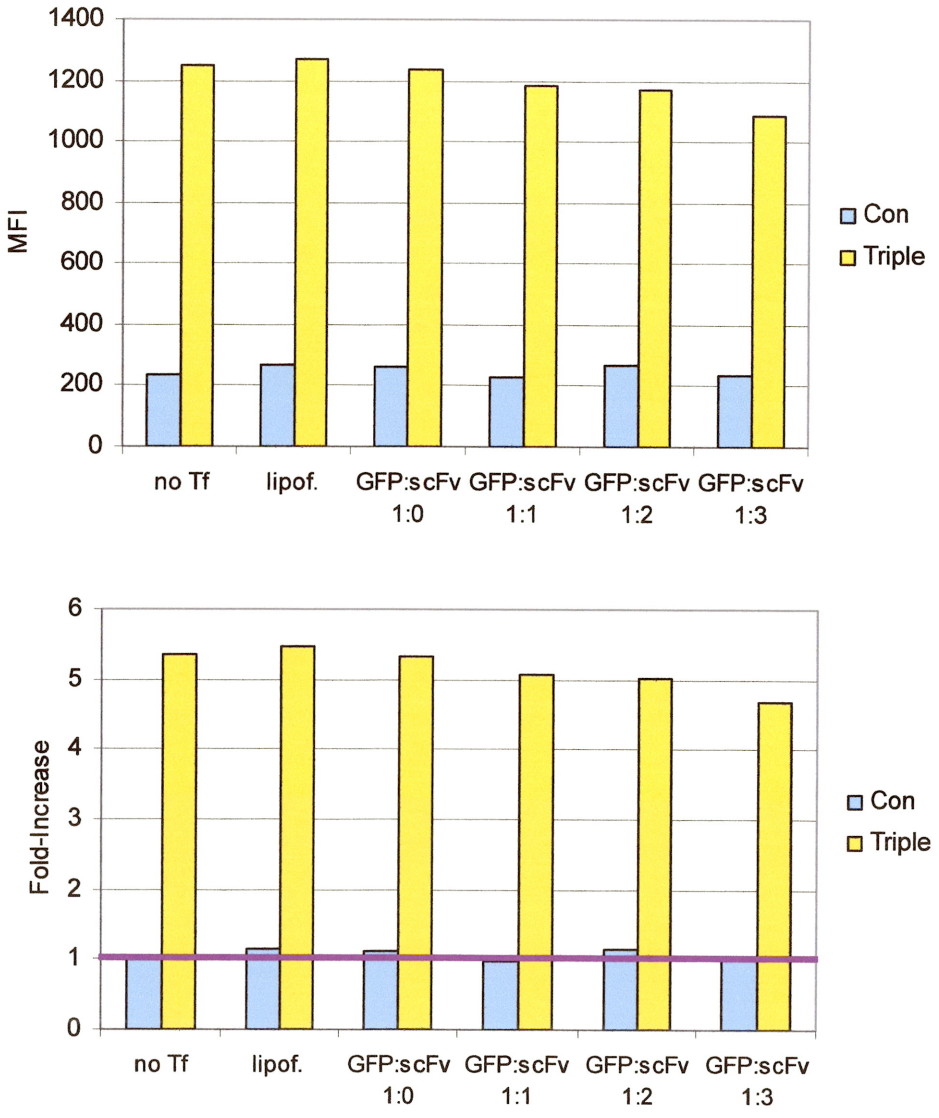


Figure 53: Inhibition of VCAM-1 expression using a single chain anti-VCAM-1 antibody transfection.
When about 70% confluent, MCE cells were transfected for 3 hours at 37°C with different ratios of GFP and scFv (a single chain antibody directed against VCAM-1), using lipofectamine. Cells were then left to recover in complete medium and incubated for 24 hours in control medium (MCE) or medium containing a cocktail of pro-inflammatory cytokines (MCE*). The expression of VCAM-1 was finally analysed using flow cytometry. The top panel presents the Medium Fluorescence Intensity (MFI) while the bottom one expresses the fold-increase in VCAM-1 expression with 1 being the value of VCAM-1 expression in resting untransfected MCE cells. Keys: Tf= transfection, Lipof.=lipofectamine only

3.4.3- Conclusion

In our attempt to prevent corneal allograft rejection, we investigated the down-regulation of VCAM-1 expression in MCE cells, using 1) vitamin E or 2) a single chain antibody directed against VCAM-1.

One experiment showed a complete inhibition of VCAM-1 up-regulation by pro-inflammatory cytokines, using vitamin E. The experiment needs however to be repeated as data were not reproduced in a subsequent attempt.

Similarly, MCE cells transfected transiently with a single chain antibody directed against VCAM-1, showed a reduced up-regulation of the adhesion molecule after stimulation by pro-inflammatory cytokines. The effect is however marginal and needs to be confirmed in experiments with higher transfection efficiency.

Provided they are confirmed, these data present two different means to diminish the up-regulation of VCAM-1 by pro-inflammatory cytokines in corneal cells. Using these techniques, the adhesion of inflammatory cells to the transplanted cornea and therefore allograft rejection could be prevented in this model.

3.5- VCAM-1, a target for therapy in corneal transplantation?

Several studies report an up-regulation of pro-inflammatory cytokines associated to the rejection of corneal allografts. In the vascular endothelium, such elevated concentrations lead to an increase of some adhesion molecule expression. This was the starting point of this study, where we investigated the expression of a panel of adhesion molecules in whole corneal tissues and in a model of corneal endothelium, the MCE cell line.

Although RT-PCR showed the presence of mRNA for several of the adhesion molecules tested in the MCE cells and in whole corneas, VCAM-1 was the only protein tested detected in both models by FACS analysis, immunofluorescence or histology. The expression of VCAM-1 in these cells was up-regulated by pro-inflammatory cytokines (TNFα and IL-1α), and even further by a combination of TNFα with IFNγ. The expression of the VAP-1 protein however was not investigated due to the lack of antibody in our laboratory. The presence of mRNA for this molecule both in the MCE cell line and in corneal tissue is however very important considering the relatively restricted distribution of this adhesion molecule (synovial vessels, HSEC, smooth muscle cells, fat cells, DC in germinal centers).

When investigating the relative role of adhesion molecules in the adhesion of different cell populations to the MCE cells, we found that VCAM-1 and its ligand VLA-4 played a great role in the interaction. The partial inhibition of cell adhesion obtained with antibodies directed against these molecules however suggested a role for other molecules. Although the molecule is a potential candidate, the role of VAP-1 could not be investigated, but will be as soon as an antibody is available in the laboratory.

VCAM-1 was also found in large quantities at the donor / host interface of a rejected cornea. No such a pattern was demonstrated in a syngeneic graft stained for this same adhesion molecule.

Altogether, these data strongly supported an implication of VCAM-1 in the rejection of corneal allograft and made of it a candidate target for therapy. In the end of this study, our efforts therefore concentrated at inhibiting its up-regulation by pro-inflammatory cytokines. In one experiment, vitamin E was able to knock down the

up-regulation of VCAM-1 by a combination of TNFα, IFNγ and IL-1α. The transfection of MCE cells with a single chain antibody directed against VCAM-1 also led to a marginally reduced expression of the adhesion molecule.

Although they need confirmation, and though, in both cases, they can only provide a transient reduction of the expression of VCAM-1 in the MCE cells, these last results are very encouraging. Nevertheless, can these findings in a murine model be transferred to the human species?

CHAPTER 4

Adhesion Molecules in the Human Cornea

Adhesion molecules in the human cornea

4.1- Expression of adhesion molecules in the human cornea

We previously established in the first part of the study that among several adhesion molecules tested, VCAM-1 only was expressed both in a mouse corneal endothelial (MCE) cell line and in whole mouse corneas. We also demonstrated that the adhesion molecule was up-regulated by pro-inflammatory cytokines and was involved, with its ligand VLA-4, in the adhesion of several human and murine cell populations to the cell line. Finally, VCAM-1 was also found in rejected corneal allografts. All these results implicated the molecule in corneal allograft rejection. Preliminary data showed that its up-regulation could be reduced using vitamin E or transfection of a single chain antibody against VCAM-1, bringing a new insight in the prevention of corneal allograft rejection.

The second part of this study is looking at the expression of VCAM-1 (among other adhesion molecules) in the human species, and the effect of pro-inflammatory cytokines on these molecules. This was investigated using first RT-PCR on whole cornea specimens, and then using immunofluorescence on corneal endothelium flat-mounts. Some work was also dedicated to the generation of a human corneal endothelium cell line, which would have provided a very useful model for this study.

4.1.1- Optimisation of RT-PCR for human adhesion molecules

In order to define the effect of cytokines on the expression of adhesion molecules in human corneal cells, an RT-PCR technique specific for human ICAM-1, VCAM-1 and E-Selectin was set up. The conditions for each primers (the annealing temperature, and the $MgCl_2$ concentration used in the reaction) were optimised using EA-Hy 926 cells incubated for 1h to 24h with control media or media containing 200 or 600 IU/ml TNFα. Total mRNA was extracted and the mRNA for a housekeeping gene, GAPDH, and for adhesion molecules was detected using RT-PCR analysis and an ethidium bromide-stained gel. PCR reactions using GAPDH, ICAM-1, VCAM-1 and E-Selectin primers generated respectively a 567, 219, 241, and a 235 bp PCR product. Gel documents were then analysed using a densitometry software.

As shown in figure 1, the PCR analysis for GAPDH showed a homogeneous band (567 bp as expected) in all the samples. RT-PCR for ICAM-1 demonstrated a constitutive expression of ICAM-1 as attested by the presence of a 219 bp PCR product. Expression was increased by TNFα stimulation and peaked around 4 hours in the low-dose experiment and around 2 hours when a high dose of TNFα was used. VCAM-1 and E-Selectin were barely detectable in unstimulated EA-Hy cells (very faint bands seen in original gel). Their expression was however increased after 4 hours of low-dose TNFα stimulation (200 IU/ml) and after 2 hours of the higher-dose condition (600 IU/ml). Unlike VCAM-1, whose expression remained elevated after 24h, E-Selectin was only transiently expressed and had returned to its weak basal level after 8 hours (200 IU/ml) and 4 hours (600 IU/ml).

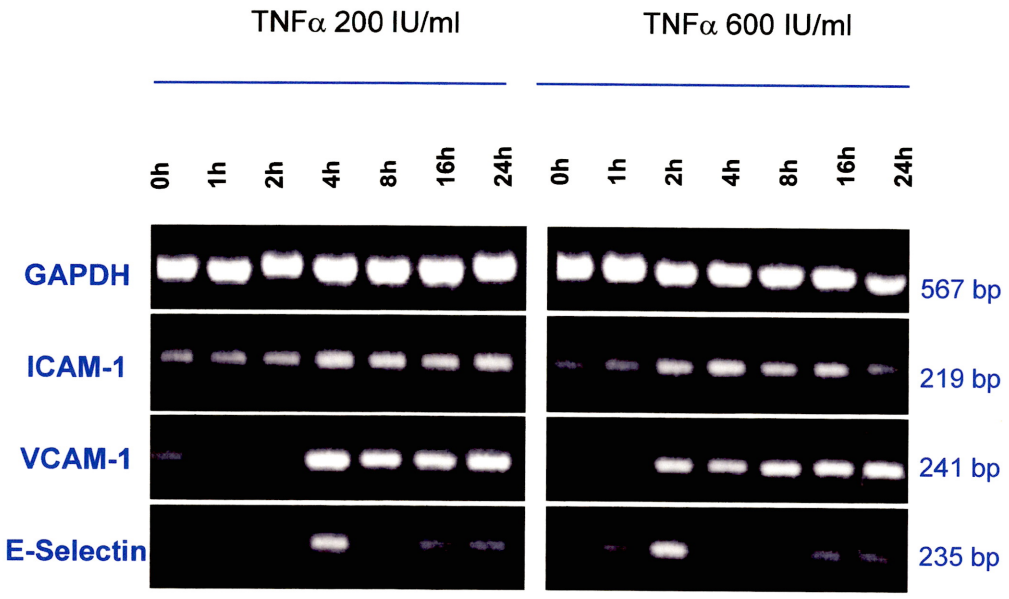


Figure 1: RT-PCR of GAPDH, ICAM-1, VCAM-1 and E-selectin mRNA in TNFα-treated EA-hy 926 cells.
Total mRNA was extracted from EA-hy monolayers stimulated for 1 to 24h with a low dose (200 IU/ml) or a high dose (600 IU/ml) TNFα and used in RT-PCR reactions to detect human GAPDH, ICAM-1, VCAM-1 and E-selectin mRNA. The PCR products were visualised by electrophoresis on a 1.5 % agarose gel stained with 10 mg/ml ethidium bromide. The photograph shows a constitutive expression of ICAM-1, peaking at 4 and 2 hours in the low and high doses of TNFα stimulation. VCAM-1 and E-selectin are barely detectable in unstimulated cells and in early time points (weak bands seen in original gel) but are both induced after 4 hours (low dose) and 2 hours (high dose) of stimulation. VCAM-1 is still highly expressed after 24h whereas E-selectin expression is only transient.

The Pixel Density (PD) analysis (figure 2) of the above gel showed a constitutive ICAM-1 mRNA expression in EA-Hy cells and an increase after 1h of TNFα stimulation, peaking at 4h with a 2.1- and 6.2-fold increase respectively in the low-dose (A) and high-dose (B) conditions. As seen on the gel, VCAM-1 and E-Selectin mRNA were barely detectable before 4h (low-dose (A)) and 2h (high dose (B)) of TNFα stimulation. VCAM-1 mRNA was then induced up to 8 fold in (A) and more than 300 times in the high dose condition after 24h of stimulation. In the low-dose condition, E-Selectin mRNA was increased 7 fold after 4h, whereas there was a 400-fold increase between 0h and 2h of high-dose TNFα stimulation. After 4h in (A) and 2h in (B), E-Selectin mRNA returned to its basal level of expression. E-Selectin data were however slightly confusing.

These data showed that EA-Hy 926 cells provided a convenient positive control for ICAM-1 expression in our corneal experiments. VCAM-1 and E-Selectin expression on these cells, however, was weak and depended on the stimulus concentration. This rendered them unsuitable and we therefore looked further for positive controls.

To overcome the problems encountered with EA-Hy cells, we decided to use stable transfectants. DVCAM cells consist of a mouse fibroblastic cell line, DAP-3, transfected with the human gene for VCAM-1. CHO-E cells are Chinese hamster CHO cells transfected with a gene coding for the human E-Selectin. The cells were tested using the RT-PCR technique optimised on EA-Hy cells.

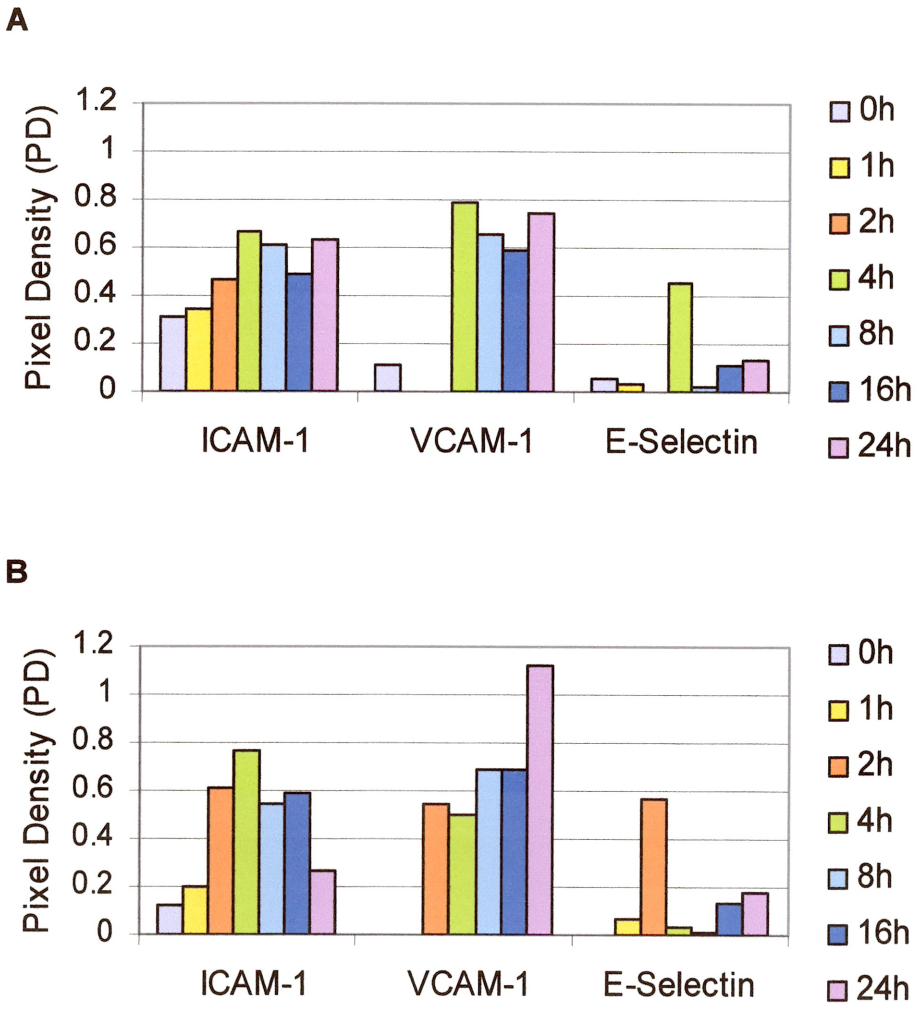


Figure 2: Pixel density analysis of ICAM-1, VCAM-1 and E-Selectin PCR products visualised on an ethidium bromide stained gel (fig. 1).
The photograph was analysed using a densitometer software and the mean pixel density (PD) obtained for ICAM-1, VCAM-1 and E-Selectin was corrected with the corresponding mean PD obtained for GAPDH. Graphs A and B show the results obtained for EA-Hy 926 cells stimulated respectively with 200 and 600 IU/ml TNFα.

As expected, the PCR for human ICAM-1 did not generate any product, as DVCAM and CHO-E are murine and Chinese hamster cells respectively. In the DVCAM cell line, PCR for human VCAM-1 generated a strong 241 bp band but no product was detected using E-Selectin primers. On the contrary, the CHO-E cell line was positive for E-Selectin but not for VCAM-1. Both untransfected cell lines (DAP-3 and CHO) were negative for the three human adhesion molecules tested (figure 3). Noteworthy, the use of primers for mouse GAPDH generated bands in all the samples, even though CHO cells are not murine cells. This confirms the conservation of the GAPDH gene across species. This experiment further demonstrated the specificity of our technique. Consequently, EA-Hy 926 cells were used as a positive control for ICAM-1, whereas DVCAM and CHO-E cells were used respectively in PCR for human VCAM-1 and E-Selectin.

4.1.2- Detection of mRNA for adhesion molecules in some human corneas

Adhesion molecules can be up regulated in vascular endothelium using various cytokines. We therefore investigated whether it was the case in human corneal cells. Post mortem human corneas were cut into 1/4 or 1/8 fragments and stimulated with 200 IU/ml TNFα (10 ng/ml) from 1h to 32h (cornea #1) or stimulated for 4h at variable doses of TNFα (0, 2, 20 or 200 IU/ml) (cornea #2). mRNA was extracted and RT-PCR for human ICAM-1, VCAM-1 and E-Selectin were performed.

Figure 4 shows the gel electrophoresis performed on PCR products from cornea #1. No constitutive expression of ICAM-1 mRNA was detected, the expression was however induced after 1h and the elevated expression remained after 32h of stimulation.

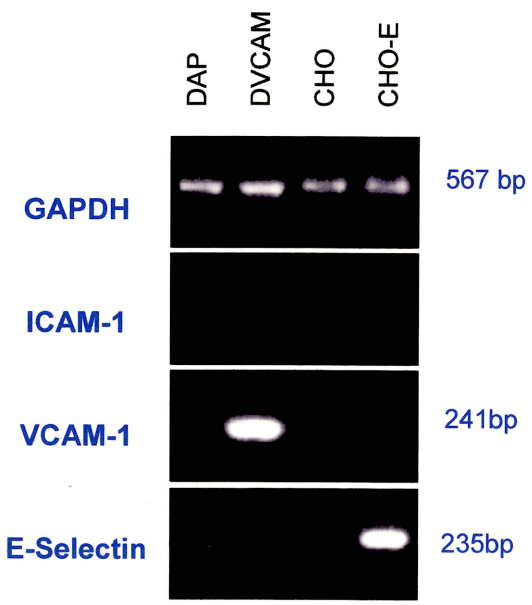


Figure 3: RT-PCR of GAPDH, ICAM-1, VCAM-1 and E-Selectin mRNA in DAP-3, DVCAM, CHO and CHO-E cells.
mRNA extracted from DAP-3, DVCAM, CHO and CHO-E cells was used in RT-PCR for human GAPDH, ICAM-1, VCAM-1 and E-Selectin. The PCR products were then run on an ethidium bromide-stained 1.5 % agarose gel. The photograph shows the expression of VCAM-1 and E-Selectin only, in the DVCAM and CHO-E cell lines respectively. No ICAM-1 was detected. Control cells (DAP and CHO) were negative for all the adhesion molecules tested.

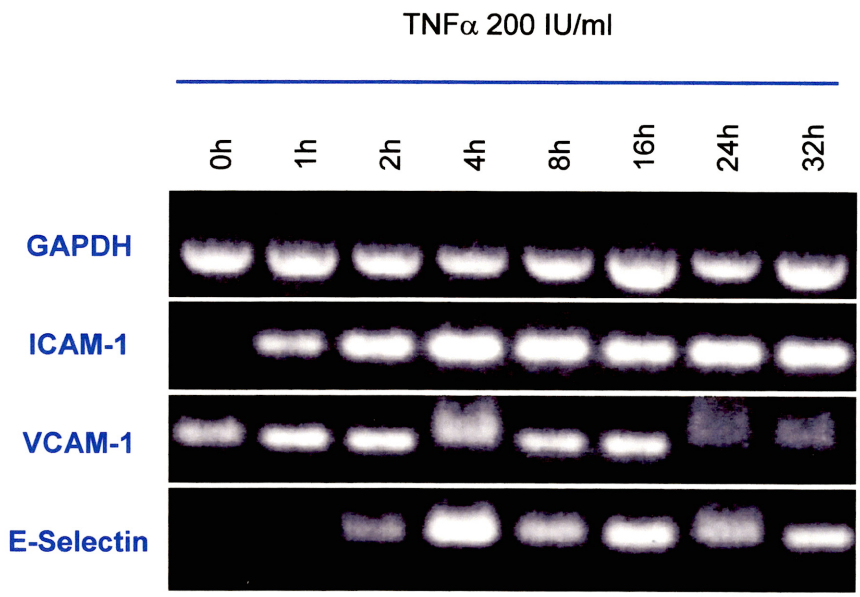


Figure 4: RT-PCR of GAPDH, ICAM-1, VCAM-1 and E-Selectin mRNA in one human cornea.
The mRNA extracted from a cornea stimulated with 200 IU/ml TNFα for 1h to 32h was used in RT-PCR for human GAPDH, ICAM-1, VCAM-1 and E-Selectin. The gel analysis shows a constitutive expression of VCAM-1 mRNA only. The mRNA expression of the three adhesion molecules tested is increased after 1h for ICAM-1 and VCAM-1, 2h for E-Selectin.

On the other hand, VCAM-1 mRNA was constitutively expressed and was increased after 1h of stimulation. E-Selectin mRNA could not be detected in the non-stimulated cornea samples. Its expression was however induced after 2 hours, peaking at 4h.

The pixel density analysis of this gel is shown on figure 5. As seen on the gel, VCAM-1 was the only tested adhesion molecule mRNA constitutively present in the non-stimulated cornea samples. TNFα induced a two-fold increase in its expression after 4h. The expression of ICAM-1 and E-Selectin mRNA also peaked at 4h, from negligible constitutive expression, with a 2.5-fold increase for ICAM-1 between 1h and 4h and a 3.6 fold increase for E-Selectin between 2h and 4h.

In order to evaluate whether the action of TNFα on corneal cells was dose-dependent, one human cornea (cornea #2) was stimulated with various concentrations of TNFα, and RT-PCR for adhesion molecules were performed. The densitometer analysis of the gel (not shown) is shown on figure 6: the graph shows no ICAM-1 mRNA expression after 4h in the non-stimulated cornea, whereas VCAM-1 and E-Selectin mRNA are expressed at low levels. Stimulation with 2 IU/ml TNFα (0.1 ng/ml) for 4h induced mRNA of all three adhesion molecules. Increased concentrations of TNFα did not further increase their expression. These data suggested that the action of TNFα on corneal cells was dose-dependent after 4h, in the range tested.

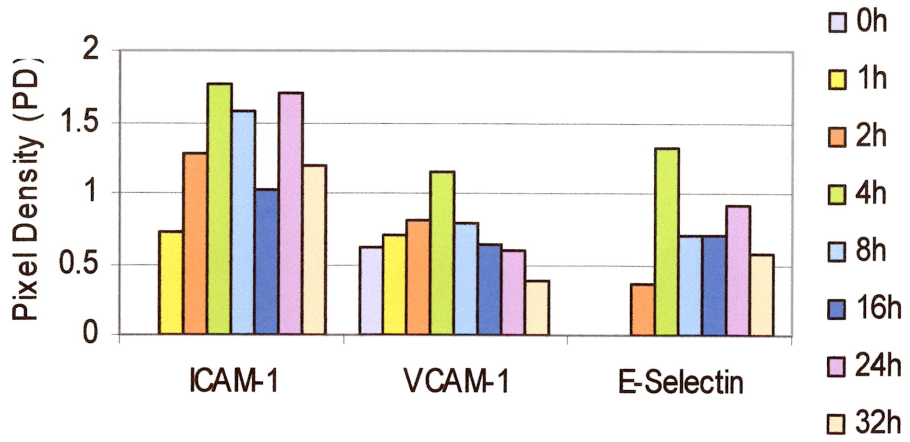


Figure 5: Pixel density analysis of ICAM-1, VCAM-1 and E-selectin bands after TNFα stimulation of a human cornea for 1 to 32h.
The gel shown in figure 9 was analysed using a densitometer. The graph shows the results obtained after GAPDH correction. Only VCAM-1 mRNA is constitutively expressed. All adhesion molecules mRNA tested are increased with TNFα stimulation, with a peak of expression at 4h.

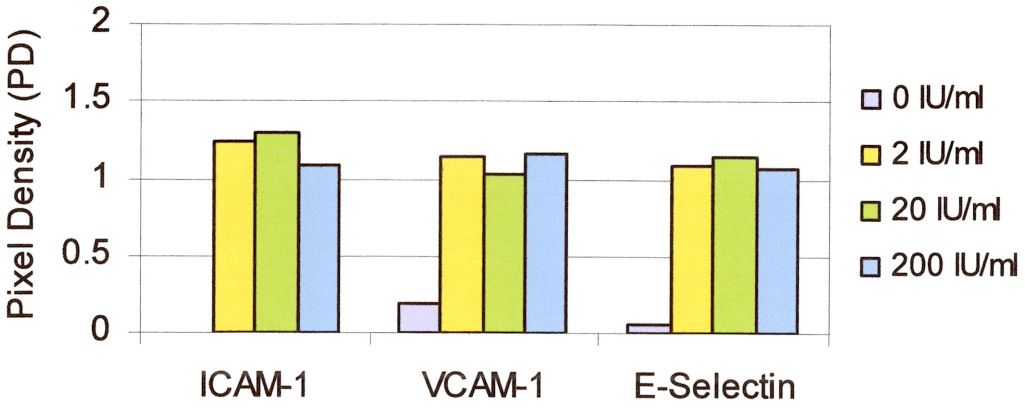


Figure 6: Pixel density analysis of ICAM-1, VCAM-1 and E-selectin PCR products after stimulation of a human cornea for 4h with 0.1 to 10 ng/ml TNFα.
The gel (not shown) was analysed using a densitometer. The graph shows the results obtained after GAPDH correction. After 4h, only VCAM-1 and E-selectin are expressed, in the non stimulated samples. The expression of ICAM-1, VCAM-1 and E-selectin is induced in the stimulated samples in a dose-dependent manner.

More human corneas were then stimulated with control medium or medium containing 200 IU/ml TNFα for 4h. However, the data presented above were not reproduced. None of the corneas analysed expressed the adhesion molecules tested, whether stimulated or not (table1).

	DONOR			CONTROL			TNFα		
		SEX	AGE	I	V	E	I	V	E
1	Post Mortem	Male	88	-	+	-	+	++	+
2	Post Mortem	Male	48	-	+	+/-	++	++	++
3	Post Mortem	Male	77	+/-	-	-	+/-	-	-
4	Post Mortem	Female	88	-	-	-	-	-	-
5	NC	NC	NC	-	-	-	-	-	-
6	Keratoconus	Male	30	-	-	-	-	-	-
7	Post Mortem	NC	NC	-	-	-	-	-	-

Table 1: RT-PCR analysis of adhesion molecule mRNA expression in human corneas.
The mRNA extracted from human corneas stimulated with control medium or medium containing 200 IU/ml TNFα for 4h was used in RT-PCR for human ICAM-1 (I), VCAM-1 (V), and E-Selectin (E). The table summarises the band intensity on the gels obtained from PCR performed on 7 human corneas.
Keys: - = no band, +/- = faint band, + = strong band.

Differences between individuals, for example age, sex or the length of corneal storage, could explain the discrepancies in the basal levels of expression of the three adhesion molecules in non-stimulated corneas. However, the most logical explanation for the difference between the first two corneas analysed and the others lies in the preparation of the samples: the limbus was removed in the second series of

corneas analysed (cornea #3 to #7), but not in corneas #1 and #2. The adhesion molecules mRNA detected in the first two corneas were most certainly extracted from the limbal vessels.

4.1.3- Expression of adhesion molecule proteins in human corneal endothelium

In order to confirm our data showing the absence of adhesion molecules mRNA in the human cornea, one human cornea was excised and the endothelium was stained for ICAM-1, VCAM-1 and E-Selectin proteins. The human cornea or control cells (EA-Hy 926 for ICAM-1, DVCAM for VCAM-1 and CHO-E for E-Selectin) were incubated with PBS or with a primary antibody, washed twice in PBS and incubated with a secondary antibody conjugated to FITC. The staining was then analysed using a fluorescent microscope and the image captured with a digital camera. Figures 7A and 7B show the results obtained after incubation with PBS and a relevant primary antibody respectively. All positive controls showed the expression of the relevant adhesion molecule (figure 7B), but the human corneal endothelium looked exactly as the negative controls (figure 7A) and did not express the three proteins tested (figure 7B).

4.1.4- Conclusion

Taken together, these findings demonstrate that the human cornea does not express ICAM-1, VCAM-1 or E-Selectin. They also show that their expression cannot be induced by TNFα in the human cornea.

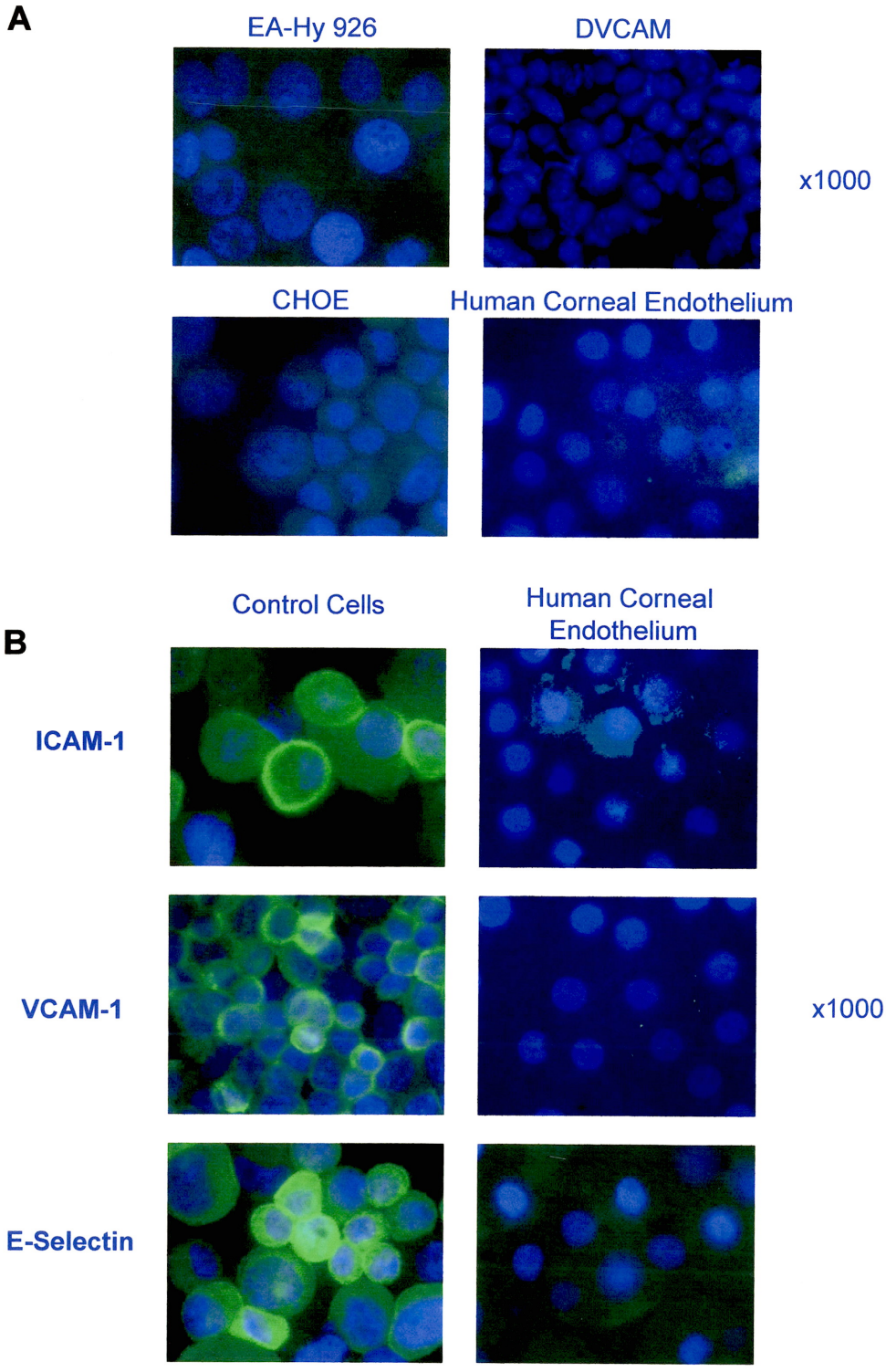


Figure 7: Adhesion molecule protein expression in human corneas (original magnification x1000).
Human corneas or control cells (EA-hy 926 for ICAM-1; DVCAM for VCAM-1; CHO-E for E-Selectin) were incubated with PBS (A) or the relevant primary antibody (1μg/ml) (B), washed twice in PBS and incubated with a secondary rabbit anti-rat IgG conjugated to FITC, before analysis with a fluorescent microscope (original magnification x1000) and capture of the picture with a digital camera.

4.2- Generation of a human corneal endothelial (HCE) cell line

All the experiments in this project were carried out using a murine or a human model. For the murine study, we had access to a mouse corneal endothelial cell line. The human study, on the other hand, was limited by a short supply of human tissue and the absence of human corneal endothelial (HCE) cell line in the laboratory or very much anywhere. To raise this cell line, we used either some collagen I-coated plates or the technique previously described by Blake *et al.* (Blake *et al.*, 1997): briefly, primary cultures of bovine corneal endothelial (BCE) cells were prepared and maintained until confluence. Cells were then stripped from the underlying matrix by a detergent treatment, and matrices were used to support the proliferation of endothelial cells derived from human corneas.

4.2.1- Generation of a BCE cell culture and matrix preparation

Bovine corneal endothelial (BCE) cells were successfully cultured and formed, upon reaching confluence, a highly ordered cobblestone-like monolayer. Cells displayed a rough hexagonal shape and were closely apposed one to another, as shown in figure 8.

4.2.2- Generation of a HCE cell culture

Human cornea-derived endothelial cells were cultured either on matrix-coated plates (as described above) or on collagen I-coated plates. Briefly, the endothelium of excised human corneas was covered with trypsin and endothelial cells were then gently scrapped off. Dislodged cells were then washed, resuspended in growth medium and transferred to collagen I- or BCE matrix-coated plates. Several attempts

were made using both coatings, but the culture of HCE cells proved to be very difficult: several cultures were contaminated by fibroblasts, easily identified by their elongated morphology; in other cultures, no cell grew at all. In most cases, however, endothelial cells failed to adhere and proliferate and were discarded when the medium was changed.

One culture of HCE using collagen I-coated plates was eventually successful. The cells showed typical endothelial morphology and formed a highly ordered cobblestone-like organisation when reaching confluence (figure 9). However, cells did not survive the first passage and the lack of new human cornea specimens prevented further attempts.

4.2.3- Conclusion

The only successful culture of human corneal endothelial (HCE) cells, in our hands, was lost after the first passage and the lack of specimens prevented further attempts. However, the problem will now be overcome as Dr N. Joyce (Schepens Eye Research Institute, Boston, MA) recently supplied the laboratory with the recipe for a new culture medium containing multiple growth factors. Cell cycle studies suggest that HCE *in vivo* are arrested in the G1-phase of the cell cycle. Senoo *et al.* have shown that these cells can proliferate, when exposed to mitogens (EGF and FGF) in conditions where contact inhibition has been transiently removed by EDTA (ethylene-diamine-tetra-acetic acid) (Senoo *et al.*, 2000). This will considerably increase our chances of success.

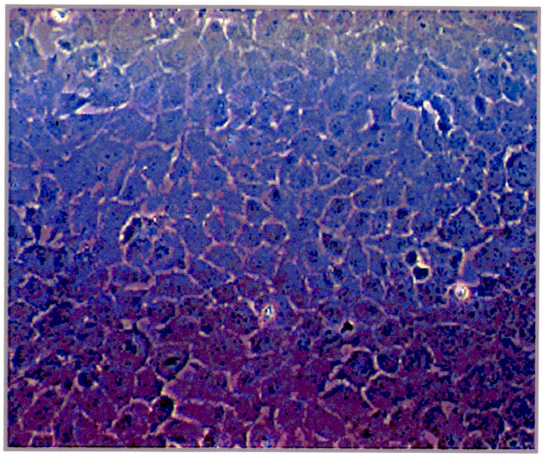
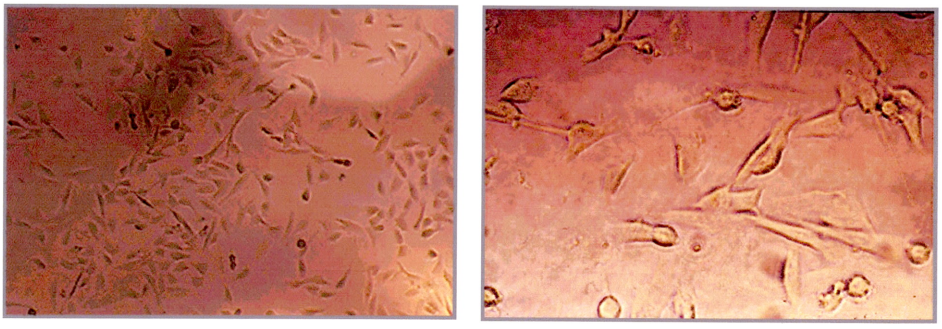


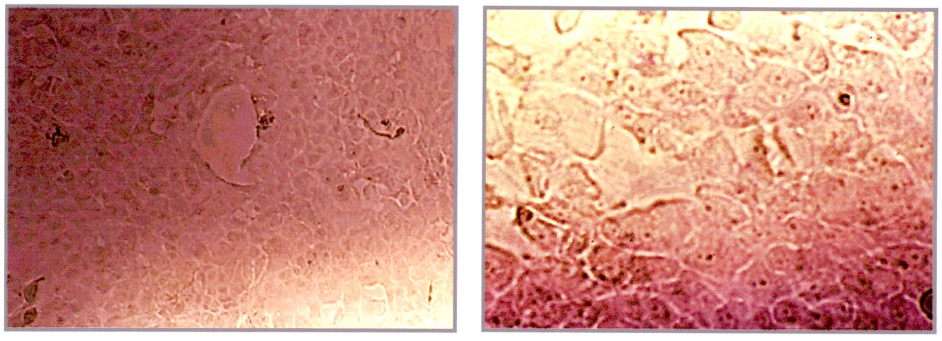
Figure 8: Inverted-phase micrograph of a confluent 4th-passage BCE cell culture (x400).
Cells form a highly ordered cobblestone-like monolayer.

A



x64 x320

B



x64 x320

Figure 9: Inverted-phase micrograph of HCE cells in culture (passage 0).
The phographs show the culture of HCE cells before (A) and after (B) reaching confluence. When confluent, endothelial cells form a typical cobblestone-like monolayer.

4.3- Conclusion

Using RT-PCR, several specimens of human corneas were analysed for the presence of ICAM-1, VCAM-1 and E-Selectin mRNA. The specimens were also submitted to various incubations with pro-inflammatory cytokines in order to determine their effects on adhesion molecule expression.

As opposed to the mouse corneas studied previously, none of these adhesion molecules tested were found in the human corneas analysed, apart from the one found in the limbus vessels. Furthermore, TNFα, responsible for the up-regulation of VCAM-1 in the mouse cornea, could not induce their expression. The absence of adhesion molecules in the human specimens was also confirmed by immunofluorescence. The second part of this study therefore highlighted a fundamental difference between corneas of the murine and human species.

The attempts to generate a human endothelial cell line were not very successful, partly due to the low supply of human specimens. One attempt resulted nonetheless in the culture of healthy human corneal endothelial cells, but these cells did not survive the first passage. To further investigate this difference between human and murine corneas, the generation of this cell line is of crucial importance. This should however be facilitated by the supply of a new culture medium in our laboratory.

CHAPTER 5

Discussion

Discussion

Corneal diseases are a major cause of blindness worldwide. In many cases, transplantation is the only treatment. Corneal transplantation, or keratoplasty, is the most common and the most successful solid organ transplantation procedure in humans. The graft survival rate after 1, 5 and 10 years are as high as 90%, 75% and 60% for low-risk groups (diagnosis of keratoconus, primary or secondary endothelial failure) (Williams *et al.*, 1997). This high acceptance rate is the result of immune privilege, an active phenomenon that allows a graft of foreign tissue to enjoy prolonged or permanent survival. However, for high-risk groups (acquired conditions that led to corneal inflammation or vascularisation) the long-term acceptance rate at 10 years falls to less than 35% (Williams *et al.*, 1997).

Although several factors are associated with corneal graft failure (Williams *et al.*, 1992), corneal allograft rejection is the most frequent cause. The specific immune mechanisms behind this are not yet fully understood, but several studies reported various degrees of neovascularisation and infiltration of the graft with macrophages, T cells (Pepose *et al.*, 1985; Wackenheim-Urlacher *et al.*, 1995; Larkin *et al.*, 1997b; Kuffova *et al.*, 1999), and a small number of NK cells (Larkin *et al.*, 1997b; Kuffova *et al.*, 1999; Kuffova *et al.*, 2001). Corneal allograft rejection is also associated with elevated pro-inflammatory cytokines (TNFα, IFNγ and IL-1β), as opposed to syngeneic grafts or accepted allografts (Torres *et al.*, 1996; Sano *et al.*, 1998; King *et al.*, 2000; Rayner *et al.*, 2000).

Several studies have investigated cytokines as a possible target to prevent allograft rejection of the cornea, and attempted to inhibit pro-inflammatory cytokines

or Th1 cytokines. However, due to the pleiotropy and the redundancy of the cytokine network, these strategies lead to a systemically compromised immunity, while the inhibited effects are often "replaced" by those of redundant cytokines. It appears therefore more feasible, and above all more efficient to stop the effects of the cytokines and to target molecules further down the line: the adhesion molecules. Pro-inflammatory cytokines are responsible for the induction or up-regulation of adhesion molecule expression on vascular endothelium, where they play a key role in the recruitment and retention of cells to the site of inflammation. Therefore, their role in the pathogenesis of corneal allograft rejection deserves further investigation as they could potentially provide not only a target for anti-adhesive therapy, but also possibly a suitable marker for allograft rejection.

As detailed in our introduction, corneal allograft rejection may occur in all three structures of the cornea, namely the epithelium, the stroma and the endothelium. The rejection of the latter is however irreversible and the most relevant clinically as it leads eventually to a loss of vision. Our study therefore concentrated on the endothelial structure of the cornea, and on the interactions, via adhesion molecules, between the endothelium and the infiltrated inflammatory cells that would ultimately destroy it.

5.1- Adhesion molecules and the mouse cornea

Using a cell line model and corneal tissues, the expression in the corneal endothelium of a large panel of adhesion molecules has been investigated by RT-PCR, FACS analysis and immunostaining. Their role in the adhesion of several human and murine populations to the corneal endothelium was then explored using

adhesion assays and blocking antibodies. Histology was also used to explore a possible correlation between the expression of particular adhesion molecules and rejection in our mouse model of corneal transplantation. Finally, the modulation of VCAM-1, a possible target for anti-adhesive therapy, was attempted using vitamin E or transfection with an anti-VCAM-1 single chain antibody.

5.1.1- Expression of adhesion molecules in the mouse cornea

Both mRNA and protein expressions of adhesion molecules were investigated in two models of corneal endothelium: a mouse corneal endothelial (MCE) cell line and excised corneas, all derived from BALB/c mice. The effect of pro-inflammatory cytokines on the adhesion molecule expression was also analysed.

RT-PCR revealed similar patterns of adhesion molecule expression in the cell line and in the endothelium from whole excised tissue: pixel density analysis of PCR bands revealed small quantities of ICAM-1 mRNA, but a larger amount of VCAM-1 and VAP-1 mRNA. Only E-Selectin and NCAM-1 mRNA were found in the cell line but not in the tissue. Stimulation with TNFα, IFNγ, IL-1α or a combination of the three decreased the expression of both VAP-1 and NCAM-1 mRNA, but increased the mRNA for ICAM-1. Noticeably, in their study on human hepatic endothelial cells, Lalor *et al.* also reported the very marginal effect of pro-inflammatory cytokines on VAP-1 expression (Lalor *et al.*, 2002a). VCAM-1 and E-Selectin mRNA were slightly increased by all cytokines except IFNγ.

Due to the lack of antibody, the expression and the function of VAP-1 and NCAM-1 were not investigated in this study. The presence of VAP-1 mRNA in the MCE cells and in corneal endothelium is however of great importance. The molecule

mediates lymphocyte-endothelial interactions in chronic kidney rejection and may be involved as well in the corneal allograft rejection process (Kurkijarvi *et al.*, 2001). The VAP-1 molecule presents a rather limited distribution (synovial vessels, sinusoidal endothelial cells in the liver, high endothelium in lymphatic organs). The sinusoidal endothelium and the corneal endothelium present some similarities: low-shear stress (the aqueous humor in the AC is drained by the trabecular meshwork at a very slow rate), absence or low expression of E-and P-selectins under normal and inflammation conditions, and finally absence or low expression of CD31 (as shown in this study). The lack of selectins in these two systems may reflect a lack of requirement for selectin-mediated rolling in conditions of low flow. Besides its role in the capture of leukocytes, VAP-1 may also be involved in their transendothelial migration, therefore compensating for the lack of CD31 in these endothelial cells (Lalor *et al.*, 2002b). All these remarks tend to point for a role of VAP-1 in the corneal endothelium and maybe in corneal allograft rejection. The presence of the protein must therefore be confirmed and the role of the molecule must be tested in adhesion assays as well as in our model of mouse corneal allograft rejection.

At the protein level, VCAM-1 was the only protein tested that was detected in the MCE cell line and in the endothelium from excised cornea. ICAM-1, E-Selectin and P-Selectin but not PECAM-1 were detected in moderate amounts by FACS analysis but not using the other techniques (immunofluorescence and histology). The small discrepancy between the FACS data and the results obtained by immunostaining is most certainly due to the higher sensitivity of cytofluorimetry. Cytokine stimulation slightly increased the expression of these molecules, but these increased levels of protein were insignificant, compared to the level of VCAM-1. The expression of

VCAM-1 was greatly enhanced by TNFα stimulation and a synergetic effect of IFNγ on VCAM-1 up-regulation by TNFα was also observed.

Our data highlight major differences between the expression of adhesion molecules at the mRNA and at the protein levels. This suggests that post-transcriptional modifications and /or post-translational mechanisms regulate their expression on corneal endothelium. This is well illustrated by VCAM-1 whose level of mRNA, constitutively high, is not much affected by cytokine stimulation. The protein expression on the other hand is doubled by TNFα stimulation and is 5 times higher than in resting cells after stimulation by TNFα and IFNγ combined. In this case, the presence of large quantities of VCAM-1 mRNA allows a rapid response to cytokines. The VCAM-1 ligand, VLA-4, which belongs to the integrin family, is also constitutively expressed on leukocytes but requires activation by specific signals (IL-8, thrombin, phorbol ester or T cell activation) to mediate adhesion. Hence, both ligands are readily available to engage in cell-to-cell interactions when environmental conditions allow, which therefore diminish response time in case of inflammation. In such context, one can postulate that after corneal grafting, the expression of VCAM-1 is up-regulated by TNFα, released after surgical inflammation. In a syngeneic setting, TNFα levels finally return to their basal levels and so does VCAM-1. In the case of an allograft however, the IFNγ released by infiltrating $CD4^+$ T cells further increases the expression of VCAM-1, which is now available in large quantities to mediate the recruitment, and the adhesion of more inflammatory cells.

The expression of VCAM-1 outside vascular endothelium is not unusual as one report detected it on macrophages and on endothelial cells in inflamed synovial tissues of patients with rheumatoid arthritis (RA) and osteoarthritis, as well as on vascular smooth muscle cells of RA patients (Koch *et al.*, 1991). Another study found occasional VCAM-1 expression on follicular dendritic cells of peripheral lymph nodes and tonsils, on splenic macrophages in the red pulp, and on hepatic Kupffer cells, in normal human tissues (Rice *et al.*, 1991). The same study also reported the expression of VCAM-1 on parietal epithelial cells of the glomerular capsule in the normal human kidney (Rice *et al.*, 1991). Finally, VCAM-1 has also been reported on myoblasts and myotubes and is involved (as well as its ligand VLA-4) in myogenesis (Rosen *et al.*, 1992). In this study, VCAM-1 was detected by immunofluorescence and histology on mouse corneal epithelial and endothelial cells, and by FACS and RT-PCR on mouse corneal endothelial cells. The role of VCAM-1 on corneal epithelial cells is not known. Its presence may be linked to a non-immunologic function of the molecule that would remain to be identified. Rice and co-workers did not find any VCAM-1 in the skin (either on epidermis, fibroblasts or endothelium), in the brain or in the gastrointestinal tract epithelium (Rice *et al.*, 1991).

Our data show a great consistency between the results obtained on the MCE cell line and on the endothelium of excised mouse corneas. This therefore confirms the adequacy of the model we have chosen for this study.

To the best of our knowledge, this is the first extensive study investigating the expression pattern of a large panel of adhesion molecules on mouse corneal endothelium. One study from Guymer *et al.* (Guymer and Mandel, 1991) looked at

the expression of ICAM-1 in the fresh uncultured murine cornea and detected no protein by immunoperoxidase staining. Using a similar technique, our data show a very discreet staining associated with keratocytes in the stroma of freshly excised murine corneas. Consistent with the Guymer *et al.* study (Guymer and Mandel, 1991), we found no expression of ICAM-1 in the endothelium, by immunostaining of MCE cells and corneal cryosections or fluorescent staining of corneal endothelium flat-mounts. FACS analysis of our cell line model showed only a very moderate expression.

As far as we know, the expression pattern, in the fresh mouse cornea, of the other adhesion molecules we tested has not been reported in the literature. Some reports, however, mention their expression in the human corneal endothelium. In the only study looking at P-Selectin expression (Vorkauf *et al.*, 1995), it was found weakly expressed in normal corneas and up-regulated after inflammation. PECAM-1, on the other hand, was found in only one case of inflamed cornea by Golberg *et al.* (Goldberg *et al.*, 1994). VCAM-1 was only reported in vascular endothelium in the stroma of inflamed or rejected human corneas, but not in the corneal endothelium (Philipp and Gottinger, 1993; Philipp, 1994; Goldberg *et al.*, 1994; Vorkauf *et al.*, 1995). Actually, only the study from Vorkauf *et al.* clearly distinguishes between vascular and corneal endothelium (Vorkauf *et al.*, 1995). In addition, some studies investigated the expression of adhesion molecules in corneas several months after the onset of rejection (Philipp, 1994) or in corneas where the corneal endothelium was not present ('burnt out corneas') (Whitcup *et al.*, 1993).

5.1.2- Function of adhesion molecules in the mouse cornea

During corneal allograft rejection, a number of inflammatory cells infiltrate the graft via the donor/recipient interface and invade the graft. The predominant cells are macrophages and T cells most of which present the helper T cell (CD4) marker (Larkin *et al.*, 1997a) (Larkin *et al.*, 1997b) (Pepose *et al.*, 1985), and DC (Kuffova *et al.*, 1999; Kuffova *et al.*, 2001). A number of inflammatory cells however reach the corneal endothelium from the recipient iris vessels via the anterior chamber and aggregate to the endothelial layer, which they ultimately destroy (Larkin *et al.*, 1997b). The high quantity of infiltrated inflammatory cells in the corneal stroma suggests the first route of entry plays a large role in the mouse. This is supported by our data (increased expression of VCAM-1 at the donor/host interface in the rejected allograft) and by the work of others (Kuffova *et al.*, 2001). However, as in human and in rats, inflammatory cell aggregates on the endothelium (rejection lines) are observed in mouse corneal allografts (unpublished observations), suggesting that the second route of entry via the AC is also involved in the rejection process. It is however difficult to evaluate the respective role of these two routes in the mouse as sampling of the aqueous humor is technically challenging.

The presence of VCAM-1 on the corneal endothelium in the mouse but not in human may indicate that the infiltration of inflammatory cells via the AC involves different pathways of cell-cell interactions in the two species. The role of adhesion molecule expression in the mouse corneal endothelium was therefore investigated. An adhesion assay was set up to investigate the adhesion of several human and murine cell populations to our corneal endothelial cell line model. The technique was successfully developed using DAP-3/DVCAM mouse cells and was then transferred

to MCE cells. Unlike studies in the vascular endothelium, this technique performed under static conditions is perfectly adapted to study the adhesion to corneal endothelium in the anterior chamber of the eye where low shear forces apply. Using this technique we investigated the role of ICAM-1, and VCAM-1, and of their counterparts LFA-1 and VLA-4, in the adhesion of human T cells, PBMC and PMN and of murine splenocytes and macrophages to the MCE cells. Murine neutrophils were not tested due to technical difficulties in purifying this population in this species. The effect of cytokines stimulation of the monolayer and/or of the populations we tested was also investigated.

Our experiments showed that on one hand, human T cells adhered more to the resting MCE monolayer when stimulated, as did human PMN and human PBMC. On the other hand, the stimulation of murine splenocytes by pro-inflammatory cytokines had no effect on their capacity to adhere to MCE cells. The stimulation of these cells populations produced similar effect on the adhesion to activated MCE cells. The stimulation of the monolayer itself increased the adherence of most of the cell populations tested, however, overall, the stimulation of the monolayer was less effective in increasing cell adherence that the stimulation of the adhering cell populations used in the assay. This finding is in complete agreement with our analysis of adhesion molecule patterns of expression on resting and stimulated MCE cells. According to our data, VCAM-1 is the only adhesion molecule among the one we tested that saw its expression increased by pro-inflammatory cytokines stimulation. Only ICAM-1, E- and P-Selectin were also found marginally increased by FACS. Therefore, the minor increase (compared to the one observed when the other cells are stimulated) in cell adherence observed in our assays reflects the minor

changes occurring on the MCE cells surface after cell activation. In addition, the stimulation of the MCE cells does not induce the expression of a novel adhesion molecule VCAM-1, but only its up-regulation. However small, these changes might represent a subtle mechanism of regulation of inflammatory cell recruitment. As already detailed above, the presence of VCAM-1 constitutively on the cell surface means that small changes in the environment increase its expression and lead to a rapid recruitment of inflammatory cells. These data therefore suggested a role for VCAM-1 in the recruitment of inflammatory cells to corneal endothelium. Experiments with blocking antibodies supported this hypothesis.

The antibody directed against ICAM-1 was only tested on the Jurkat cell line and no effect on cell adhesion was observed. Experiments with this antibody were not pursued as the molecule was not detected in the MCE cell line and as several reports in the literature showed no reduction of corneal allograft incidence of rejection after intraperitoneal injection of anti-ICAM-1 monoclonal antibody around the time of grafting (He *et al.*, 1994; Yamagami *et al.*, 1996).

On the other hand, blocking of the VCAM-1 molecule expressed on the corneal endothelial cell line reduced the adhesion of human T cells and resting splenocytes, but not of macrophages, PMN, PBMC (except when both cell types were activated) and activated splenocytes. This is worth noting the absence of effect on macrophages, cells that normally express VCAM-1 after activation and on PMN. The latter are thought not to express VLA-4, the counterligand for VCAM-1 and the general assumption is that the VCAM-1/VLA-4 pathway is not involved in the recruitment and function of neutrophils. It is however noteworthy that functional α4-integrins can indeed be expressed on neutrophils as reviewed by Johnston *et al.*

(Johnston and Kubes, 1999). Although at very low levels, depending upon species, and probably only on activated neutrophils, the expression of VLA-4 might be involved in the recruitment of neutrophils in chronic inflammatory processes (Johnston and Kubes, 1999).

Immunosuppression to cardiac allografts by anti-VCAM-1 and anti-VLA-4 therapy has been reported in mice (Isobe *et al.*, 1994; Suzuki *et al.*, 1999). However, failure of an anti-VCAM-1 mAb to induce the prolongation of corneal allograft survival (unpublished data) was mentioned in one report by Hori *et al.* (Hori *et al.*, 1997). Unfortunately, authors did not produce any details about the experimental conditions, nor the results and the combined use of anti-VCAM-1 and anti-VLA-4 mAb has not been mentioned.

Inhibition of human cell populations adhesion to MCE cells was also attempted using a mouse antibody directed against the β2 integrin subunit of human LFA-1 (TS1). This antibody reduced the adhesion of activated purified T cells to resting MCE cells and of resting and activated T cells to activated MCE cells. There is one possible reason why anti-ICAM-1 mAb had no effect on the suppression of human T cell adhesion while anti-LFA-1 mAb reduced the adhesion by 16% to 24% according to conditions of cell stimulation. Since ICAM-1 is not the only ligand for LFA-1, other ligands ICAM-2 and ICAM-3 or the newly discovered JAM molecules, must be blocked at the same time to produce the same effect.

On the contrary, the effect of the monoclonal antibody directed against the β2 integrin subunit of mouse LFA-1 (M18/2) reduced only marginally the adhesion of splenocytes and showed no effect on macrophages. However, before reaching any conclusion on the lack of effect of the latter antibody on murine cell adhesion to

MCE cells, experiments will need repeating with another antibody as one report found that the one we used had no blocking activity (Hori *et al.*, 1997).

Several studies have reported an improved survival rate of corneal allografts after injection of an anti-LFA-1 antibody as a peritransplant treatment in mice (He *et al.*, 1994; Yamagami *et al.*, 1996; Hori *et al.*, 1997). However, one should not expect necessarily a direct correlation between the capacity of a monoclonal antibody against one given adhesion molecule to block cell adhesion on one hand, and its beneficial effect on corneal allograft rejection on the other hand. Adhesion molecules are known to produce co-stimulatory signals and LFA-1 is involved in several immunologic events, including leukocyte adhesion to endothelium, but also interaction between antigen presenting cells and T cells.

In our hands, the inhibition of cell adhesion using an anti-VLA-4 antibody proved to be more efficient than the use of the anti-LFA-1 antibody (at least on human cells, as it is difficult to comment on the effect of the anti-LFA-1 antibody on mouse cells, as explained above). This strongly suggests a role for a VCAM-1/VLA-4 interaction in the adhesion process to mouse corneal endothelial cells. Again, this hypothesis is supported by the literature where a prolongation of corneal allograft survival in mice treated with anti-VLA-4 mAb alone or combined to anti-LFA-1 has been demonstrated (Hori *et al.*, 1997; Hori *et al.*, 1998).

Our data show that the combination of anti-VLA-4 mAb and anti-LFA-1 mAb is more powerful in reducing cell adhesion to MCE cells, than both antibodies used alone. It is noteworthy that the Hori *et al.* study found that the combine use of these antibodies induced a specific immunosuppression in murine corneal allografts. The combined treatment significantly increased corneal allograft survival more than the

use of these antibodies alone and was also associated with reduced mononuclear cell infiltration and stromal oedema, and depressed cytotoxic T cell response to donor alloantigens (Hori *et al.*, 1997). In a second report, the same team also reported the induction of immunologic tolerance by the combined use of anti-LFA-1 and anti-VLA-4 antibodies in corneal allograft transplantation (Hori *et al.*, 1998). These reports obviously tighten the need for more experiments in our mouse system using another anti-LFA-1 antibody. They also remind the limitations of these experiments. First as mentioned above, a role for one adhesion molecule in the recruitment and adhesion to endothelium of a defined cell type does not necessarily imply a role in the rejection process. Secondly, as stated by Hori *et al.*, the fact that specific acceptance is maintained more than 8 weeks after the mAbs administration indicates that specific immunosuppression and ignorance or tolerance is achieved and maintained by a mechanism other than the blockade of molecular bindings by mAb. Nonetheless, our data are in agreement with these studies and the use in the assay of an extended range of first cell types, and second, of monoclonal antibodies in combinations, should provide interesting results, in particular the addition to MCE cells of purified T $CD4^+$ and T $CD8^+$ cells, or purified mouse neutrophils.

Our system also needs to be applied to whole excised corneas, fresh or stimulated with pro-inflammatory cytokines. Preliminary data have not identified an increase in cell adhesion after cytokine treatment of the explant but methods for counting adherent cells are not completely satisfactory and there is lots of room for improvement.

Finally but not the least interesting, the use of the adhesion assay on frozen corneal sections sampled at different time points during graft rejection should

provide new information on the cell populations recruited to the endothelium during this process.

5.1.3- Consequences of adhesion molecules expression on mouse corneal allograft fate

To the best of our knowledge, comparison of adhesion molecules pattern of expression on normal mouse corneas and mouse corneas exposed to allograft rejection has never been reported in the literature. In our study, we looked using immunohistochemistry, at the expression of ICAM-1, VCAM-1 and PECAM-1 on cryosections of corneal allografts just after rejection was established. The pattern of expression was compared to those on ungrafted corneas and isografts. Our initial aim was to include intermediate time-points but these could not be analysed for technical reasons. For similar reasons, the range of adhesion molecules tested was limited to the three molecules listed above.

Our data did not highlight major differences in the pattern of expression of ICAM-1 and VCAM-1 between the ungrafted and isografted corneas. PECAM-1, however, was found in the outer stroma in the isograft but not in the ungrafted cornea. ICAM-1 was found scarcely associated with keratocytes and was not detected in the corneal endothelium in either case. This relates to a study from Guymer *et al.* that found no ICAM-1 staining in the fresh uncultured mouse cornea, using a similar immunoperoxidase detection system (Guymer and Mandel, 1991). VCAM-1 was found associated with keratocytes in the normal and isografted cornea. As already established using PCR and FACS on our cell line model, and staining of corneal flat-mounts, the mouse corneal endothelium presented a strong staining for

VCAM-1. A positive staining was also detected in the endothelium of the isograft. As far as we know, this finding has never been reported in the literature.

In the allograft, the staining for ICAM-1, VCAM-1 and PECAM-1 was mainly associated with stromal cells and infiltrating cells. The staining was less abundant for PECAM-1 than for the other two molecules. Overall, data showed an increased expression of ICAM-1, VCAM-1 and PECAM-1 in stromal and infiltrating cells at the time of rejection. The endothelium, already damaged at this late stage of rejection, was not visible. It is therefore of crucial importance to establish, (and this is what we intended in the first place), a more precise timing of adhesion molecule up-regulation and to follow the events leading to the corneal endothelium destruction.

Kuffova *et al.*, studying the kinetics of cell traffic in the murine corneal allograft response, reported that the infiltration of the graft with inflammatory cells took place immediately after surgery. The first infiltrating cells were myeloid cells, followed by T cells and the only difference between allografts and isografts was the ability of T cells, in the allograft, to cross the host-donor interface early in the alloresponse (2 days) (Kuffova *et al.*, 2001). This finding can be put in perspective with our observations that VCAM-1 and to a lesser extent, PECAM-1 was found hugely expressed at the donor-recipient border. Some of our preliminary data (not shown) also showed a gradual increase in VCAM-1 and PECAM-1 expression, at this interface, in the earlier phases of rejection. This strongly suggests a role for VCAM-1 (and PECAM-1) in the recruitment and migration of infiltrating T cells into the graft.

It would also be interesting to analyse these samples using RT-PCR, even though immunohistology gives us precious information on the location of adhesion

molecules. Finally, DNA microchips array would provide a very useful tool to look at the differential expression of adhesion molecules genes in iso- and allografts. However, the histological analysis of earlier time-points before the onset of rejection remains crucial to establish a correlation between the expression of VCAM-1 and the recruitment of inflammatory cells in the allograft.

5.1.4- Modulation of VCAM-1 expression in MCE cells

Our data reported for the first time the constitutive expression of VCAM-1 on mouse corneal endothelium and its up-regulation by a synergetic action of TNFα and IFNγ. Experiments using adhesion assays strongly suggested a role for the VCAM-1/VLA-4 interaction in the recruitment of T cells or splenocytes. Finally, comparison of corneal iso- and allografts demonstrated an increased expression of VCAM-1 on keratocytes, on infiltrating cells and principally at the donor-recipient interface in the allograft, at the time of rejection. Overall, our data suggested an important role for VCAM-1 in immunologic rejection after corneal transplantation, and our efforts therefore concentrated in modulating its expression in our MCE cell model.

First, we attempted to reduce VCAM-1 expression in MCE cells using vitamin E, a reagent that inhibits the up-regulation of VCAM-1 in a human saphenous vein model, in our laboratory. Preliminary data were very encouraging and showed that vitamin E, at high concentrations, was capable of totally preventing the up-regulation of VCAM-1 by pro-inflammatory cytokines in MCE cells. The anti-inflammatory effect of vitamin E was however not observed when the experiment was repeated a second time. The inhibiting effect of vitamin E on VCAM-1 up-regulation by cytokines observed in the first set of data needs therefore to be confirmed. The

inhibitory effect of vitamin E is only transient (tests in our laboratory showed a transient effect of up to 8 hours on human saphenous veins (unpublished data)). As our main goal is to stably modify corneas before they are transplanted, this might prove to be a problem in the future. Eight hours is not long enough to realistically consider repeated administration of the drug before and after transplantation. Daily topical administration of corticosteroids is already the fate of patients that undergo corneal transplantation and vitamin E will not be a very powerful tool, unless we find ways of prolonging its effect.

At lower doses however, vitamin E increased the expression of adhesion molecules on the MCE cells. It is noteworthy that the increased effect of cytokines on VCAM-1 up-regulation after low doses of vitamin E was also observed in the human saphenous vein model (unpublished data). This was however not the case with other cell models (HUVECs and HAECs). In these models, the inhibitory effect of vitamin E was observed with a dose as low as 20 μM (Wu *et al.*, 1999) or 50 μM (Zapolska-Downar *et al.*, 2000). Different cell types therefore respond differently to the antioxidant. Our data were observed in two different species (mouse corneal and human saphenous vein EC), this therefore could not explain this discrepancy. Although the anti-inflammatory effect of vitamin E is only observed in our model at doses far above the physiological level (around 50 μM) (Zapolska-Downar *et al.*, 2000), we did not observed any cell toxicity when vitamin E was added at high doses.

Although non-specific, vitamin E presents the advantage of selectively inhibiting the up-regulation of adhesion molecules induced by pro-inflammatory cytokines. Their basal level is not affected and therefore side effects are kept to a minimum. In

addition, the substance is present in the body under normal physiological conditions and will therefore not trigger any immune reaction. Our efforts should therefore concentrate on producing long-term effects in our model with this therapeutic agent.

Another strategy used to down-regulate the expression of VCAM-1 in the MCE cells involved the use of a single chain antibody (scFv) directed against the surface receptor. This scFv was developed in the pig, but preliminary results showed a 13% reduction in VCAM-1 expression in MCE cells after transfection with the scFv. This effect results effectively from the transfection of only 20% of the cells. A 100% transfection rate would therefore produce an effect equivalent to a 65% reduction in VCAM-1 expression, which is very encouraging. Recent data in the laboratory support our work: the stable transfection of scFv produced a great reduction in the constitutive expression of VCAM-1 in our MCE cell model. The effect of the transfectants on cytokine-induced up-regulation of VCAM-1 has yet to be tested.

The ultimate goal is to stably transfect a donor cornea with the anti-VCAM-1 single chain antibody before its transplantation into the recipient bed and such, to prevent its rejection. Alternatively, transfection of fresh non-immortalised corneal endothelial cells and their transplantation could provide new means to reconstruct corneas with endothelial defects.

The simple anatomy of cornea and the ability to store the organ *in vivo* for long periods facilitates its genetic modification and even allows checking the efficiency of the procedure before transplantation (George *et al.*, 2000). The cornea is therefore an ideal candidate for gene therapy and the scFv technique is the strategy of choice in the prevention of allograft rejection in this organ. The modulation of VCAM-1

expression using the scFv strategy offers several advantages: unlike vitamin E whose effects are not only targeted to VCAM-1, this is a highly specific technique. Furthermore, unlike other strategies that involve the systemic administration of an inhibitor, resulting in systemic immunocompromise, VCAM-1 targeting with intrabodies allows graft-specific inhibition of the molecule. In addition, we have associated the use of intrabodies to a non-viral (lipofectamine) gene transfer technique. Unlike viral vectors whose effectiveness is limited by their high immunogenicity, lipofectamine transfer is relatively safe (George *et al.*, 2000). Finally, the toxicity and immunogenicity associated with the use of intrabodies themselves appear to be minimal.

One possible disadvantage of the technique as it is developed so far, is the inhibitory effect observed on constitutive VCAM, in our stable transfectants (unpublished data). VCAM-1 distribution outside the vascular endothelium is rather limited and often restricted to conditions of inflammation. However, nature and evolution rarely leave anything to chance; therefore, the constitutive expression of VCAM-1 on corneal endothelium has most certainly a role to play. Even though the reason for its presence has not been elucidated yet, its complete inhibition could have detrimental effects. The technique needs therefore to be adjusted. The control of the scFv gene under an inducible promoter could probably solve this problem. The expression of the gene could for example be triggered by the presence of inflammatory cytokines. Alternatively, the expression of the gene could be turned on by the administration of a drug. Again, cornea would be a great candidate for this kind of strategy: it is the only transplanted organ whose early signs of rejection are clearly visible by clinical examination. Top-up doses of drug could therefore trigger

the expression of the intrabodies when necessary, maybe reverting the rejection. In conclusion, this technique offers a variety of advantages for the treatment of corneal allograft rejection, and the opportunities will develop even more with the discovery of new biological targets. If its role in the development of allograft rejection is confirmed, VAP-1 could be the next target.

Finally, in the unlikely case (preliminary results are very encouraging), the strategies developed in this study fail to inhibit VCAM-1 up-regulation by TNFα and IFNγ in the mouse cornea, a variety of techniques reported in the literature can be adapted to our MCE cell model. These include the use of dopamine (Kapper *et al.*, 2002), of cell-derived apolipoprotein E (Stannard *et al.*, 2001), or of albumin (Zhang and Frei, 2002), which inhibit TNFα-mediated up-regulation of VCAM-1 in HUVECs or HAECs. Finally, RNAi or RNA interference is a new emerging concept that involves the use of double stranded RNA (dsRNA) to silence gene expression. In the near future, this technique will be available in our laboratory to specifically inhibit VCAM-1 expression in our model.

5.2- Adhesion molecules and the human cornea

Our work in the mouse has demonstrated the unexpected constitutive expression of VCAM-1 in the corneal endothelium. Its up-regulation by pro-inflammatory cytokines, known to be associated with rejection, and its involvement in the adhesion of several cell types to the corneal endothelium (as demonstrated in our adhesion assays) made this molecule a potential target for therapy in the prevention of corneal allograft rejection. This part of the study has been facilitated by the use of a corneal endothelium model, the MCE cell line and furthermore, preliminary experiments

attempting the specific inhibition of VCAM-1 in the corneal endothelium are very encouraging.

The second part of our study investigated the expression of adhesion molecules in the human cornea. In contrast to the murine study, a model of human corneal endothelium was not available in our laboratory and pretty much anywhere else when the study was started. Therefore, in addition to experiments investigating the expression of adhesion molecules in the human cornea using RT-PCR and fluorescent microscopy, the second part of this project has involved attempts to generate a human corneal endothelial (HCE) cell line.

5.2.1- Expression of adhesion molecules in the human cornea

RT-PCR for human ICAM-1, VCAM-1 and E-Selectin were performed on post-mortem human corneal samples. Early experiments showed the constitutive expression of VCAM-1 mRNA and its induction after exposure to TNFα. In these samples (corneas #1 and #2), ICAM-1 and E-Selectin mRNA were up-regulated by the cytokine. More samples were then processed but these findings could not be reproduced. The first hypothesis was that human cornea did not present a consistent pattern of adhesion molecule expression, and that factors such as sex, age of the donor, or even the length of storage before the RT-PCR was carried out could influence the results. However, as the number of samples increased, we began to think that the origin of the discrepancy between the first two samples (corneas #1 and 2) and the subsequent ones (corneas #3 to 7) lied in the sample preparation: the limbal region of the excised cornea was removed in all the samples except in the first two. Most certainly the adhesion molecules mRNA detected in the first two corneas

were isolated from limbal vessels, hence the kinetic of up-regulation of the adhesion molecules, typical of vascular endothelium. At the time, however, the lack of specimens prevented us to test the presence of von Willebrand factor mRNA in these samples. This would have certainly confirmed the absence of blood vessels in corneas #3 to #7. These data suggest a role for limbal vessels in the recruitment of leukocytes, via the up-regulation of adhesion molecules at times of inflammation: during keratoplasty, surgery induces the release of TNFα and this relates to the increased risk of rejection in pre-vascularised recipient beds.

The absence of adhesion molecules in the human corneal endothelium was confirmed by immunostaining of adhesion molecule proteins in corneal flat-mounts. None of the three adhesion molecules tested was detected on the endothelium of normal unstimulated human corneas. The induction of these proteins by TNFα was not investigated due to a shortage of samples but the RT-PCR results showing the absence of mRNA for ICAM-1, VCAM-1 and E-Selectin speak for themselves. The absence of VCAM-1 in particular has to be noted as the first part of this report highlighted its potential role in the recruitment of inflammatory cells in the murine cornea. As far as VCAM-1 expression is concerned, this is not an isolated case as Lidington *et al.* reported that in contrast to human cells, endothelial cells (EC) isolated from murine heart, lung and lymph nodes also express large quantities of VCAM-1 constitutively (Lidington *et al.*, 2002).

In the literature, the pattern of adhesion molecule expression in the normal human cornea or human corneas exposed to pro-inflammatory cytokines or allograft rejection has been studied more intensively than in the murine model. Noticeably, among all the work carried out on this subject, the study from Vorkauf and co-

workers (Vorkauf *et al.*, 1995) is the only one that clearly distinguishes between corneal and vascular endothelium, when our RT-PCR data in human samples illustrate the importance of this distinction.

Data in the literature are conflicting. ICAM-1 was found moderately expressed in normal corneal endothelium in four reports (Foets *et al.*, 1992; Vorkauf *et al.*, 1995) but could not be detected by Whitcup *et al.* (Whitcup *et al.*, 1993).

E-Selectin was found in inflamed corneal endothelium only by Vorkauf *et al.* (Vorkauf *et al.*, 1995) but other authors admitted using corneas several months after the onset of rejection (Philipp, 1994) or corneas with chronic inflammation or only few well-preserved corneal endothelial cells (Whitcup *et al.*, 1993). Even expressed at the onset of rejection, E-Selectin could not have been detected in these studies.

When detected, VCAM-1, however, was always reported in vascular endothelium in the stroma of inflamed or rejected corneas, but not in the corneal endothelium (Philipp and Gottinger, 1993; Philipp, 1994; Goldberg *et al.*, 1994; Vorkauf *et al.*, 1995).

These results highlight a major difference in the adhesion molecule pattern of expression in the human and the murine species. According to our data, none of the adhesion molecules we tested is induced in pro-inflammatory conditions, which suggests none of them are involved in the recruitment or the adhesion of inflammatory cells to the human corneal endothelium. Yet, during rejection, the human corneal endothelium suffers severe destruction after adhesion of inflammatory cells. Therefore, more work is required to discover the mechanisms of corneal endothelium destruction and the need for a model of human corneal endothelium has never been so obvious.

5.2.2- Generation of a human corneal endothelial (HCE) cell line

The short supply of human corneal tissues and the absence of a human corneal endothelial cell line in our laboratory, and pretty much anywhere at the time this project was started, proved to be very limiting. Our efforts therefore concentrated on culturing human corneal endothelial cells, with the ultimate objective to raise an immortalised cell line.

Many studies have been performed using corneal endothelial cells in culture, from various animal sources (rabbit, mouse, rat). It has been, however very difficult to grow and maintain long-term cultures of human corneal endothelial (HCE) cells: unlike rodents, human corneal endothelium has a limited regenerative capacity, under normal physiological conditions. Joyce and co-workers showed that the cells had the capability to divide but were arrested in the G1-phase of the cell cycle (Joyce *et al.*, 1996a; Joyce *et al.*, 1996b). Among the factors that may be responsible for maintaining these cells in arrest is TGFβ, which suppresses S-phase entry in cultured endothelial cells (Chen *et al.*, 1999). In addition, a contact-inhibition-like mechanism may actively suppress the proliferation of mature endothelial monolayers (Senoo and Joyce, 2000; Senoo *et al.*, 2000).

One technique reported by Blake *et al.* suggested using the matrix generated by primary cultures of bovine corneal endothelial cells as a support for the proliferation of human cells (Blake *et al.*, 1997). This technique was used in conjunction with the growth of cells on collagen-I coated plates.

The very short supply of tissues proved again very limiting. The use of several specimens conjointly would have increased our chances of success but the supply was too little to risk wasting too many on a technique that was not reliable yet.

Several attempts were made using both coatings, but cultures were contaminated with fibroblasts, or endothelial cells failed to proliferate. Although one culture was successful, it did not survive the first passage. We did not have the chance to further characterise the cells, but the morphology (cobblestone-like) was typical of endothelial cells.

Since then, the work of Joyce and colleagues has considerably improved chances of success. A more recent technique consists in dissecting Descemet's membrane and the associated cells from the stroma. Endothelial cells are then released using EDTA and grown in medium containing multiple growth factors (FGF and EGF) (Senoo *et al.*, 2000). This technique has been used to repopulate the denuded Descemet's membrane of another cornea *ex vivo* (Chen *et al.*, 2001) and opens the door for corneal endothelial cell transplantation. In the near future, a human corneal endothelial cell line will be available and more information will be available on corneal endothelium fate during allograft rejection, providing more targets and strategies for therapy.

5.3- Conclusion

Despite the widespread assumption that corneal transplantation does not require improvements, immunological rejection still accounts for a large number of graft failures, in particular in high-risk recipient beds. During this process, inflammatory cells infiltrate the graft and the corneal endothelium is eventually destroyed. Recruitment of these inflammatory cells involves cell-cell interactions mediated via cell adhesion molecules.

The pattern of expression of these adhesion molecules was therefore investigated in the mouse and human corneas. We showed for the first time the constitutive expression of VCAM-1 and its up-regulation by pro-inflammatory cytokines in mouse corneal endothelial cells. A role for the molecule and its ligand VLA-4 in the adhesion of several cell populations to the corneal endothelium was also demonstrated. This could lead to new directions of research focused on manipulating the VCAM-1/VLA-4 pathway, in order to prevent corneal allograft rejection. Our preliminary experiments also showed encouraging data on the inhibition of VCAM-1 up-regulation by pro-inflammatory cytokines, after treatment with vitamin E or transfection with a single chain antibody directed against VCAM-1. Cornea would be an ideal candidate for such therapy as it can be stored for several months before transplantation. This provides a "window of opportunities" and allows time for manipulations in order to render the graft more "acceptable".

Interestingly, VCAM-1 was not detected in the human corneal endothelium. This work therefore illustrates a fundamental difference between the expression of VCAM-1 in the human and murine corneal endothelium.

This finding stresses the need for a good model of human corneal endothelium and reminds that one must remain prudent when extrapolating from a murine to a human model.

Credits

The mouse model of corneal allograft rejection was developed in the laboratory by Dr D.F.P. Larkin and Dr. Navid Ardjomand. The grafts on BALB/c mice and their follow-up were carried out by Dr Ardjomand, who also prepared the histological sections.

The human T cells used in the adhesion assays were purified by Dr W. Jordan.

Abbreviations

AA	Adhesion assay
ACAID	Anterior chamber-associated immune deviation
ACGR	Australian Corneal Graft Registry
afd	Autoclaved filtered deionised
APC	Antigen-presenting cells
BCE	Bovine corneal endothelial cells
BES	N,N-Bis(2-hydroxyethyl)-2-aminoethanesulfonic acid
bFGF	Basic fibroblast growth factor (FGF-2)
BM	Bone marrow
bp	Base pair
BZ	Bowman's zone
CAM	Cell adhesion molecules
CD_4	Antigenic marker of helper/inducer T cells
CD_8	Antigenic marker of cytotoxic/suppressor T cells
cDNA	Complementary DNA
CHO	Chinese hamster ovarian cells
CMV	Cytomegalovirus
cm^2	Centimetre square
CTFS	Corneal Transplant Follow Up Study
CTL	Cytotoxic lymphocytes
DAB	Diaminobenzidine
DAPI	4,6-Diamidino-2-phenylindole
DC	Dendritic cells
DM	Descemet's membrane
DNA	Deoxyribonucleic acid
dNTP	Deosynucleoside triphosphate
dsRNA	Double stranded RNA
DTT	Dithiothreitol
EBSS	Earle's balanced salt solution
EC	Endothelial cells
EDTA	Ethylenediaminetetraacetate
e.g.	Example
EGF	Epidermal growth factor
ELISA	Enzyme-linked immunosorbent assay
ER	Endoplasmic reticulum
Fab	Antigen-binding fragment
FACS	Fluorescent-activated cell sorter
FasL	Fas-Ligand
FCS	Fetal calf serum
FITC	Fluorescein isothiocyanate
GAPDH	Glyceraldehyde 3-phosphate dehydrogenase
GFP	Green fluorescent protein
GM-CSF	Granulocyte-macrophage colony-stimulating factor

h	Hours
HAECs	Human aortic endothelial cells
HCE	Human corneal endothelial cells
HLA	Human leukocyte antigen
HPRT	Hypoxanthine phosphoribosyl transferase
HSEC	Hepatic sinusoidal endothelial cells
HUVECs	Human umbilical vein endothelial cells
ICAM	Intercellular adhesion molecule
IF	Immunofluorescence
IFN	Interferon
Ig	Immunoglobulin
IgSF	Immunoglobulin superfamily
IH	Immunohistology
IL	Interleukin
IL-1RA	IL-1 receptor antagonist
IL-2R	IL-2 Receptor
IP-10	Inducible Protein-10
IU	International unit
JAM	Junctional adhesion molecule
K	Keratocytes
LC	Langerhans cells
LFA-1	Leukocyte function-associated molecule-1
LPS	Lipopolysaccharide
M	Marker
M	Molar
mAb	Monoclonal antibody
MCE	Mouse corneal endothelial cells
MCP	Monocyte chemoattractant protein
MEM	Minimum essential medium
MFI	Median fluorescence intensity
Mϕ	Macrophage
mg	Milligramme
μg	Microgramme
MHC	Major histocompatibility complex
mins	Minutes
MIP	Macrophage inducible proteins
ml	Millilitre
μl	Microlitre
mm	Millimetre
mm^2	Millimetre square
mM	Millimolar
μm	Micrometre
μM	Micromolar
M-MLV RT	Moloney Murine Leukemia Virus Reverse Transcriptase
mRNA	Messenger RNA

MSH	Melanocyte stimulating hormone
NCAM	Neural cell adhesion molecule
ng	Nanogramme
NK	Natural killer cells
O.C.T.	Optimal cutting tissue
OD	Optical density
PAF	Platelet activating factor
PBMC	Periphral blood mononuclear cells
PBS	Phosphate buffered solution
PCR	Polymerase chain reaction
PD	Pixel density
PECAM	Platelet endothelial cell adhesion molecule
pg	Picogramme
PGE_2	Prostaglandin 2
PLN	Peripheral lymph nodes
PMA	Phorbol myristate acetate
PMN	Polymorphonuclear cells
POD	Postoperative days
PSGL	P-Selectin glycoprotein ligand
RANTES	Regulated upon activation of normal T cell expressed and secreted
RBC	Red blood cells
RNA	Ribonucleic acid
RNAi	RNA interference
rpm	Rotation per minute
RT	Room temperature
RT-PCR	Reverse transcription PCR
SCR	Short consensus repeat
secs	Seconds
scFv	Single chain antibody
SSAO	Semicarbazide-sensitive mono-amine oxidase
Tc	T cytotoxic cells
TCR	T cell receptor
TES	N-tris[hydroxymethyl]methyl-2-aminoethanesulfonic acid
Tf	Transfection
TGF	Transforming growth factor
Th	T helper cells
TNF	Tumor necrosis factor
VAP-1	Vascular adhesion protein-1
VCAM-1	Vascular cell adhesion molecule-1
VLA-4	Very late antigen-4
%	Percentage
°C	Celsius degree

References

Alldredge, O. C., and Krachmer, J. H. (1981). Clinical types of corneal transplant rejection. Their manifestations, frequency, preoperative correlates, and treatment. Arch Ophthalmol *99*, 599-604.

Alon, R., Fuhlbrigge, R. C., Finger, E. B., and Springer, T. A. (1996). Interactions through L-selectin between leukocytes and adherent leukocytes nucleate rolling adhesions on selectins and VCAM-1 in shear flow. J Cell Biol *135*, 849-65.

Barclay. (1997). The Leukocyte Antigen Facts Book (London: Academic Press Limited, Harcourt Brace & Company Publishers).

Bevilacqua, M. P. (1993). Endothelial-leukocyte adhesion molecules. Annu Rev Immunol *11*, 767-804.

Bird, R. E., Hardman, K. D., Jacobson, J. W., Johnson, S., Kaufman, B. M., Lee, S. M., Lee, T., Pope, S. H., Riordan, G. S., and Whitlow, M. (1988). Single-chain antigen-binding proteins. Science *242*, 423-6.

Blake, D. A., Yu, H., Young, D. L., and Caldwell, D. R. (1997). Matrix stimulates the proliferation of human corneal endothelial cells in culture. Invest Ophthalmol Vis Sci *38*, 1119-29.

Blatt, D. H., Leonard, S. W., and Traber, M. G. (2001). Vitamin E kinetics and the function of tocopherol regulatory proteins. Nutrition *17*, 799-805.

Boisjoly, H. M., Tourigny, R., Bazin, R., Laughrea, P. A., Dube, I., Chamberland, G., Bernier, J., and Roy, R. (1993). Risk factors of corneal graft failure. Ophthalmology *100*, 1728-35.

Bourne, W. M., Nelson, L. R., and Hodge, D. O. (1997). Central corneal endothelial cell changes over a ten-year period. Invest Ophthalmol Vis Sci *38*, 779-82.

Bowen, J. A., and Hunt, J. S. (1999). Expression of cell adhesion molecules in murine placentas and a placental cell line. Biol Reprod *60*, 428-34.

Brissette-Storkus, C. S., Reynolds, S. M., Lepisto, A. J., and Hendricks, R. L. (2002). Identification of a novel macrophage population in the normal mouse corneal stroma. Invest Ophthalmol Vis Sci 43, 2264-71.

Bron, A. J., Tripathi, R. C., and Tripathi, B. J. (1997). Wolff's Anatomy of the Eye and Orbit, 8th Edition: Lippincott Williams & Wilkins Publishers).

Callanan, D., Peeler, J., and Niederkorn, J. Y. (1988). Characteristics of rejection of orthotopic corneal allografts in the rat. Transplantation *45*, 437-43.

Chan, A. C. (1998). Vitamin E and atherosclerosis. J Nutr *128*, 1593-6.

Chen, K. H., Azar, D., and Joyce, N. C. (2001). Transplantation of adult human corneal endothelium ex vivo: a morphologic study. Cornea *20*, 731-7.

Chen, K. H., Harris, D. L., and Joyce, N. C. (1999). TGF-beta2 in aqueous humor suppresses S-phase entry in cultured corneal endothelial cells. Invest Ophthalmol Vis Sci *40*, 2513-9.

Claesson, M., Elder, M. J., and Larkin, D. F. (1997). A method for separation and staining of flat mounts of human corneal endothelium. Acta Ophthalmol Scand *75*, 131-3.

Comer, R. M., Daya, S. M., and O'Keefe, M. (2001). Penetrating keratoplasty in infants. J Aapos *5*, 285-90.

Coster, D. J., and Williams, K. A. (1992). Transplantation of the cornea. Med J Aust *157*, 405-8.

Cousins, S. W., McCabe, M. M., Danielpour, D., and Streilein, J. W. (1991). Identification of transforming growth factor-beta as an immunosuppressive factor in aqueous humor. Invest Ophthalmol Vis Sci *32*, 2201-11.

Dana, M. R., Yamada, J., and Streilein, J. W. (1997). Topical interleukin 1 receptor antagonist promotes corneal transplant survival. Transplantation *63*, 1501-7.

Davenpeck, K. L., Sterbinsky, S. A., and Bochner, B. S. (1998). Rat neutrophils express alpha4 and beta1 integrins and bind to vascular cell adhesion molecule-1 (VCAM-1) and mucosal addressin cell adhesion molecule-1 (MAdCAM-1). Blood *91*, 2341-6.

Dekaris, I., Gabric, N., Mazuran, R., Karaman, Z., and Mravicic, I. (2001). Profile of cytokines in aqueous humor from corneal graft recipients. Croat Med J *42*, 650-6.

Ebnet, K., and Vestweber, D. (1999). Molecular mechanisms that control leukocyte extravasation: the selectins and the chemokines. Histochem Cell Biol *112*, 1-23.

Edgell, C. S., McDonald, C. C., and Graham, J. B. (1983). Permanent cell line expressing human factor VIII-related antigen established by hybridization. PNAS *80*, 3734-7.

Elner, V. M., Elner, S. G., Pavilack, M. A., Todd, R. F. d., Yue, B. Y., and Huber, A. R. (1991). Intercellular adhesion molecule-1 in human corneal endothelium. Modulation and function. Am J Pathol *138*, 525-36.

Faruqi, R., de la Motte, C., and DiCorleto, P. E. (1994). Alpha-tocopherol inhibits agonist-induced monocytic cell adhesion to cultured human endothelial cells. J Clin Invest *94*, 592-600.

Foets, B. J., van den Oord, J. J., Volpes, R., and Missotten, L. (1992). In situ immunohistochemical analysis of cell adhesion molecules on human corneal endothelial cells. Br J Ophthalmol *76*, 205-9.

Forrester JV, D. A., McMenamin P and Lee WR. (1996). The Eye: Basic Sciences in Practice, 1 Edition: W B Saunders Company Ltd).

Fuggle, S. V., and Koo, D. D. (1998). Cell adhesion molecules in clinical renal transplantation. Transplantation *65*, 763-9.

Fujikawa, L. S., Colvin, R. B., Bhan, A. K., Fuller, T. C., and Foster, C. S. (1982). Expression of HLA-A/B/C and -DR locus antigens on epithelial, stromal, and endothelial cells of the human cornea. Cornea *1*, 213-222.

George, A. J., Arancibia-Carcamo, C. V., Awad, H. M., Comer, R. M., Fehevari, Z., King, W. J., Kadifachi, M., Hudde, T., Kerouedan-Lebosse, C., Mirza, F., Barbaros Oral, H., Rayner, S. A., Tan, P. H., Tay, E., and Larkin, D. F. (2000). Gene delivery to the corneal endothelium. Am J Respir Crit Care Med *162*, S194-200.

Goldberg, M. F., Ferguson, T. A., and Pepose, J. S. (1994). Detection of cellular adhesion molecules in inflamed human corneas. Ophthalmology *101*, 161-8.

Guymer, R. H., and Mandel, T. E. (1991). Monoclonal antibody to ICAM-1 prolongs murine heterotopic corneal allograft survival. Aust N Z J Ophthalmol *19*, 141-4.

Hahne, M., Jager, U., Isenmann, S., Hallmann, R., and Vestweber, D. (1993). Five tumor necrosis factor-inducible cell adhesion mechanisms on the surface of mouse endothelioma cells mediate the binding of leukocytes. J Cell Biol *121*, 655-64.

Hamrah, P., Liu, Y., Zhang, Q., and Dana, M. R. (2003). The corneal stroma is endowed with a significant number of resident dendritic cells. Invest Ophthalmol Vis Sci *44*, 581-9.

Hamrah, P., Zhang, Q., Liu, Y., and Dana, M. R. (2002). Novel characterization of MHC class II-negative population of resident corneal Langerhans cell-type dendritic cells. Invest Ophthalmol Vis Sci *43*, 639-46.

He, Y., Mellon, J., Apte, R., and Niederkorn, J. Y. (1994). Effect of LFA-1 and ICAM-1 antibody treatment on murine corneal allograft survival. Invest Ophthalmol Vis Sci *35*, 3218-25.

Hegde, S., and Niederkorn, J. Y. (2000). The Role of Cytotoxic T Lymphocytes in Corneal Allograft Rejection. Invest Ophthalmol Vis Sci *41*, 3341-3347.

Hohlbaum, A. M., Moe, S., and Marshak-Rothstein, A. (2000). Opposing effects of transmembrane and soluble Fas ligand expression on inflammation and tumor cell survival. J Exp Med *191*, 1209-20.

Hori, J., Isobe, M., Yamagami, S., Mizuochi, T., and Tsuru, T. (1997). Specific immunosuppression of corneal allograft rejection by combination of anti-VLA-4 and anti-LFA-1 monoclonal antibodies in mice. Exp Eye Res *65*, 89-98.

Hori, J., Joyce, N. C., and Streilein, J. W. (2000). Immune privilege and immunogenicity reside among different layers of the mouse cornea. Invest Ophthalmol Vis Sci *41*, 3032-42.

Hori, J., Isobe, M., Yamagami, S., and Tsuru, T. (1998). Acceptance of second corneal allograft by combination of anti-VLA-4 and anti-LFA-1 monoclonal antibodies in mice. Transplant Proc *30*, 200-1.

Huston, J. S., Levinson, D., Mudgett-Hunter, M., Tai, M. S., Novotny, J., Margolies, M. N., Ridge, R. J., Bruccoleri, R. E., Haber, E., Crea, R., and et al. (1988). Protein engineering of antibody binding sites: recovery of specific activity in an anti-digoxin single-chain Fv analogue produced in Escherichia coli. Proc Natl Acad Sci U S A *85*, 5879-83.

Iademarco, M. F., Barks, J. L., and Dean, D. C. (1995). Regulation of vascular cell adhesion molecule-1 expression by IL-4 and TNF-alpha in cultured endothelial cells. J Clin Invest *95*, 264-71.

Inoue, K., Amano, S., Oshika, T., Sawa, M., and Tsuru, T. (2000). A 10-year review of penetrating keratoplasty. Jpn J Ophthalmol *44*, 139-45.

Isobe, M., Suzuki, J., Yagita, H., Okumura, K., Yamazaki, S., Nagai, R., Yazaki, Y., and Sekiguchi, M. (1994). Immunosuppression to cardiac allografts and soluble antigens by anti-vascular cellular adhesion molecule-1 and anti-very late antigen-4 monoclonal antibodies. J Immunol *153*, 5810-8.

Janeway C.A., Travers P., Walport M., Capra J.D.(1999). Immunobiology, Fourth Edition, Garland Publishing.

Johnston, B., and Kubes, P. (1999). The alpha4-integrin: an alternative pathway for neutrophil recruitment? Immunol Today *20*, 545-50.

Joo, C. K., Pepose, J. S., and Stuart, P. M. (1995). T-cell mediated responses in a murine model of orthotopic corneal transplantation. Invest Ophthalmol Vis Sci *36*, 1530-40.

Joyce, N. C., Meklir, B., Joyce, S. J., and Zieske, J. D. (1996a). Cell cycle protein expression and proliferative status in human corneal cells. Invest Ophthalmol Vis Sci *37*, 645-55.

Joyce, N. C., Navon, S. E., Roy, S., and Zieske, J. D. (1996b). Expression of cell cycle-associated proteins in human and rabbit corneal endothelium in situ. Invest Ophthalmol Vis Sci *37*, 1566-75.

Kao, F. T., and Puck, T. T. (1968). Genetics of somatic mammalian cells, VII. Induction and isolation of nutritional mutants in Chinese hamster cells. Proc Natl Acad Sci U S A *60*, 1275-81.

Kapoor, R., Sakai, L. Y., Funk, S., Roux, E., Bornstein, P., and Sage, E. H. (1988). Type VIII collagen has a restricted distribution in specialized extracellular matrices. J Cell Biol *107*, 721-30.

Kapper, S., Beck, G., Riedel, S., Prem, K., Haak, M., van der Woude, F. J., and Yard, B. A. (2002). Modulation of chemokine production and expression of adhesion molecules in renal tubular epithelial and endothelial cells by catecholamines. Transplantation *74*, 253-60.

Khatib, A. M., Kontogiannea, M., Fallavollita, L., Jamison, B., Meterissian, S., and Brodt, P. (1999). Rapid induction of cytokine and E-selectin expression in the liver in response to metastatic tumor cells. Cancer Res *59*, 1356-61.

Khodadoust, A. A., and Silverstein, A. M. (1969). Transplantation and rejection of individual cell layers of the cornea. Invest Ophthalmol *8*, 180-95.

King, W. J., Comer, R. M., Hudde, T., Larkin, D. F., and George, A. J. (2000). Cytokine and chemokine expression kinetics after corneal transplantation [In Process Citation]. Transplantation *70*, 1225-33.

Koch, A. E., Burrows, J. C., Haines, G. K., Carlos, T. M., Harlan, J. M., and Leibovich, S. J. (1991). Immunolocalization of endothelial and leukocyte adhesion molecules in human rheumatoid and osteoarthritic synovial tissues. Lab Invest *64*, 313-20.

Kuffova, L., Lumsden, L., Vesela, V., Taylor, J. A., Filipec, M., Holan, V., Dick, A. D., and Forrester, J. V. (2001). Kinetics of leukocyte and myeloid cell traffic in the murine corneal allograft response. Transplantation *72*, 1292-8.

Kuffova, L., Holan, V., Lumsden, L., Forrester, J. V., and Filipec, M. (1999). Cell subpopulations in failed human corneal grafts. Br J Ophthalmol *83*, 1364-9.

Kurkijarvi, R., Jalkanen, S., Isoniemi, H., and Salmi, M. (2001). Vascular adhesion protein-1 (VAP-1) mediates lymphocyte-endothelial interactions in chronic kidney rejection. Eur J Immunol *31*, 2876-84.

Lalor, P. F., Edwards, S., McNab, G., Salmi, M., Jalkanen, S., and Adams, D. H. (2002a). Vascular adhesion protein-1 mediates adhesion and transmigration of lymphocytes on human hepatic endothelial cells. J Immunol *169*, 983-92.

Lalor, P. F., Shields, P., Grant, A., and Adams, D. H. (2002b). Recruitment of lymphocytes to the human liver. Immunol Cell Biol *80*, 52-64.

Larkin, D. F., Alexander, R. A., and Cree, I. A. (1997a). Infiltrating inflammatory cell phenotypes and apoptosis in rejected human corneal allografts. Eye *11*, 68-74.

Larkin, D. F., Calder, V. L., and Lightman, S. L. (1997b). Identification and characterization of cells infiltrating the graft and aqueous humour in rat corneal allograft rejection. Clin Exp Immunol *107*, 381-91.

Li, X. Y., D'Orazio, L. T., and Niederkorn, J. Y. (1996). Role of Th1 and Th2 cells in anterior chamber-associated immune deviation. Immunology *89*, 34-40.

Lidington, E. A., Rao, R. M., Marelli-Berg, F. M., Jat, P. S., Haskard, D. O., and Mason, J. C. (2002). Conditional immortalization of growth factor-responsive cardiac endothelial cells from H-2K(b)-tsA58 mice. Am J Physiol Cell Physiol *282*, C67-74.

Liu, Y., Hamrah, P., Zhang, Q., Taylor, A. W., and Dana, M. R. (2002). Draining lymph nodes of corneal transplant hosts exhibit evidence for donor major histocompatibility complex (MHC) class II-positive dendritic cells derived from MHC class II-negative grafts. J Exp Med *195*, 259-68.

Maeno, A., Naor, J., Lee, H. M., Hunter, W. S., and Rootman, D. S. (2000). Three decades of corneal transplantation: indications and patient characteristics. Cornea *19*, 7-11.

Marelli-Berg, F. M., Peek, E., Lidington, E. A., Stauss, H. J., and Lechler, R. I. (2000). Isolation of endothelial cells from murine tissue. J Immunol Methods *244*, 205-15.

Masuyama, J., Minato, N., and Kano, S. (1986). Mechanisms of lymphocyte adhesion to human vascular endothelial cells in culture. T lymphocyte adhesion to endothelial cells through endothelial HLA-DR antigens induced by gamma interferon. J Clin Invest *77*, 1596-605.

McEver, R. P. (1994). Selectins. Cuu Opin Immunol 6, 75-84

Medawar, P. B. (1948). Immunity to homologous grafted skin. B J Exp Pathol *29*, 58-69.

Nicholls, S. M. (1996). Non-HLA antigens and HLA-DR matching in corneal transplantation. Br J Ophthalmol *80*, 780-2.

Niederkorn, J. Y. (1990). Immune privilege and immune regulation in the eye. Adv Immunol *48*, 191-226.

Ostermann, G., Weber, K. S., Zernecke, A., Schroder, A., and Weber, C. (2002). JAM-1 is a ligand of the beta(2) integrin LFA-1 involved in transendothelial migration of leukocytes. Nat Immunol *3*, 151-8.

Ottonello, L., Tortolina, G., Amelotti, M., and Dallegri, F. (1999). Soluble Fas ligand is chemotactic for human neutrophilic polymorphonuclear leukocytes. J Immunol *162*, 3601-6.

Pavilack, M. A., Elner, V. M., Elner, S. G., Todd, R. F. d., and Huber, A. R. (1992). Differential expression of human corneal and perilimbal ICAM-1 by inflammatory cytokines. Invest Ophthalmol Vis Sci *33*, 564-73.

Peeler, J., Niederkorn, J., and Matoba, A. (1985). Corneal allografts induce cytotoxic T cell but not delayed hypersensitivity responses in mice. Invest Ophthalmol Vis Sci *26*, 1516-23.

Pepose, J. S., Nestor, M. S., Gardner, K. M., Foos, R. Y., and Pettit, T. H. (1985). Composition of cellular infiltrates in rejected human corneal allografts. Graefes Arch Clin Exp Ophthalmol *222*, 128-33.

Petruzzelli, L., Takami, M., and Humes, H. D. (1999). Structure and function of cell adhesion molecules. Am J Med *106*, 467-76.

Philipp, W. (1994). Leukocyte adhesion molecules in rejected corneal allografts. Graefes Arch Clin Exp Ophthalmol *232*, 87-95.

Philipp, W., and Gottinger, W. (1993). Leukocyte adhesion molecules in diseased corneas. Invest Ophthalmol Vis Sci *34*, 2449-59.

Piali, L., Hammel, P., Uherek, C., Bachmann, F., Gisler, R. H., Dunon, D., and Imhof, B. A. (1995). CD31/PECAM-1 is a ligand for alpha v beta 3 integrin involved in adhesion of leukocytes to endothelium. J Cell Biol *130*, 451-60.

Pigott, R., and Power, C. (1993). The Adhesion Molecule Facts Book (London: Academic Press Limited, Harcourt Brace & Company Publishers).

Pleyer, U., Steuhl, K. P., Weidle, E. G., Lisch, W., and Thiel, H. J. (1992). Corneal graft rejection: incidence, manifestation, and interaction of clinical subtypes. Transplant Proc *24*, 2034-7.

Pober, J. S., and Cotran, R. S. (1991). Immunologic interactions of T lymphocytes with vascular endothelium. Adv Immunol *50*, 261-302.

Ralph, P., Moore, M. A., and Nilsson, K. (1976). Lysozyme synthesis by established human and murine histiocytic lymphoma cell lines. J Exp Med *143*, 1528-33.

Ramrakha, P., Edwards, R., Nunez, D., Palmer, D., Haskard, D., Dorling, A., George, A., and Lechler, R. Intrabody-mediated phenotypic knockout of vascular cell adhesion molecule (VCAM) on porcine endothelial cells. Submitted.

Rayner, S. A., King, W. J., Comer, R. M., Isaacs, J. D., Hale, G., George, A. J., and Larkin, D. F. (2000). Local bioactive tumour necrosis factor (TNF) in corneal allotransplantation. Clin Exp Immunol *122*, 109-116.

Rice, G. E., Munro, J. M., Corless, C., and Bevilacqua, M. P. (1991). Vascular and nonvascular expression of INCAM-110. A target for mononuclear leukocyte adhesion in normal and inflamed human tissues. Am J Pathol *138*, 385-93.

Richardson, J. H., and Marasco, W. A. (1995). Intracellular antibodies: development and therapeutic potential. Trends Biotechnol *13*, 306-10.

Rondon, I. J., and Marasco, W. A. (1997). Intracellular antibodies (intrabodies) for gene therapy of infectious diseases. Annu Rev Microbiol *51*, 257-83.

Rosen, G. D., Sanes, J. R., LaChance, R., Cunningham, J. M., Roman, J., and Dean, D. C. (1992). Roles for the integrin VLA-4 and its counter receptor VCAM-1 in myogenesis. Cell *69*, 1107-19.

Salmi, M., and Jalkanen, S. (2001). VAP-1: an adhesin and an enzyme. Trends Immunol *22*, 211-6.

Sano, Y., Osawa, H., Sotozono, C., and Kinoshita, S. (1998). Cytokine expression during orthotopic corneal allograft rejection in mice. Invest Ophthalmol Vis Sci *39*, 1953-7.

Senoo, T., and Joyce, N. C. (2000). Cell cycle kinetics in corneal endothelium from old and young donors. Invest Ophthalmol Vis Sci *41*, 660-7.

Senoo, T., Obara, Y., and Joyce, N. C. (2000). EDTA: a promoter of proliferation in human corneal endothelium. Invest Ophthalmol Vis Sci *41*, 2930-5.

Skurkovich, S., Kasparov, A., Narbut, N., and Skurkovich, B. (2002). Treatment of corneal transplant rejection in humans with anti- interferon-gamma antibodies. Am J Ophthalmol *133*, 829-30.

Sonoda, Y., and Streilein, J. W. (1993). Impaired cell-mediated immunity in mice bearing healthy orthotopic corneal allografts. J Immunol *150*, 1727-34.

Sonoda, Y., and Streilein, J. W. (1992). Orthotopic corneal transplantation in mice--evidence that the immunogenetic rules of rejection do not apply. Transplantation *54*, 694-704.

Stannard, A. K., Riddell, D. R., Sacre, S. M., Tagalakis, A. D., Langer, C., von Eckardstein, A., Cullen, P., Athanasopoulos, T., Dickson, G., and Owen, J. S. (2001). Cell-derived apolipoprotein E (ApoE) particles inhibit vascular cell adhesion molecule-1 (VCAM-1) expression in human endothelial cells. J Biol Chem *276*, 46011-6.

Streilein, J. W., Masli, S., Takeuchi, M., and Kezuka, T. (2002). The eye's view of antigen presentation. Hum Immunol *63*, 435-43.

Streilein, J. W. (1993). Immune privilege as the result of local tissue barriers and immunosuppressive microenvironments. Curr Opin Immunol *5*, 428-32.

Stuart, P. M., Griffith, T. S., Usui, N., Pepose, J., Yu, X., and Ferguson, T. A. (1997). CD95 ligand (FasL)-induced apoptosis is necessary for corneal allograft survival. J Clin Invest *99*, 396-402.

Suzuki, J., Isobe, M., Izawa, A., Takahashi, W., Yamazaki, S., Okubo, Y., Amano, J., and Sekiguchi, M. (1999). Differential Th1 and Th2 cell regulation of murine cardiac allograft acceptance by blocking cell adhesion of ICAM-1/LFA-1 and VCAM-1/VLA-4. Transpl Immunol *7*, 65-72.

Tamura, Y., Konomi, H., Sawada, H., Takashima, S., and Nakajima, A. (1991). Tissue distribution of type VIII collagen in human adult and fetal eyes. Invest Ophthalmol Vis Sci *32*, 2636-44.

Tan, P., Chan, C., Xue, S., Dong, R., Anathesayanan, B., Kerouedan, C., Manunta, M., Lombardi, G., Larkin, D., Cheshire, N., Wolfe, J., Haskard, D., Taylor, K., and George, A. Human Saphenous Vein Enothelial Cells (HSVEC) - A robust model for vascular biology. Submitted.

Thornhill, M. H., Li, J., and Haskard, D. O. (1993). Leucocyte endothelial cell adhesion: a study comparing human umbilical vein endothelial cells and the endothelial cell line EA-hy-926. Scand J Immunol *38*, 279-86.

Torres, P. F., De Vos, A. F., van der Gaag, R., Martins, B., and Kijlstra, A. (1996). Cytokine mRNA expression during experimental corneal allograft rejection. Exp Eye Res *63*, 453-61.

Vail, A., Gore, S. M., Bradley, B. A., Easty, D. L., and Rogers, C. A. (1993). Corneal transplantation in the United Kingdom and Republic of Ireland. Br J Ophthalmol *77*, 650-6.

Varki, A. (1994). Selectin ligands. Proc Natl Acad Sci U S A 91, 7390-7

Volker-Dieben, H. J., Claas, F. H., Schreuder, G. M., Schipper, R. F., Pels, E., Persijn, G. G., Smits, J., and D'Amaro, J. (2000). Beneficial effect of HLA-DR matching on the survival of corneal allografts. Transplantation *70*, 640-8.

Vorkauf, W., Vorkauf, M., Nolle, B., and Duncker, G. (1995). Adhesion molecules in normal and pathological corneas. An immunohistochemical study using monoclonal antibodies. Graefes Arch Clin Exp Ophthalmol *233*, 209-19.

Wackenheim-Urlacher, A., Kantelip, B., Falkenrodt, A., Piqot, X., Tongio, M. M., Montard, M., and Delbosc, B. (1995). T-cell repertoire of normal, rejected, and pathological corneas: phenotype and function. Cornea *14*, 450-6.

Waldock, A., and Cook, S. D. (2000). Corneal transplantation: how successful are we? Br J Ophthalmol *84*, 813-5.

Waring, G. O. d., Bourne, W. M., Edelhauser, H. F., and Kenyon, K. R. (1982). The corneal endothelium. Normal and pathologic structure and function. Ophthalmology *89*, 531-90.

Weiss, A., Wiskocil, R. L., and Stobo, J. D. (1984). The role of T3 surface molecules in the activation of human T cells: a two-stimulus requirement for IL 2 production reflects events occurring at a pre-translational level. J Immunol *133*, 123-8.

Whitcup, S. M., Nussenblatt, R. B., Price, F. W., Jr., and Chan, C. C. (1993). Expression of cell adhesion molecules in corneal graft failure. Cornea *12*, 475-80.

Whitsett, C. F., and Stulting, R. D. (1984). The distribution of HLA antigens on human corneal tissue. Invest Ophthalmol Vis Sci *25*, 519-24.

Williams, K. A., Muehlberg, S. M., Lewis, R. F., and Coster, D. J. (1997). Long-term outcome in corneal allotransplantation. The Australian Corneal Graft Registry. Transplant Proc *29*, 983.

Williams, K. A., Roder, D., Esterman, A., Muehlberg, S. M., and Coster, D. J. (1992). Factors predictive of corneal graft survival. Report from the Australian Corneal Graft Registry. Ophthalmology *99*, 403-14.

Williams, K. A., Ash, J. K., and Coster, D. J. (1985). Histocompatibility antigen and passenger cell content of normal and diseased human cornea. Transplantation *39*, 265-9.

Wilson, S. E., Weng, J., Blair, S., He, Y. G., and Lloyd, S. (1995). Expression of E6/E7 or SV40 large T antigen-coding oncogenes in human corneal endothelial cells indicates regulated high-proliferative capacity. Invest Ophthalmol Vis Sci *36*, 32-40.

Wu, D., Koga, T., Martin, K. R., and Meydani, M. (1999). Effect of vitamin E on human aortic endothelial cell production of chemokines and adhesion to monocytes. Atherosclerosis *147*, 297-307.

Yamada, J., Zhu, S. N., Streilein, J. W., and Dana, M. R. (2000). Interleukin-1 receptor antagonist therapy and induction of anterior chamber-associated immune deviation-type tolerance after corneal transplantation. Invest Ophthalmol Vis Sci *41*, 4203-8.

Yamada, J., Yoshida, M., Taylor, A. W., and Streilein, J. W. (1999). Mice with Th2-biased immune systems accept orthotopic corneal allografts placed in "high risk" eyes. J Immunol *162*, 5247-55.

Yamagami, S., Miyazaki, D., Ono, S. J., and Dana, M. R. (1999). Differential chemokine gene expression in corneal transplant rejection. Invest Ophthalmol Vis Sci *40*, 2892-7.

Yamagami, S., Tsuru, T., Isobe, M., Obata, H., and Suzuki, J. (1996). The role of cell adhesion molecules in allograft rejection after penetrating keratoplasty in mice. Clinical and immunohistochemical study. Graefes Arch Clin Exp Ophthalmol *234*, 382-7.

Yusuf-Makagiansar, H., Anderson, M. E., Yakovleva, T. V., Murray, J. S., and Siahaan, T. J. (2002). Inhibition of LFA-1/ICAM-1 and VLA-4/VCAM-1 as a therapeutic approach to inflammation and autoimmune diseases. Med Res Rev *22*, 146-67.

Zapolska-Downar, D., Zapolski-Downar, A., Markiewski, M., Ciechanowicz, A., Kaczmarczyk, M., and Naruszewicz, M. (2000). Selective inhibition by alpha-tocopherol of vascular cell adhesion molecule-1 expression in human vascular endothelial cells. Biochem Biophys Res Commun *274*, 609-15.

Zhang, W. J., and Frei, B. (2002). Albumin selectively inhibits TNF alpha-induced expression of vascular cell adhesion molecule-1 in human aortic endothelial cells. Cardiovasc Res *55*, 820-9.

Zhu, S., Dekaris, I., Duncker, G., and Dana, M. R. (1999). Early expression of proinflammatory cytokines interleukin-1 and tumor necrosis factor-alpha after corneal transplantation. J Interferon Cytokine Res *19*, 661-9.